AIM ASSOCIATES
ARCHITECTURE AND INTEGRATED DESIGN TEAM MANAGEMENT
100 FAIR STREET, PETALUMA, CALIFORNIA 94952-2515 707•763•3300 x2 george@aimgreen.com

October 11, 2023

Regarding: General Plan Flood Mapping

Dear General Plan Advisory Committee and Petaluma City Council:

This letter asks for clarifications of contradictions I noticed between the Community Meeting 9/27/2023 about Sea Level Rise Flood Mapping for the General Plan and Petaluma's Greenhouse Gas Reduction Plan 9/2023.

During the 9/27/2023 meeting I asked if the flood maps included the more sever rain storms that will come with climate change. I was told that increased rain intensity was not included in the flood models because it is hard to predict and the average amount of rain for the year is not likely to increase. I am concerned because in California hundred year level storms are occurring only decades apart.

The contradiction is that on page 12 of the *Blueprint for Carbon Neutrality Petaluma's Greenhouse Gas Reduction Plan,* September 2023, it says

> "The City's updated flood model will incorporate projections for other factors that influence flood risk, including sea level rise, astronomical tides and storm- induced bay water levels, precipitation intensity, and impervious land cover. The General Plan will address anticipated hazards related to flooding and sea level rise through land use decisions and adaptation policies."

Since the General Plan and the resulting zoning maps and ordinances will be baed on the flood maps it is imperative that the flood modeling incorporate the best available science predicting atmospheric river level rain intensity. To be most useful they need to includie the range of scenarios as presented in that attached research papers. Highlights are noted on the next two pages. Transparency necessitates listing the sources rain intensity and duration used in the models.

Your colleague in working towards an equitable & sustainable society!

A. George Beeler, Principal Architect
NCARB 27839 Certification, Licensed California C9542, New York 13740

LIVING FUTURE
PROFESSIONAL MEMBER

Community service:
California Technical Forum
Safety Assessment Program Evaluator CA OES

Attached are scientifically robust studies that have been done for predictions of the range of rain storm possibilities for Petaluma and Northern CA.

A. The attached research paper **Increasing precipitation volatility in twenty-first-century California** says the following:

1. Page 427, first page of this article, First paragraph: "large twenty-first-century increases in the frequency of wet extremes, including a more than threefold increase in sub-seasonal events comparable to California's 'Great Flood of 1862'. As a consequence, a 25% to 100% increase in extreme dry-to-wet precipitation events is projected, despite only modest changes in mean precipitation."

2. Page 428: Large increase in extreme wet-event frequency: We find large, statistically robust increases in the simulated frequency of extremely heavy precipitation events on multiple time scales. All of California experiences a 100–200% increase in the occurrence of very high cumulative seasonal precipitation (of a magnitude comparable to the 2016–2017 season on a statewide basis) by the end of the twenty-first century (Fig. 1).

3. Page 428: these findings suggest that California's major urban centers (including San Francisco and Los Angeles) are more likely than not to experience at least one such extremely severe storm sequence between 2018 and 2060 (Fig. 2b,c) on a business-as-usual emissions trajectory. On a statewide basis, the overall frequency of 1862 magnitude events increases on the order of 300–400% by the end of the twenty-first century (Supplementary Fig. 2).

B. The attached research paper **Climate change is increasing the risk of a California megaflood** By Xingying Huang and Daniel L. Swain in SCIENCE ADVANCES RESEARCH ARTICLE **CLIMATOLOGY** https://www.science.org/doi/10.1126/sciadv.abq0995

1. **Introduction** Observed extreme precipitation and severe subregional flood events during the 20th century—including those in 1969, 1986, and 1997—hint at this latent potential, but despite their substantial soci- etal impacts, none have rivaled (from a geophysical perspective) the benchmark "Great Flood of 1861–1862" (henceforth, GF1862).

   Recent estimates suggest that floods equal to or greater in mag- nitude to those in 1862 occur five to seven times per millennium [i.e., a 1.0 to 0.5% annual likelihood or 100- to 200-year recurrence interval (RI)] (*5*, *8*).
   The extraordinary impacts resulting from GF1862 provided mo- tivation for a 2010 California statewide disaster scenario—known as "ARkStorm" (ARkStorm 1.0)—led by the U.S. Geological Survey in conjunction with a large, interdisciplinary team.

We find that climate change has already increased the risk of a
Ensemble (CESM1-LENS) and subsequently choosing from among GF1862-like
megaflood scenario in California, but that future cli-
the top 3 ranked events in each climate era to dynamically down- mate warming
will likely bring about even sharper risk increases.

2. **Cumulative and extreme precipitation** In general, cumulative precipitation in ARkFuture is be- tween 35 and 60% higher than in ARkHist for northern and central California (al- though locally >80% higher), with lesser increases in far southern California (fig. S7, A and B). On a statewide average basis, 30-day precipitation is ~45% higher in ARkFuture.
3. **Discussion** An extensive body of existing research has linked climate change to increasingly extreme precipitation events, even in locations where changes in mean precipitation are nonrobust. Our analysis suggests that the present-day (circa 2022) likelihood of historically rare to unprecedented 30-day precipitation accumulations has already increased substantially and that even modest additional increments of global warming will bring about even larger increases in likelihood. …we emphasize that recognizing and mitigating the societal risks associated with this subtly but substantially escalating natural hazard is a critically important consideration from a climate adaptation perspective.

C. The attached research paper **Fourth Climate Change Assessment San Francisco Bay Area Region** https://www.energy.ca.gov/sites/default/files/2019-11/Reg_Report-SUM-CCCA4-2018-005_SanFranciscoBayArea_ADA.pdf

1. page 20 In other words, a once-in-20- year storm would become a once-in-seven-year or more frequent storm. Similarly, Swain et al. (2018) estimate that a once-every-200-year sequence of storms comparable to that which caused the great California food of 1862 could occur every 40-50 years by 2100 under a high emissions scenario (RCP8.5).

nature climate change

ARTICLES

https://doi.org/10.1038/s41558-018-0140-y

Increasing precipitation volatility in twenty-first-century California

Daniel L. Swain[1,2*], Baird Langenbrunner[3,4], J. David Neelin[3] and Alex Hall[3]

Mediterranean climate regimes are particularly susceptible to rapid shifts between drought and flood—of which, California's rapid transition from record multi-year dryness between 2012 and 2016 to extreme wetness during the 2016–2017 winter provides a dramatic example. Projected future changes in such dry-to-wet events, however, remain inadequately quantified, which we investigate here using the Community Earth System Model Large Ensemble of climate model simulations. Anthropogenic forcing is found to yield large twenty-first-century increases in the frequency of wet extremes, including a more than threefold increase in sub-seasonal events comparable to California's 'Great Flood of 1862'. Smaller but statistically robust increases in dry extremes are also apparent. As a consequence, a 25% to 100% increase in extreme dry-to-wet precipitation events is projected, despite only modest changes in mean precipitation. Such hydrological cycle intensification would seriously challenge California's existing water storage, conveyance and flood control infrastructure.

Mediterranean climate regimes are renowned for their distinctively dry summers and relatively wet winters—a globally unusual combination[1]. Such climates generally occur near the poleward fringe of descending air in the subtropics, where semi-permanent high-pressure systems bring stable conditions during most of the calendar year[2]. Here, the majority of precipitation occurs during the passage of transient storm events during a short rainy season[3]—a distinct seasonality brought about by an equatorward shift in the mid-latitude storm track during winter[4]. The same factors that imbue such regions with their temperate mean climate state, however, are also conducive to dramatic swings between drought and flood[4–6]. Subtle year-to-year jetstream shifts can generate disproportionately large precipitation variability[7]—yielding highly non-uniform precipitation distributions[8] and increasing the intrinsic likelihood of hydroclimatic extremes[4,9]. These effects are often amplified in California, where a combination of complex topography and over 1,000 km of latitudinal extent yield a great diversity of microclimates within the broader 'dry summer' regime[1].

California's rapid shift from severe drought to abundant precipitation (and widespread flooding) during the 2016–2017 winter[10] offers a compelling example of one such transition in a highly populated, economically critical and biodiverse region[11,12]. Immediately following one of the most intense multi-year droughts on record between 2012 and 2016 (refs [13–15]), the state experienced several months of heavy precipitation associated with an extraordinarily high number of atmospheric river storms during November–March 2016–2017 (ref. [10]). While the heaviest precipitation was concentrated in northern Sierra Nevada watersheds, hundreds of roads throughout California were damaged by floodwaters and mudslides (including a major bridge collapse)[16]. In February 2017, heavy runoff in the Feather River watershed contributed to the failure of the Oroville Dam's primary spillway—culminating in a crisis that forced the emergency evacuation of nearly a quarter of a million people[17].

Previous studies focusing on future changes in California precipitation have generally reported modest[18–20] (and/or uncertain) changes in regional mean precipitation[7,20]. More recent work, however, has suggested an increased likelihood of wet years[20–23] and subsequent flood risk[9,24] in California—which is consistent with broader theoretical and model-based findings regarding the tendency towards increasing precipitation intensity[25] in a warmer (and therefore moister) atmosphere[26,27]. Meanwhile, while evidence shows that anthropogenic warming has contributed to an increased risk of California drought via increasing temperatures[28,29] and increased frequency of seasonally persistent high-pressure ridges[8,14,30,31], attribution studies focusing directly on precipitation have yielded mixed results[18,32]. Contributing additional uncertainty are climate model simulations suggesting that the boundary between mean subtropical drying and mid-latitude wetting will probably occur over California[33], potentially yielding strong latitudinal gradients in the precipitation response. Thus, while there is already substantial evidence that climate change will induce regional hydroclimatic shifts, a cohesive picture has yet to emerge—presenting serious challenges to decision-makers responsible for ensuring the resilience of California's water infrastructure[11].

Importance of large ensemble approach

We use specific flood and drought events from California's history as baselines for exploring the changing character of precipitation extremes. Our use of a large ensemble of climate model simulations[34]—the Community Earth System Model Large Ensemble (CESM-LENS)—allows us to directly quantify changes in large-magnitude extremes. This approach offers a substantial advantage over traditional climate model experiments, which yield too small a sample size of statistically rare extreme events to draw robust inferences without making assumptions regarding the underlying precipitation distribution[35]. By selecting a wide range of wet, dry and dry-to-wet transition (that is, 'whiplash') events informed by historical analogues, we aim to provide a comprehensive perspective on the changing risks of regional hydroclimate extremes in a manner directly relevant to climate adaptation and infrastructure planning efforts.

[1]Institute of the Environment and Sustainability, University of California, Los Angeles, Los Angeles, CA, USA. [2]The Nature Conservancy, Arlington, VA, USA. [3]Department of Atmospheric and Oceanic Sciences, University of California, Los Angeles, Los Angeles, CA, USA. [4]Department of Earth System Science, University of California, Irvine, Irvine, CA, USA. *e-mail: dlswain@ucla.edu

We assess simulated changes in the frequency of California precipitation extremes caused by increasing atmospheric greenhouse gas concentrations. Our overall approach is to (1) determine approximate frequency of occurrence for each event of interest based on direct observations or historical accounts, (2) calculate the magnitude of events within a preindustrial control climate model simulation that occur with comparable frequency to those observed and (3) quantify subsequent frequency changes in similar events under a scenario of continued growth in greenhouse gas concentrations.

We focus on changes in frequency of precipitation events exceeding particular thresholds for two key reasons. First, historical civil engineering and risk management practices have been predicated on a largely stationary climate[36], and the majority of existing water storage and conveyance structures have been constructed under such assumptions. Second, a frequency-based approach also offers the considerable advantage of implicit climate model bias correction. While all global climate models exhibit some degree of mean precipitation bias in topographically complex California[9], the use of a long preindustrial control simulation to define return interval thresholds allows us to make internally consistent comparisons between simulated precipitation distributions at different levels of radiative forcing. We can therefore select CESM-LENS precipitation thresholds corresponding to approximate return intervals of real-world historical events, which serve as analogues for impacts.

Large increase in extreme wet-event frequency

We find large, statistically robust increases in the simulated frequency of extremely heavy precipitation events on multiple timescales. All of California experiences a 100–200% increase in the occurrence of very high cumulative seasonal precipitation (of a magnitude comparable to the 2016–2017 season on a statewide basis) by the end of the twenty-first century (Fig. 1). This simulated increase in seasonal wet extremes across California is part of a broader regional increase extending across the Pacific coast. Seasonal precipitation of this magnitude (equivalent to that associated with the 25 year preindustrial control (PIC) return interval) has only occurred a handful of times over the lifespan of California's modern water infrastructure. It represents a rarely exceeded but not unprecedented threshold, for which there are analogues in the recent historical record.

We note, however, that California's most severe floods do not necessarily coincide with its wettest winters. Instead, regional flood events are more directly linked to persistent storm sequences on sub-seasonal timescales, which are capable of bringing a significant fraction of annual average precipitation over a brief period[3,6,37]. Thus, to better characterize changes in the frequency of such 'high consequence, low probability' precipitation events, we use a sub-seasonal threshold motivated by the extraordinary sequence of 'atmospheric river' storms that brought extremely severe flooding to much of California during the winter of 1861–1862 (refs [38,39]). We define 40 day precipitation accumulations exceeding the 200 year preindustrial return interval as a measure of occurrences comparable to this benchmark event (see Methods).

Given the severe impacts even one such occurrence would have on California's existing infrastructure and population centres[40], we assess cumulative twenty-first-century risk beginning in the present winter season (2017–2018). Figure 2 shows that at least two-thirds (66.66%) of LENS ensemble members simulate two or more 1862-magnitude events over this interval across virtually all of California—which represents a dramatic increase in likelihood relative to preindustrial simulations (where, by definition, the cumulative 83 year likelihood of a single occurrence is less than 50%). Strikingly, these findings suggest that California's major urban centres (including San Francisco and Los Angeles) are more likely than not to experience at least one such extremely severe storm sequence between 2018 and 2060 (Fig. 2b,c) on a business-as-usual emissions trajectory. On a statewide basis, the overall frequency of 1862-magnitude events increases on the order of 300–400% by the end of the twenty-first century (Supplementary Fig. 2).

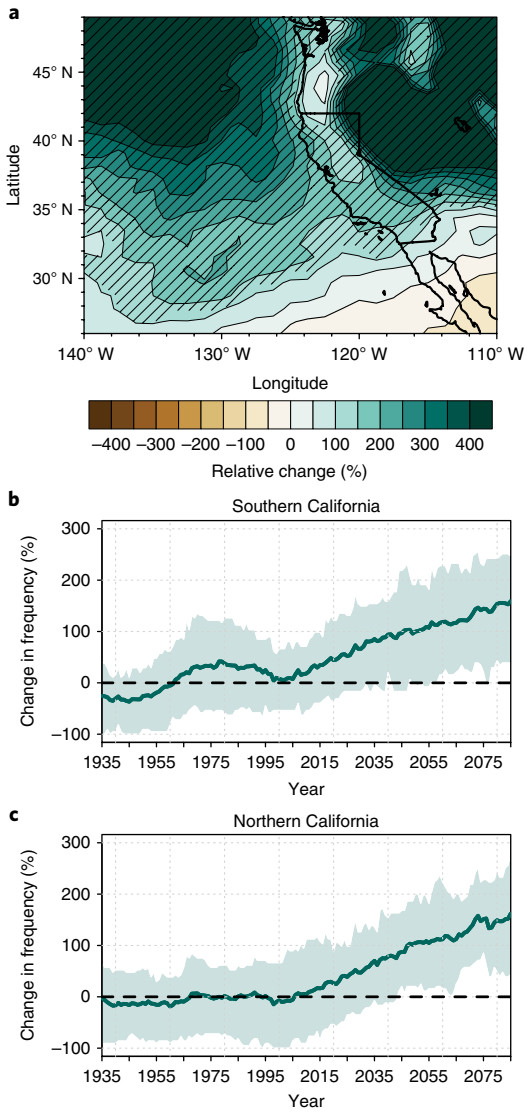

Fig. 1 | Change in frequency of extremely wet seasons. a, Relative (%) change in frequency of extremely wet seasons (meeting or exceeding the 25 year PIC return interval for November–March precipitation) at end of the twenty-first century (2070–2100, RCP8.5 forcing) relative to the preindustrial era (1850 forcing). Cross-hatching signifies 90% statistical confidence ($P < 0.10$) in robustness of frequency shifts across the full 40-member CESM-LENS ensemble. **b**,**c**, Time series showing relative (%) change in frequency of extremely wet seasons in each year from 1935 to 2085 (solid green curve) for a cluster of grid boxes in Southern California (**b**) and Northern California (**c**). Data are smoothed over 30 year intervals, and the green shaded range encompasses two-thirds (66.66%) of the CESM-LENS ensemble spread (that is, the 16.66th and 83.33th percentile bounds). Dashed black horizontal lines in **b** and **c** denote zero change in frequency.

These increases in extreme wet-event frequency across the large ensemble emerge in an essentially monotonic fashion throughout most of California beginning between around 2010–2020 for both seasonal (25 year) wet events (Supplementary Fig. 3a) and sub-seasonal (200 year) wet events (Supplementary Fig. 3b). In addition to the robust ensemble-mean signal by mid-to-late century for both

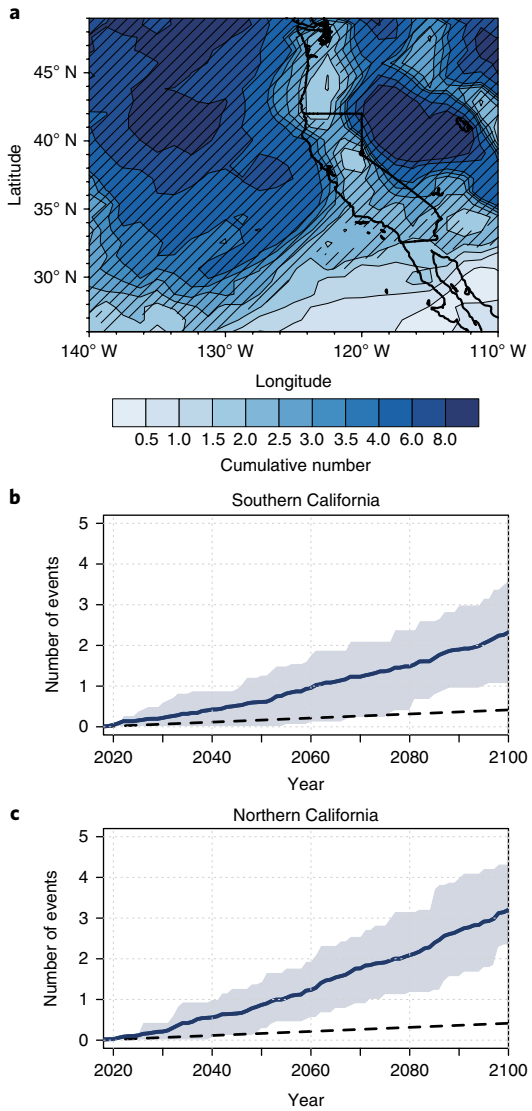

Fig. 2 | Cumulative occurrence of extremely wet sub-seasonal storm sequences. a, Cumulative number of extremely wet sub-seasonal storm sequences (meeting or exceeding the 200 year PIC return interval for cumulative 40 day precipitation) occurring in CESM-LENS between 2018 and 2100 under RCP8.5 forcing. Cross-hatching signifies regions where at least two-thirds (66.66%) of CESM-LENS ensemble members simulate two or more such occurrences. **b**,**c**, Time series showing cumulative number of extremely wet sub-seasonal storm sequences during 2018–2100 (solid blue curve) for a cluster of grid boxes in Southern California (**b**) and Northern California (**c**). Blue shaded range encompasses two-thirds (66.66%) of the CESM-LENS ensemble spread (that is, the 16.66th and 83.33th percentile bounds). Dashed black curve depicts baseline cumulative occurrence over an equivalent time interval assuming constant preindustrial climate forcings.

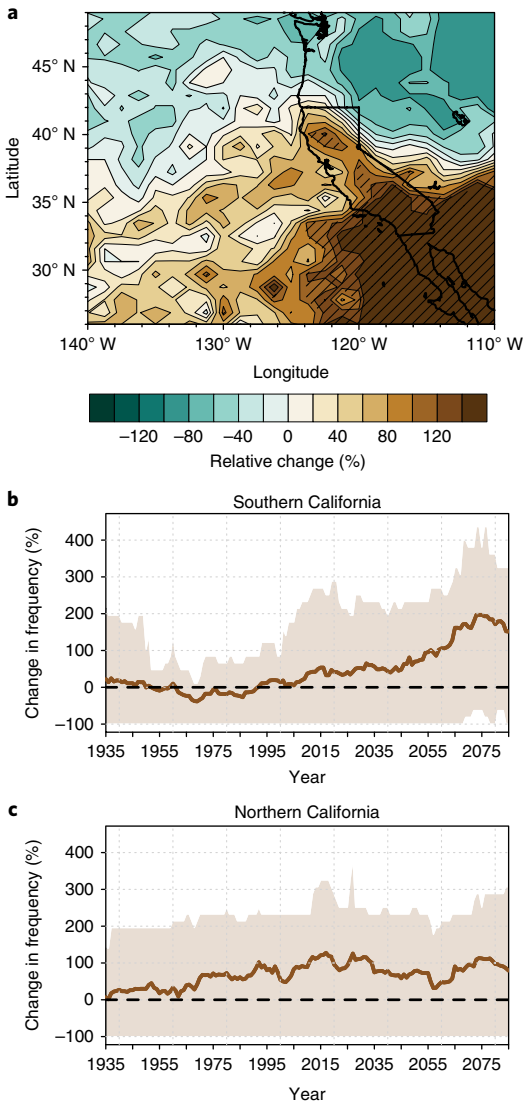

Fig. 3 | Change in frequency of extremely dry seasons. a, Relative (%) change in frequency of extremely dry seasons (meeting or falling below the 100 year PIC return interval for low November–March precipitation) at end of the twenty-first century (2070–2100, RCP8.5 forcing) relative to the preindustrial era (1850 forcing). Cross-hatching signifies 90% statistical confidence ($P < 0.10$) in robustness of frequency shifts across the full 40-member CESM-LENS ensemble. **b**,**c**, Time series showing relative (%) change in frequency of extremely dry seasons in each year 1935–2085 (solid brown curve) for a cluster of grid boxes in Southern California (**b**) and Northern California (**c**). Data are smoothed over 30 year intervals, and the brown shaded range encompasses two-thirds (66.66%) of the CESM-LENS ensemble spread (that is, the 16.66th and 83.33th percentile bounds). Dashed black horizontal lines in **b** and **c** denote zero change in frequency.

extreme wet events, these results also imply that an increased likelihood of large precipitation accumulations relative to a preindustrial climate may already exist. However, we note that a handful of outlying ensemble members suggest a chance that internal variability could delay emergence of an attributable signal by several decades (Fig. 1b,c and Fig. 2b,c).

Shifts in extreme dry-event frequency

The simulated frequency of extremely dry years also increases across nearly all of California (Fig. 3). An increased likelihood of these extremely dry rainy seasons (that is, exceeding the 100 year return interval, analogous to the 1976–1977 drought and slightly drier than 2013–2014) first emerges weakly across portions of the state as early as the 1980s, before emerging in a statistically robust manner across Northern California around 2010–2020 and Southern California later in the century (around 2060; Supplementary Fig. 4a). Notable are especially large increases (>140%) in frequency that occur across Southern California after 2050 (Fig. 3b and Supplementary Fig. 4a), though we emphasize that substantial increases on the order of +80% extend across most of Northern California. Except

for southernmost California, much of this increased risk emerges during the twentieth and early twenty-first centuries (Fig. 3b,c and Supplementary Fig. 4a)—suggesting that the likelihood of individual dry seasons may already be increased relative to the preindustrial period.

In contrast, changes in the occurrence of extremely dry consecutive years analogous to the record-low 3 year cumulative statewide precipitation observed during 2013–2015 (100 year return interval on a 3 year basis) exhibit a more complex temporal and spatial structure (Supplementary Fig. 4b). By the end of the twenty-first century, only far southern California experiences a robust increase in the frequency of consecutively dry seasons (Supplementary Fig. 2), while the rest of California does not experience statistically significant changes. Further analysis shows that this divergence between single and consecutive dry-season frequency shifts arises from the increased pace of future wet-year increases relative to dry-year increases, which is especially pronounced across Northern California (Supplementary Fig. 5c). These findings suggest that future multi-year droughts in California may exhibit an increased propensity to be interrupted by very wet interludes.

Emergence of 'precipitation whiplash' signal

Given the large simulated increase in the frequency of both dry and wet extremes, we test whether the frequency of rapid transitions between dry and wet conditions—similar to the precipitation whiplash that occurred between the recent 2012–2016 drought and 2016–2017 floods—also increases. For the purposes of this study, we define precipitation whiplash as the occurrence of two consecutive years during which rainy season (November–March) precipitation falls under the PIC 20th percentile (in the first year) and subsequently exceeds the PIC 80th percentile (in the following year). Figure 4 confirms such an increase during the twenty-first century throughout California. We report a strong latitudinal gradient in the year-to-year (interannual) whiplash response to anthropogenic forcing, ranging from an ~100% increase across Southern California to an ~25% increase in Northern California (Fig. 4a). These whiplash increases first emerge in the south relatively early in the twenty-first century (2010–2020) before spreading progressively northward in a statistically robust manner in the following decades (especially after 2050; Supplementary Fig. 5). We also investigate changes in month-to-month (sub-seasonal) precipitation variability during the canonical wet season. We report modest but widespread increases of 20–30% across a broad swath of the northeastern Pacific region, again extending across all of California (Supplementary Fig. 2c).

Together, these shifts represent a marked increase in both the interannual and intraseasonal variability of precipitation, especially in Southern California—which is noteworthy for two distinct reasons. First, natural precipitation variability in this region is already large[6], and projected future whiplash increases would amplify existing swings between dry and wet years (and between dry and wet months within the rainy season). Second, the robust emergence of a precipitation whiplash signal across a wide range of timescales (Fig. 4 and Supplementary Fig. 2c) is remarkable, as large-scale atmospheric variability over the North Pacific relevant to California precipitation is dominated by different physical processes and associated remote teleconnections on sub-seasonal (for example, the Madden–Julian Oscillation[41]) and interannual (for example, El Nino–Southern Oscillation (ENSO)[42]) timescales.

Increasingly sharp seasonality of California wet season

We find a distinct sharpening of California's future mean seasonal cycle (Fig. 5). While winter mean precipitation increases across most of California, mean precipitation during autumn (September–November) and especially spring (March–May) decreases nearly everywhere, which is consistent with previous findings from the Coupled Model Intercomparison Project Phase 5 (CMIP5) ensemble[43]. This striking contrast between the drying marginal and wetting core rainy season months results in a large ensemble-mean increase (35% to 85% from north to south) in the ratio of overall wet season precipitation falling between November and March relative to cumulative precipitation during the four months of September, October, April and May (Fig. 5). This increase in sharpness of precipitation seasonality suggests that the already distinct contrast between California's long, dry summers and relatively brief, wet winters will probably become even more

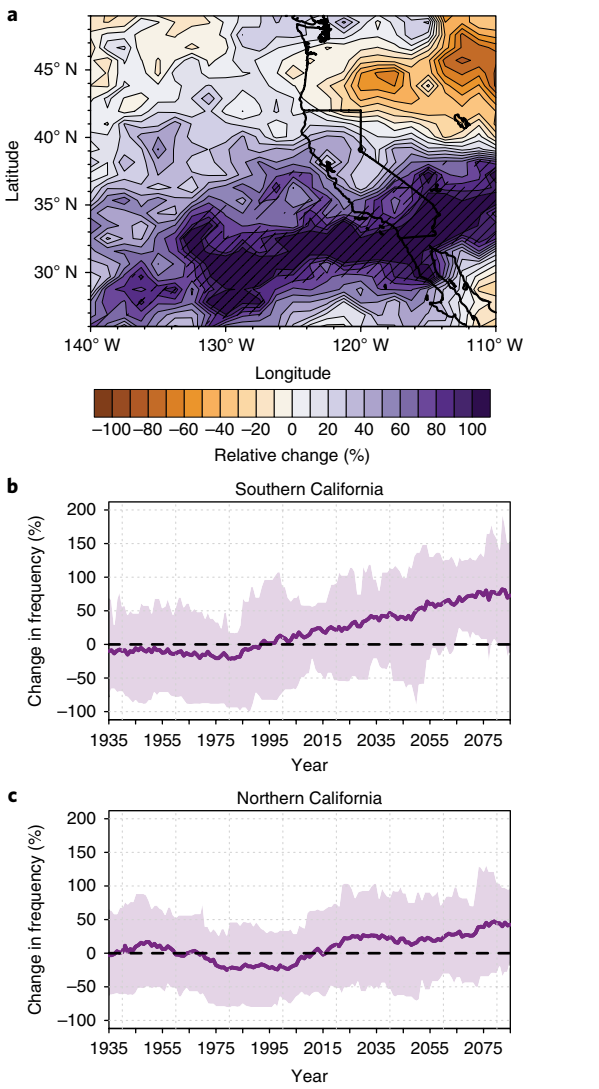

Fig. 4 | Change in frequency of precipitation whiplash events. a, Relative (%) change in frequency of dry-to-wet precipitation whiplash events (years with November–March precipitation at or above the 80th preindustrial percentile immediately followed by a year with precipitation below the 20th preindustrial percentile) at end of the twenty-first century (2070–2100, RCP8.5 forcing) relative to the preindustrial era (1850 forcing). Cross-hatching signifies 90% statistical confidence ($P < 0.10$) in robustness of frequency shifts across the full 40-member CESM-LENS ensemble. **b**,**c**, Time series showing relative (%) change in frequency of whiplash events in each year 1935–2085 (solid purple curve) for a cluster of grid boxes in Southern California (**b**) and Northern California (**c**). Data are smoothed over 30 year intervals, and the purple shaded range encompasses two-thirds (66.66%) of the CESM-LENS ensemble spread (that is, the 16.66th and 83.33th percentile bounds). Dashed black horizontal lines in **b** and **c** denote zero change in frequency.

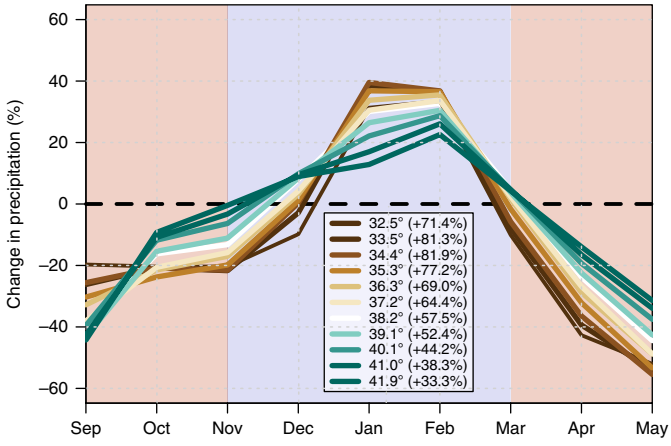

Fig. 5 | Shifts in precipitation seasonality. Relative changes in CESM-LENS monthly mean precipitation at the end of the twenty-first century (2070–2100) as a percent of the PIC climatology for each calendar month for a range of latitudes spanning the California coast. Percentages in the legend denote relative changes in mean 'seasonal sharpness' at each latitude, defined as the ratio between precipitation falling during the core rainy season (November–March; blue background shading) to that cumulatively falling during the marginal rainy season (September–October, April–May; red background shading). Curves are colour coded by latitude (and therefore by mean seasonal precipitation, which increases monotonically with latitude). Dashed black horizontal line denotes zero change in magnitude.

pronounced during the twenty-first century. While a comprehensive assessment is beyond the scope of this study, we note that autumn and spring drying trends have recently begun to emerge in observations across California (Supplementary Fig. 7)—suggesting that the projected concentration of precipitation into an even narrower season may already be underway.

Increase in extremes despite modest mean change

The substantial increases in California precipitation extremes over a wide range of timescales and intensities occur despite only modest changes in rainy season mean precipitation. By the end of the twenty-first century, the CESM-LENS ensemble mean depicts modest cool-season wetting over the northern portion of the state (<20–30%; Fig. 5), with little change in the south (~0%; Supplementary Fig. 6)—similar to the CMIP5 multi-model ensemble-mean response (Supplementary Fig. 6). Yet over the same interval, the frequencies of both extreme dry seasons and whiplash events increase by over 50% over much of the state (Figs. 3 and 4), and the frequency of extreme wet events increases by well over 100% nearly everywhere (Fig. 1 and Supplementary Fig. 2). This remarkable divergence between simulated future mean and extreme climate is especially pronounced across Southern California. For example: simulated mean precipitation in Southern California exhibits little trend by the end of the twenty-first century (Supplementary Fig. 5), despite an ~200% increase in extremely dry seasons (Fig. 3), an ~150% increase in extremely wet seasons (Fig. 1), a >500% increase in extreme sub-seasonal precipitation events (Fig. 2 and Supplementary Fig. 2) and an ~75% increase in year-to-year whiplash (Fig. 4). Importantly, these findings suggest that lingering uncertainty regarding the magnitude (and even sign) of regional mean precipitation change does not preclude statistically robust conclusions regarding changes in precipitation extremes.

Changes in processes responsible for extremes

We confirm that simulated large-scale atmospheric circulation patterns associated with California wet and dry extremes are substantially similar to those observed historically (Supplementary Fig. 12). Wet years are linked to strong low-pressure anomalies over the northeastern Pacific Ocean (Fig. 6a), with downstream enhancement of the storm track just west of California[7,14]. Dry years coincide with seasonally persistent high pressure extending across the northeastern Pacific (Fig. 6d), which reinforces the climatological mean ridge along the West Coast[14] and prevents storms from reaching California[44].

We find that future (representative concentration pathway 8.5 (RCP8.5)) wet and dry years are linked to broadly similar atmospheric circulation anomalies as those in the past (PIC; Fig. 6b,e)—suggesting that the spatial character of large-scale features driving California precipitation extremes may remain relatively stationary. However, given that subtle storm track perturbations can yield disproportionately large shifts in California precipitation[7,14,20], we note two potentially important differences between the RCP8.5 and PIC composites. In future wet years, low pressure over the North Pacific is deeper to the west of California (Fig. 6b), which previous work using models in the CMIP5 experiment has suggested is linked to a localized eastward extension of the jetstream[7,20]. In RCP8.5 dry years, atmospheric pressure anomalies in the immediate vicinity of California are similar to PIC dry years (Fig. 6e), but are higher in adjacent regions—suggesting a broader, more longitudinally oriented atmospheric ridge pattern and subsequent poleward storm track shift.

We also report large increases in atmospheric water vapour during both future wet and dry years. While this moistening is not in itself surprising—given the well-understood thermodynamic consequences of the Clausius–Clapeyron relation[45]—we point out that RCP8.5 dry years occur in an atmosphere moister than that during even the wettest years of the PIC simulation (Fig. 6c,f). The fact that California dry years occur more frequently (Fig. 3) suggests that simulated (thermodynamic) moistening must be counteracted (at least periodically) by changes in the frequency and/or intensity of atmospheric circulation patterns that prevent precipitation-bearing storms from reaching California, such as persistent high-pressure systems[14] or transient poleward shifts in the East Pacific storm track[7]. Conversely, the (thermodynamic) increase in water vapour would probably reinforce the (dynamic) effect of deeper North Pacific low pressure during wet years—which may underlie the relatively larger simulated increase in extreme wet-event frequency (versus dry-event frequency). Nonetheless, we emphasize that further work is necessary to better understand underlying changes in both remote (tropical[31,44] and Arctic teleconnections[46–48]) and regional-scale (that is, atmospheric rivers[9] and orographic precipitation) influences.

Societal implications of hydrological intensification

Collectively, our findings suggest that anthropogenic warming will bring about large increases in the frequency of California hydroclimatic extremes similar or greater in magnitude to those that have historically caused widespread disruption. These changes in the character of California precipitation emerge in a large single-model ensemble despite only modest trends in mean precipitation—strongly suggesting that the region's already variable year-to-year climate is likely to become even more volatile. Historically observed impacts of droughts and floods may in many cases offer reasonable analogues for the human and environmental impacts of future events of a similar magnitude, but increasingly wide swings between dry and wet conditions will threaten to upset the already precarious balance between competing flood control and water storage imperatives in California.

Moreover, we report a substantial increase in the projected risk of extreme precipitation events exceeding any that have occurred over the past century—meaning that such events would be unprecedented in California's modern era of extensive water infrastructure. Few of the dams, levees and canals that currently protect millions living in California's flood plains and facilitate the movement of

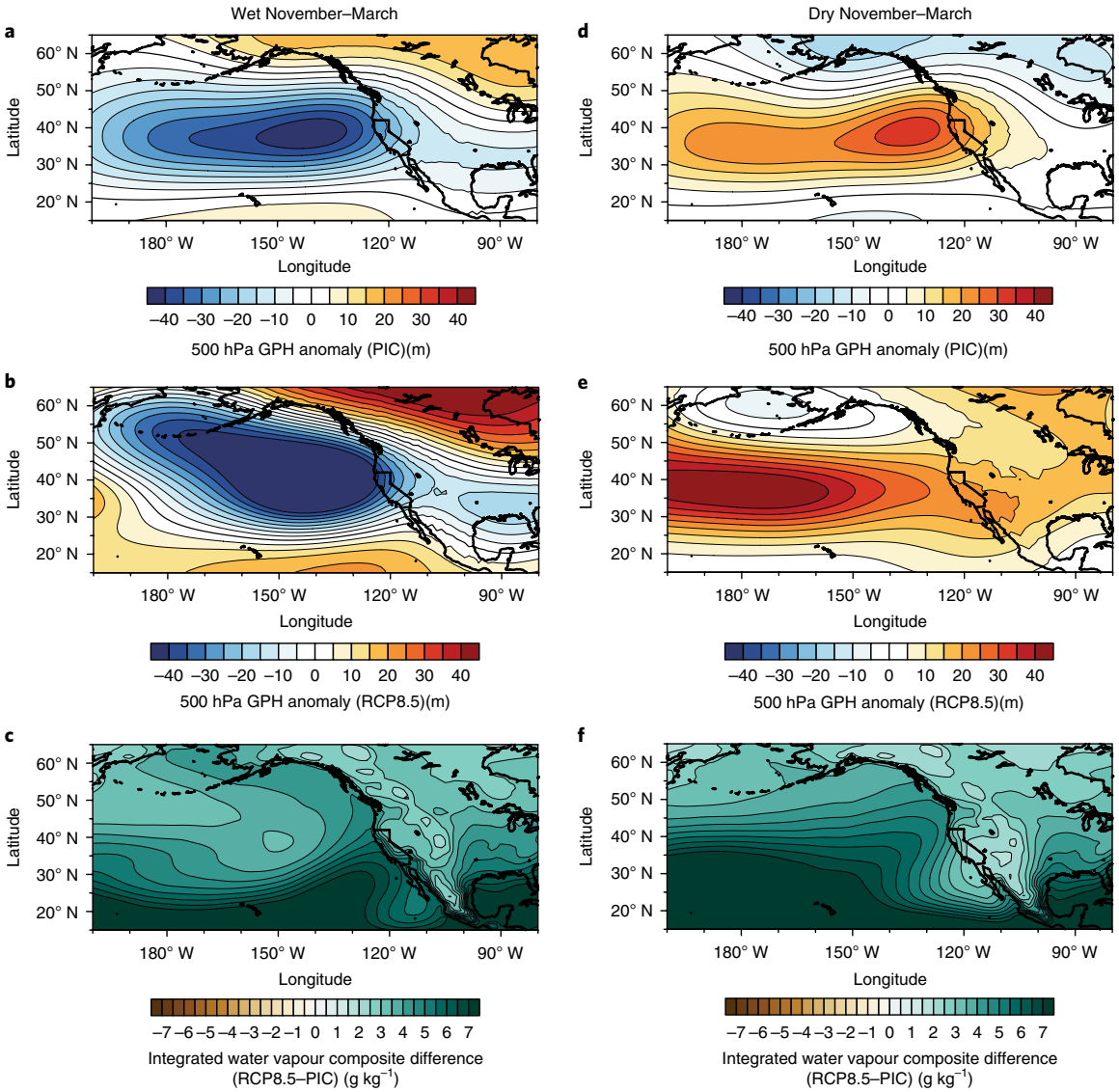

Fig. 6 | Large-scale atmospheric conditions linked to California precipitation extremes. a,**d**, Composite maps depicting anomalies in November–March 500 hPa GPH during wet (80th percentile, left column) and dry (20th percentile, right column) March–November seasons in the CESM-LENS simulation. **b**,**e**, RCP8.5 (2081–2100) composite anomaly patterns for GPH (see Methods). **c**,**f**, Difference between RCP8.5 (2081–2100) and PIC composite anomaly patterns for column-integrated water vapour.

water from Sierra Nevada watersheds to coastal cities have been tested by a deluge as severe as the extraordinary 1861–1862 storm sequence—a repeat of which would probably lead to considerable loss of life and economic damages approaching a trillion dollars[39,40]. Our results suggest that such an event is more likely than not to occur at least once between 2018 and 2060, and that multiple occurrences are plausible by 2100 on a business-as-usual emissions trajectory. Therefore, recognizing that risks associated with hydroclimatic extremes may rise more rapidly than the gradual projected shift in regional mean precipitation might otherwise suggest will be a critical step in ensuring resilience amid a warming climate.

Methods

Methods, including statements of data availability and any associated accession codes and references, are available at https://doi.org/10.1038/s41558-018-0140-y.

Received: 23 November 2017; Accepted: 20 March 2018;
Published online: 23 April 2018

References

1. Kottek, M., Grieser, J., Beck, C., Rudolf, B. & Rubel, F. World map of the Köppen-Geiger climate classification updated. *Meteorol. Z.* **15**, 259–263 (2006).
2. Karnauskas, K. B. & Ummenhofer, C. C. On the dynamics of the Hadley circulation and subtropical drying. *Clim. Dynam.* **42**, 2259–2269 (2014).
3. Dettinger, M. Atmospheric rivers as drought busters on the US West Coast. *J. Hydrometeorol.* **14**, 1721–1732 (2013).
4. Stephen, H. S., Terry, L. R. & Michael, D. M. *Encyclopedia of Climate and Weather* (Oxford Univ. Press, New York, 2011).
5. Horton, D. et al. Contribution of changes in atmospheric circulation patterns to extreme temperature trends. *Nature* **522**, 465–469 (2015).
6. Dettinger, M. D., Ralph, F. M., Das, T., Neiman, P. J. & Cayan, D. R. Atmospheric rivers, floods and the water resources of California. *Water* **3**, 445–478 (2011).
7. Langenbrunner, B., Neelin, J. D., Lintner, B. R. & Anderson, B. T. Patterns of precipitation change and climatological uncertainty among CMIP5 models, with a focus on the midlatitude Pacific storm track. *J. Clim.* **28**, 7857–7872 (2015).
8. Swain, D. et al. The extraordinary California drought of 2013/2014: character, context, and the role of climate change. *Bull. Am. Meteorol. Soc.* **95**, S3–S7 (2014).

9. Dettinger, M. Historical and future relations between large storms and droughts in California. *San Francisco Estuary Watershed Sci.* **14**, 1 (2016).
10. Wang, S. Y. S., Yoon, J.-H., Becker, E. & Gillies, R. California from drought to deluge. *Nat. Clim. Change* **7**, 465–468 (2017).
11. Swain, D. A tale of two California droughts: lessons amidst record warmth and dryness in a region of complex physical and human geography. *Geophys. Res. Lett.* **42**, 9999–10003 (2015).
12. Cowling, R. M., Rundel, P. W., Lamont, B. B., Kalin Arroyo, M. & Arianoutsou, M. Plant diversity in Mediterranean-climate regions. *Trends Ecol. Evol.* **11**, 362–366 (1996).
13. Griffin, D. & Anchukaitis, K. J. How unusual is the 2012–2014 California drought?. *Geophys. Res. Lett.* **41**, 9017–9023 (2014).
14. Swain, D., Horton, D., Singh, D. & Diffenbaugh, N. Trends in atmospheric patterns conducive to seasonal precipitation and temperature extremes in California. *Sci. Adv.* **2**, e1501344 (2016).
15. Robeson, S. Revisiting the recent California drought as an extreme value.*Geophys. Res. Lett.* **42**, 6771–6779 (2015).
16. Serna, J. California faces $860-million repair bill for roads battered by record winter storms. *Los Angeles Times* (3 April 2017).
17. Schmidt, S., Hawkins, D & Phillips, K. 188,000 evacuated as California's massive Oroville Dam threatens catastrophic floods. *Washington Post* (3 February 2017).
18. Seager, R. et al. Causes of the 2011–14 California drought. *J. Clim.* **28**, 6997–7024 (2015).
19. Simpson, I. R., Seager, R., Ting, M. & Shaw, T. A. Causes of change in Northern Hemisphere winter meridional winds and regional hydroclimate. *Nat. Clim. Change* **6**, 65–70 (2016).
20. Neelin, J. D., Langenbrunner, B., Meyerson, J. E., Hall, A. & Berg, N. California winter precipitation change under global warming in the Coupled Model Intercomparison Project Phase 5 ensemble. *J. Clim.* **26**, 6238–6256 (2013).
21. Berg, N. & Hall, A. Increased interannual precipitation extremes over California under climate change. *J. Clim.* **28**, 6324–6334 (2015).
22. Wang, S.-Y. S., Huang, W.-R. & Yoon, J.-H. The North American winter 'dipole' and extremes activity: a CMIP5 assessment. *Atmos. Sci. Lett.* **16**, 338–345 (2015).
23. Yoon, J.-H. Increasing water cycle extremes in California and in relation to ENSO cycle under global warming. *Nat. Commun.* **6**, 8657 (2015).
24. Dettinger, M. Climate change, atmospheric rivers, and floods in California—a multimodel analysis of storm frequency and magnitude changes. *J. Am. Water Resour. Assoc.* **47**, 514–523 (2011).
25. Giorgi, F. et al. Higher hydroclimatic intensity with global warming. *J. Clim.* **24**, 5309–5324 (2011).
26. Trenberth, K. E., Dai, A., Rasmussen, R. M. & Parsons, D. B. The changing character of precipitation. *Bull. Am. Meteorol. Soc.* **84**, 1205–1217 (2003).
27. Donat, M. G., Lowry, A. L., Alexander, L. V., Ogorman, P. A. & Maher, N. More extreme precipitation in the world's dry and wet regions. *Nat. Clim. Change* **6**, 508–513 (2016).
28. Diffenbaugh, N., Swain, D. & Touma, D. Anthropogenic warming has increased drought risk in California. *Proc. Natl Acad. Sci. USA* **112**, 3931–3936 (2015).
29. Williams, A. P. et al. Contribution of anthropogenic warming to California drought during 2012–2014. *Geophys. Res. Lett.* **42**, 6819–6828 (2015).
30. Wang, S. Y., Hipps, L., Gillies, R. R. & Yoon, J.-H. Probable causes of the abnormal ridge accompanying the 2013–2014 California drought: ENSO precursor and anthropogenic warming footprint. *Geophys. Res. Lett.* **41**, 3220–3226 (2014).
31. Swain, D. L. et al. Remote linkages to anomalous winter atmospheric ridging over the northeastern Pacific. *J. Geophys. Res. Atmos.* **122**, 12194–12209 (2017).
32. Angélil, O. et al. An independent assessment of anthropogenic attribution statements for recent extreme temperature and rainfall events. *J. Clim.* **30**, 5–16 (2017).
33. IPCC *Climate Change 2013: The Physical Science Basis* (eds Stocker, T. F. et al.) (Cambridge Univ. Press, 2013).
34. Kay, J. E. et al. The Community Earth System Model (CESM) Large Ensemble project: a community resource for studying climate change in the presence of internal climate variability. *Bull. Am. Meteorol. Soc.* **96**, 1333–1349 (2015).
35. Diffenbaugh, N. S. et al. Quantifying the influence of global warming on unprecedented extreme climate events. *Proc. Natl Acad. Sci. USA* **114**, 4881–4886 (2017).
36. Jakob, D. in *Extremes in a Changing Climate: Detection, Analysis and Uncertainty* (eds AghaKouchak, A., Easterling, D., Hsu, K., Schubert, S. & Sorooshian, S.) 363–417 (Springer, New York, 2013).
37. Ralph, F. M. et al. Flooding on California's Russian River: role of atmospheric rivers. *Geophys. Res. Lett.* **33**, L13801 (2006).
38. Engstrom, W. N. The California Storm of January 1862. *Quat. Res.* **46**, 141–148 (1996).
39. Porter, K. et al. *Overview of the ARkStorm Scenario* Report No. 2010-1312 (United States Geological Survey, 2011).
40. Wing, I. S., Rose, A. Z. & Wein, A. M. Economic consequence analysis of the ARkStorm scenario. *Nat. Hazards Rev.* **17**, A4015002 (2016).
41. Jones, C., Waliser, D. E., Lau, K. M. & Stern, W. Global occurrences of extreme precipitation and the Madden–Julian Oscillation: observations and predictability. *J. Clim.* **17**, 4575–4589 (2004).
42. Hoell, A. et al. Does El Niño intensity matter for California precipitation? *Geophys. Res. Lett.* **43**, 819–825 (2016).
43. Diffenbaugh, N. S. & Giorgi, F. Climate change hotspots in the CMIP5 global climate model ensemble. *Climatic Change* **114**, 813–822 (2012).
44. Teng, H. & Branstator, G. Causes of extreme ridges that induce California droughts. *J. Clim.* **30**, 1477–1492 (2016).
45. Trenberth, K. E., Dai, A., Rasmussen, R. M. & Parsons, D. B. The changing character of precipitation. *Bull. Am. Meteorol. Soc.* **84**, 1205–1217 (2003).
46. Cvijanovic, I. et al. Future loss of Arctic sea-ice cover could drive a substantial decrease in California's rainfall. *Nat. Commun.* **8**, 1947 (2017).
47. Lee, M.-Y., Hong, C.-C. & Hsu, H.-H. Compounding effects of warm sea surface temperature and reduced sea ice on the extreme circulation over the extratropical North Pacific and North America during the 2013–2014 boreal winter. *Geophys. Res. Lett.* **42**, 1612–1618 (2015).
48. Blackport, R. & Kushner, P. J. Isolating the atmospheric circulation response to Arctic sea ice loss in the coupled climate system. *J. Clim.* **30**, 2163–2185 (2017).

Acknowledgements

Our work was supported by a grant from the University of California, Los Angeles Sustainable LA Grand Challenge (D.L.S., J.D.N. and A.H.), by National Science Foundation grant AGS-1540518 (J.D.N. and B.L.) and by US Department of Energy Grant 201603457-04 (A.H.). The NatureNet Science Fellows Program provided funding to D.L.S. through a collaboration between The Nature Conservancy and the University of California, Los Angeles.

Author contributions

D.L.S., B.L., J.D.N, and A.H. conceived of the study and designed the analyses. D.L.S. and B.L. provided analysis tools and conducted the analyses. D.L.S. wrote the manuscript and B.L., J.D.N. and A.H. provided comments and feedback.

Competing interests

The authors declare no competing interests.

Additional information

Supplementary information is available for this paper at https://doi.org/10.1038/s41558-018-0140-y.

Reprints and permissions information is available at www.nature.com/reprints.

Correspondence and requests for materials should be addressed to D.L.S.

Publisher's note: Springer Nature remains neutral with regard to jurisdictional claims in published maps and institutional affiliations.

Methods

Datasets used in this study. The CESM-LENS is a large ensemble of fully coupled model simulations designed to explore multiple realizations of internal climate system variability on long timescales. We used precipitation output from an 1,800 year PIC run and 40 separate simulations of the twentieth century (20C; 1920–2005) and RCP8.5 (2005–2100) climate change scenario[49]. Each of the 40 20C + RCP8.5 realizations is generated using the same climate model but with slightly perturbed initial conditions, which yield different time sequences of daily- to decadal-scale internal variability[50]. Thus, CESM-LENS offers an opportunity to examine robust changes in extreme events across a wide range of simulated internal variability—a considerable advantage relative to other investigations that have historically been limited by the shortness of the observational record and the relative infrequency of extreme hydroclimatic events in smaller ensembles.

We also used precipitation output from climate model simulations generated as part of the CMIP5 project[49] for comparison with CESM-LENS simulations. We constructed a multi-model ensemble consisting of 78 realizations from 35 distinct climate models, where each distinct model receives equal weight in the ensemble mean and fields are interpolated to a common 2.5° grid.

We used the National Climatic Data Center's nClimDiv observational divisional dataset to determine the relative rank of historical precipitation events to estimate approximate return intervals (Supplementary Fig. 2). Existing biases between simulated and observed precipitation were implicitly accounted for using the methodology described below. Finally, we used gridded observational precipitation data to validate CESM-LENS precipitation (see section on Suitability of CESM-LENS for simulating California precipitation).

Quantifying changes in frequency of extreme hydroclimatic events. We seek to quantify changes in the frequency of extreme wet, dry and whiplash events in a manner that implicitly accounts for model biases and sidesteps parametric assumptions regarding the underlying shape of the precipitation distribution. In doing so, we focus on relative changes in the frequency of occurrence of events exceeding fixed thresholds defined using the PIC simulation. PIC atmospheric greenhouse gas concentrations are maintained at constant levels similar to those before the start of the Industrial Revolution (that is, year 1850 levels)—representing a counterfactual climate without human influence. We subsequently compare the relative change in frequency of specific events in the 20C + RCP8.5 simulations. The 20C forcing includes rising greenhouse gas and aerosol concentrations close to those observed in the historical record, and RCP8.5 forcing includes projected greenhouse gas increases between 2005 and 2100 based on a business-as-usual emissions trajectory[49]. We examine the RCP8.5 simulations as they most closely resemble the observed emissions trajectory to date[51], and they provide a larger signal-to-noise ratio for statistically rare extreme events[52].

We restrict our analysis of extremes to the months of November to March, representing the peak of the California rainy season[14]. While the seasonal peak of monthly precipitation occurs earlier in Northern California than in Southern California, extreme winter-like precipitation events associated with mid-latitude cyclonic activity can occur during any of these calendar months throughout the state. Thus, data for November–March are pooled to create a single, spatially explicit rainy season distribution of precipitation accumulations in each grid box.

Using direct observational (and indirect historical) records, we first estimate the approximate return interval for each event of interest. Our definition of return interval (R) is consistent with that widely used in the climate and civil engineering literature[36]: the likelihood of occurrence in any given year of an event with an n year return interval is $1/n$. Using this fixed return interval, we then calculate the precipitation value (p) in the CESM-LENS PIC simulation that occurs with frequency $1/n$ at each climate model grid box. In the 40-member ensemble, we then count exceedances of the specific return values and normalize the PIC and 20C + RCP8.5 runs on an events-per-year basis.

Once these counts are tabulated across all ensemble members and each season, we calculate percent changes in the frequency F of a given event at time t relative to the PIC period:

$$\Delta F_t = \frac{F_t - F_{\mathrm{PIC}}}{F_{\mathrm{PIC}}} \quad (1)$$

This approach is modelled after ref. [35] and references therein. We note that our use of a fixed return interval, rather than percentile values, allows us to directly compare precipitation extremes spanning timescales from monthly to multi-annual. For example: the 98th percentile of daily precipitation might be expected to occur several days per year, but the 98th percentile of annual precipitation might be expected to occur only twice per century.

Definition of precipitation whiplash. Given the potential for adverse human impacts of rapid transitions between dry and wet conditions in California (as occurred during 2016–2017), we formalize two precipitation whiplash metrics across a range of timescales. We define year-to-year (interannual) whiplash years to be those during which seasonal (November–March) precipitation accumulation meets or exceeds the PIC 80th percentile and which were immediately preceded by a year with seasonal precipitation at or below the PIC 20th percentile. We define within-season (intraseasonal) whiplash as the standard deviation of monthly precipitation within individual rainy seasons across the ensemble.

Selection of extreme events and climate model analogues. *2016–2017 (wet) analogue with 25 year return interval.* This threshold is based on the extremely wet 2016–2017 winter, during which record wet seasonal precipitation (return interval >100 years) occurred across portions of Northern California and relatively smaller positive anomalies occurred over Southern California (return interval ~10 years), yielding a mean statewide return interval of approximately 15–25 yr for November–March. Given the strong latitudinal gradient in relative abnormality of seasonal precipitation during this period—and the consequent variation in adverse societal impacts across the state—we use a 25 yr return interval as a compromise threshold.

1861–1862 (wet) analogue with 200 year return interval. This threshold is based on the extraordinary sequence of atmospheric river storm events that brought extremely severe and widespread flooding to much of California during the 1861–1862 winter. Much of what is known about the 'Great Flood of 1862' has been pieced together from informal historical accounts and newspaper records from the then-nascent State of California[38,52]. Such records suggest that the most intense period of nearly continuous precipitation occurred between late December 1861 and late January 1862 over an approximately 40 day period, yielding rainfall accumulations over 1 m in some locations[38]. While this event occurred before the advent of reliable meteorological observations in California, palaeoclimate evidence from sediment records in coastal river systems suggests that events comparable to the 1861–1862 flood are associated with an approximately 200 year return interval[53]. Given the substantial uncertainties regarding the exact duration, magnitude and recurrence interval of the 1861–1862 event, we define our analogue as the 40 day cumulative precipitation during all November–March periods with a return interval of 200 years in the PIC simulation. The magnitude of this event is larger than that envisioned in the 'ARkStorm' natural hazard contingency planning scenario jointly developed by the United States Geological Survey and the State of California[39] but smaller in magnitude compared with several other probable events in the past millennium[53].

Recent research has suggested that a modern recurrence of the 1861–1862 flood would probably have a catastrophic human and socioeconomic toll[39,40]. Thus, despite the fact that such an event remains unlikely in any given year even under strong greenhouse forcing, a multi-fold relative increase in physical event likelihood combined with a high degree of socioeconomic vulnerability collectively yield a substantial increase in the overall risk associated with such an event over a period of decades[54].

1976–1977 (dry) analogue with 100 year return interval. This threshold is based on the extremely dry conditions that occurred during winter 1976–1977, which was the driest such period in California's 122 year observational record. This short-lived but intense drought led to acute water shortages in regions dependent on surface runoff from smaller hydrological basins and without direct access to State Water Project or Central Valley Project reservoirs. We conservatively assume a 100 year return period for this single-year event analogue threshold.

2012–2016 (dry) analogue with 100 year return interval. This threshold is based on the multi-year drought that occurred in California between late 2012 and early 2016. A substantial fraction of overall drought magnitude and associated impacts can be attributed to extremely warm temperatures that coincided with the lack of precipitation during successive winters[28,29], and while 2013 was the driest calendar year on record in California[8], no individual November–March period was the drier than 1976–1977. Nevertheless, the driest consecutive 3 year period (and consecutive November–March seasons) on record in California did indeed occur between 2013 and 2016 (ref. [14]), and we use this 3-year threshold as a benchmark for a high-impact, multi-year drought. We emphasize that the widespread environmental impacts of this event were substantially exacerbated by record warm temperatures—which are expected to be a signature of future droughts in this region as the climate warms[28,55]. Consistent with the single-year dry event, we conservatively assume a 100 year return interval.

Quantification of statistical significance. All figures showing spatial changes (latitude–longitude and time–latitude maps) represent 30 year running means in the 20C + RCP8.5 simulations. In all significance assessments below, these 30 year mean changes in event frequency are compared with resampled (bootstrapped) time series from the PIC simulation. Confidence intervals represent climate change signals that fall outside the sampled range of PIC variability with 90% confidence, representing a high statistical bar given the very wide range of simulated internal variability that exists within CESM-LENS[50].

Change-in-frequency maps. To provide a robust measure of statistical significance for change-in-frequency maps (Figs. 1–4 and Supplementary Fig. 2), we used a bootstrap resampling approach. For seasonal extreme events (25 year wet events and 100 year dry events), we generated 10,000 random time series by selecting wet season precipitation totals from the full 1,800 year PIC run (with replacement).

The length of each time series corresponds to the return interval of the event itself: in this instance, either 25 or 100 years. Next, in each resampled time series, the number of exceedances of 25 or 100 year events was calculated and translated into a ratio relative to the full PIC count, producing a distribution of 10,000 bootstrapped ratio values at each grid point. Finally, these distributions were used to determine the rarity of the simulated ratios relative to internal variability in the PIC run. In all map plots, cross-hatching for wet (dry) events represent a value at or above (at or below) the 90th (10th) PIC percentile—signifying 90% confidence ($P<0.1$) that ratios fall outside of the PIC internal variability. In time series plots shown in Figs. 1–4, error bars represent two-thirds of the spread (±33.3%) of 40 ensemble members, and the average is calculated on a 30 year running mean basis to distinguish long-term trends from interannual variability.

We used a modified version of the bootstrap resampling approach described above for the 200 year event change-in-frequency map (Fig. 2 and Supplementary Fig. 2). Given the computational constraint of large-N resampling using this dataset, 100 resampled time series were constructed for this particularly extreme event (we confirm that $N=100$ is a sufficiently large sample size for estimates of precipitation values to stabilize). For each time series, 200 years were chosen at random (each of which contains a distribution of 40 day running sums of November–March precipitation). We note that temporal autocorrelation can become problematic when counting occurrences using 40 day running sums for high-magnitude events. To ensure that our frequency counts do not unintentionally count these extremes twice, our algorithm skips ahead by 40 days each time a 200-year-magnitude event is encountered. As for other extreme events, we calculated the ratio of event frequencies between the full PIC run and the bootstrapped time series at each grid point.

For change-in-frequency maps of seasonal whiplash events (Fig. 4a), 10,000 block bootstrapped time series were generated using randomly chosen segments of 100 consecutive years. This consecutive-year (block) approach is necessary because our whiplash definition depends on sequential dry-to-wet transitions; thus, to appropriately sample the internal variability, the underlying temporal sequence in the PIC simulation must be preserved.

For change-in-frequency maps of month-to-month precipitation variability (Supplementary Fig. 2c), P values are calculated using 10,000 bootstrapped 40 year time series of November–March PIC precipitation. In each bootstrap iteration, 40 years were selected at random and with replacement, and the standard deviation across 200 (40 × 5) November–March model months was calculated for comparison with the CESM-LENS 40-member ensemble. Distributions of these month-to-month variability measures were generated at each grid point and normalized by the full PIC run to represent ratios.

For time series plots referring to either Southern California or Northern California, we use a spatially smoothed mean value (defined as the average value within a 3×3 grid box cluster centred on the original CESM-LENS grid box closest to the actual latitude/longitude of Los Angeles and San Francisco, respectively).

Time–latitude plots. The bootstrapped time series discussed above are also used to calculate statistical significance for time–latitude plots. After these bootstrapped time series were generated, further calculations were completed using the average of three contiguous west-to-east-oriented grid boxes along the California coast at each relevant latitude. As before, P values <0.1 resulting from the significance test imply rejection of the null hypothesis that the ratios in the time–latitude plots are within the range of simulated internal variability in the PIC simulation. In the present case, rejection of the null hypothesis is interpreted to mean that the 20C + RCP8.5 distribution is statistically distinguishable from the 'climate without humans' control.

Analysis of large-scale atmospheric conditions linked to extremes. We created anomaly composite maps for 500 hPa geopotential heights (GPH; Fig. 6a,d) and column-integrated water vapour (Fig. 6c,f) for wet years (exceeding the 80th preindustrial percentile) and dry years (falling below the 20th percentile) in the LENS simulations during both the full 1,800 year PIC simulation and across the 40 ensemble members of the RCP8.5 simulation between 2081 and 2100 (yielding a sample size of 760 model years). To simplify visual comparison of the anomaly patterns (where spatial gradients determine the geostrophic wind field) a spatially constant component of the thermal dilation[5,14] of the atmosphere (Supplementary Fig. 8a) was removed by subtracting the field mean difference in GPH (RCP8.5 minus PIC for a broad region near California (20° N–60° N, 180° E–250° E) from all grid points before generating RCP8.5 anomaly fields (Fig. 6a,d). We also compare the difference in anomalies between the RCP8.5 and PIC for wet and dry years (Fig. 6b,c,e,f) to emphasize the relative similarity of the underlying atmospheric circulation features between these periods.

Suitability of CESM-LENS for simulating California precipitation. The majority of findings in this study were derived using a global climate model operating at relatively coarse spatial resolutions (nominally 1°, or ~100 km, for the CESM configuration in LENS[34]). Given the importance of fine-scale topography in influencing California precipitation extremes[6], the relative spatial coarseness of model data used in this study precludes quantitative estimates of future runoff volume and flood flows at the watershed scale. Indeed, we note that that a local minimum in the relative increase in wet extremes exists along the axis of maximum topographic slope in the CESM-LENS boundary conditions (Supplementary Fig. 9b), suggesting a possible nonlinearity in orographic precipitation scaling with warming (a possibility supported by recent high-resolution modelling experiments, for example, ref. [56]). In the present study, however, our focus on relative (rather than absolute) changes in the frequency of various precipitation extremes across broad regions implicitly accounts for possible simulated precipitation biases arising from coarse model resolution and other sources.

We reiterate that CESM-LENS, while state-of-the-art, is a single-model ensemble. Substantial intermodel differences do exist in the simulated atmospheric response to anthropogenic forcing[7], but we have chosen to focus on results using exclusively CESM-LENS data for two reasons. First, CESM-LENS includes 40 ensemble members over a 180 year simulation (1920–2100)—yielding a very large (7,200-model year) sample size, allowing us to directly examine very rare extreme events (such as the '200 year flood') without making assumptions about the character of the underlying statistical distribution. Combining this with the 1,800 year PIC simulation allows for evaluation of very rare events that would otherwise not be possible in the observational record or CMIP5 experiments. Recent evidence suggests that (1) CESM reproduces both the mean and variability of observed California precipitation with reasonable fidelity[9] (Supplementary Fig. 10), (2) the CESM-LENS single-model ensemble mean lies close to the median of the CMIP5 multi-model ensemble mean in the vicinity of California (Supplementary Fig. 6) and (3) CESM reproduces remote teleconnections (that is, those associated with ENSO) critical to California precipitation[57] (Supplementary Fig. 11).

To independently confirm that CESM-LENS is an appropriate tool for investigating changes in California precipitation, we compare simulated versus observed precipitation distributions for the 20C historical period for Northern and Southern California. We perform this validation using a gridded observational dataset (the Global Precipitation Climatology Project (GPCP) version 2.3[58]). To generate distributions for Northern and Southern California regions (depicted as white boxes in Supplementary Fig. 9), we sum November–March precipitation over land-only grid boxes with centroids that fall within a 200 km radius of San Francisco and Los Angeles, respectively, during the 1980–2016 period of mutual overlap between the CESM-LENS 20C simulations and the GPCP dataset.

We find that despite slight positive bias in median seasonal precipitation (<5% for Southern California and +9% for Northern California), the overall shape of the CESM-LENS distribution for both regions is statistically indistinguishable from observations at the 5% level using a Kolgoromov–Smirnoff test (Supplementary Fig. 10). We note that the CESM-LENS distribution tends to have slightly longer tails than observations, but this is unsurprising given that the effective sample size of the historical simulation (1,440 model years) is much larger than for the observational dataset (40 years) and the range of distribution among the 40 realizations encompasses the GPCP data (see horizontal bars in Supplementary Fig. 10). As our overall methodology implicitly accounts for mean biases in precipitation, and our focus is on extreme events in the upper and lower the tails of the distribution, the outcome of this validation exercise strongly suggests CESM-LENS is capable of capturing both the median and underlying interannual variability of California hydroclimate.

Having confirmed these measures of fidelity of simulated California precipitation in CESM-LENS relative to observations, we assess whether the ensemble also captures the large-scale physical processes and teleconnections responsible for precipitation variability in this region. To test whether CESM-LENS plausibly reproduces the observed ENSO teleconnection, we perform linear regression of 500 hPa GPH on sea surface temperatures in the 'Nino3.4' region of the tropical eastern Pacific Ocean using data from both CESM-LENS and National Centers for Environmental Prediction/National Center for Atmospheric Research (NCEP/NCAR) R1[59]. The spatial pattern of the GPH teleconnection is substantially similar between CESM-LENS simulations and the R1 reanalysis (corroborating results previously shown in ref. [57]), and is characterized by a deepening of North Pacific low pressure and a more modest decrease in mid-tropospheric heights eastward over California and the southern tier of the United States (Supplementary Fig. 11a,b) during El Niño events. We further confirm that the mean position and magnitude of the cool-season (November–March) jetstream is close to that in observations (Supplementary Fig. 11b,c), though we also point out that even subtle biases could potentially lead to latitudinal shifts in the location of precipitation extreme changes discussed here (an issue that has been raised in previous work[60]). Finally, the large-scale atmospheric circulation patterns during California wet and dry years, respectively, exhibit similar spatial patterns and magnitudes to those observed during historical wet and dry years (Supplementary Fig. 12), especially in key regions near the US West Coast. Collectively, these results suggest that CESM-LENS is an appropriate tool for use in characterizing changes in regional precipitation extremes in the vicinity of California.

Code availability. The code used in the analyses described in this study is available from the corresponding author upon reasonable request.

Data availability. Precipitation data from the CESM-LENS simulations are available from the University Corporation for Atmospheric Research (http://www.

cesm.ucar.edu/projects/community-projects/LENS/data-sets.html). Precipitation data for California are available from the National Oceanic and Atmospheric Administration National Climatic Data Center (nClimDiv, www.ncdc.noaa.gov/monitoring-references/maps/us-climate-divisions.php) and National Oceanic and Atmospheric Administration Earth System Research Laboratory (NOAA ESRL) (GPCP, https://www.esrl.noaa.gov/psd/data/gridded/data.gpcp.html). CMIP5 ensemble data were obtained from Lawrence Livermore National Laboratory's Earth System Grid portal (https://esgf.llnl.gov) via the Royal Netherlands Meteorological Institute Climate Explorer (https://climexp.knmi.nl). Geopotential height and wind data from NCEP/NCAR R1 are available from NOAA ESRL (https://www.esrl.noaa.gov/psd/data/gridded/data.ncep.reanalysis.html) and additional composite data were created using the NOAA ESRL plotting tool (https://www.esrl.noaa.gov/psd/cgi-bin/data/composites/printpage.pl).

References

49. Taylor, K. E., Stouffer, R. J. & Meehl, G. A. An overview of CMIP5 and the experiment design. *Bull. Am. Meteorol. Soc.* **93**, 485–498 (2012).
50. Deser, C., Phillips, A. S., Alexander, M. A. & Smoliak, B. V. Projecting North American climate over the next 50 years: uncertainty due to internal variability. *J. Clim.* **27**, 2271–2296 (2014).
51. Fuss, S. et al. Betting on negative emissions. *Nat. Clim. Change* **4**, 850–853 (2014).
52. Dettinger, M.D. & Ingram, B.L. The coming megafloods. *Sci. Am.* **308**, 64–71 (2012).
53. Malamud-Roam, F. P., Lynn Ingram, B., Hughes, M. & Florsheim, J. L. Holocene paleoclimate records from a large California estuarine system and its watershed region: linking watershed climate and bay conditions. *Quat. Sci. Rev.* **25**, 1570–1598 (2006).
54. IPCC *Managing the Risks of Extreme Events and Disasters to Advance Climate Change Adaptation* (eds Field, C.B. et al.) (Cambridge Univ. Press, 2012).
55. Overpeck, J. T. The challenge of hot drought. *Nature* **503**, 350–351 (2013).
56. Sandvik, M. I., Sorteberg, A. & Rasmussen, R. Sensitivity of historical orographically enhanced extreme precipitation events to idealized temperature perturbations. *Clim. Dynam.* **50**, 143–157 (2018).
57. Allen, R. J. & Luptowitz, R. El Niño-like teleconnection increases California precipitation in response to warming. *Nat. Commun.* **8**, 16055 (2017).
58. Adler, R. F. et al. The Version-2 Global Precipitation Climatology Project (GPCP) monthly precipitation analysis (1979–present). *J. Hydrometeorol.* **4**, 1147–1167 (2003).
59. Kalnay, E. et al. The NCEP/NCAR 40-year reanalysis project. *Bull. Am. Meteorol. Soc.* **77**, 437–471 (1996).
60. Hagos, S. M., Leung, L. R., Yoon, J.-H., Lu, J. & Gao, Y. A projection of changes in landfalling atmospheric river frequency and extreme precipitation over western North America from the Large Ensemble CESM simulations. *Geophys. Res. Lett.* **43**, 1357–1363 (2016).

CLIMATOLOGY

Climate change is increasing the risk of a California megaflood

Xingying Huang[1]*† and Daniel L. Swain[2,3,4]*†

Despite the recent prevalence of severe drought, California faces a broadly underappreciated risk of severe floods. Here, we investigate the physical characteristics of "plausible worst case scenario" extreme storm sequences capable of giving rise to "megaflood" conditions using a combination of climate model data and high-resolution weather modeling. Using the data from the Community Earth System Model Large Ensemble, we find that climate change has already doubled the likelihood of an event capable of producing catastrophic flooding, but larger future increases are likely due to continued warming. We further find that runoff in the future extreme storm scenario is 200 to 400% greater than historical values in the Sierra Nevada because of increased precipitation rates and decreased snow fraction. These findings have direct implications for flood and emergency management, as well as broader implications for hazard mitigation and climate adaptation activities.

INTRODUCTION

California is a region more accustomed to water scarcity than overabundance in the modern era. Between 2012 and 2021, California experienced two historically severe droughts—at least one of which was likely the most intense in the past millennium (*1*, *2*)—resulting in widespread agricultural, ecological, and wildfire-related impacts (*3*, *4*) and ongoing drought-focused public policy conversations. Yet, historical and paleoclimate evidence shows that California is also a region subject to episodic pluvials that substantially exceed any in the meteorological instrumental era (*5*)—potentially leading to underestimation of the risks associated with extreme (but infrequent) floods. Observed extreme precipitation and severe subregional flood events during the 20th century—including those in 1969, 1986, and 1997—hint at this latent potential, but despite their substantial societal impacts, none have rivaled (from a geophysical perspective) the benchmark "Great Flood of 1861–1862" (henceforth, GF1862). This event, which was characterized by weeks-long sequences of winter storms, produced widespread catastrophic flooding across virtually all of California's lowlands—transforming the interior Sacramento and San Joaquin valleys into a temporary but vast inland sea nearly 300 miles in length (*6*) and inundating much of the now densely populated coastal plain in present-day Los Angeles and Orange counties (*7*). Recent estimates suggest that floods equal to or greater in magnitude to those in 1862 occur five to seven times per millennium [i.e., a 1.0 to 0.5% annual likelihood or 100- to 200-year recurrence interval (RI)] (*5*, *8*).

The extraordinary impacts resulting from GF1862 provided motivation for a 2010 California statewide disaster scenario—known as "ARkStorm" (ARkStorm 1.0)—led by the U.S. Geological Survey in conjunction with a large, interdisciplinary team (*9*). The meteorological scenario underpinning the ARkStorm 1.0 exercise involved the synthetic concatenation of two nonconsecutive extreme storm events from the 20th century (*10*). Subsequent analysis suggested that such an event would likely produce widespread, catastrophic flooding and subsequently lead to the displacement of millions of people, the long-term closure of critical transportation corridors (*9*), and ultimately to nearly $1 trillion in overall economic losses (2022 dollars) (*11*).

Meanwhile, a growing body of research suggests that climate change is likely increasing the risk of extreme precipitation events along the Pacific coast of North America (*12*, *13*), including California (*14*–*16*), and of subsequent severe flood events (*17*, *18*). The primary physical mechanism responsible for this projected regional intensification of extreme precipitation is an increase in the strength of cool-season atmospheric river (AR) events (*19*–*21*). Previous analyses have suggested that the thermodynamically driven increase in atmospheric water vapor with warming is directly responsible for most of this projected AR intensification [e.g., (*16*)], with the remainder contributed by shifts in regional atmospheric circulation. There is also evidence that increased radiative forcing may result in an eastward shifted expression of atmospheric circulation anomalies associated with both the Madden-Julian Oscillation (*22*) and the El Niño–Southern Oscillation (ENSO)–forced component of the Pacific North American pattern (*23*)—both of which would increase the subseasonal variability of cool season precipitation over and near California. Compounding the increase in extreme precipitation associated with AR events are warming temperatures themselves (*24*)—which raise the mean elevation of snow accumulation in mountainous areas (*25*), increase instantaneous runoff rates as rain falls at the expense of snow (*18*), and raise the risk of "rain on snow" events (*26*). Collectively, these previous research findings motivate the question of whether climate change may substantially affect the odds of "low probability but high consequence" flood events.

Here, we describe the overall design and implementation of, as well as results from, "ARkStorm 2.0"—a new severe storm and flood scenario reimagined for the climate change era. Leveraging recent advances in atmospheric modeling by coupling a high-resolution weather model to a climate model large ensemble, we assess the meteorological characteristics of extreme storm sequences (henceforth referred to as "megastorm" events) as well as the subsequent extreme runoff and adverse hydrologic outcomes such meteorological conditions (henceforth, "megaflood" events) would produce under both present-day and warmer future climate regimes. This work builds

[1]Climate and Global Dynamics Laboratory, National Center for Atmospheric Research, Boulder, CO. USA. [2]Institute of the Environment and Sustainability, University of California, Los Angeles, Los Angeles, CA, USA. [3]Capacity Center for Climate and Weather Extremes, National Center for Atmospheric Research, Boulder, CO, USA [4]The Nature Conservancy of California, Sacramento, CA, USA.
*Corresponding author. Email: xyhuang@ucar.edu (X.H.); dlswain@ucla.edu (D.L.S.)
†These authors contributed equally to this work as co-first authors.

upon previous research by explicitly considering long-duration (30-day) storm sequences (rather than single-storm events) most relevant to flood hazard management and disaster preparedness, characterizing large-scale ocean and atmosphere conditions associated with such severe storm sequences, and assessing the likelihood of these events over a wide range of potential levels of global warming. We find that climate change has already increased the risk of a GF1862-like megaflood scenario in California, but that future climate warming will likely bring about even sharper risk increases.

RESULTS

Large-scale and regional climate conditions associated with megaflood scenarios

We design two separate megastorm scenarios capable of causing a megaflood in California—one drawn from the recent historical climate (circa 1996–2005; henceforth "ARkHist") and another from a hypothetical warmer future climate (2071–2080 in the "high warming" RCP8.5 emissions scenario; henceforth "ARkFuture"). Each scenario comprises a multiweek sequence of consecutive severe winter storm events similar to what is reported to have occurred during the peak of the GF1862 event. Specific events are selected by ranking the 30-day cumulative precipitation on a California statewide basis simulated by the 40-member Community Earth System Model Large Ensemble (CESM1-LENS) and subsequently choosing from among the top 3 ranked events in each climate era to dynamically downscale using a high-resolution weather model [the Weather Research and Forecasting (WRF) model v4.3]. Further details can be found in Materials and Methods.

We find that both ARkHist and ARkFuture events occur during simulated warm-phase ENSO (El Niño) years, although the El Niño event that co-occurs with ARkFuture is much stronger [Niño 3.4 sea surface temperature (SST) anomaly = +1.48 K] than that with ARkHist (+0.56 K). Both events have maximum SST anomalies located in the tropical central Pacific (Fig. 1, A and B), which would be consistent with so-called "central Pacific" or "Modoki" El Niño (*27*). Warm (positive)

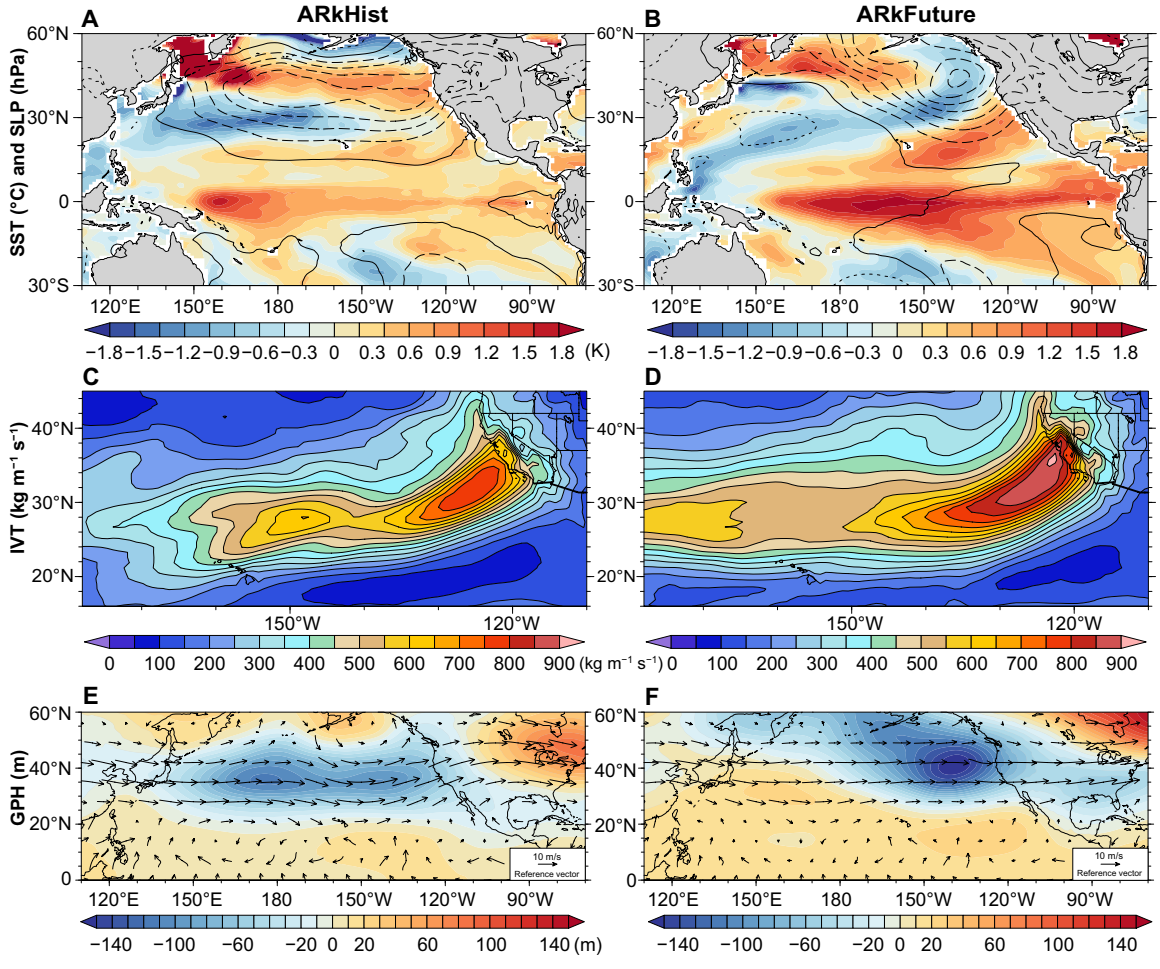

Fig. 1. Large-scale conditions during California megastorm scenarios. (**A** and **B**) Mean SST anomalies (color contours, K) and mean SLP (hPa) anomalies (dashed/solid contours) during ARkHist (A) and ARkFuture (B). SST and SLP are detrended before anomaly calculation using monthly data from each corresponding CESM1-LENS member (baseline period 1980 to 2005 for ARkHist; 2060–2090 for ARkFuture); solid (dashed) SLP contours denote positive (negative) anomalies in increments of 2 hPa. (**C** and **D**) Composite instantaneous vertically IVT (kg m^{-1} s^{-1}) for all hours in which California mean precipitation exceeds 1.5-mm ARkHist (C) and ARkFuture (D) using WRF 81-km simulations. Mean 30-day 500-hPa geopotential height (GPH, detrended) anomalies (color contours, m) and mean absolute 850-hPa wind vectors (m/s) (black arrows) during ARkHist (**E**) and ARkFuture (**F**).

SST anomalies are also present in the western Bering Sea and Sea of Okhotsk, as well as along the immediate California coast, in both cases. In addition, a broad region of negative sea level pressure (SLP) anomalies is centered over the Gulf of Alaska and adjacent portions of western North America—consistent with traditional El Niño teleconnections—although the zone of negative SLP anomalies extends farther westward across the North Pacific in ARkHist.

We acknowledge, however, that these large-scale patterns and associations with ENSO are drawn from only two individual scenario instances, and we cannot determine from this analysis alone whether these relationships are robust across a wider range of potential megastorm events. To offer a more systematic assessment, we consider the top 4 ranked 30-day California precipitation events in the CESM1-LENS historical and warmer future snapshot periods (fig. S1). We find that all eight such events are associated with anomalously warm conditions in the tropical Pacific Ocean, and Niño 3.4 SST anomalies are uniformly positive (+0.33, +0.56, +2.28, and + 1.56 K for the top 4 historical events and + 1.17, +1.95, +1.48, and + 1.39 K for future events, respectively, using detrended SST). However, it has recently been demonstrated that dynamic ENSO indices can better capture the spatial diversity of ENSO events and their subsequent western U.S. hydroclimate teleconnections (*28*). We thus calculate the ENSO Longitude Index (ELI)—an ENSO metric that tracks the average longitudinal position of ENSO-associated deep convection and accounts for the nonlinear response of convective activity to SST (*29*). As with Nino 3.4 SST anomalies, all eight such events are again associated with anomalously warm conditions in the tropical Pacific Ocean, but ELI values more clearly illustrate a wider range of ENSO spatial variability and dynamical intensity (ELI = 169.9°E, 171.6°E, 185.1°E, and 181.5°E for the top 4 historical events and ELI = 174.2°E, 181.0°E, 176.8°E, and 179.1°E for future events, respectively, using detrended SST).

Using the ELI categorizations defined in (*29*), this suggests that two of four events each in the historical and future simulations occur under "strong El Niño" conditions (ELI $\geq$ 179°E), and one of four historical and two of four future events occur under "moderate El Niño" conditions (170°E $\leq$ ELI < 179°E), with the final historical event falling nominally under the "moderate" threshold. Collectively, seven of eight historical and future potential California megastorm events occur under moderate or strong El Niño conditions as defined by the ELI (eight of eight, if rounding to the nearest degree of longitude). These findings strongly suggest that there is a substantially elevated likelihood of month-long storm sequences capable of producing very large precipitation accumulations during moderate to strong El Niño conditions and that the conspicuous anomalous deepening of the Gulf of Alaska low present in most of these eight events (fig. S3) is plausibly linked to El Niño teleconnections [which would be consistent with (*28*)].

Much previous work has focused on the critical role AR storms ("ARs") play in California hydroclimate—both as beneficial bolsterers of water supply and as the cause of hazardous floods (*30*–*32*). Composite analysis of 30-day averaged vertically integrated water vapor transport (IVT) and animations of IVT over the 30-day scenarios (movies S1 and S2) confirm that ARs are the primary storm mode during both ARkHist and ARkFuture (Fig. 1, C and D) scenarios, with a well-defined moisture transport axis extending northeastward from just north of the Hawaiian Islands to central California. This alignment is suggestive of 30-day mean storm trajectories capable of entraining large quantities of subtropical moisture (i.e., a "Pineapple Express"–type pattern), although with considerable upstream longitudinal extension of the IVT corridor westward of Hawaii (particularly in the future scenario; Fig. 1, C and D). This overall zonal pattern (but with localized meridional flow near California) is consistent with that recently associated with "AR families" occurring during El Niño conditions (*33*), which tend to be characterized by a strengthened subtropical Pacific jet stream and a persistently anomalous Gulf of Alaska cyclone that together favor long-duration periods of successive AR activity across California. While the general spatial structure of IVT is similar for both scenarios, ARkFuture exhibits mean 30-day composite IVT values that are ~25% higher than ARkHist.

Both severe storm sequences are associated with strong westerly (zonal) winds throughout nearly the entire atmospheric column (fig. S4), with a pronounced vertical maximum of ~60 m/s located around jet stream level (200 to 250 hPa) between 30°N and 35°N. Zonal winds are stronger in ARkFuture, especially in the upper troposphere (by >10 m/s above ~400 hPa). Analysis of 500-hPa geopotential height fields (Fig. 1, E and F) indicates that both events are associated with a broad region of negative mid-tropospheric height anomalies over the North Pacific to the west of California, although the negative height anomaly is more localized to the northeastern Pacific in ARkFuture. This suggests that both ARkStorm scenarios are associated with a robust Pacific jet, which is dynamically consistent with the eastward extension of the wintertime Pacific jet associated with both El Niño (Fig. 1, A and B) [e.g., (*28*)] and climate change [e.g., (*34*)], although the 30-day mean low-level (850-hPa) flow pattern exhibits a slightly more zonal pattern (with less of a meridional component over the northeastern Pacific) in ARkFuture relative to ARkHist. Visual inspection of movies S1 and S2 further confirm that both 30-day scenario storm sequences are characterized by the occurrence of multiple deep extratropical cyclones just west of or over California, which is consistent with recent results in (*35*), which found that AR-associated precipitation in the San Francisco Bay Area increased more for ARs directly associated with extratropical cyclones than those without.

We also find that composite atmospheric instability is relatively high during both ARkStorm scenarios. A 30-day composite convective available potential energy (CAPE) exhibits a broad region of >300 J/kg west of the northern California coast during ARkHist, with an even wider region of CAPE (>300 J/kg) (and locally >400 J/kg) in ARkFuture (fig. S5). The values might be unremarkable in a different geographic context, but in coastal California, ARs are typically associated with primarily stratiform or dynamically forced precipitation, and California ARs tend to be characterized by moist-neutral (versus conditional unstable) vertical profiles (*36*). Modest increases in atmospheric instability have been associated with outsized impacts during certain historical California storm events, increasing the risk of flash flooding/debris flows (*37*) and severe wind gusts (*38*) (fig. S6).

Cumulative and extreme precipitation

In both ARkHist and ARkFuture, 30-day cumulative precipitation is extremely high. In ARkHist, we find broad regions exceeding 500 mm of cumulative precipitation, with widespread areas exceeding 1000 mm in the Sierra Nevada (SN) and more isolated pockets exceeding 1000 mm in the Coast Ranges, Transverse Ranges, and far southern end of the Cascade Range (domain maximum of ~2150 mm; Fig. 2A). In ARkFuture, spatial patterns of event total precipitation

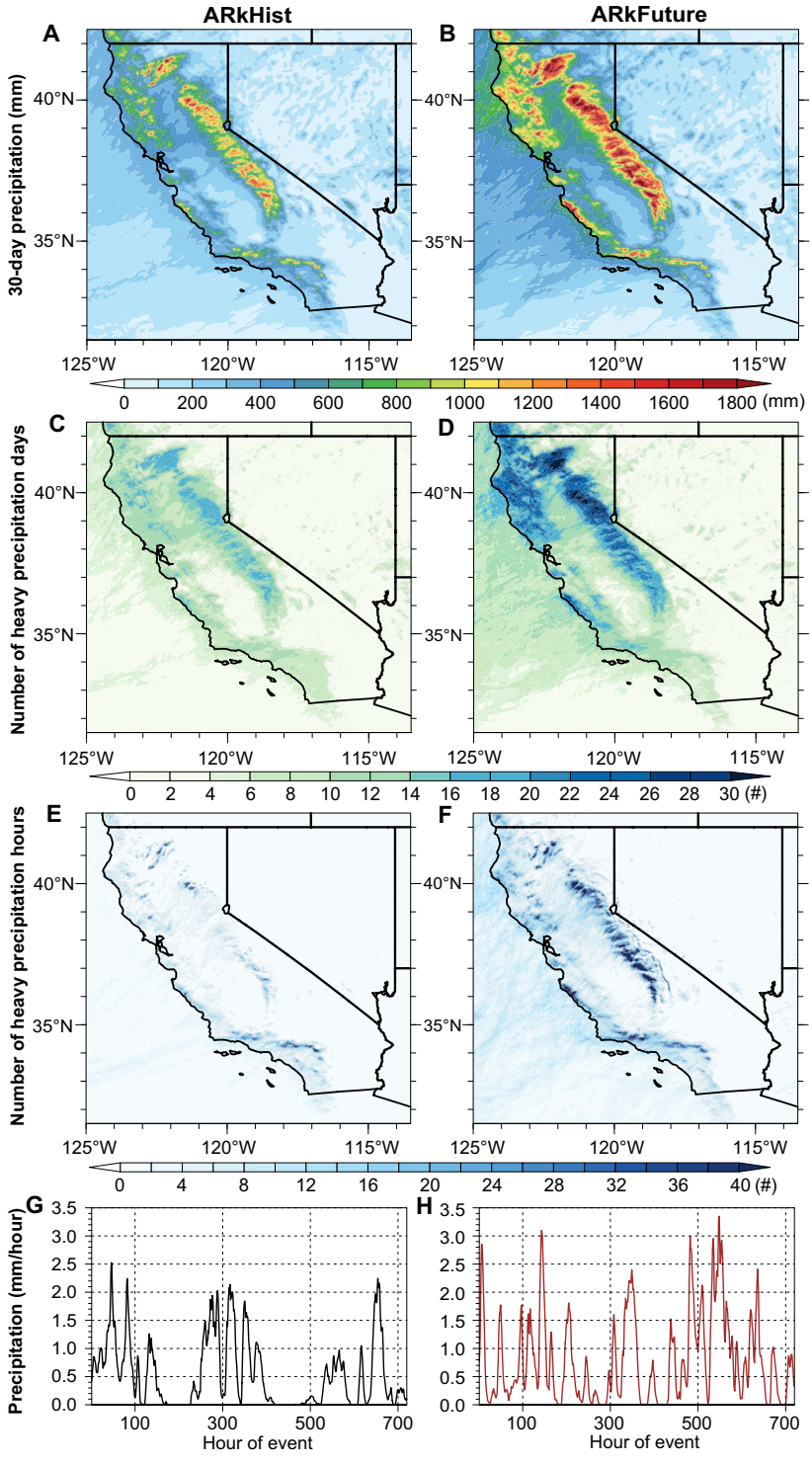

Fig. 2. Precipitation associated with California megastorm scenarios. (**A** and **B**) Cumulative 30-day precipitation (mm) during ARkHist (A) and ARkFuture (B). (**C** and **D**) Cumulative number of heavy precipitation days (days with precipitation > 20 mm/day) during ARkHist (C) and ARkFuture (D). (**E** and **F**) Cumulative number of heavy precipitation hours (hours with precipitation >10 mm/hour) during ARkHist (E) and ARkFuture (F). (**G** and **H**) Time series depicting hourly precipitation (mm/hour) on a cumulative California statewide basis during ARkHist (G) and ARkFuture (H). Data depicted in all panels are from the innermost 3-km WRF domain.

are similar but are uniformly characterized by heavier accumulations, with broad areas in both northern and southern California exceeding 700 mm and widespread areas in the abovementioned mountain areas above 1400 mm (domain maximum of ~3200 mm; Fig. 2B). We note that these values are comparable to maximum precipitation informally reported during the GF1862, which exceeded 2500 mm in at least two locations on the SN western slope over a slightly longer (~40-day) period (*6*). In general, cumulative precipitation in ARkFuture is between 35 and 60% higher than in ARkHist for northern and central California (although locally >80% higher), with lesser increases in far southern California (fig. S7, A and B). On a statewide average basis, 30-day precipitation is ~45% higher in ARkFuture.

Although absolute increases in cumulative precipitation are highest in mountainous areas (fig. S7A), relative increases in event total precipitation are greatest in areas that are not prone to orographic enhancement of precipitation during prevailing southwesterly winds (fig. S7B). Thus, some of the largest relative increases in precipitation (locally >80%) instead occur in regions that are less historically accustomed to receiving extreme precipitation during these events, such as inland valleys and otherwise wind-shadowed areas, which is consistent with earlier work (*16*).

Both ARkStorm scenarios are also notable for their very high precipitation intensities. We quantify this on several time scales, focusing on the frequency (over the 30-day scenario periods) with which precipitation intensity exceeds fixed daily and hourly thresholds [the number of days with precipitation > 20 mm/day and the number of hours with precipitation > 10 mm/hour, henceforth "heavy precipitation days" (HPDs) and "heavy precipitation hours" (HPHs)]. In ARkHist, we find that nearly all coastal areas experience at least 8 (of 30) days with precipitation exceeding 20 mm, and most mountain areas exceed 14 such days (except the Transverse Ranges in southern California, Fig. 2C). In ARkFuture, we find a sharp increase in the number of HPDs, especially in northern and central California, where most coastal areas exceed 16 (of 30) HPDs and most mountain areas exceed 20 such days (Fig. 2D and fig. S7, C and D). In some small pockets in the northern SN and far southern Cascades, all 30 days of the ARkFuture scenario are HPDs. HPD increases are substantially smaller in magnitude across southern California (mostly on the order of one to five additional days) but still nearly ubiquitous (fig. S7C).

Because of their particular relevance in the context of flash flood and debris flow risk (*39*), we specifically consider the occurrence of short-duration precipitation extremes in both ARkStorm scenarios. We find that the highest number of such hours occur in orographically favored areas, with the highest frequency of occurrence in the southern California Transverse Ranges and the Feather River watershed in the northern SN during ARkHist (Fig. 2, E and F). In ARkFuture, we report large and widespread increase in the occurrence of HPHs across essentially the entire domain. The largest increases [+25 to 40 cumulative hours (fig. S7, E and F)] occur broadly across the SN and (locally) in Santa Lucia Mountains—shifting the domain-wide maximum in HPH from southern to northern California. We find large relative increases (~200 to 300%) in the frequency of HPH and a large increase in the spatial extent of affected regions in ARkFuture. On a statewide average basis, we find that the frequency of HPH is ~220% higher in ARkFuture versus ARkHist (Fig. 2, G and H). Oakley *et al.* (*40*) conducted a literature review on published hourly rainfall rates in California and/or similar Mediterranean climate regions thought to be sufficient to trigger shallow landslides and debris flows in susceptible terrain, noting a range (5 to 20 mm/hour) that encompasses our HPH threshold (10 mm/hour) in the present study. These findings, therefore, likely have large implications from a flash flood and debris flow risk perspective.

California-wide average cumulative precipitation during the 30-day periods encompassing both extreme storm sequence scenarios represents a considerable fraction of the total annual [October-September water year (WY)] precipitation occurring during both ARkHist (~447 mm or 46% of the WY total) and ARkFuture (~586 mm, of 40% of the WY total). Compared to the climatological mean WY precipitation across all 40 ensemble members during the baseline periods (1996–2005 and 2071–2080, respectively); however, these events represent an even larger fraction of average annual precipitation—60% of WY precipitation in ARkHist and 71% of WY precipitation in ARkFuture. This also means that both the ARkHist and ARkFuture occur during anomalously wet WYs overall (32 and 77% wetter than the contemporaneous averages in ARkHist and ARkFuture, respectively). This would be dynamically consistent, from an ENSO teleconnection perspective, with the strong relationship between moderate to strong El Niño events (as characterized by the ELI) and anomalously wet cool-season conditions in California (*29*). It also has significant implications from a potential flood hazard perspective, as soil conditions are likely to be more saturated than average during anomalously wet WYs, likely amplifying runoff and further elevating the risk of flooding.

To systematically contextualize the precipitation-related results arising from these two specific downscaled extreme storm scenarios drawn from CESM1-LENS relative to all top-ranked 30-day precipitation events in multiple large ensembles—including the CanESM2, GFDL-CM3, and CSIRO-Mk3.6 ensembles [as described in (*41*)]. We conducted an intercomparison of these events during the historical and future study periods. We found that of the top 4 ranked megastorm events (as quantified by California-wide cumulative 30-day precipitation), all 16 events across the four single-model large ensembles have larger cumulative precipitation in the warmer future scenario versus their counterparts drawn from cooler historical climate snapshot period (fig. S1). We further show that hourly precipitation maxima are also higher in future versus historical megastorm events in all four large ensembles (fig. S2).

We also note that there are substantial differences across the large ensembles regarding the absolute magnitude of the 30-day precipitation associated with the top four ranked storm sequences, with CESM1-LENS exhibiting the largest precipitation accumulations (fig. S1). However, a direct comparison between these absolute precipitation values is not possible in this context because of the widely differing number of ensemble members and potential and biases in the representation of extreme precipitation in specific models. Nevertheless, we emphasize that the overall consistency of the response of both 30-day cumulative and hourly precipitation in the warmer future versus cooler historical megastorms, in relative terms within each respective large ensemble, suggests that many of the key conclusions drawn from the two synthetic case studies drawn from CESM1-LENS and emphasized in this analysis are likely to be generalizable.

Precipitation phase, freezing level height, and snow water equivalent

The heaviest precipitation during both ARkStorm scenarios occurs over mountainous terrain—particularly in the SN—and a substantial fraction of that high elevation accumulation falls in the form of snow. In ARkHist, a substantial fraction of the higher elevation portions

of the SN receives more than 1000 mm (Fig. 3A) of snow water equivalent (SWE) over the 30-day event (yielding a domain maximum of 7.7 m of accumulated snowfall). Estimates of peak on-the-ground SWE range from around ~300 mm in the southern Sierra to 470 mm in the central Sierra (fig. S8), with even higher maxima over localized mountain peaks (Fig. 3). This extremely heavy snowfall would likely be highly disruptive to infrastructure and emergency response activities.

In ARkFuture, we find that the event-averaged precipitation phase changes from primarily snow to primarily rain at low to mid-elevations (~1200 to 2000 m) but remains primarily snow at very high elevations (≥2500 m) in the SN (Fig. 3, D and E). This results in a spatial dipole pattern of SWE changes, with large (>50%) SWE decreases at lower elevations but large SWE increases at the highest elevations (≥3000 m) of the SN and southern Cascades (locally >50%, yielding cumulative total SWE as high as 1800 mm and a domain maximum of 10.4 m of accumulated snowfall) (Fig. 3, B and C). Further, there is a stark contrast between the large SWE and snow-to-rain ratio decrease in the northern SN versus a substantial SWE increase and lesser snow-to-rain ratio decrease in the southern SN (Fig. 3F) (likely because of lower elevations in the northern Sierra). We report widespread increases in the mean atmospheric freezing level height during ARkFuture (statewide freezing level of ~2230 m for the 30-day window) versus ARkHist (freezing level of ~1940 m; Fig. 3, G and H)—supporting prior studies finding that warmer temperatures during future extreme storm events will fundamentally alter mountain hydrology and subsequent watershed response [e.g., (*18*) and (*25*)].

Very large increase in cumulative and peak runoff during ARkFuture

We find that both ARkStorm scenarios are likely to generate very high runoff across a wide range of watersheds and topographies. Projected increases in ARkFuture runoff, however, are widespread and extremely high in magnitude. On a statewide basis, peak runoff during ARkFuture is more than double that during ARkHist (Fig. 3, I and J). In certain key watersheds, however, the relative differences are even larger: In all three SN subregions, the peak runoff is 200 to 400% higher in ARkFuture (fig. S9). A ~100% increase in peak runoff is also observed in the South Coast and Cascade subregions, with a 60% increase along the North Coast.

Event total cumulative runoff increases are similarly large, with increases of 100% or more across most of the SN western slope, the southern Cascades, the Santa Lucias, and also in several major urban areas with a high impervious surface fraction (including the Los Angeles, Sacramento, and San Jose metropolitan areas; fig. S9B). Even greater fractional increases are found for extreme runoff periods (defined as hours with surface runoff of >10 mm/hour; fig. S9, C and D), which increase from being almost negligible in ARkHist (generally three or fewer total hours, except in the Los Angeles Basin) to being widespread across nearly all of California's major urban areas and mountain ranges (with many locations experiencing >10 such extreme runoff hours). In addition, we find that runoff efficiency during ARkFuture relative to ARkHist (measured as the ratio of total 30-day runoff to 30-day precipitation) increases by ~50% (from ~0.19 to ~0.29)—suggesting that a considerably higher fraction of precipitation is likely to immediately contribute to potential food risk in the warmer future scenario.

Given the geographic concentration of numerous critical pieces of water and flood management infrastructure on the western slopes of the SN Mountains and in California's Central Valley, we conduct additional analysis focused on the Sacramento and San Joaquin River watersheds that encompass these regions [as defined by their respective U.S. Geological Survey (USGS) Hydrologic Unit Code (HUC) footprints; fig. S10]. We find large and ubiquitous increases in the upper tail of the empirical distribution of both precipitation and surface runoff at both hourly and 24-hour temporal aggregations in ARkFuture relative to ARkHist, although the relative increases are larger for the San Joaquin basin than the Sacramento Basin (Fig. 4). Here, again, we find that the relative increases in the uppermost tail of the surface runoff distributions are much larger than that of the precipitation distributions. At the 24-hour aggregation level, the upper tail of the surface runoff distributions is largely nonoverlapping in both basins (Fig. 4, G and H)—with virtually no overlap at all in the San Joaquin basin during ARkFuture relative to ARkHist. This points to the potential for historically unprecedented surface runoff regimes during future extreme storms in a strong warming scenario—especially in the watersheds draining the western slopes of the central and southern SN, with major implications for operation of critical water infrastructure in these regions.

We attribute these notably high increases in runoff, which greatly exceed fractional increases in precipitation, to the nonlinear hydrologic effects of increasing both total precipitation (via increased AR intensity) and decreasing the snow-to-rain fraction (due to AR warming and the solid-to-liquid phase change of precipitation). This so-called "double whammy effect," whereby both the volume of precipitation falling on watersheds and the fraction of that precipitation that immediately becomes runoff at higher elevations increases substantially, can be responsible for unexpectedly large increases in runoff volume (*18*). We also suggest that there is arguably a "triple whammy" effect at play in the case of ARkFuture: In addition to the previous two factors, there is evidence for multiple intense "rain on snow" events (*26*) in both scenarios (Fig. 3, G and H) that correspond temporally with event-maximum runoff peaks (Fig. 3, I and J). However, we acknowledge that antecedent hydrologic conditions—particularly soil moisture and the extent/moisture content of snowpack leading up to the event—could potentially have large influences on simulated runoff and ultimately on potential flood risks. In this analysis, we only consider the specific antecedent conditions that were actually present in the respective large ensemble members leading up to the simulated events. Although a comprehensive assessment of the various antecedent hydrological contributors to surface runoff is beyond the scope of the present manuscript, more systematic assessments will be conducted in later stages of the ARkStorm 2.0 project.

Megaflood risk increases robustly as function of climate warming

We assess the cumulative and annual likelihood of a 30-day megastorm sequence capable of causing a California megaflood and find that both increase strongly as a function of climate warming. On a high warming emissions trajectory (RCP8.5), we find that the cumulative likelihood of an ARkHist level event begins to accelerate after the year ~2020 period, with corresponding accelerations becoming apparent earlier (~2000) for lesser (50-year RI) and later (~2030) for higher magnitude (200-year RI) events (Fig. 5A).

To accommodate the various Earth system and sociopolitical uncertainties that complicate future predictions of possible greenhouse gas emission trajectories and to facilitate direct comparison

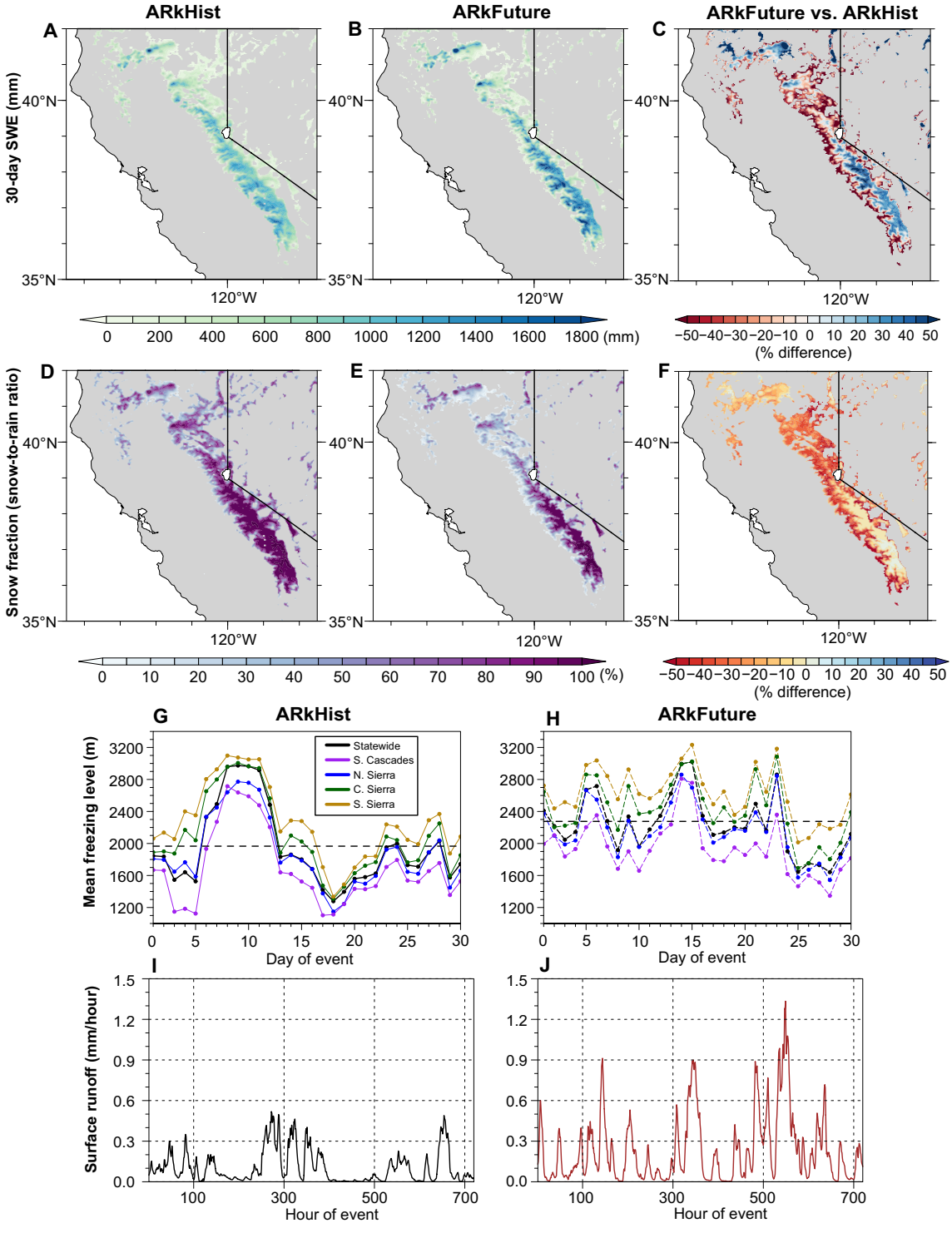

Fig. 3. Snowfall and surface runoff associated with California megastorm scenarios. (**A** and **B**) Cumulative 30-day gross SWE (mm) during ARkHist (A) and ARkFuture (B). (**C**) Difference in cumulative SWE (mm) between ARkFuture and ARkHist. (**D** and **E**) Mean snow fraction (snow-to-rain ratio, in percent) during ARkHist (D) and ARkFuture (E). (**F**) Difference (%) in mean snow fraction between ARkFuture and ARkHist. (**G** and **H**) Mean freezing level (m) during ARkHist (G) and ARkFuture (H). (**I** and **J**) Time series depicting hourly surface runoff (mm/hour) on a cumulative California statewide basis during ARkHist (I) and ARkFuture (J). Data depicted in all panels are from the innermost 3-km WRF domain.

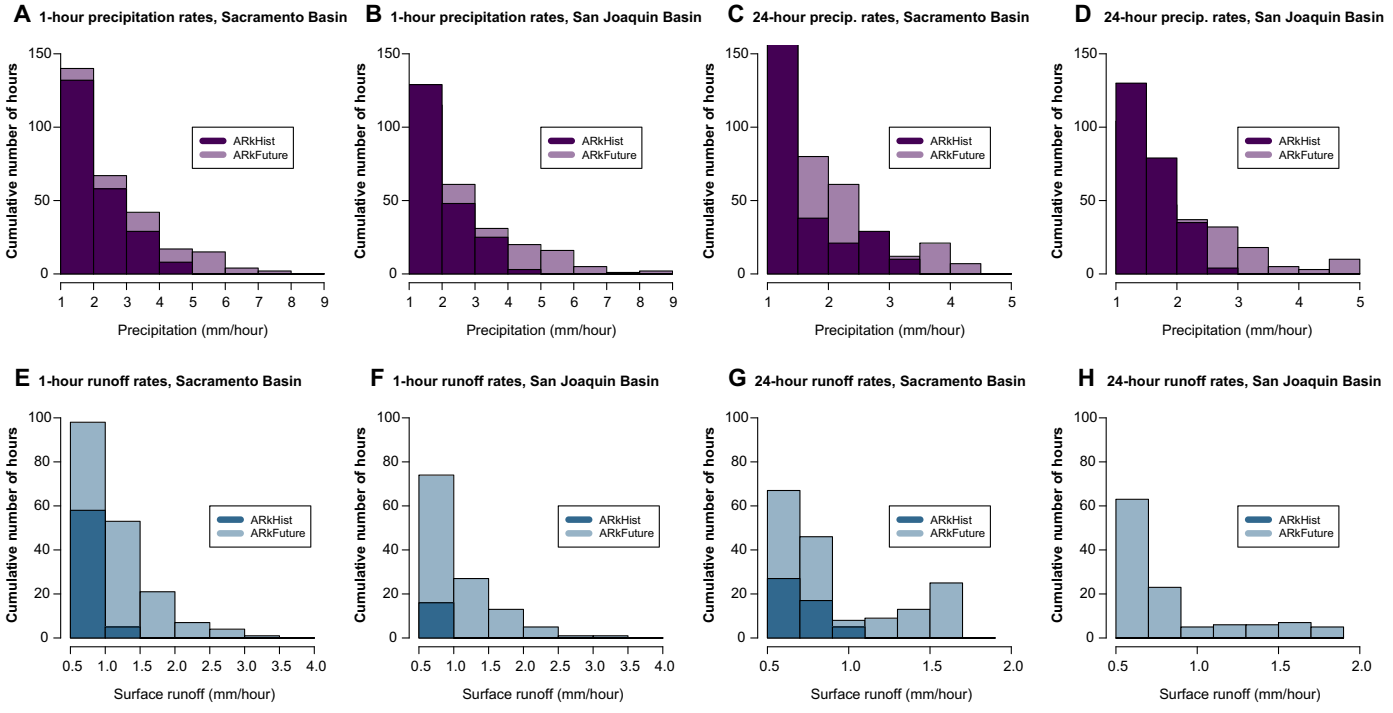

Fig. 4. Upper tail of precipitation and surface runoff distribution for Sacramento and San Joaquin River watersheds. Empirical histograms depicting the cumulative number of hours (over the 30-day scenarios) at or above specific precipitation [purple bars (**A** to **D**)] and surface runoff [blue bars (**E** to **H**)] thresholds (in units of mm/hour) at two levels of temporal aggregation (1 hour and 24 hours) for two key California watersheds as outlined by HUC Subregion 1802 (the Sacramento River watershed) and HUC subregion 1804 (the San Joaquin River watershed). Data are drawn from the WRF 3-km domain for ARkHist (darker bars) and ARkFuture (lighter bars) and are calculated as average values for each entire watershed. Values less than 1 mm/hour for precipitation and 0.5 mm/hour for surface runoff are excluded from this upper tail analysis.

with various proposed targets linked to specific planetary warming levels, we conduct further analysis to estimate changes in megastorm risk as a function of the warming itself. We find that the annual likelihood of an ARkHist level event increases rapidly for each 1°C of global warming [by ~0.012/year per degree C from a baseline of ~0.01/year]; Fig. 5B) and that this approximately linear relationship ($P < 0.001$) appears to hold even at very high levels of warming (~+4°C). We find that climate change to date (as of 2022) has already increased the annual likelihood of an ARkHist event by ~105% relative to 1920 in the CESM1-LENS ensemble and of an even higher magnitude (200-year RI) event by ~234%. This finding is consistent with prior work reporting progressively larger increases in projected extreme precipitation events for increasing event magnitudes [e.g., (*42*)]. We further find that by ~2060, on a high emissions trajectory, the annual likelihood of an ARkHist level event increases by ~374% and by ~683% for a formerly 200-year RI event. These statistics represent notably large increases in risk of California megastorm events due to climate change, as they transform an event that previously would have occurred once every two centuries into one that may occur approximately three times per century.

DISCUSSION

Our analyses suggest that the fundamental characteristics of the plausible worst-case California megafloods of the future will be familiar: Similar to their contemporary and historical counterparts, they will be characterized by a week-long sequences of recurrent, strong to extreme ARs during the cool season and coinciding with a persistently strong Pacific jet stream. Yet, we also find evidence of some critical differences: Future extreme storm sequences will bring more intense moisture transport and more overall precipitation, along with higher freezing levels and decreased snow-to-rain ratios that together yield runoff that is much higher than that during historical events. In addition, we find even larger increases in hourly rainfall rates during individual storm events, which have high potential to increase the severity of geophysical hazards such as flash flooding and debris flows. This is especially true in the vicinity of large or high-intensity wildfire burn areas, which are themselves increasing due to climate change (*39*) and yielding large increases in associated compound hazards (*43*).

An extensive body of existing research has linked climate change to increasingly extreme precipitation events [e.g., (*44*–*47*)], even in locations where changes in mean precipitation are nonrobust (*48*, *49*). There is further evidence that climate warming increases the intensity of ARs in many regions (*20*), including California (*16*, *19*). The strongest ARs are expected to strengthen considerably at the expense of the weakest—shifting the balance from "primarily beneficial" AR events to "primarily hazardous" ones (*21*)—an intensification brought about primarily via the direct thermodynamic effect of warming (*16*).

Our analysis goes beyond these prior works to demonstrate that climate change is robustly increasing both the frequency and magnitude of extremely severe storm sequences capable of causing megaflood events in California. Our analysis suggests that the present-day (circa 2022) likelihood of historically rare to unprecedented 30-day precipitation accumulations has already increased substantially and that even modest additional increments of global warming will

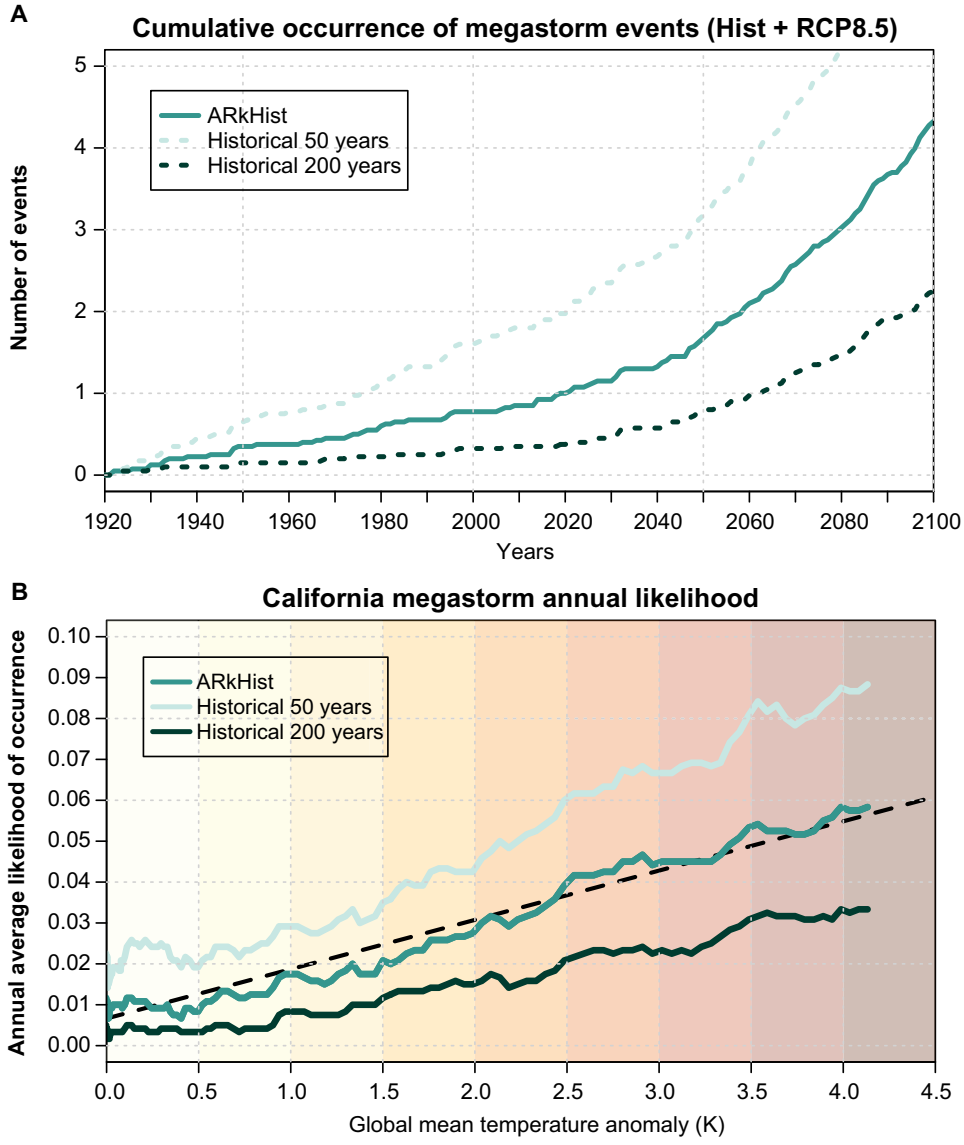

Fig. 5. Climate change and California megastorm risk. (**A**) Cumulative occurrence of extreme 30-day precipitation accumulations on a California statewide basis as simulated by the CESM1-LENS ensemble. The three blue-green curves denote cumulative occurrence of events equal or greater in magnitude to the ARkHist scenario, as well as for events with approximate RIs of 50 and 200 years. Data are drawn from the historical CESM1-LENS simulations for 1920–2005 and from the RCP8.5 scenario for 2006–2100. (**B**) Annual likelihood of extreme 30-day cumulative precipitation events as a function of projected global mean surface temperature (GMST; K) anomaly across the 40-member ensemble. Blue-green curves correspond to definitions in (A). GMST anomaly is defined relative to a baseline calculated from the CESM1-LENS preindustrial control run, and both annual likelihood and GMST are smoothed on a 30-year running mean basis.

bring about even larger increases in likelihood. Critically, this finding means that existing international emissions policies, which are estimated to yield cumulative warming of well over 2°C (*50*), will entail large further increases in the likelihood of a California megaflood event. We further find that all of the most intense 30-day megastorm events in the CESM1-LENS ensemble occur during moderate to strong ENSO warm phase (El Niño) conditions—both in the historical and warmer future scenarios—suggesting that these events may potentially exhibit some degree of predictability at seasonal scale. For these reasons, we emphasize that recognizing and mitigating the societal risks associated with this subtly but substantially escalating natural hazard is a critically important consideration from a climate adaptation perspective.

Recent evidence suggests that increases in western United States flood risk caused by anthropogenic warming may have been counteracted in recent decades by natural variability, but that further warming and shifts in natural variability will eventually "unmask" this accumulated increase in regional flood risk (*51*). Additional work suggests that the response of flood risk to climate change is likely to exhibit threshold behavior, at least in certain climatological and hydrological regimes (*52*), with a precipitation extremeness threshold dictating whether flood risk decreases (for smaller events, due to the antecedent soil aridification effect of warming temperatures) or increases (for the largest events, due to the overwhelming effect of large increases in precipitation intensity). Both of these considerations are especially germane to California—a region where most

contemporary public policy and climate adaptation efforts emphasize drought and wildfire risk due to lack of recent experience with widespread severe floods. Collectively, the findings from previous work and this study illustrate the growing urgency of planning for and mitigating the hazards from potentially catastrophic floods in California in a warming climate.

The extreme storm scenario development and subsequent analyses described here represent the first phase of the broader ARkStorm 2.0 exercise, which is eventually expected to encompass a full suite of follow-on hydrologic and inundation modeling, hazard assessments, and tabletop disaster response exercises. We plan to work with local, regional, and federal stakeholders to integrate quantification of physical hazards resulting from an "ARkStorm"-level event in California within disaster resilience and climate adaptation frameworks. Our initial atmospheric modeling results presented here demonstrate that extremely severe winter storm sequences once thought to be exceptionally rare events are likely to become much more common under essentially all plausible future climate trajectories—suggesting that 20th century hazard mapping, emergency response plans, and even physical infrastructure design standards may already be out of date in a warmer 21st century climate. Still, region-wide and high-resolution runoff inundation modeling capable of accounting for the effects of various active and passive flood management infrastructure will be required to fully quantify the extent of flood-related hazards and associated societal impacts resulting from these two ARkStorm 2.0 scenarios, and these simulations are actively being planned for the project's future phases.

Yet, potential solutions to increasing flood risk do exist. Examples of climate-aware strategies that have the potential to mitigate harm during a 21st century California megaflood include floodplain restoration and levee setbacks, which would lessen flood risk in urban areas while offering environmental cobenefits (*53*); forecast-informed reservoir operations, which would afford reservoir operators greater flexibility in the face of uncertainty (*54*); and revised emergency evacuation and contingency plans that accommodate the possibility of inundation and transportation disruption extending far beyond that which has occurred in the past century. Some of these interventions—such as flood-managed aquifer recharge—even have the potential to reduce flood damages while simultaneously improving resilience to future regional droughts (*55*). Ultimately, our hope is that the analysis described here can serve as a geographically portable framework for scenario-based emergency response and regional adaptation endeavors in the climate change era, both within and beyond California.

MATERIALS AND METHODS

Overall ARkStorm 2.0 scenario design

ARkStorm 2.0 is a wide-reaching extreme storm and flood scenario for California that seeks to build upon previous disaster contingency and emergency response planning efforts. This endeavor is intended to build upon previous efforts in the original ARkStorm exercise (ARkStorm 1.0), which was completed in 2010 (*9*) and involved a broad consortium of local, state, and federal agencies. It was found that the hypothetical storm scenario used in ARkStorm 1.0 would have produced widespread, deep inundation of a large fraction of the Sacramento and San Joaquin valley floors, as well as widespread, life-threatening flooding in other highly populated parts of California. Total economic losses (the sum of direct damages and indirect losses due to business and economic disruption) were projected to exceed $750 billion [2010 dollars (*11*)]. This would be equivalent to approximately $1 trillion in 2022 dollars, making it the most expensive geophysical disaster in global history to date. Partly for this reason, this hypothetical event was informally dubbed California's "other Big One:" Such a flood event in modern California would likely exceed the damages from a large magnitude earthquake by a considerable margin.

In ARkStorm 1.0, the scenario design involved the artificial concatenation of two of the most intense individual storm sequences in the observed 20th century climate [from January 1969 to February 1986; (*9*)], with additional manual adjustments to the persistence of individual ARs to amplify cumulative precipitation totals. Historical atmospheric reanalysis data were used to obtain boundary conditions for simulating these concatenated events using the Weather Research and Forecasting Model (v3.0.1) at spatial resolution ranging from 2 to 6 km across California. Precipitation and other variables from this single simulation were then used to estimate flood and other related impacts.

In ARkStorm 2.0, we update and upgrade the methods used in ARkStorm 1.0 in several fundamental ways. First, we use a hypothetical extreme event selection method that is both systematic and internally consistent from an atmospheric dynamical perspective: Rather than artificially concatenating multiple historical events, we leverage the large sample size afforded by large ensemble climate model simulations to draw upon a much wider range of physically plausible event sequences that are available by considering the roughly century-long observational record alone (and we make no manual adjustments to storm sequencing). Second, we use a newer and more sophisticated weather model (WRF V4.3) with generally higher spatial resolution (3 km across all of California and adjacent regions). Last and most critically, we design and implement two separate scenarios—ARkHist and ARkFuture—with the combined aim of comparing a "lesser" present era severe storm sequence to a much more intense but physically plausible future sequence amplified by climate change. The overall approach of embedding a high-resolution weather model within existing climate model large ensemble simulations is similar to that described in (*16*) and has the dual advantage of not only expanding the statistical sample size of physically plausible but observationally rare or unprecedented precipitation events (in CESM1-LENS) but also attaining the high degree of physical realism afforded by simulating extreme ARs in a high-resolution setting (*38*).

Selection of specific extreme storm sequences

Both ARkHist and ARkFuture are intended to capture multiweek sequences of discrete severe storm events that produce extremely high cumulative precipitation over a 30-day period. The use of a 30-day accumulation period is motivated by the desire to conduct a realistic emergency management contingency exercise as part of ARkStorm 2.0 and the prior knowledge that multiple successive storm events often challenge infrastructure and response systems to a greater degree than shorter-duration events. We first calculate the cumulative 30-day precipitation for the state of California from all 40 ensemble members from the CESM1-LENS (*56*) from two decade long "snapshot" intervals during which high-frequency (6 hourly) data are available for dynamical downscaling: 1996–2005 (using the historical scenario, which aims to replicate real-world aerosol and greenhouse gas climate forcings) and 2071–2080 (using the RCP8.5 scenario,

which assumes continued rapid growth of greenhouse gas emissions over the 21st century).

Among the available global climate model large ensemble datasets, CESM1-LENS stands out with its comprehensive suite of three-dimensional, high-frequency (6 hourly) atmospheric variables, which provide the forcing conditions required for dynamical downscaling simulations. We note that, while it might otherwise be desirable to sample from a wider time period than the two specific decades included in these snapshots, these are the only two such intervals for which a comprehensive suite of three-dimensional, high-temporal frequency (6 hourly) atmospheric conditions were retained in the original CESM1-LENS experiment, and so, it is not possible to conduct high-resolution WRF simulations during other intervals because of the unavailability of needed initial and boundary conditions. However, as the snapshot periods include data from 40 independent ensemble members initialized decades before the assessment period—each with their own sequences of internal variability—these snapshot periods nonetheless include a wide range of potentially relevant internal ocean-atmospheric oscillations.

We also note that although real-world greenhouse gas forcings are likely to be lower than assumed in the RCP8.5 scenario (*57*), this is the only scenario for which high-frequency data are available as part of the CESM1-LENS dataset (*56*). We further emphasize that although RCP8.5 is considered to be a high warming scenario, we explicitly intend to design a plausible "worst case scenario" storm and flood sequence in this analysis, and therefore, the use of a high-end emissions trajectory is appropriate.

We then rank all such 30-day cumulative precipitation events from each CESM1-LENS snapshot period, drawing from an effective sample size of 400-model years in each instance (10 years × 40 ensemble members). To ensure statistical independence of the dataset and that long-lasting events are not double counted, we require at least a 30-day separation between storm sequences. From among the top 3 ranked events in each period, we manually select a single 30-day storm sequence that exhibits large precipitation intensity peaks in both northern and southern California, as well as a pattern of 30-day cumulative precipitation that is spatially well distributed throughout both northern and southern portions of the state. This subjective aspect of the extreme event scenario selection process is critically important from the broader perspective of ARkStorm 2.0, which is designed to be a statewide exercise in which flood and emergency management capacity is severely tested. Therefore, we manually selected the respective ARkHist and ARkFuture events from among the top three ranked events such that each would bring a high level of impacts to the entire state rather than just a portion of the region. In so doing, we ultimately select the second ranked event for ARkHist (calendar date range: 9 February 2002 to 12 March 2002 in ensemble member #20) and the third ranked event for ARkFuture (calendar date range: 11 January 2072 to 11 February 2072 in ensemble member #2). Further analysis suggests that the selected ARkHist event has an approximate RI of ~85 years in the 1971–2020 era climate, and the ARkFuture event has an approximate RI of ~333 years in a 2051–2100 era high warming climate and is empirically unprecedented (i.e., a >400-year RI) in the 1971–2020 era climate (fig. S11).

LENS-WRF event-targeted downscaling approach

For each selected 30-day storm sequence, we use a high-resolution (3 km), nonhydrostatic regional weather model (WRF V4.3) embedded within initial and boundary conditions from CESM1 large ensemble (a framework known as "LENS-WRF") to perform dynamical downscaling as originally developed by (*16*). We use a full suite of three-dimensional atmospheric initial and boundary conditions from the high-frequency (6 hourly) temporal data available from the CESM1-LENS output files and conduct ~50-day long WRF simulations for each 30-day scenario event (allowing for ~1 week of model spin-up and ~1 week of event follow-up). Land surface initial and boundary conditions (including three-dimensional soil temperature, soil moisture, and snow depth) are drawn from the corresponding model member at monthly frequency (as this is the highest temporal resolution retained for three-dimensional land surface conditions in CESM1-LENS) such that they are spatiotemporally congruent with the atmospheric conditions.

In this analysis, we use a nonhydrostatic configuration of WRF-ARW (V4.3) including four nested domains with progressively finer spatial resolutions of 81, 27, 9, and 3 km (see fig. S12 for the detailed domain configuration). The outer three domains cover a large portion of the northeastern Pacific Ocean and the innermost 3-km domain also covers a broad oceanic region—as well as all of California and Nevada—to better represent near-coastal processes and sea-air interactions. WRF is configured using 44 vertical levels (with model top pressure at 50 hPa and vertical velocity damping turned on) and forced with time-varying SST (from CESM1-LENS). A higher density of vertical levels is prescribed near the surface to improve the representation of lower-level processes.

WRF physics parameterizations applied in these simulations include the Thompson graupel scheme (*58*), the Kain-Fritsch (new Eta) cumulus scheme (*59*) (for 81-, 27-, and 9-km domains only; cumulus parameterizations are turned off for the innermost 3-km domain), the Dudhia shortwave radiation scheme (*60*); the "rrtm" longwave radiation scheme (*61*), the Yonsei University (YSU) boundary layer scheme (*62*), the revised MM5 Monin-Obukhov surface layer scheme (*63*), and the Noah-multiple parameterization (MP) land surface model (*64*). The Noah-MP model includes a multilayer snowpack capable of liquid water storage and melt/refreeze cycles, direct representation of heat exchange due to phase changes, and a snow interception component allowing for canopy interception (*64*).

Model validation and fitness for purpose

The overall performance of both CESM (as implemented in CESM1-LENS) and WRF have been previously assessed and validated in the context of both mean and extreme cool season precipitation in California. Swain *et al.* (*14*) found that the simulated distribution of CESM1-LENS cool-season precipitation was statistically indistinguishable from observations during the recent historical period in both northern and southern California. In addition, Huang *et al.* (*38*) found that high-resolution (3 km), nonhydrostatic WRF simulations nested within boundary and initial conditions from atmospheric reanalysis (i.e., pseudo-observations) were capable of simulating real-world extreme AR events (including extreme IVT) and associated extreme precipitation—including spatial patterns of orographic enhancement. However, we acknowledge that this validation does not obviate the potential for parametric and/or structural uncertainties that could lead to model biases that are difficult to quantify (as it is not possible to directly validate large ensemble climate model representation of specific extreme events). Nonetheless, the LENS-WRF configuration used in the present analysis is capable of generating physically realistic extreme storm events and is an appropriate tool for use in the context of "plausible worst case" scenario development.

Contextualization of CESM1-LENS relative to other large ensembles

We conduct additional analysis using daily precipitation data from several other large single-model ensembles [the 50-member CanESM2 (Canadian Earth System Model, Second Generation) at ~2.8° × 2.8° horizontal resolution, 20-member GFDL-CM3 (Geophysical Fluid Dynamics Laboratory Coupled Model, Version 3) at 2.0° × 2.5° horizontal resolution, and 30-member CSIRO-Mk3.6 (Commonwealth Scientific and Industrial Research Organisation Model, Version 3) at ~1.875° × 1.875° horizontal resolution] to aid in contextualization of the study's primary focus on results driven by CESM1-LENS (40 members at 1° × 1° horizontal resolution). We note that CESM1-LENS has the highest horizontal resolution, by a wide margin, as well as the second largest number of ensemble members of these four large ensembles. To conduct as systematic an intercomparison as possible, we extract precipitation data for each of the top 4 ranked events in each ensemble and during each ARkHist and ARkFuture snapshot period. The results of this analysis are discussed in Results and can be visualized in figs. S1 and S2.

HUC region precipitation and runoff analysis

We select two "four-digit/subregional" HUC regions, as defined by the USGS, for more detailed analysis of regional precipitation and surface runoff during ARkHist and ARkFuture scenarios: HUC 1802 (Sacramento subregion, which includes the Sacramento River basin and Goose Lake watershed) and HUC 1804 (San Joaquin subregion, which includes the San Joaquin River basin; see fig. S10 for geographic outlines). We select these HUC regions, particularly, because they encompass most or all of the major SN western slope water storage and flood control reservoirs, as well as broad swaths of land in California's Central Valley that are highly susceptible to large-scale flooding and are home to numerous flood control structures. We extract precipitation and runoff data from the WRF 3-km domain at 1 hour frequencies from geographic regions delineated by the respective HUC subregion shapefiles made available via the USGS (at https://apps.nationalmap.gov/downloader). We then plot empirical histograms of the upper tail of the precipitation (all values above 1 mm/hour) and runoff (all values above 0.5 mm/hour) distributions for each selected HUC region temporally aggregated at two different durations (1 and 24 hours) in both historical and future scenarios (Fig. 4).

Public availability of ARkStorm 2.0 atmospheric simulation data

Boundary and initial condition input files (derived from CESM1-LENS) and output files from the WRF simulations are archived on the DesignSafe web platform (*65*) via DOI: 10.17603/ds2-mzgn-cy51 (*66*).

SUPPLEMENTARY MATERIALS

Supplementary material for this article is available at https://science.org/doi/10.1126/sciadv.abq0995

REFERENCES AND NOTES

1. D. Griffin, K. Anchukaitis, How unusual is the 2012–2014 California drought? *Geophys. Res. Lett.* **41**, 9017–9023 (2014).
2. S. Robeson, Revisiting the recent California drought as an extreme value. *Geophys. Res. Lett.* **42**, 6771–6779 (2015).
3. M. Goss, D. L. Swain, J. T. Abatzoglou, A. Sarhadi, C. A. Kolden, A. P. Williams, N. S. Diffenbaugh, Climate change is increasing the likelihood of extreme autumn wildfire conditions across California. *Environ. Res. Lett.* **15**, 094016 (2020).
4. D. J. McEvoy, D. W. Pierce, J. F. Kalansky, D. R. Cayan, J. T. Abatzoglou, Projected changes in reference evapotranspiration in California and Nevada: Implications for drought and wildland fire danger. *Earth's Future* **8**, e2020EF001736 (2020).
5. F. P. Malamud-Roam, B. Lynn Ingram, M. Hughes, J. L. Florsheim, Holocene paleoclimate records from a large California estuarine system and its watershed region: Linking watershed climate and bay conditions. *Quat. Sci. Rev.* **25**, 1570–1598 (2006).
6. J. Null, J. Hulbert, California washed away: The great flood of 1862. *Weatherwise* **60**, 26–30 (2007).
7. W. N. Engstrom, The California storm of January 1862. *Quatern. Res.* **46**, 141–148 (1996).
8. I. L. Hendy, L. Dunn, A. Schimmelmann, D. K. Pak, Resolving varve and radiocarbon chronology differences during the last 2000 years in the Santa Barbara Basin sedimentary record, California. *Quat. Int.* **310**, 155–168 (2013).
9. K. Porter, A. Wein, C. Alpers, A. Baez, P. Barnard, J. Carter, A. Corsi, J. Costner, D. Cox, T. Das, M. Dettinger, J. Done, C. Eadie, M. Eymann, J. Ferris, P. Gunturi, M. Hughes, R. Jarrett, L. Johnson, Hanh Dam Le-Griffin, D. Mitchell, S. Morman, P. Neiman, A. Olsen, S. Perry, G. Plumlee, M. Ralph, D. Reynolds, A. Rose, K. Schaefer, J. Serakos, W. Siembieda, J. Stock, D. Strong, I. S. Wing, A. Tang, P. Thomas, K. Topping, C. Wills, L. Jones, C. Scientist, D. Cox, *Overview of the ARkStorm scenario* (U.S. Geological Survey, 2011).
10. M. D. Dettinger, F. Martin Ralph, M. Hughes, T. Das, P. Neiman, D. Cox, G. Estes, D. Reynolds, R. Hartman, D. Cayan, L. Jones, Design and quantification of an extreme winter storm scenario for emergency preparedness and planning exercises in California. *Nat. Hazards* **60**, 1085–1111 (2012).
11. I. S. Wing, A. Z. Rose, A. M. Wein, Economic Consequence Analysis of the ARkStorm Scenario. *Nat. Hazards Rev.* **17**, A4015002 (2016).
12. K. E. Kunkel, North American trends in extreme precipitation. *Nat. Hazards* **29**, 291–305 (2003).
13. M. C. Kirchmeier-Young, X. Zhang, Human influence has intensified extreme precipitation in North America. *Proc. Natl. Acad. Sci.* **117**, 13308–13313 (2020).
14. D. L. Swain, B. Langenbrunner, J. D. Neelin, A. Hall, Increasing precipitation volatility in 21st-century California. *Nat. Clim. Chang.* **8**, 427–433 (2018).
15. L. Dong, L. R. Leung, J. Lu, Y. Gao, Contributions of extreme and non-extreme precipitation to California precipitation seasonality changes under warming. *Geophys. Res. Lett.* **46**, 13470–13478 (2019).
16. X. Huang, D. L. Swain, A. D. Hall, Future precipitation increase from very high resolution ensemble downscaling of extreme atmospheric river storms in California. *Sci. Adv.* **6**, eaba1323 (2020).
17. T. W. Corringham, F. M. Ralph, A. Gershunov, D. R. Cayan, C. A. Talbot, Atmospheric rivers drive flood damages in the western United States. *Sci. Adv.* **5**, eaax4631 (2019).
18. X. Huang, S. Stevenson, A. D. Hall, Future warming and intensification of precipitation extremes: A "double whammy" leading to increasing flood risk in California. *Geophys. Res. Lett.* **47**, e2020GL088679 (2020).
19. M. Dettinger, Climate change, atmospheric rivers, and floods in California - A multimodel analysis of storm frequency and magnitude changes. *J. Am. Water Resour. Assoc.* **47**, 514–523 (2011).
20. A. E. Payne, M. E. Demory, L. R. Leung, A. M. Ramos, C. A. Shields, J. J. Rutz, N. Siler, G. Villarini, A. Hall, F. M. Ralph, Responses and impacts of atmospheric rivers to climate change. *Nat. Rev. Earth Environ.* **1**, 143–157 (2020).
21. A. M. Rhoades, M. D. Risser, D. A. Stone, M. F. Wehner, A. D. Jones, Implications of warming on western United States landfalling atmospheric rivers and their flood damages. *Weather Clim. Extremes* **32**, 100326 (2021).
22. W. Zhou, D. Yang, S.-P. Xie, J. Ma, Amplified Madden-Julian oscillation impacts in the Pacific–North America region. *Nat. Clim. Chang.* **10**, 654–660 (2020).
23. Z.-Q. Zhou, S.-P. Xie, X.-T. Zheng, Q. Liu, H. Wang, Global warming–induced changes in El Niño teleconnections over the North Pacific and North America. *J. Climate* **27**, 9050–9064 (2014).
24. K. R. Gonzales, D. L. Swain, K. M. Nardi, E. A. Barnes, N. S. Diffenbaugh, Recent warming of landfalling atmospheric rivers along the West Coast of the United States. *J. Geophys. Res. Atmos.* **124**, 6810–6826 (2019).
25. E. R. Siirila-Woodburn, A. M. Rhoades, B. J. Hatchett, L. S. Huning, J. Szinai, C. Tague, P. S. Nico, D. R. Feldman, A. D. Jones, W. D. Collins, L. Kaatz, A low-to-no snow future and its impacts on water resources in the western United States. *Nat. Rev. Earth Environ.* **2**, 800–819 (2021).
26. F. V. Davenport, J. E. Herrera-Estrada, M. Burke, N. S. Diffenbaugh, Flood size increases nonlinearly across the Western United States in response to lower snow-precipitation ratios. *Water Resources Res.* **56**, e2019WR025571 (2020).
27. M. B. Freund, B. J. Henley, D. J. Karoly, H. V. McGregor, N. J. Abram, D. Dommenget, Higher frequency of Central Pacific El Niño events in recent decades relative to past centuries. *Nat. Geosci.* **12**, 450–455 (2019).
28. C. M. Patricola, J. P. O'Brien, M. D. Risser, A. M. Rhoades, T. A. O'Brien, P. A. Ullrich, D. A. Stone, W. D. Collins, Maximizing ENSO as a source of western US hydroclimate predictability. *Climate Dynam.* **54**, 351–372 (2020).

29. I. N. Williams, C. M. Patricola, Diversity of ENSO events unified by convective threshold sea surface temperature: A nonlinear ENSO index. *Geophys. Res. Lett.* **45**, 9236–9244 (2018).
30. M. D. Dettinger, F. M. Ralph, T. Das, P. J. Neiman, D. R. Cayan, Atmospheric rivers, floods and the water resources of California. *Water* **3**, 445–478 (2011).
31. B. Guan, D. E. Waliser, F. M. Ralph, E. J. Fetzer, P. J. Neiman, Hydrometeorological characteristics of rain-on-snow events associated with atmospheric rivers. *Geophys. Res. Lett.* **43**, 2964–2973 (2016).
32. F. M. Ralph, J. J. Rutz, J. M. Cordeira, M. Dettinger, M. Anderson, D. Reynolds, L. J. Schick, C. Smallcomb, A scale to characterize the strength and impacts of atmospheric rivers. *Bull. Am. Meteorol. Soc.* **100**, 269–289 (2019).
33. M. A. Fish, J. M. Done, D. L. Swain, A. M. Wilson, A. C. Michaelis, P. B. Gibson, F. M. Ralph, Large-scale environments of successive atmospheric river events leading to compound precipitation extremes in California. *J. Climate* **35**, 1515–1536 (2022).
34. I. R. Simpson, T. A. Shaw, R. Seager, A diagnosis of the seasonally and longitudinally varying midlatitude circulation response to global warming. *J. Atmos. Sci.* **71**, 2489–2515 (2014).
35. C. M. Patricola, M. F. Wehner, E. Bercos-Hickey, F. V. Maciel, C. May, M. Mak, O. Yip, A. M. Roche, S. Leal, Future changes in extreme precipitation over the San Francisco Bay Area: Dependence on atmospheric river and extratropical cyclone events. *Weather Clim. Extremes* **36**, 100440 (2022).
36. D. Swain, B. Lebassi-Habtezion, N. Diffenbaugh, Evaluation of nonhydrostatic simulations of Northeast Pacific atmospheric rivers and comparison to in situ observations. *Mon. Weather Rev.* **143**, 3556–3569 (2015).
37. N. S. Oakley, J. T. Lancaster, M. L. Kaplan, F. M. Ralph, Synoptic conditions associated with cool season post-fire debris flows in the Transverse Ranges of southern California. *Nat. Hazards* **88**, 327–354 (2017).
38. X. Huang, D. L. Swain, D. B. Walton, S. Stevenson, A. D. Hall, Simulating and evaluating atmospheric river-induced precipitation extremes along the U.S. Pacific Coast: Case studies from 1980 to 2017. *J. Geophys. Res. Atmos.* **125**, e2019JD031554 (2020).
39. N. S. Oakley, A warming climate adds complexity to post-fire hydrologic hazard planning. *Earth's Future* **9**, e2021EF002149 (2021).
40. N. S. Oakley, J. T. Lancaster, B. J. Hatchett, J. Stock, F. M. Ralph, S. Roj, S. Lukashov, A 22-year climatology of cool season hourly precipitation thresholds conducive to shallow landslides in California. *Earth Interact.* **22**, 1–35 (2018).
41. C. Deser, F. Lehner, K. B. Rodgers, T. Ault, T. L. Delworth, P. N. DiNezio, A. Fiore, C. Frankignoul, J. C. Fyfe, D. E. Horton, J. E. Kay, R. Knutti, N. S. Lovenduski, J. Marotzke, K. A. McKinnon, S. Minobe, J. Randerson, J. A. Screen, I. R. Simpson, M. Ting, Insights from Earth system model initial-condition large ensembles and future prospects. *Nat. Clim. Chang.* **10**, 277–286 (2020).
42. D. L. Swain, O. E. J. Wing, P. D. Bates, J. M. Done, K. A. Johnson, D. R. Cameron, Increased flood exposure due to climate change and population growth in the United States. *Earth's Future* **8**, e2020EF001778 (2020).
43. D. Touma, S. Stevenson, D. L. Swain, D. Singh, D. A. Kalashnikov, X. Huang, Climate change increases risk of extreme rainfall following wildfire in the western United States. *Sci. Adv.* **8**, eabm0320 (2022).
44. P. A. Gorman, T. Schneider, The physical basis for increases in precipitation extremes in imulations of 21st-century climate change. *Proc. Natl. Acad. Sci.* **106**, 14773–14777 (2009).
45. M. G. Donat, A. L. Lowry, L. V. Alexander, P. A. O'Gorman, N. Maher, More extreme precipitation in the world's dry and wet regions. *Nat. Clim. Chang.* **6**, 508–513 (2016).
46. E. M. Fischer, R. Knutti, Observed heavy precipitation increase confirms theory and early models. *Nat. Clim. Chang.* **6**, 986–991 (2016).
47. S. Pfahl, P. A. O'Gorman, E. M. Fischer, Understanding the regional pattern of projected future changes in extreme precipitation. *Nat. Clim. Chang.* **7**, 423–427 (2017).
48. A. G. Pendergrass, R. Knutti, F. Lehner, C. Deser, B. M. Sanderson, Precipitation variability increases in a warmer climate. *Sci. Rep.* **7**, 17966 (2017).
49. C. W. Thackeray, A. M. DeAngelis, A. Hall, D. L. Swain, X. Qu, On the connection between global hydrologic sensitivity and regional wet extremes. *Geophys. Res. Lett.* **45**, 11,343–311,351 (2018).
50. Emissions Gap Report 2021: The heat is on—A world of climate promises not yet delivered (2021).
51. B. Bass, J. Norris, C. Thackeray, A. Hall, Natural variability has concealed increases in Western US flood hazard since the 1970s. *Geophys. Res. Lett.* **49**, e2021GL097706 (2022).
52. M. I. Brunner, D. L. Swain, R. R. Wood, F. Willkofer, J. M. Done, E. Gilleland, R. Ludwig, An extremeness threshold determines the regional response of floods to changes in rainfall extremes. *Commun. Earth Environ.* **2**, 173 (2021).
53. J. Opperman Jeffrey, G. E. Galloway, J. Fargione, J. F. Mount, B. D. Richter, S. Secchi, Sustainable floodplains through large-scale reconnection to rivers. *Science* **326**, 1487–1488 (2009).
54. C. J. Delaney, R. K. Hartman, J. Mendoza, M. Dettinger, L. D. Monache, J. Jasperse, F. M. Ralph, C. Talbot, J. Brown, D. Reynolds, S. Evett, Forecast informed reservoir operations using ensemble streamflow predictions for a multipurpose reservoir in Northern California. *Water Resour. Res.* **56**, e2019WR026604 (2020).
55. X. He, B. P. Bryant, T. Moran, K. J. Mach, Z. Wei, D. L. Freyberg, Climate-informed hydrologic modeling and policy typology to guide managed aquifer recharge. *Sci. Adv.* **7**, eabe6025 (2021).
56. J. E. Kay, C. Deser, A. Phillips, A. Mai, C. Hannay, G. Strand, J. M. Arblaster, S. C. Bates, G. Danabasoglu, J. Edwards, M. Holland, P. Kushner, J. F. Lamarque, D. Lawrence, K. Lindsay, A. Middleton, E. Munoz, R. Neale, K. Oleson, L. Polvani, M. Vertenstein, The Community Earth System Model (CESM) large ensemble project: A community resource for studying climate change in the presence of internal climate variability. *Bull. Am. Meteorol. Soc.* **96**, 1333–1349 (2015).
57. P. M. Forster, A. C. Maycock, C. M. McKenna, C. J. Smith, Latest climate models confirm need for urgent mitigation. *Nat. Clim. Chang.* **10**, 7–10 (2020).
58. G. Thompson, P. R. Field, R. M. Rasmussen, W. D. Hall, Explicit forecasts of winter precipitation using an improved bulk microphysics scheme. Part II: Implementation of a new snow parameterization. *Monthly Weather Rev.* **136**, 5095–5115 (2008).
59. J. S. Kain, The Kain-Fritsch convective parameterization: An update. *J. Appl. Meteorol.* **43**, 170–181 (2004).
60. J. Dudhia, Numerical study of convection observed during the winter monsoon experiment using a mesoscale two-dimensional model. *J. Atmos. Sci.* **46**, 3077–3107 (1989).
61. E. J. Mlawer, S. J. Taubman, P. D. Brown, M. J. Iacono, S. A. Clough, Radiative transfer for inhomogeneous atmospheres: RRTM, a validated correlated-k model for the longwave. *J. Geophys. Res. Atmos.* **102**, 16663–16682 (1997).
62. M. Nakanishi, H. Niino, An improved Mellor-Yamada level-3 model: Its numerical stability and application to a regional prediction of advection fog. *Bound.-Lay. Meteorol.* **119**, 397–407 (2006).
63. P. A. Jiménez, J. Dudhia, J. F. González-Rouco, J. Navarro, J. P. Montávez, E. García-Bustamante, A revised scheme for the WRF surface layer formulation. *Mon. Weather Rev.* **140**, 898–918 (2012).
64. G.-Y. Niu, Z. L. Yang, K. E. Mitchell, F. Chen, M. B. Ek, M. Barlage, A. Kumar, K. Manning, D. Niyogi, E. Rosero, M. Tewari, Y. Xia, The community Noah land surface model with multiparameterization options (Noah-MP): 1. Model description and evaluation with local-scale measurements. *J. Geophys. Res. Atmos.* **116**, D12109 (2011).
65. E. Rathje, C. Dawson, J. E. Padgett, J.-P. Pinelli, D. Stanzione, A. Adair, P. Arduino, S. J. Brandenberg, T. Cockerill, C. Dey, M. Esteva, F. L. Haan Jr, M. Hanlon, A. Kareem, L. Lowes, S. Mock, G. Mosqueda, *DesignSafe: A New Cyberinfrastructure for Natural Hazards Engineering* (ASCE Natural Hazards Review, 2017).
66. X. Huang, D. L. Swain, ARkStorm2.0: Atmospheric Simulations Depicting Extreme Storm Scenarios Capable of Producing a California Megaflood (DesignSafe-CI, 2022); https://doi.org/10.17603/ds2-mzgn-cy51.

Acknowledgments: We thank M. McCarthy, C. Albano, D. Cox, and M. Anderson for discussions that helped shape the initial storm scenario design. We also thank A. Gettelman and S. Stevenson for assistance in facilitating this work and underlying simulations. We acknowledge high-performance computing support from Cheyenne (doi: 10.5065/D6RX99HX) provided by NCAR's Computational and Information Systems Laboratory, sponsored by the National Science Foundation. **Funding:** This work was supported by the Yuba Water Agency grant (to X.H. and D.L.S.), the California Department of Water Resources grant (to X.H. and D.L.S.), and the National Science Foundation award #1854761 (to D.L.S.) and a joint collaboration between the Institute of the Environment and Sustainability at the University of California, Los Angeles; the Center for Climate and Weather Extremes at the National Center for Atmospheric Research; and the Nature Conservancy of California (to D.L.S.). **Author contributions:** Conceptualization: X.H. and D.L.S. Methodology: X.H. and D.L.S. Investigation: X.H. and D.L.S. Visualization: X.H. and D.L.S. Writing—original draft: D.L.S. and X.H. Writing—review and editing: X.H. and D.L.S. **Competing interests:** The authors declare that they have no competing interests. **Data and materials availability:** All data needed to evaluate the conclusions in the paper are present in the paper and/or the Supplementary Materials. Data from the parent CESM1-LENS simulations are publicly available via https://cesm.ucar.edu/projects/community-projects/LENS/data-sets.html. Data from the CSIRO, GFDL, and CanESM2 large ensembles are publicly available at the Multi-Model Large Ensemble Archive via https://cesm.ucar.edu/projects/community-projects/MMLEA. Source code for WRF 4.3 may be found at https://github.com/wrf-model/WRF. Specific forcing files from CESM1-LENS used in the WRF simulations, as well as WRF output and configuration files for the simulations described here and code used in the underlying analysis, are archived on the NSF DesignSafe platform at https://doi.org/10.17603/ds2-mzgn-cy51.

Submitted 17 March 2022
Accepted 28 June 2022
Published 12 August 2022
10.1126/sciadv.abq0995

ScienceAdvances

Climate change is increasing the risk of a California megaflood

Xingying Huang and Daniel L. Swain

Sci. Adv. **8** (31), eabq0995. DOI: 10.1126/sciadv.abq0995

CALIFORNIA'S FOURTH
CLIMATE CHANGE
ASSESSMENT

San Francisco Bay Area Region Report

Coordinating Agencies:

GOVERNOR'S OFFICE OF PLANNING AND RESEARCH · STATE OF CALIFORNIA ·

STATE OF CALIFORNIA ENERGY COMMISSION

CALIFORNIA natural resources AGENCY

Introduction to California's Fourth Climate Change Assessment

California is a global leader in using, investing in, and advancing research to set proactive climate change policy, and its Climate Change Assessments provide the scientific foundation for understanding climate-related vulnerability at the local scale and informing resilience actions. The Climate Change Assessments directly inform State policies, plans, programs, and guidance to promote effective and integrated action to safeguard California from climate change.

California's Fourth Climate Change Assessment (Fourth Assessment) advances actionable science that serves the growing needs of state and local-level decision-makers from a variety of sectors. This cutting-edge research initiative is comprised of a wide-ranging body of technical reports, including rigorous, comprehensive climate change scenarios at a scale suitable for illuminating regional vulnerabilities and localized adaptation strategies in California; datasets and tools that improve integration of observed and projected knowledge about climate change into decision-making; and recommendations and information to directly inform vulnerability assessments and adaptation strategies for California's energy sector, water resources and management, oceans and coasts, forests, wildfires, agriculture, biodiversity and habitat, and public health. In addition, these technical reports have been distilled into summary reports and a brochure, allowing the public and decision-makers to easily access relevant findings from the Fourth Assessment.

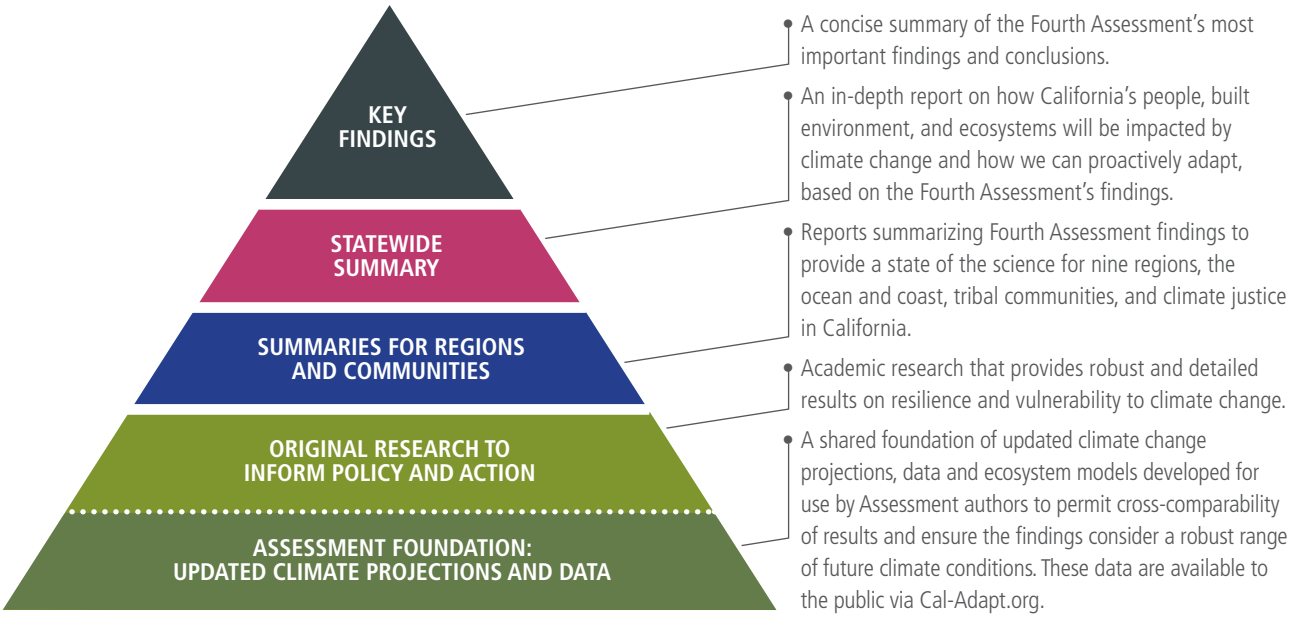

All research contributing to the Fourth Assessment was peer-reviewed to ensure scientific rigor as well as, where applicable, appropriate representation of the practitioners and stakeholders to whom each report applies.

For the full suite of Fourth Assessment research products, please visit: www.ClimateAssessment.ca.gov

San Francisco Bay Area Region

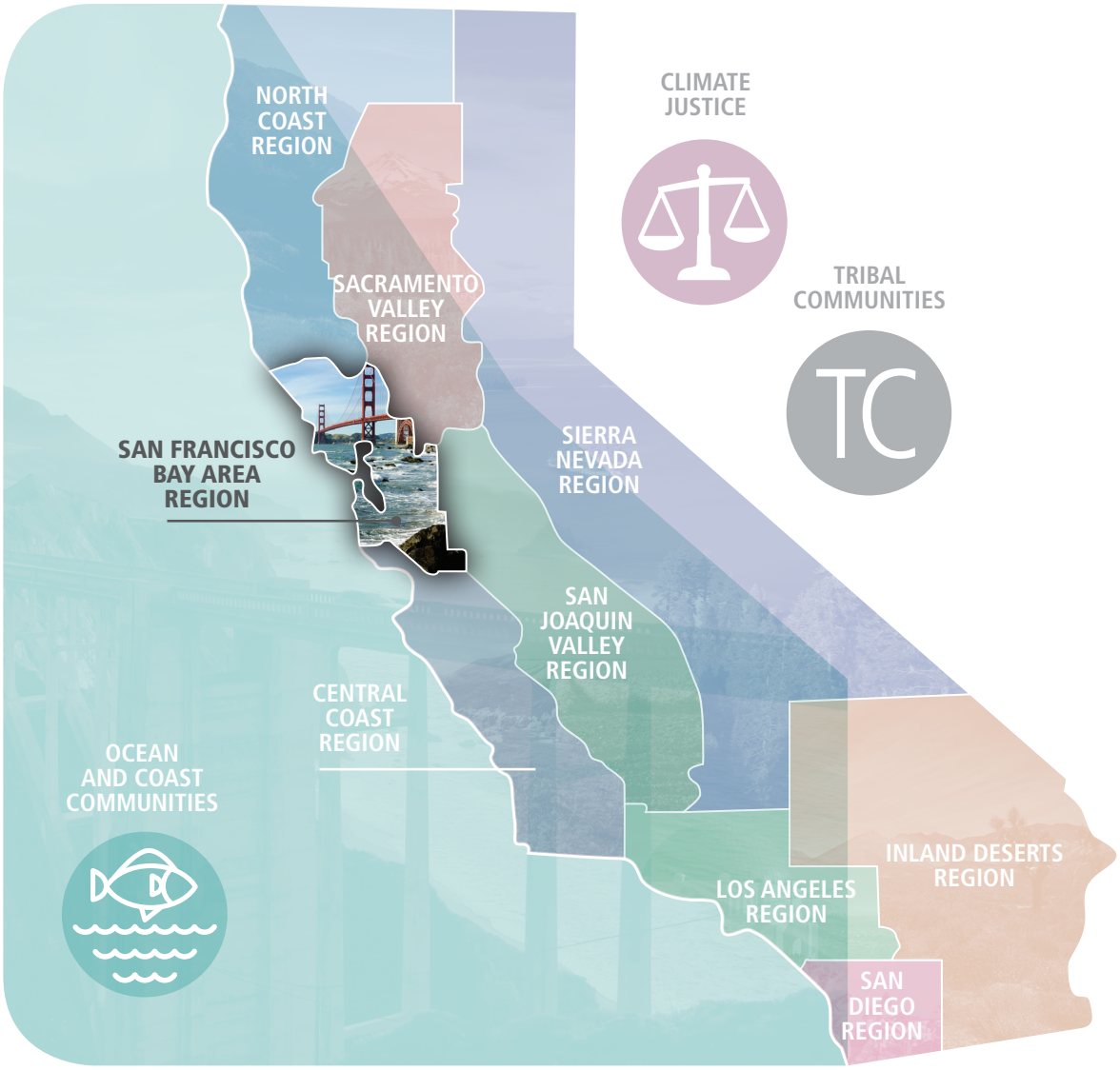

The San Francisco Bay Area Region Summary Report is part of a series of 12 assessments to support climate action by providing an overview of climate-related risks and adaptation strategies tailored to specific regions and themes. Produced as part of California's Fourth Climate Change Assessment as part of a pro bono initiative by leading climate experts, these summary reports translate the state of climate science into useful information for decision-makers and practitioners to catalyze action that will benefit regions, the ocean and coast, frontline communities, and tribal and indigenous communities.

The San Francisco Bay Area Region Summary Report presents an overview of climate science, specific strategies to adapt to climate impacts, and key research gaps needed to spur additional progress on safeguarding the San Francisco Bay Area Region from climate change.

San Francisco Bay Area Region Authors

COORDINATING LEAD AUTHOR

David Ackerly, *University of California, Berkeley*

LEAD AUTHORS

Andrew Jones, *Lawrence Berkeley National Laboratory*

Mark Stacey, *University of California, Berkeley*

Bruce Riordan, *University of California, Berkeley*

CONTRIBUTING AUTHORS

Patrick Barnard *USGS*

Steven Beissinger *UC Berkeley*

Gregory Biging *UC Berkeley*

Allison Brooks *Bay Area Regional Collaborative*

Emile Elias *USDA-ARS*

Letitia Grenier *Estuary Institute*

Bruce Herbold *Estuarine Ecology Consultant*

Lisa Micheli *Pepperwood Foundation*

Max Moritz *UC Berkeley*

Scott Moura *UC Berkeley*

Kara Nelson *UC Berkeley*

Mary Ann Piette *Lawrence Berkeley National Laboratory*

John Radke *UC Berkeley*

Alan Rhoades *Lawrence Berkeley National Laboratory*

Whendee Silver *UC Berkeley*

Kerri Steenwerth *USDA-ARS*

Jennifer Stokes-Draut *UC Berkeley*

Alicia Torregrosa *USGS*

Paul Waddell *UC Berkeley*

Michael Wehner *Lawrence Berkeley National Laboratory*

TECHNICAL EDITOR

Jack Chang *UC Berkeley*

STAKEHOLDER ADVISORY COMMITTEE

David Behar *San Francisco Public Utilities Commission*

Anne Crealock *Sonoma County Water Agency*

Kara Gross *Joint Venture Silicon Valley*

Andy Gunther *Bay Area Economic Climate Change Consortium*

Sandra Hamlat *East Bay Regional Parks*

Jay Jasperse *Sonoma County Water Agency*

Michael Kent *Contra Costa County*

Jack Liebster *Marin County*

Lindy Lowe *Port of San Francisco*

Sona Mohnot *The Greenlining Institute*

Tom Robinson *Bay Area Open Space Council*

Sam Veloz *Point Blue Conservation Science*

Doug Wallace *EBMUD*

CITATION: Ackerly, David, Andrew Jones, Mark Stacey, Bruce Riordan. (University of California, Berkeley). 2018. ***San Francisco Bay Area Summary Report.*** California's Fourth Climate Change Assessment. Publication number: CCCA4-SUM-2018-005.

Table of Contents

Highlights from the SF Bay Area Report

The San Francisco Bay Area spans nine counties and 100 cities and towns with a population of more than 7 million people and a $750 billion economy (~30% of California's total). The Mediterranean climate, with mild, wet winters and a warm, sun-drenched summer, supports extraordinary biological diversity and a thriving wine and dairy industry. This report examines the potential impacts of 21st century climate change on the physical climate, social systems and built environment, and natural and agricultural systems of the Bay Area. The geography of the region sets the stage for understanding how rising temperatures, changes in precipitation and fog, and rising sea levels will impact the region (section 1). We then examine projected impacts on social systems and infrastructure, from coastal flooding to wildfire and public health, with attention to the effects of social inequity on the vulnerability and resilience of local communities (section 2). Finally, we examine the impacts of climate change on biodiversity and open space conservation, and the effects on agriculture, with a focus on vineyards and rangelands (section 3). Where possible, we summarize proposed climate mitigation and adaptation strategies in a regional context to highlight potential actions and solutions necessary to meet these diverse challenges.

The impacts of climate change are already being felt in the San Francisco Bay Area and Northern California.

- Overall, the Bay Area's average annual maximum temperature increased by 1.7°F (0.95 °C) from 1950-2005.
- Several studies suggest that coastal fog along the California coast, so critical to our Bay Area climate, is less frequent than before.
- Sea level in the Bay Area has risen over 20 centimeters (8 inches) in the last 100 years.
- The powerful 2015-16 El Niño, one of the three largest in the historical record, resulted in winter wave energy that was over 50% larger than the typical winter in the Bay Area, driving unprecedented outer coast beach erosion.
- The 2012-2016 California drought led to the most severe moisture deficits in the last 1,200 years and a 1-in-500 year low in Sierra snowpack. The 2012-2016 record low snowpack resulted in $2.1 billion in economic losses and 21,000 jobs lost in the agricultural and recreational sectors statewide and exacerbated an ongoing trend of groundwater overdraft.

These changes are projected to increase significantly in the coming decades over the region.

- Even with substantial global efforts to reduce greenhouse gas emissions, the Bay Area will likely see a significant temperature increase by mid-century. By the end of the century, the difference between lower and higher global emissions scenarios will make a major difference in how much Bay Area temperatures rise.
- Precipitation in the Bay Area will continue to exhibit high year-to-year variability - "booms and busts" - with very wet and very dry years. The Bay Area's largest winter storms will likely become more intense, and potentially more damaging, in the coming decades. Under a high emissions scenario, average Sierra Nevada snowpack is projected to decline by nearly 20% in the next 2-3 decades, 30% to 60% in mid-century and by over 80% in late century.

- Future increases in temperature, regardless of whether total precipitation goes up or down, will likely cause longer and deeper California droughts, posing major problems for water supplies, natural ecosystems, and agriculture.
- California's Fourth Climate Change Assessment projects median sea level rise between 0.74 m (RCP 4.5) and 1.37 m (RCP8.5) for 2100 along the California coast. However, recent science studies, using advanced models and ice sheet observations, suggest the possibility of extensive loss from Antarctic ice sheets in the 21st century — possibly producing sea level rise by 2100 that could approach 3 meters.
- Even with high levels of emissions reductions, research now suggests that at least 2 meters of sea level rise is inevitable over the next several centuries due to the lag of sea level rise in response to increasing global temperatures.

Changes in temperature, precipitation, and sea level rise will produce substantial impacts on Bay Area social systems and the built environment.

- The three-way relationship between land use, transportation infrastructure, and energy systems — all of which are vulnerable to climate impacts — is perhaps the most critical interdependence in determining the future growth and prosperity of the Bay Area.
- Future land use decisions will significantly influence the Bay Area's efforts to address climate change, affecting building and transportation energy, urban water demand, and wildfire ignitions. For example, the critical lack of affordable housing in the core of the region is forcing households further south, north, and inland, with negative energy and environmental consequences. At the same time, building energy demand is higher in inland regions (warmer summers/cooler winters) so reducing Bay Area energy consumption will strongly depend on where new housing and business growth are located.
- Much of the Bay Area's transportation system — airports, roads, and railways — is concentrated along the bay where flooding from sea level rise and storm surge is a major vulnerability.
- The Bay Area electrical grid is vulnerable to power outages during wind and wildfire events while much of our natural gas transmission system is located along waterways and will be impacted by flooding from sea level rise and extreme storm events.
- Warmer summers will increase summer energy demand across the region, with the largest increase expected in coastal cities as air conditioning adoption grows there.
- Climate impacts — such as earlier melting of snowpack, increasing seawater intrusion into groundwater, increased rates of evapotranspiration, and levee failures or subsidence that contaminate Delta supplies — will affect both the quantity of water available and the quality of supplies.
- Wastewater treatment plants, historically located along bay shorelines where effluent discharge was convenient, are now highly vulnerable to future sea level rise. Rising bay water and groundwater levels will also increase salinity intrusion and subsurface flooding. Climate change will require improved stormwater management in the Bay Area as extreme storm events increase in size and frequency.
- Bay Area public health is threatened by a number of climate-related changes, including more extreme heat events, increased air pollution from ozone formation and wildfires, longer and more frequent droughts, and flooding from sea level rise and high-intensity rain events.

- High levels of socioeconomic inequity in the Bay Area create large differences in the ability of individuals to prepare for and recover from heat waves, floods, and wildfires. Financial resources as well as improved social structures are important to enhance community resilience and reduce these disparities.
- Heat waves pose increased health risks due to urban heat islands and lack of local experience and cooling infrastructure (air conditioning) in bayside cities. These risks are compounded for low-income communities.
- Natural infrastructure can play an important role in climate change adaptation, enhancing biodiversity and ecosystem services while reducing societal risks.
- While bayside communities are on the front lines for future flood risk, many may have limited ability or resources to pursue adaptation strategies. Without inclusive engagement among communities, disparities in economic and political power will undermine regional solutions and leave communities acting independently, with highly variable results for resilience and community health.

Climate change will produce substantial impacts on Bay Area natural and managed resource systems.

- The future climate of the Bay Area will become less suitable for evergreen forests — redwoods and Douglas fir — and more favorable for hot adapted vegetation such as chaparral shrub land.
- The ability of vegetation to respond to the rapidly changing conditions in the 21st century is poorly understood. It is possible that vegetation will be increasingly "out of sync" with climate and vulnerable to heat and drought.
- The most threatening effect of climate change to Bay Area wildlife is the impact of rising sea levels on wetlands because of the limited potential for wetlands to move inland and become established. At the same time, less rainfall, more summer heat, and increased drought will hurt amphibians and reptiles, while heat and wildfires may negatively affect upland birds, mammals, amphibians, and reptiles. Some wildlife species may need to shift locations as the vegetation they inhabit transforms with a changing climate.
- The Bay Area's mild climate and accessible open spaces are vital to the region's quality of life. Regional conservation efforts, including coordinated open space protection design and implementation of landscape corridors, climate-smart conservation, and restoration practices, will enhance success in a changing climate.
- In the Bay Area, future fire activity will be driven by both changes in urban development and in climate. Land use planning, together with fire-safe building standards and near-building vegetation management, are important strategies for managing future fire risk to people and structures.
- Forests can play an important role in carbon sequestration. Fuel and fire management will be critical, as fire is the primary source of carbon loss from forests. Recently, carbon loss from fires exceeded carbon uptake by vegetation in California.
- Nearly every aspect of Bay-Delta ecosystems will be affected by climate change as a result of rising sea levels, increases in air temperatures, changes in precipitation, changes in sediment supply and more. All natural areas of the shore will need to adapt or transform.

- The interruption of natural processes over the past 200 years as the region has developed has decreased natural Bay-Delta resiliency. A dynamic, resilient ecosystem has become a rigid landscape with brittle features that will have trouble adapting. New approaches that use natural shoreline infrastructure, like beaches, marshes, and mudflats, together with managed retreat where necessary, can create more resilient shorelines that respond well to changing conditions.
- Nearly 70% of California's existing area of wine production will be vulnerable under future climate change projections by mid-century. Wine grape production in the Bay Area could be vulnerable to extreme temperatures and temperature-related water scarcity.
- The sensitivity of Bay Area rangeland vegetation to precipitation dynamics makes these ecosystems particularly vulnerable to climate change. Changes in rainfall regimes are also likely to affect plant production and associated patterns in soil carbon and greenhouse gas production. Grazing and rangeland management practices can play a significant role in enhancing soil moisture and belowground carbon sequestration. Current research highlights the potential role of compost together with grazing on California pasturelands as a targeted strategy to increase carbon sequestration.

A growing number of Bay Area local governments, regional agencies, nonprofits, and private sector stakeholders are taking actions that advance climate adaptation and resilience.

- Projects include comprehensive vulnerability assessments, plans for infrastructure improvements, new governance structures, and actual on-the-ground projects to address sea level rise, drought and other climate impacts.
- Examples include Resilient by Design: Bay Area Challenge, the Sonoma County Regional Climate Authority, Adaptation to Rising Tides, the Bay Area Regional Reliability Project, Bay Area Regional Health Inequities Initiative (BARHII), San Francisco Climate & Health Profile, RISeR SF Bay, Marin County C-SMART, Sea Change San Mateo County, Climate Ready North Bay, and the San Francisco Bay Restoration Authority.

Introduction

The San Francisco Bay Area spans nine counties and 100 cities and towns with a population of more than 7 million people and a $750 billion economy (~30% of California's total). The Mediterranean-type climate, with mild, wet winters and a warm sun-drenched summer, supports extraordinary biological diversity and a thriving wine and dairy industry. The amenable climate is one factor that has drawn people from across the U.S. and all corners of the globe, contributing to the growth of the region's economy and the rise of Silicon Valley. San Francisco was the gateway to the Gold Rush, and that spirit of opportunity and innovation has permeated California culture and been reflected in continuing cycles of boom and bust. Economic growth has been accompanied by social inequity and accompanying disparities in health, education, and job opportunities. The current housing crisis has reflected that disparity with waves of displacement unfolding across the region.

FIGURE 1

The Bay Area, as defined for the Fourth Assessment. Note that the eastern half of Solano County is included in the Sacramento Valley report.

This report examines the potential impacts of 21st century climate change on the physical climate, social systems, and built environment, and natural and agricultural systems of the Bay Area. The geography of the region, adjacent to the cool Pacific Ocean and wrapped around San Francisco Bay, sets the stage to understand how rising temperatures, changes in precipitation and fog, and rising sea levels will impact the region. We then examine projected impacts on social systems and infrastructure, from coastal flooding to wildfire and public health, with attention to the effects of social inequity on the vulnerability and resilience of local communities. Lastly, we examine impacts of climate change on biodiversity and open space conservation, and the effects on agriculture, with a focus on vineyards and rangelands. Where possible, we summarize proposed climate mitigation and adaptation strategies in a regional context to highlight potential actions and solutions necessary to meet these diverse challenges.

Regional Climate Science

With its diverse microclimates, highly variable rainfall, dependency on snow-fed mountain water supply, extensive shorelines, and propensity for wildfire, it is not surprising that the physical climate of the Bay Area is changing in complex ways. This first section examines recent historical trends in temperature, precipitation, snowpack, extreme storms, drought, and sea level, as well as their projected changes over the course of the 21st century and key uncertainties, such as the changing role of fog in shaping microclimates.

Except where noted, the temperature and precipitation data we present are drawn from the downscaled daily products prepared for California's Fourth Climate Change Assessment by Pierce et al. (2018), using a statistical downscaling technique known as Localized Constructed Analogues (LOCA) (Pierce et al. 2014). Pierce et al. (2018) downscaled daily temperature and precipitation projections from 32 global climate models (GCMs) over California to a spatial resolution of 1/16° (around 6 kilometers, or 3.7 miles). The dataset includes observationally based historical data covering 1950-2005 that were used to train the statistical model, as well as historical downscaled data sets from the GCMs covering the same period. It also includes future projections spanning from 2006 to 2100 based on two greenhouse gas emissions scenarios - Representative Concentration Pathways (RCP) 4.5 and 8.5. RCP4.5 represents a mitigation scenario where global CO_2 emissions peak by 2040, while RCP8.5 represents a business-as-usual scenario where CO_2 emissions continue to rise throughout the 21st century (van Vuuren *et al.* 2011). A subset of 10 downscaled GCMs were shown to adequately sample changes across the entire ensemble of 32 models, and results from this 10-member ensemble are used for figures in this report. Public access to the downscaled data, along with mapping and other visualization tools, can be found at Cal-Adapt[1]. We also draw insight and data from a larger literature, including the National Climate Assessment and the IPCC 5th Assessment Report, to inform the confidence with which various aspects of the climate system are expected to change. These datasets are described in more detail where they are presented below.

Where applicable, we note key uncertainties and model limitations, as well as phenomena for which there is a high degree of confidence. Projection uncertainties can arise from a number of factors including the representation of physical processes in models, model resolution, and natural variability in the climate system. For instance, while theory suggests that storm tracks will shift northward as a result of climate change, the global climate model runs used to drive LOCA downscaled products do not show such a trend for North America (Collins *et al.* 2013) and are likely too coarse to detect any such changes less than 100 kilometers (about 60 miles) with confidence. Moreover, it is important to remember that the actual climate and weather experienced contains elements of both natural and human factors. For instance, annual mean precipitation in the Western U.S. is naturally highly variable, meaning that it is difficult to detect climate change-driven trends. On the other hand, there is high confidence that temperatures are rising and trends that are directly associated with temperature, such as decreased snowpack and more intense extreme precipitation events, can be characterized with greater confidence.

Methods for downscaling global climate models to finer spatial scales introduce an additional layer of uncertainty. Different downscaling procedures may, in general, produce different results due to biases in regional climate models or limitations of statistical assumptions. LOCA belongs to a class of statistical downscaling methods that use historic

1 www.cal-adapt.org

patterns as a basis to infer finer scale outcomes in space and time from Global Climate Models. However, future climate change might lead to dynamic changes in the local patterns of circulation that would not be captured by such statistical approaches. For instance, the observed trend of greater fog frequency over the ocean yet less frequency over land could be pointing to future changes in fog and sea breeze that would alter the temperature differential between the coast and inland areas. Such changes would not be captured in Global Climate Models (because they are too coarse) or in LOCA downscaling (because it is based on historic spatial patterns). Changes in fog and sea breeze in the Bay Area remain an active area of research as discussed in the fog section below.

Temperature

HIGHLIGHTS

- Overall, the Bay Area average annual maximum temperature increased by 1.7°F (0.95 °C) from 1950 to 2005.
- Even with substantial global efforts to reduce greenhouse gas emissions in the coming decades, the Bay Area will likely see a significant increase in temperature by mid-century.
- By the end of the century, the difference between lower and higher global emissions scenarios will make a major difference in how much Bay Area temperatures rise.
- While all parts of the Bay Area are projected to get warmer, inland areas will heat up more than coastal areas.
- Warming near the coast will be affected by changes in fog and sea breeze, but the influence of climate change on these highly localized features of the Bay Area climate is poorly understood at this time.

The Bay Area is characterized by a Mediterranean-type climate, defined by its cool, wet winters and warm, dry summers. Unique microclimates are created by regional topography, oceanic currents, fog exposure, and onshore winds (Cayan & Peterson 1993; Kottek *et al.* 2006). The combination of these processes acts like a natural air conditioner resulting in low interannual and daily temperature variability compared with much of California (O'Brien *et al.* 2013; Torregrosa *et al.* 2014, 2016). However, over the 20th century, some studies suggest that eastern Pacific summertime fog has declined substantially (Johnstone & Dawson 2010), and the influence of climate change on historical and future changes in fog prevalence remains an unresolved issue (see Fog section, below).

Regardless, increased surface temperatures have increased summertime cooling costs for residents of the Bay Area, especially at night when onshore winds diminish (Gershunov & Guirguis 2012). In addition, the built environment has played a role in shaping the local climatology of the San Francisco Bay Area, mainly through the effects of the urban heat island, which can be moderated by urban forestry and the cooling effects of irrigation in urban landscapes. For instance, landscape irrigation practices are estimated to reduce daytime summer temperatures across the urbanized portions of the Bay Area by an average of 1.8°F (1.0 °C) (Vahmani & Jones 2017).

Figure 2 highlights the annual average maximum surface temperature trend (annual average of the highest temperature on each day of the year) across the nine counties of the region produced from LOCA downscaling for California's Fourth Assessment (Pierce *et al.* 2018). Annual average maximum temperatures remained within the

relatively narrow range of 67.5°F to 71.9°F (19.7 °C to 22.2 °C) over the period 1950-2005, with an overall average maximum temperature of 69.5°F (20.1 °C). The estimated upward trend of 1.7°F (0.95 °C)in the Bay Area over this period is consistent with the global mean temperature change attributable to anthropogenic influences over a similar timeframe (Bindoff *et al.* 2013). By mid-century (2040-2069), the projected mean annual maximum temperature for the Bay Area, across multiple climate models, exceeds the maximum historical annual mean, regardless of which emissions trajectory is chosen. Thus, even with significant efforts to mitigate climate change (RCP4.5), the Bay Area will likely see annual mean warming on the order of approximately 3.3°F (1.8 °C) by mid-century. This increment increases to 4.4°F (2.4 °C) warming by mid-century under the high-emissions RCP8.5 scenario. The difference between emissions scenarios becomes more apparent by end of century (2070-2100), when the multi-model average shows warming on the order of 4.2°F (2.3 °C) for RCP4.5 and 7.2°F (4.0 °C) for the RCP8.5 scenario.

FIGURE 2

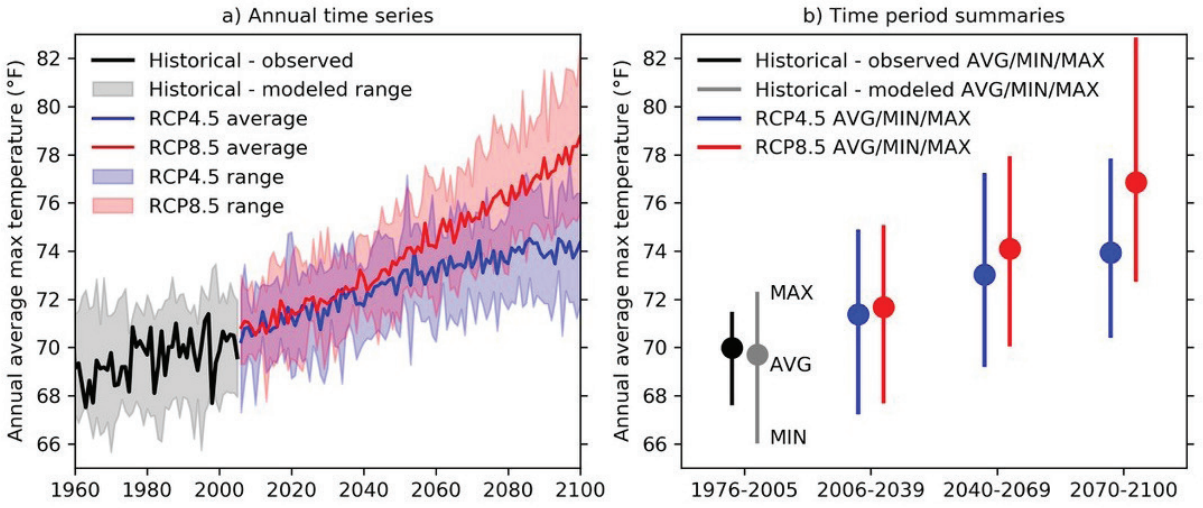

Observed historical (black), modeled historical (grey), and projected future (RCP4.5 - blue, RCP8.5 - red) annual average maximum temperature over the Bay Area. (a) Annual time series of data (future projections begin in 2006), with solid lines representing observed annual mean in the historical period and model-averages in the future. Shading represents the spread across models. (b) Summary of multi-year average (circles) and spread (vertical lines) across four time periods: 1975-2005 (historical), 2006-2039 (early-21st century), 2040-2069 (mid-21st century), and 2070-2100 (late-21st century). Note that the spread of values in panel b is smaller for the observed historical data compared to both the modeled historical data and modeled future data because the modeled quantities reflect model-to-model variability in addition to year-to-year variability, whereas the observed historical data only reflects year-to-year variability. Unit is °F.

Changes in annual mean maximum temperatures do not convey information about changes in heat extremes, which typically occur over the course of one to several days, nor do they convey spatial differences in the pattern of warming across the sub-regions and microclimates of the Bay Area. Figure 3 shows the spatial change in the annual mean of maximum daily temperatures across the nine counties under RCP4.5 and RCP8.5. Coastal cooling processes, such as fog and onshore winds, buffer some of the surface temperature increase in regions close to the coast and San Francisco Bay whereas regions further inland warm at a faster rate. However, as noted elsewhere in the report, the LOCA downscaling procedure does not explicitly account for potential changes in the characteristics of local phenomena such as fog and sea breeze. Thus, the maps shown in Figures 3 and 4 reflect an assumption that current fog and sea breeze patterns remain the same relative to larger scale temperature conditions in the future. The differential warming signal between the coast and inland areas is also apparent in Figure 4, which highlights the average change in the hottest day of the year. Under RCP8.5, the average hottest day of year is projected to increase by a minimum of 6.3°F (3.5 °C) near the coast up to 10°F (5.6 °C) further inland. Under RCP4.5, warming trends for the average hottest day of year reduce to 3.9°F (2.2 °C) near the coast up to 6.4°F (3.6 °C) further inland.

FIGURE 3

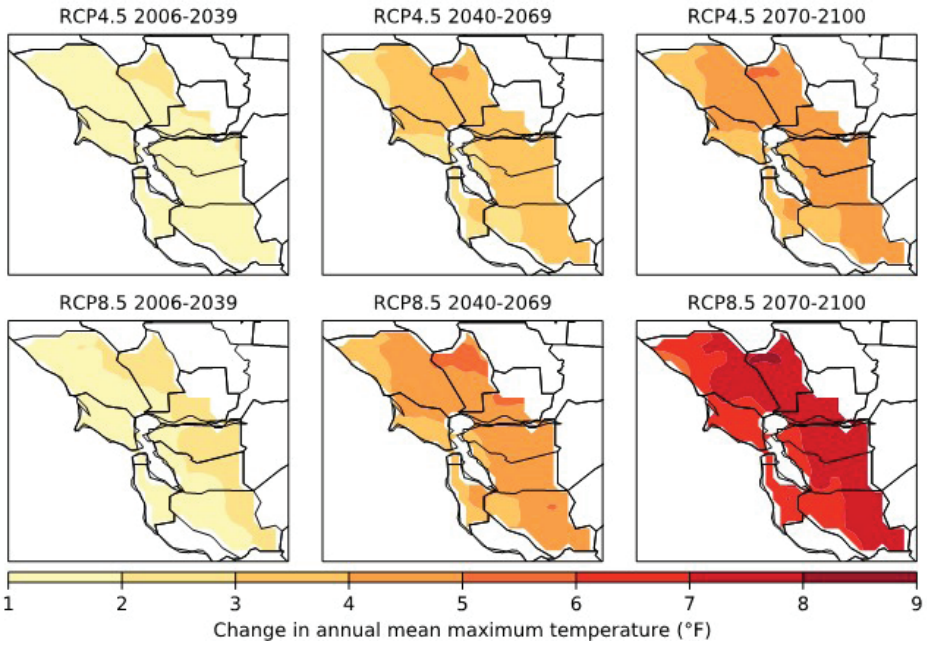

Spatial patterns of projected model-average change in annual mean maximum temperature (unit: °F) under RCP4.5 and RCP8.5 for three time periods: 2006-2039 (early-21st century), 2040-2069 (mid-21st century), and 2070-2100 (late 21st-century). Unit is °F.

FIGURE 4

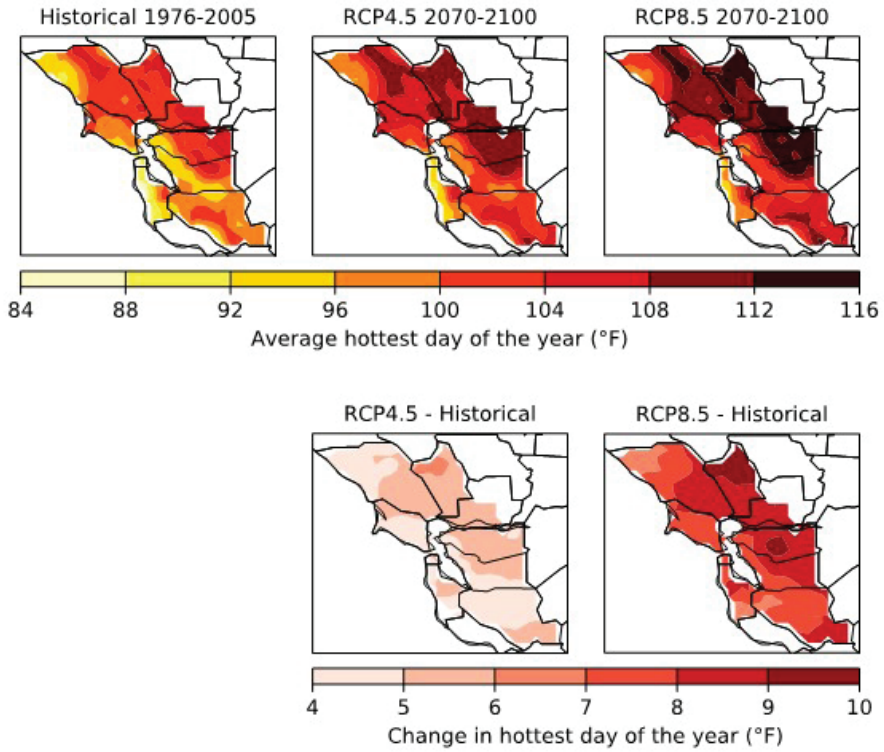

Top row: Average hottest day of the year in the historical (1976-2005) period, and in the late-21st century (2070-2100) under RCP4.5 and RCP8.5. Bottom row: change (late-21st century minus historical) in the hottest day of the year under RCP4.5 and RCP8.5. Unit is °F. All data are derived from LOCA.

Precipitation, Drought and Snowpack

HIGHLIGHTS

- Precipitation in the Bay Area will continue to exhibit high year-to-year variability - "booms and busts" - with very wet and very dry years.
- Our largest storms, called "atmospheric rivers," contribute on average 40% of the Sierra snowpack and can also produce heavy rainfall and substantial flood risk.
- The Bay Area's largest winter storms will likely become more intense, and potentially more damaging, in the coming decades.
- Future increases in temperature, regardless of whether *total* precipitation goes up or down, will likely cause longer and deeper California droughts, posing major problems for water supplies, natural ecosystems, and agriculture.
- The 2012-2016 California drought led to the most severe moisture deficits in the last 1,200 years and a 1-in-500 year low in Sierra snowpack. Importantly, paleoclimatic records show that mega-droughts spanning multiple decades have occurred in California's past.
- Consecutive years of low or no snowpack are especially worrisome. The 2012-2016 record low snowpack resulted in $2.1 billion in economic losses, 21,000 jobs lost in the agricultural and recreational sectors statewide and exacerbated an ongoing trend of groundwater overdraft.
- Under a high emissions scenario, average Sierra Nevada snowpack is projected to decline by nearly 20% in the next 2-3 decades, 30% to 60% in mid-century, and by over 80% in late century.

California precipitation is the most episodic in the nation, often with relatively long duration between storms (Dettinger *et al.* 2011). As a result, large, discrete storms provide a substantial fraction of California's rainy season total precipitation, and annual precipitation is highly variable from year to year. There are two emerging perspectives on how climate change is affecting precipitation in California. On one hand, any changes in annual mean precipitation that occur are currently expected to be relatively small compared to the range of natural variability experienced in the region (USGCRP 2017). On the other hand, atmospheric theory and climate models both indicate that the largest individual storms are becoming more intense with climate change (Pall *et al.* 2017; Prein *et al.* 2017; Risser & Wehner 2017), and there is some evidence that this might also be accompanied by more frequent extremely dry precipitation periods, as well as more frequent "whiplash" events that swing from extremely dry to extremely wet conditions in California (Swain *et al.* 2018), further enhancing variability in a system already characterized by "booms and busts." We describe these changes in both mean annual precipitation and extreme events further below.

Mean Precipitation Changes

The high variability of mean annual precipitation in California makes it difficult to detect a strong signal in future projections of annual precipitation. Moreover, the physical processes that lead to regional precipitation change as a result of global climate change are complex and vary by region, leading to a higher degree of model uncertainty

compared to projections of temperature change. As the planet warms, the atmosphere holds more water, but the consequences for rainfall vary across the globe (Allen & Ingram 2002; Collins *et al.* 2013). Across North America, even under the strongest emissions scenario (RCP8.5), little change is projected for summer and fall precipitation, but larger changes may occur in winter and spring (USGCRP 2017). In general, precipitation in northern regions is projected to increase while precipitation in the southern regions, especially the Southwest, is projected to decrease. California straddles the boundary between these regions, contributing to the high uncertainty about future precipitation that has been reported through several generations of climate modeling (i.e., IPCC AR3, AR4, and AR5; Collins *et al.* 2013).

This relatively small signal in mean annual precipitation relative to variability can be seen in the downscaled LOCA data for mean annual precipitation in the Bay Area as seen in Figure 5. Mean annual precipitation ranged considerably from year to year over 1950-2005, from 11.7 inches to 61.1 inches (29.7 cm to 155 cm). Thus, while the multi-model average projections do show a small increase in annual precipitation (i.e. 2.5 inches (6.4 cm) per year in RCP4.5 and 4.6 inches (11.7 cm) per year in RCP8.5 by end of century (2070-2100) relative to the baseline period of 1976-2005), these changes are nearly imperceptible relative to the high interannual variability, with a range of almost 50 inches (130 cm) in total rainfall between the driest and wettest years in the historical record.

There is also concern that even if statewide mean precipitation does not change, there could be important local changes due to a northward shift in storm tracks as large-scale patterns of atmospheric circulation are expected to shift away from the equator toward the poles in a warmer climate. The degree to which this phenomenon will impact regional precipitation within California is still poorly understood. We note that the coarse horizontal resolution (~100-200km) of the global climate models used as input to the LOCA downscaling procedure may be too large to resolve such a shift, in which case the shift would not be reflected in downscaled climate data products based on them. The IPCC WG1 AR5 (Collins *et al.* 2013) reveals that end-of-21st century winter storm track shifts under the RCP8.5 forcing scenario are small and not statistically robust in the Eastern Pacific basin. Although these projected shifts are larger in the Western Pacific, North Atlantic, and throughout the Southern Hemisphere, confidence in these projections off the coast of California is *low* due to model limitations.

FIGURE 5

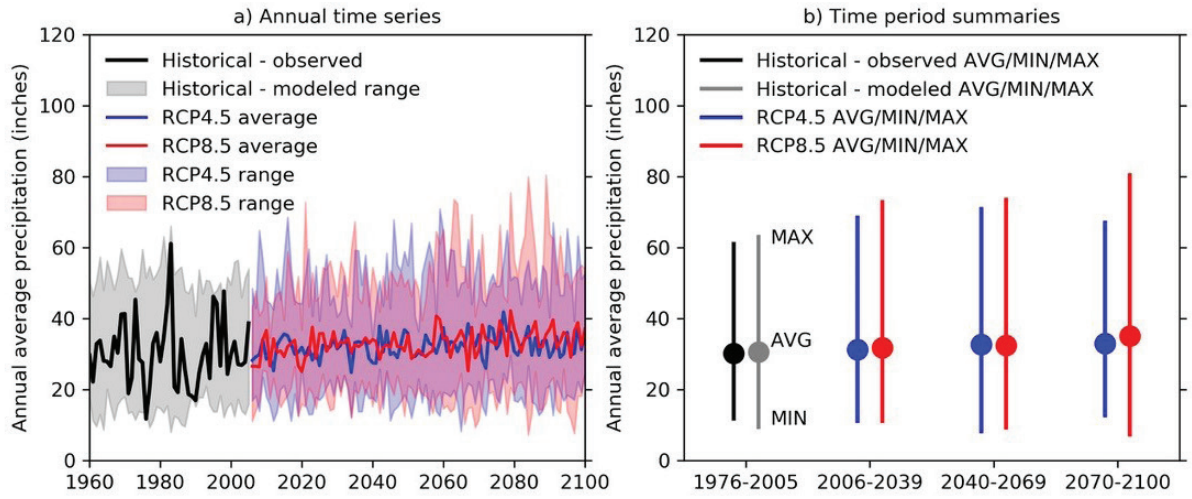

Observed historical (black), modeled historical (grey), and projected future (RCP4.5 - blue, RCP8.5 - red) annual average precipitation over the Bay Area. (a) Annual time series of data (future projections begin in 2006), with solid lines representing observed annual mean in the historical period and model-averages in the future. Shading represents the spread across models. (b) Summary of multi-year average (circles) and spread (vertical lines) across four time periods: 1976-2005 (historical), 2006-2039 (early-21st century), 2040-2069 (mid-21st century), and 2070-2100 (late-21st century). Unit is inches.

Extreme Precipitation Events — Historical and Projections

Generally, the largest California storms are what have recently been dubbed "atmospheric rivers" as they carry more water than seven to 15 Mississippi Rivers combined (Ralph & Dettinger 2011) and often bring an end to drought conditions (Dettinger 2013). These storms result in heavy rainfall over a narrow area (Gimeno *et al.* 2014). Moreover, they contribute an average of 40% of the annual snowpack in California (Guan *et al.* 2013). However, they also present substantial flood risk, especially for the Russian River (Ralph *et al.* 2006) and the Sierra Nevada region, where they account for 50% of rain-on-snow events despite representing only 17% of all precipitation events (Guan *et al.* 2016).

Several lines of evidence point to an enhancement of precipitation extremes due to climate change, although the degree of enhancement is an active area of research. The extreme precipitation literature in recent years has focused on how anthropogenic climate change will impact the magnitude and frequency of extreme storm events through what is known as the Clausius-Clapeyron relationship, which describes the increased capacity of the atmosphere to hold moisture as it warms. One hypothesis holds that if the atmosphere can hold more moisture, the potential for more extreme precipitation should increase as well (Allen & Ingram 2002). This hypothesis is supported by recent

global climate model simulations (Kharin *et al.* 2013); however, climate models at these horizontal resolutions (i.e., ~100-200 km) fail to reproduce observed extreme precipitation amounts (Wehner *et al.* 2010, 2014), especially atmospheric rivers that make landfall in California (Dettinger 2011). The implication for projected changes in extreme precipitation is unclear but several recent analyses suggest that certain storm types may yield precipitation increases substantially in excess of what the Clausius-Clapeyron relationship might predict (Pall *et al.* 2017; Prein *et al.* 2017; Risser & Wehner 2017). A recent analysis of precipitation extremes focused specifically on California corroborates this finding of enhanced wet extremes under climate change and also indicates higher occurrence of extremely low precipitation periods, as well as greater occurrence of "whiplash" events in which extremely dry periods are followed by extremely wet periods (Swain *et al.* 2018).

Consistent with global climate models, the downscaled LOCA projections show an increase in the magnitude of large precipitation events. Figure 6 shows changes in the average wettest day of the year for the nine counties of the Bay Area. Historically, the greatest precipitation events in the Bay Area have occurred in the coastal mountains of northern Sonoma County. Percent increases in the largest precipitation events (measured in inches of rain per day) range from 6% to 21% in RCP4.5 and as high as 37% in RCP8.5 by end of century.

Another way to measure changes in extreme precipitation is to calculate the change in return frequency of a storm of a particular magnitude. For instance, using data prepared for the IPCC WG1 AR5 by Kharin et al. (2013), we estimate that under RCP8.5, what is currently considered a 20-year return frequency one-day storm event for the Bay Area would increase in frequency by a factor of three or more by end of century. In other words, a once-in-20-year storm would become a once-in-seven-year or more frequent storm. Similarly, Swain et al. (2018) estimate that a once-every-200-year sequence of storms comparable to that which caused the great California flood of 1862 could occur every 40-50 years by 2100 under a high emissions scenario (RCP8.5).

BOX 1: IS THAT AN ATMOSPHERIC RIVER I HEAR COMING?

New $19 million advanced weather radar system for the Bay Area

Bay Area water districts are teaming up with USGS and Scripps to develop and deploy a fabulous new Bay Area weather monitoring system that will provide critical data for flood control and water supply issues during our big atmospheric river events. Being able to accurately forecast exactly where the storms will make landfall and how long they will linger over an area will provide a tremendous boost to water and flood managers. Current systems have allowed for 7-day forecasting, which limits preparations on the ground, but the new system will eventually expand to 14- and 21-day advance notices.

FIGURE 6

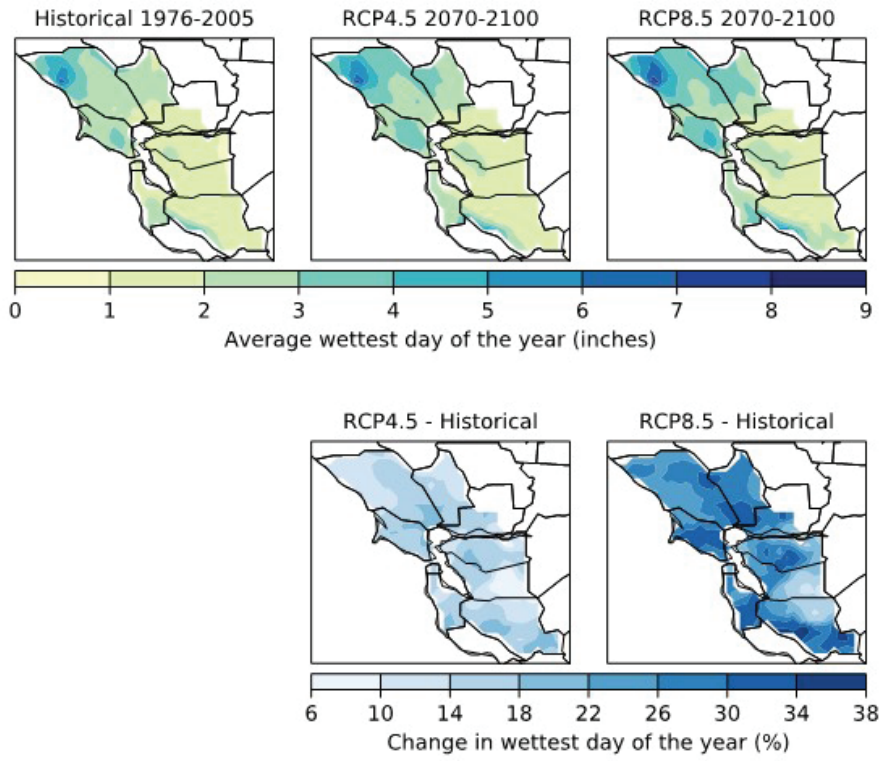

Top row: Average wettest day of the year in the historical (1976-2005) period and in the late-21st century (2070-2100) under RCP4.5 and RCP8.5. Unit is inches. Bottom row: Change (late-21st century minus historical) in the wettest day of the year under RCP4.5 and RCP8.5. Unit is percent. All data are derived from LOCA.

Drought and Snowpack

To formally quantify drought, or a prolonged period of water deficit, four main indices have been created over the last several decades including: meteorological, soil moisture, hydrological and, most recently, snow (Van Loon 2015). Each index quantifies drought with a unique lens focused on impacts on agriculture, drinking water, ecosystems, energy, and industry and/or recreation. The occurrence of drought is not uncommon in California (Griffin & Anchukaitis 2014) largely due to persistent atmospheric ridges (high pressure systems over the Pacific Ocean; Swain *et al.* 2016) and extreme and intermittent precipitation (Dettinger 2013). The 2012-2016 California drought was a prime example of the implications of atmospheric ridging as it led to the most severe moisture deficits in the last

1,200 years (Griffin & Anchukaitis 2014) and a 1-in-500 year low in Sierra Nevada snowpack (Belmecheri *et al.* 2016). The 2012-2016 drought was associated with significant declines in groundwater across the state, particularly in the Central Valley region[2], continuing a long-term overdraft trend that tends to accelerate during periods of drought[3]. Paleoclimatic records have shown that even longer periods of drought, i.e., mega-droughts or persistent droughts that span decades to centuries, have occurred in California's past (Malamud-Roam *et al.* 2007; Cook *et al.* 2010). In recent years, the contribution of anthropogenic climate change to the intensity and persistence of drought has been a major topic of interest (Diffenbaugh *et al.* 2015; Mann & Gleick 2015; Seager *et al.* 2015; Swain 2015; Cheng *et al.* 2016; Angélil *et al.* 2017). Most of the studies have concluded that current and future increases in temperature, regardless of changes in precipitation, raise the probability of enhanced drought magnitude and duration in California (Wehner *et al.* 2017). This has major implications on California's agricultural industry and water supply through modifications in snowpack, soil moisture, and evapotranspiration.

Water storage in mountain snowpack is an important feature that alleviates seasonal fluctuations in rainfall. The snowpack of the Sierra Nevada acts like a natural reservoir by increasing California surface water storage by ~72% in addition to man-made surface reservoirs (Dettinger & Anderson 2015). Approximately 60% of Bay Area water supply is sourced in the Sierra Nevada (Bay-Area-IRWMP n.d.) and Sierra snowmelt provides 40% of the annual water to the San Francisco Bay Delta (Cloern *et al.* 2011). Further, mountain snowpack acts to delay the rate of release of water to man-made surface reservoirs into the summer, when precipitation is low and water demand is high (California Department of Water Resources 2015) (Figure 7). Therefore, snow drought, or consecutive years of low-to-no snowpack, has become a major topic of interest over the last decade (Harpold *et al.* 2017). This was made apparent in the drought period of 2012-2016 when the combination of warm temperatures and low precipitation led to record low Sierra Nevada snowpack (5% of normal) with economic impacts felt throughout the agricultural and recreational industries (i.e., $2.1 billion and 21,000 jobs lost) and a mandatory statewide surface water use reduction of 25% (Mote *et al.* 2016).

2 https://water.ca.gov/-/media/DWR-Website/Web-Pages/Programs/Groundwater-Management/Data-and-Tools/Files/Statewide-Reports/Fall-2017-Groundwater-Level-Data-Summary.pdf

3 http://www.ppic.org/wp-content/uploads/JTF_GroundwaterJTF.pdf

FIGURE 7

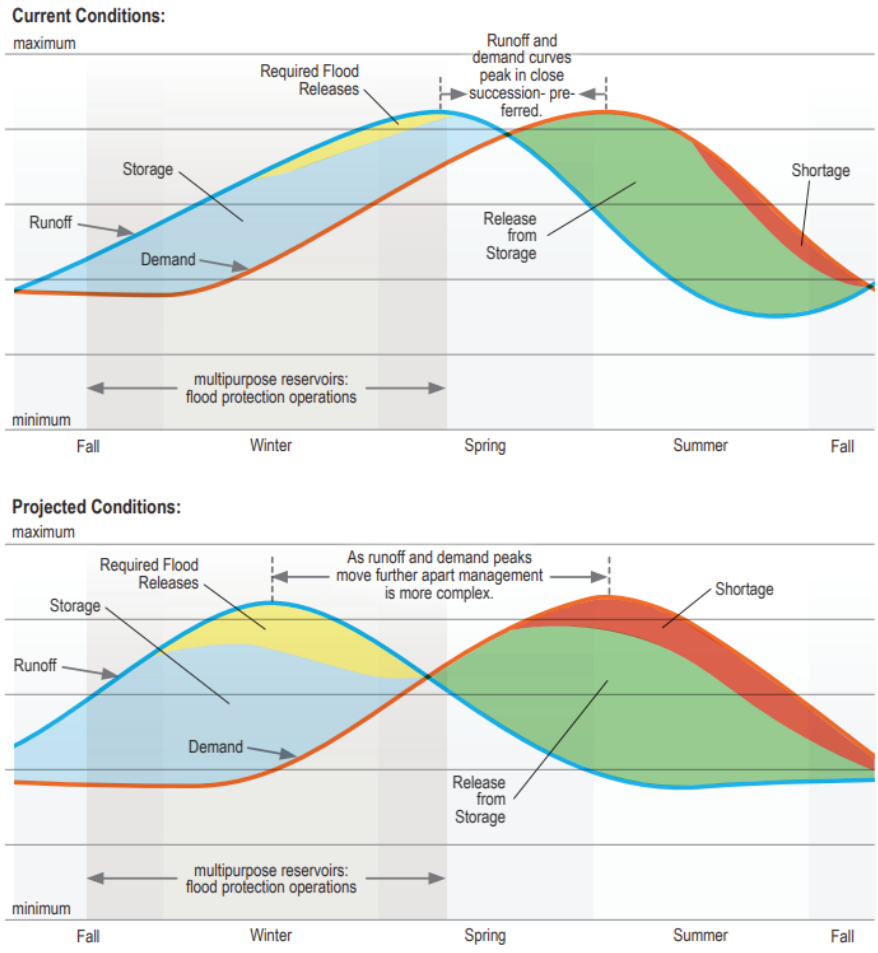

Top row: Current water supply surplus (blue shading) and demand deficit (green) curves with yellow (red) areas highlighting flood release loss (shortages). Bottom row: Same as top row, however with climate change projected onto the water supply surplus and demand deficit curves. Source: Adapted from the California Department of Water Resources (2015) report on "California Climate Science and Data for Water Resources Management."

Decline in Sierra Nevada snowpack has occurred over the last half-century (Mote *et al.* 2018) and is *very likely* to continue given the physics of climate change (Wehner *et al.* 2017). This was shown in the most recent National Climate Assessment (USGCRP 2017) where a *high confidence* was attributed to an earlier spring melt and reduced snowpack in Western U.S. states as the climate continues to warm (Wehner *et al.* 2017). This is because as surface temperatures continue to rise, the historical location of the freezing line in mountains will move upslope, snow will persist for shorter durations at low elevation, and more storms will fall as rain rather than snow (Pierce & Cayan 2013). Although snowpack decline is *very likely*, the changes will be heterogeneous in both time and space. Conventional global climate model simulations, such as those used for the IPCC, are unable to realistically represent mountainous regions due to limited spatial resolution in current models. This makes it difficult to infer snowpack change at scales where decisions are made (e.g., watershed regions). Therefore, to properly evaluate this decline, the use of regional downscaling techniques is necessary.

An intercomparison of several regional climate downscaling strategies was conducted by Rhoades et al. (2018) for the major mountain ranges of the Western U.S., including the California Sierra Nevada. By 2040-2065, average Sierra Nevada snowpack was shown to decline by 30 to 60% under a business-as-usual emission scenario across the various regional downscaling methods. Using a new downscaling technique, the authors also found that average Sierra Nevada snowpack could decline by 19% by 2025-2050 and amplify to an 83% decline by 2075-2100 (Figure 8) (Rhoades *et al.* 2018). The effect of future warming on snowpack during periods of drought is of particular concern. With increased warming, the decline in Sierra Nevada snowpack seen during the 2012-2016 drought could be exacerbated by 60 to 85% if it occurred at end-century (Berg & Hall 2017). The changes in Sierra Nevada snowpack will undeniably pressure California to preemptively invest in climate adaptation measures such as alternative water storage, water-use efficiency, and updated reservoir storage operations. Without these preemptive measures, there is *very high confidence* that reoccurring and persistent hydrological drought will define California's future (Wehner *et al.* 2017).

FIGURE 8

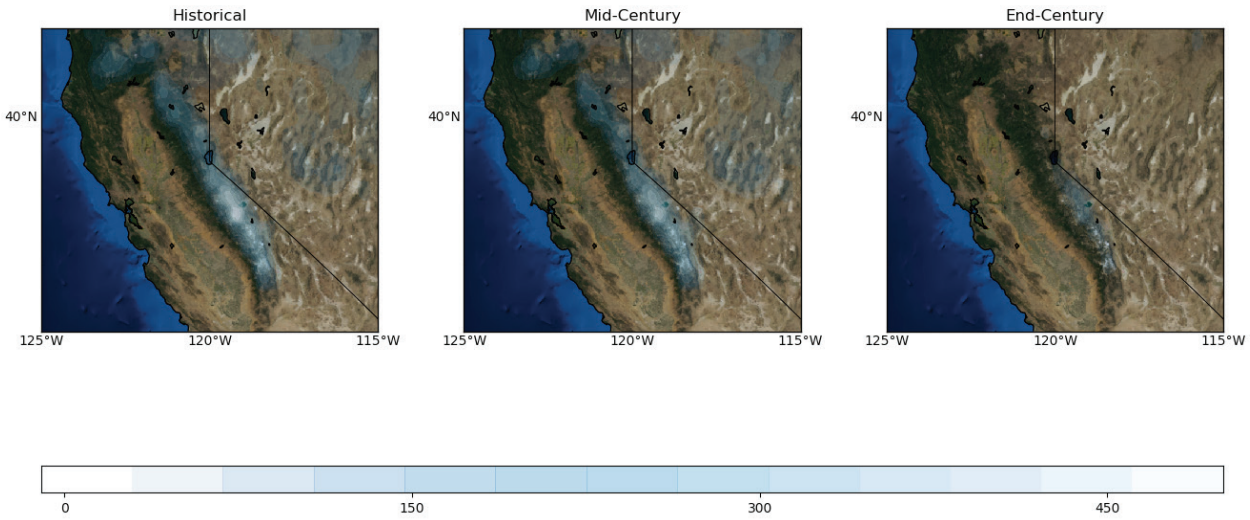

The figure highlights a new variable-resolution global climate model simulation of average winter snowpack in the California Sierra Nevada over a historical period (left), at mid-century (middle) and at end-century (right) under a business-as-usual emissions scenario (Rhoades et al. 2018). Units are mm of snow water equivalent (SWE) averaged over the winter months of December, January and February (DJF). Source: Adapted from Figure 8.2 in the National Climate Assessment 4 by Hari Krishnan at Lawrence Berkeley National Laboratory

Fog

HIGHLIGHT

- Several studies suggest that coastal fog along the California coast, so critical to our Bay Area climate, is less frequent than before. However, the causes of this decline and implications of climate change are complicated because coastal fog formation is the result of a delicate moving balance between heat and humidity from three different sources: ocean, air, and land.

Coastal fog in the San Francisco Bay Area has been such a regular summer feature that songs are written about it, pilots taking off and landing at SFO keep a watchful eye on delays caused by it, and the phenomenon is even recognized by its twitter handle #KarltheFog. Several lines of evidence suggest that coastal fog along the California coast and other coastal upwelling zones is less frequent than before. However, the story is complicated because the dynamics of coastal fog formation and disappearance are the result of a delicate moving balance between heat and humidity from three different sources: ocean, air, and land. This balance is in turn driven by upstream processes

important to fog such as the high-pressure winds causing cold water upwelling, Arctic-cooled ocean currents that lead to changing fog frequency, and turbulence that mixes the moister fog layer into the drier air layer above. These factors change the thickness and timing of the fog and the highly localized offshore and onshore movements of fog across complex topography (Koračin *et al.* 2014; Torregrosa *et al.* 2016; Clemesha *et al.* 2017a).

Some of these interactions are strongly affected by warming climates but how they all work together under changing climate conditions is not yet well understood. Planet wide changes in air patterns can cause strong change in fog at our local level, such as the resilient atmospheric ridge that parked warm dry air over California in August 2017, shutting down the usual pattern of onshore coastal fog advection into coastal ecosystems (see also September 2010 event) (Kaplan *et al.* 2017; Swain *et al.* 2018).

Long term observations of fog come from airport and ship records (Dorman *et al.* 2017) and are being augmented with satellite remote sensed data (Rossow & Dueñas 2004). Using 60 years of Arcata and Monterey airport data, Johnstone and Dawson (2010) derived a temperature-based statistical method to estimate coastal fog frequencies for the last century, which showed a 33% reduction in coastal fog. Periodic increases of coastal fog have been associated with the warm phase of the Pacific Decadal Oscillation (Witiw & Ladochy 2015), an ocean temperature index. The one dynamic simulation model for California coastal fog that exists (O'Brien *et al.* 2013) shows a long term trend of 12- 20% reduction in coastal fog over the model's 1900-2070 period. Although the model improves on regional climate models by including important turbulence processes, it did not include several feedbacks and processes that may be important for the future of fog, such as coastal upwelling and shifts in the center of summertime high pressure zones.

Fog is also affected by local conditions. Recent analyses of coastal fog in Southern California showed fog is reduced near heavy urban areas (Williams *et al.* 2015) and affected by pollution (LaDochy & Witiw 2012). Urban surfaces warm during the day, causing warmer nighttime air temperatures that prevent fog droplets from forming until the air rises high enough and cools (adiabatically) for condensation to occur. Reductions in summertime coastal fog have also been observed in other regions such as Hokkaido, Japan (Sugimoto *et al.* 2013), Kiril Islands, Russia (Zhang *et al.* 2015), and Central Europe (Egli *et al.* 2017). An opposite trend of increasing fog and low clouds in the South China region is attributed to an increase in heavy pollution that prevents rain formation (Fu & Dan 2018). Reductions in non-marine Central Valley tule fog have been correlated with lower levels of NOx and other air pollutants (Herckes *et al.* 2015; Gray *et al.* 2016).

In California, summertime fog and low clouds can move deep into northwest-oriented valleys that are well positioned to receive the summer northwestern winds that help form fog and move it inland (Torregrosa *et al.* 2016). Some of the state's most productive agricultural regions benefit from these inland incursions of fog such as the Salinas Valley, where fog moves more than 75 kilometers inland and protects lettuce and strawberries from sunburn, or the wine grape-growing regions of Sonoma and Napa, where fog penetrates inland through the San Francisco Bay and over the Petaluma Gap.

Species restricted to the coastal zone, such as coast redwood trees, grow in forests that can get up to a third of their water from fog (Burgess & Dawson 2004). The discovery that plants in fog-filled forests can take in water through their leaves (Dawson 1998) changed our understanding of fog's contribution to ecosystems. Fog drip can be lifesaving to salmonids in low flow coastal streams that would otherwise dry out during the late Mediterranean dry season. In

the high fog areas of the Santa Cruz Mountains, Sawaske and Freyberg (2015) found summer streamflow increases of 100% during fog events and increase of up to 200% with a two-day lag. Shade from summertime fog and low clouds cools coastal systems with a cascading effect: less heat (Walker & Anderson 2016) reduces the rate of plant evapotranspiration (Chung *et al.* 2017), which reduces the use of subsurface water reserves by plant roots (Burgess & Dawson 2004), leaving more water in the system (Flint *et al.* 2013). When fog disappears in late summer, it can exacerbate the climatic water deficit for entire watersheds leading to fire-ready tinder conditions and increased electrical demand as air conditioners are turned on for relief from the heat.

The importance of fog to California's water and energy balance and to human and wildlife well-being is receiving increased attention and study (Torregrosa *et al.* 2014; Clemesha *et al.* 2017b). Research on climate change impacts to fog (Wang & Ullrich 2018), the relationship between fog, species, and ecosystem resilience (Burns 2017), and even the geoengineering technique of increasing marine clouds to cool the planet (Ahlm *et al.* 2017) will help to improve forecasts of future trends and understanding of coastal fog impacts on California (Koračin 2017).

Wildfire

HIGHLIGHTS

- In the Bay Area, future fire activity will be driven by both changes in urban development and changes in climate.
- Warming temperatures combined with expansion of the wildland-urban interface are projected to increase fire risk in most of the Bay Area, though risks may decline in some areas as they become more heavily urbanized.
- Land use planning, together with fire-safe building standards and near-building vegetation management, are important strategies for managing future fire risk to people and structures.

Wildland fire is a recurrent feature of ecosystems in semi-arid climates throughout the world, including the American West and California. The Mediterranean-type climate of California (and climatically similar regions in other parts of the world) is especially fire prone, as the winter rains support vigorous plant growth and the summer dry season dries out the vegetation, making it exceedingly flammable. Hot and dry conditions, combined with offshore winds in autumn (Santa Anas in Southern California, Diablo winds in Northern California) create high risk conditions that rapidly spread fires. Fire ignitions in California are primarily due to human activity, and the dry fuels and climate contribute to higher risk of rapid fire spread. While attention to wildfire has mostly focused on the Sierra Nevada and Southern California, the large and destructive fires in the Bay Area and North Coast, particularly in 2015 and 2017, have rapidly shifted attention to the ongoing risks in these regions.

State and federal agencies have pursued aggressive policies of fire suppression, both for protection of timber resources but increasingly to protect human life and infrastructure as fires ignite and spread in areas with high population density. As is well documented in the Sierra Nevada, fire suppression can contribute to fuel buildup (i.e., dense forests where fire can spread more easily to the canopy) (Agee & Skinner 2005). There is also strong evidence that anthropogenic climate change, especially rising temperatures and periodic droughts, have made substantial contributions to the increase in area burned in wildfires in the America West (Westerling *et al.* 2006; Abatzoglou & Williams 2016). Like storms and hurricanes, however, it is difficult to pinpoint the contribution of climate change to the occurrence or severity of any individual fire event.

FIGURE 9

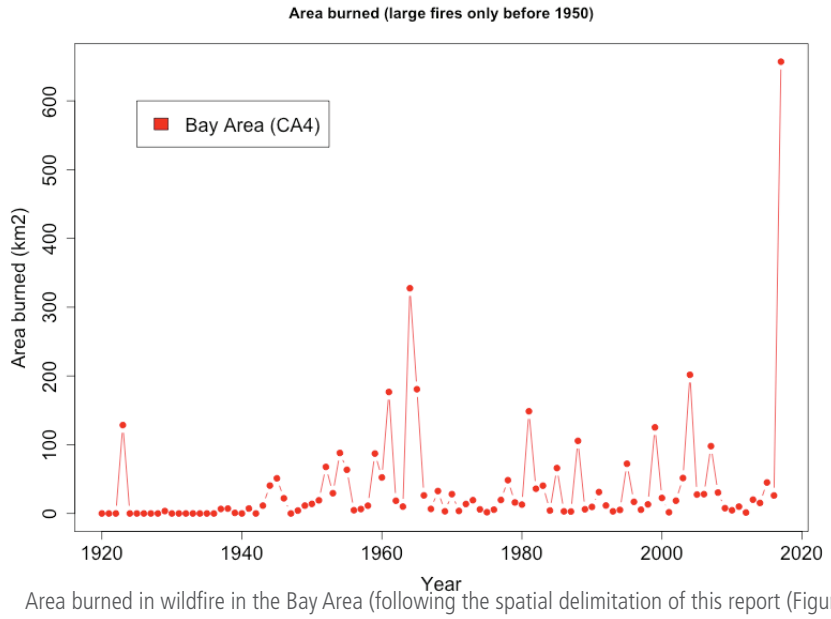

Area burned in wildfire in the Bay Area (following the spatial delimitation of this report (Figure 1). Cumulative areas derived from FRAP (1920-2016) and GeoMac[4] (2017).

4 https://www.geomac.gov/

Analysis of the Fire and Resource Assessment Program (FRAP) fire history database[5] shows recurring years with high wildfire activity (in terms of area burned) in the Bay Area (Fig. 9). Prior to 2017, the peak year was 1964, due to the large Hanly fire and the smaller Nuns and Roadside #42 fires; the perimeters of these three fires were eerily similar or contained within the 2017 Tubbs, Nuns and Atlas fires, respectively. The North Bay fires of October 2017 burned more than twice the area of any previous year, following close on the heels of the large and destructive Lake County fires of 2015. As of 2018, six of the top 20 most destructive fires in California history (in terms of buildings lost) have occurred in the Bay Area (Table 1).

TABLE 1

RANK	FIRE	DATE	COUNTY	ACRES	STRUCTURES	DEATHS
1	Tubbs	October 2017	Sonoma	36,807	5,643	22
2	Tunnel	October 1991	Alameda	1,600	2,900	25
4	Valley	September 2015	Lake, Napa, Sonoma	76,067*	1,955	4
6	Nuns	October 2017	Sonoma	54,382	1,355	2
11	Atlas	October 2017	Napa, Solano	51,624	781	6
15	Berkeley	September 1923	Alameda	130	584	0

Bay Area fires ranked in the top 20 most destructive fires in California history, in terms of structures burned. Source: CalFire.
*Note: Most of the acreage burned was in Lake County, outside of the Bay Area as defined here.

Climate change and future wildfire activity: Projections of future fire activity depend on our understanding of what controls wildfire historically in each region, how those controls may change in the future, and the ranges of uncertainty associated with key variables. At relatively broad scales, climate affects fire regimes in two different ways, either by altering vegetation growth rates (e.g., fuel accumulation) or through changes in fire season length and severity (e.g., fuel flammability and fire weather) (Krawchuk & Moritz 2014). At finer scales, recent studies demonstrate that fire exhibits a "hump-shaped" response to human development, with fire activity peaking in the wildland-urban interface (WUI) due to increased ignitions and dropping off both in more urbanized areas and in less developed rural regions and open space (Syphard *et al.* 2007; Butsic *et al.* 2015; Mann *et al.* 2016). Thus, future patterns of land use together with climate change are crucial for assessing what fire regimes may emerge in the coming decades.

5 http://frap.fire.ca.gov/data/frapgisdata-sw-fireperimeters_download

The impact of climate change on future fire activity has been the focus of considerable research in California and elsewhere (Krawchuk & Mortiz 2012). Where fires are fuel limited (as in the desert), changes in fire depend on whether future climates have higher or lower rainfall. In the Bay Area, although there is a strong moisture gradient from the coast inland, fire is not generally fuel limited. As a result, there are more consistent projections of increased fire activity (i.e., more frequent or greater area burned), due to a warmer climate (Figure 10).

Projections of the impact of development and land use change are less well developed. These effects are incorporated in two modeling studies for the Bay Area (Mann *et al.* 2016; Westerling 2018). While the studies are not directly comparable, Mann et al. suggest that future fire activity will be driven as much by changes in human development as by changes in climate. Continued development will likely dampen fire probabilities in areas closest to high-density human development, while potentially increasing fire risk where development expands in the wildland-urban interface. Westerling (2018) projected increased fire probability in most of the Bay Area, especially the dry hills around Mt. Hamilton, with reduced fire risk near urban areas and development corridors.

Given the importance of land use patterns, additional work is needed to understand their importance relative to changes in climate. It is also worth noting that local human development is under society's direct control, meaning that land use planning may be the most effective tool for managing future fire risk to human life and infrastructure. Continued building in the wildland-urban interface exposes more structures to fire risk and also alters fire probabilities. On the other hand, improved building codes and management of defensible space around structures can significantly reduce losses when fires do occur.

FIGURE 10

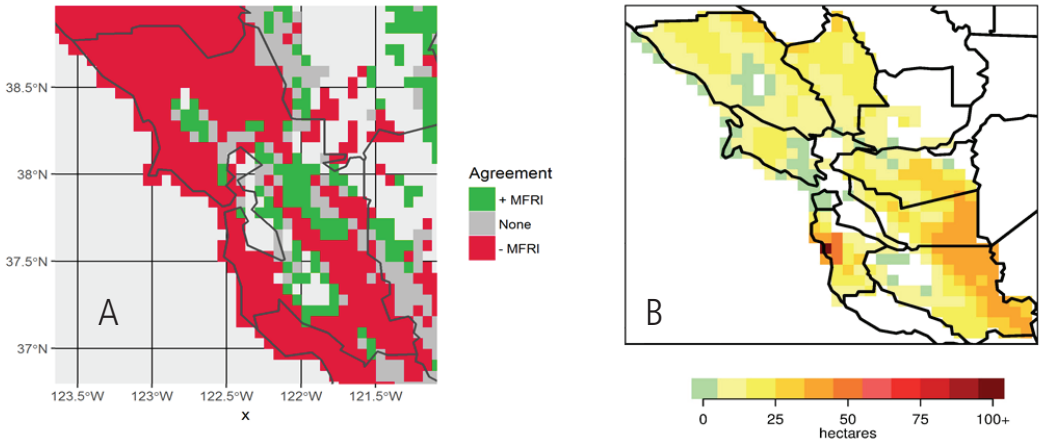

Projections for future changes in wildfire. A) Predictions for increase (red) or decrease (green) in fire frequency (2026-2050, compared to baseline of 1976-2000), showing areas of agreement across an ensemble of climate models (Mann et al. 2016). B) Composite projections from Westerling (Westerling 2018) for mid-century (2035-2064) average annual area burned under RCP 4.5 (results for RCP 8.5 are very similar).

Sea Level Rise

HIGHLIGHTS

- Sea level in the Bay Area has risen over 20 centimeters (8 inches) in the last 100 years.
- The regional signal of SLR is complicated at the local level by highly variable rates of vertical land movement across the Bay Area due to seismic effects, sediment compaction, marsh accretion, and groundwater fluctuations.
- California's Fourth Climate Change Assessment projects median sea level rise of 0.74 m (RCP 4.5) and 1.37 m (RCP8.5) for 2100 along the California coast.
- Recent science studies, using advanced models and ice sheet observations, suggest the possibility of extensive loss from Antarctic ice sheets in the 21st century — possibly producing sea level rise by 2100 that could approach 3 meters. California's Fourth Climate Change Assessment finds, under the RCP 8.5 scenario, that extremely high SLR by 2100 (as high as 2.87m at San Francisco) is plausible with very low probability.
- Even with high levels of emissions reductions, research now suggests that at least 2 meters of sea level rise is inevitable over the next several centuries due to time lags in response to increasing global temperatures.
- The powerful 2015-16 El Niño, one of the three largest in the historical record, resulted in winter wave energy that was over 50% larger than the typical winter in the Bay Area, driving unprecedented outer coast beach erosion.

Numerous studies have documented the acceleration of global (i.e., eustatic) sea level rise (SLR) during the latter part of the 20th century and early 21st century, with rates of ~1-2 mm/yr prior to 1990 as much as tripling to ~3 mm/yr during the satellite altimetry era (1993-present) (Jevrejeva *et al.* 2014; Dangendorf *et al.* 2017). Regional rates of SLR are highly variable in space and time, depending on ocean and atmospheric circulation patterns, gravitational and deformational effects due to land-based ice mass changes, and tectonics and other drivers of vertical land motion (NRC 2012).

Historical SLR rates in the San Francisco Bay Area are well documented. The Ft. Point tide gauge adjacent to the Golden Gate has the longest tide record in North America (1855-present), with a long-term rate of SLR of 1.94 mm/yr (1897-2016). Other tide gauges across the region report similar results, including Redwood City (1.99 mm/yr, 1974-2016), Alameda (0.72 mm/yr from 1939-2016) and Port Chicago (1.58 mm/yr, 1976-2016) within San Francisco Bay, and Pt. Reyes (1.98 mm/yr, 1975-2016) along the outer coast (NOAA 2018). Moderate variability among these observations (with Alameda being a significant outlier) could be attributed to factors such as record length, local vertical land motion, and datum issues.

Importantly, each of the Bay Area tide gauges shows significant acceleration since 2011. These observations are consistent with the satellite altimetry-observed West Coast acceleration of SLR from 2011-2015 due, at least in part, to a shift in low frequency climate variability in the Pacific as well as a strong El Niño peaking in fall of 2015 (Hamlington *et al.* 2016). This recent acceleration of regional SLR follows decades of dynamical SLR suppression across the U.S. West Coast, possibly related to the mode of the Pacific Decadal Oscillation (PDO) (Bromirski *et al.* 2011). It is unclear how long this recent trend of higher than eustatic rates of SLR will continue for the San Francisco Bay Area but will

largely depend on the patterns of shorter (e.g., ENSO) and longer (e.g., PDO) modes of climate variability that drive regional circulation patterns.

The regional signal of SLR is further complicated at the local level by highly variable rates of vertical land motion across the Bay Area due to co-seismic and intra-seismic land movement, sediment compaction, marsh accretion, and groundwater fluctuations. Extensive groundwater pumping in the Santa Clara Valley from 1916-1966 led to as much as 1 meter of subsidence along the shoreline of South San Francisco Bay, leading to the periodic flooding of low-relief land adjacent to the bay (Poland & Ireland 1988). Some of the submerged land has been recovered over the last several decades due to more responsible groundwater pumping practices (Schmidt & Bürgmann 2003), resulting in recent uplift of 1-2 mm/yr (Shirzaei *et al.* 2017).

Despite active tectonics, the largest recent vertical rates of change measured in the Bay Area are due to non-tectonic processes, particularly the consolidation of bay mud and artificial fill that comprise a large proportion of the land lining the Bay Area's shoreline. For example, InSAR data show that the northwestern tip of Treasure Island dropped ~20 mm/yr from 1992-2000 (Ferretti *et al.* 2004), and subsidence of up to 10 mm/yr occurred along mud-dominated shoreline areas, such as the San Francisco waterfront, San Francisco International Airport, and Foster City, though most subsidence rates in the Bay Area are less than 2 mm/yr (Bürgmann *et al.* 2006; Shirzaei & Bürgmann 2018). The recent launching of the Sentinel-1A (2014) and Sentinel-1B (2016) satellites equipped with advanced synthetic aperture radar (SAR) antenna sensors will allow for greater resolution of vertical land motion rates across the Bay Area (Shirzaei *et al.* 2017), and more precise integration of these changes into coastal flood projections (Ballard *et al.* n.d.; Barnard *et al.* 2014; Shirzaei & Bürgmann 2018).

Projected SLR over the course of the 21st century is being thoroughly discussed as part of the Fourth Assessment, and therefore only a brief summary is provided here. The National Research Council study (NRC 2012), which incorporated steric and dynamic ocean components of SLR, mountain glacier and ice sheet loss, and vertical land motion, projected 92 centimeters of relative SLR for the San Francisco Bay by 2100 (range 42-166 centimeters). More recent California-focused SLR projections, including California's Fourth Climate Change Assessment (Pierce *et al.* 2018) and "Rising Seas in California" (Ocean-Protection-Council 2018) have incorporated advanced models and observations of ice sheets, suggesting the possibility of more extensive loss from Antarctica in the 21st century than previously considered (DeConto & Pollard 2016), along with a probabilistic approach to support risk assessment (Kopp *et al.* 2014). These more recent efforts have not produced a marked change in the median projections of sea level rise by 2100; e.g., the Fourth assessment projects 0.74 m (RCP 4.5) and 1.37 m (RCP8.5) for California in general, and the Ocean Protection Council projects 0.49 m (RCP 2.6) and 0.76 m (RCP8.5) for San Francisco Bay. However, they do indicate that SLR by 2100 of ~3 meters is physically plausible. For example, under the RCP8.5 scenario, California's Fourth Climate Change Assessment projects a 0.1% and 5% chance of sea level rise reaching 2.87 m and 2.41 m by 2100, respectively (Pierce *et al.* 2018). Sweet et al. (2017) have integrated this latest SLR science into continuous probabilistic projections across North America, including San Francisco Bay, and placed them in the context of a flood risk framework, with similar upper-end SLR projections (Sweet *et al.* 2017). Median SLR projections have not changed markedly in recent years and significant uncertainty remains in terms of the timing of SLR projections (based in large part on uncertainty in emissions pathways). Even with net zero future emissions, research now suggests that at least ~2 meters of sea level is inevitable over the next several centuries due to the lag in

response time of SLR with temperature; current emission trajectories in the 21st century would commit the oceans to 9 meters of SLR eventually (Clark *et al.* 2016).[6]

Wave Conditions and El Niño: The potential changes in long-period wave energy (i.e., swell) are primarily a concern for the exposed open coast although there is some swell penetration into the Central Bay, and Hanes and Erikson (2013) documented a peak in wave energy along Crissy Field during outer coast, southwest swell events. Increases in wave heights over the last several decades have been documented along portions of the U.S. West Coast (Allan & Komar 2006; Wingfield & Storlazzi 2007; Menéndez *et al.* 2008), including the region adjacent to the Bay Area (Hanes & Erikson 2013), but these trends have more recently been found to be largely insignificant when adjusted for buoy hardware modifications (Gemmrich *et al.* 2011). The use of Global Climate Models (GCMs) to determine the future wave climate shows a projected poleward migration of storm tracks and generally a slight decrease in wave heights for the outer coast of the Bay Area (and California in general) compared to the historical record (Graham *et al.* 2013; Erikson *et al.* 2015). This future projection is consistent with the observed multi-decadal trend of poleward Hadley cell expansion since 1979 and, therefore, the location of the sub-tropical jet stream (Hu & Fu 2007). However, we note that the poleward shift in storm tracks is not consistent across all GCMs (Collins *et al.* 2013).

Periodic El Niño events exert a dominant control on coastal hazards across the region, driven by seasonally elevated water levels as high as 30 centimeters above normal, and, on average, 30% larger winter wave energy (Barnard *et al.* 2015). The powerful El Niño of 2015-16, one of the three largest in the historical record, resulted in elevated water levels of 10-20 cm and winter wave energy that was over 50% larger than the typical winter in the Bay Area, driving unprecedented outer coast beach erosion (i.e., landward shoreline retreat) that was 98% higher than normal (Barnard *et al.* 2017). The frequency and magnitude of future El Niño events, combined with SLR, will be a key driver of coastal vulnerability in the coming decades, including influencing nuisance flooding patterns due to the combination of seasonally elevated sea levels with background sea level rise. Research to date on future El Niño patterns is largely inconclusive (Collins *et al.* 2010), although a recent study suggests a potential doubling in the frequency of extreme El Niño events (Cai *et al.* 2014), such as those that occurred in 1982-83, 1997-98, and 2015-16.

6 More information on the specific impacts climate change will have on California's Ocean and Coast – including sea level rise, rising temperatures, and rising ocean acidity – can be found in a companion Fourth Assessment report (California's Ocean and Coast Summary Report 2018).

Social Systems and Built Environment

In this section, we consider the threats to social systems and the built environment in the Bay Area that are created by climate change. We examine energy consumption, including both buildings and vehicle charging; energy distribution, including electricity, natural gas, and transportation fuels; land use; infrastructure and services that support transportation and urban water resources; and direct and indirect impacts on public health in the region. In each of these areas, we describe the specific vulnerabilities that manifest in the Bay Area and note cases where Bay Area vulnerability is more or less than that for the state as a whole.

Throughout this section, we emphasize the risks for vulnerable communities, which are particularly pronounced for certain climate stressors in the Bay Area. These vulnerable populations include but are not limited to: low-income individuals and families, people of color, women, the young, the elderly, people with disabilities, people with existing health issues including mental health issues, people with limited-English proficiency (LEP), immigrants and refugees, agricultural workers and day laborers, traditional communities, people who are or have been incarcerated, people without a high school education, and other groups or a combination of groups. These populations will often not only feel the immediate impacts of climate change more significantly, but also are less able to adapt to climate changes or recover from their impacts.

Finally, it is important to note that a complex set of interdependencies underlie these vulnerabilities. An understanding of these feedbacks and dependencies across infrastructure and social systems is critical to assessing how California's social and built environments will respond in the coming century. Examples of interdependencies developed further below include the links between (1) land use, transportation infrastructure and traffic, energy consumption, and air pollution; or (2) water resources, energy consumption, and public health. In the subsections that follow, we consider each component individually and examine how it is likely to be impacted by different aspects of climate change. Within each section, we also include a brief discussion of the interdependencies that would influence outcomes within the segment under consideration. This structure does not do justice to the highly integrated aspects of social and built systems in California, but it begins to convey the complexity that must be addressed.

Transportation Infrastructure

HIGHLIGHTS

- The three-way relationship between land use, transportation infrastructure, and energy systems—all of which are vulnerable to climate impacts—is perhaps the most critical interdependence in determining the future growth and prosperity of the Bay Area.
- Much of the Bay Area's transportation system—airports, roads, and railways—is concentrated along the bay where flooding from sea level rise and storm surge is a major vulnerability.
- Disruptions to the transportation system from flood events will occur at critical links, such as highways and rail lines serving the port of Oakland, as well as low-lying roadways that connect the region's bridges and highways.

Nearly 7.2 million people live in the Bay Area, and regional residents take more than 21 million total trips on an average weekday (MTC & Caltrans 2008). In 2007, more than 82% of all trips were made by automobile, and most of the remainder were made by bus or rail transport. The Bay Area has 620 miles of freeways, 800 miles of state highways, and 19,000 miles of local roadways owned and maintained by Bay Area cities and counties (MTC & Caltrans 2008). The region's rail network has more than 600 miles of track and moves both freight and passengers (BCDC 2009). Dedicated trackways exist for Bay Area Rapid Transit (BART), the San Francisco Municipal Transportation Agency (MUNI), Sonoma-Marin Area Rail Transit (SMART), and the Valley Transportation Authority (VTA) light rail system in San Jose and the Silicon Valley. All other tracks (e.g., Amtrak, Caltrain, ACE) are shared by passenger and freight service, leading to substantial congestion. In addition, over the next 50 years, freight demand is expected to increase up to 350% (MTC 2007; BCDC 2009).

The greatest impact of climate change for the U.S. transportation system will be the flooding of roads, railways, and airport runways in coastal areas (NRC 2008), as well as sea level rise and storm surges. San Francisco Bay has approximately 1,000 miles of shoreline, and airports, roads, and railways throughout the region are concentrated along the coastline. That means coastal flooding to transportation systems is a major vulnerability (see above for a summary of sea level rise projections). Sea level rise will also be accompanied by sizable wind waves (Cayan *et al.* 2008). For example, very high seas and storm surge caused hundreds of millions of dollars in storm and flood damage around San Francisco Bay in 1997–1998 (Ryan *et al.* 1999).

To understand the effect of sea level rise on the Bay Area transportation network, Biging et al. (2012) created a high resolution digital elevation model (DEM) using data from Lidar, an airborne technology that provides very precise measurements of land surface elevation. In addition, they developed a digital surface model (DSM) of vegetation, buildings, bridges, and other infrastructure to better calculate the risk of flooding by sea level shifts and storm surges. To visualize potential inundation, they considered sea level rise scenarios in increments up to 1.4 meters, plus the equivalent of a 100-year storm event. Peak water level is modeled to an upper level that is in excess of 4 meters to visualize the extent to which transportation features and facilities become inundated. Results for the Port of Oakland (Figure 11) (Biging *et al.* 2012) are presented here to demonstrate the combined effect of progressive sea level rise and extreme storm events on inundation. With just modest sea level rise (0.5 meters), the approach to the Bay Bridge (upper portion of Figure 11) and portions of interstates 880 and 980 (running through the center-right of Figure 11) are compromised by inundation. As sea levels progress to 1.0 meters of rise (yellow) and 1.4 meters of rise (red), the inundated regions expand. At these higher sea levels, new transportation arteries

FIGURE 11

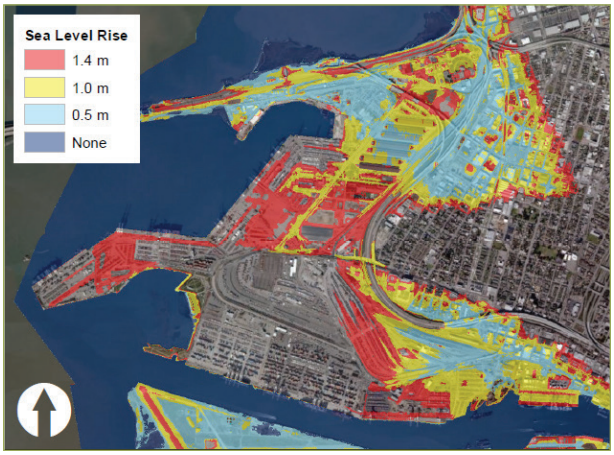

Inundation scenarios for the Port of Oakland. This delineates the area at risk of a 100-year flood event under different sea level rise elevations (none or 0 m, 0.5 m, 1.0 m, and 1.4 m). Source: Biging et al. 2012.

aren't necessarily cut, but the depth and duration of inundation will proportionally increase with rising sea levels. The result is that the Port of Oakland's vulnerability lies primarily in the links between the port and the terrestrial transportation network, which are fundamental to the port's functioning.

In addition, Biging et al. (2012) quantified the impact of sea level rise and storm events on the transportation network of the greater Bay Area by examining travel time between key nodes (high connectivity nodes) of the highway system. Figure 12 illustrates the greatest impact on individual links in the sample network by mapping the increase in access time to neighboring nodes. The results show that disruptions are greatest between east-west linkages, compared to north-south connections, and the overall regional network itself breaks down in several locations as key nodes become inaccessible. Travel times will increase significantly although much of the regional system remains accessible via secondary roadways further inland and not adjacent to areas of inundation.

BOX 2: 9 FABULOUS SLR DESIGNS FOR 9 BAY AREA COMMUNITIES

Resilient By Design: Bay Area Challenge

Financed through a $5 million grant from the Rockefeller Foundation, Resilient By Design (RBD) was a year-long collaborative design challenge bringing local, national, and international experts together with local residents and public officials. The result is nine innovative and community-based solutions that will strengthen the Bay Area's resilience to sea level rise, severe storms, flooding, and earthquakes. RBD was inspired by and modeled on the Resiliency By Design competition in the New York City area after Superstorm Sandy.

After receiving 51 submissions and undergoing an extensive jury process, RBD selected 10 winning Design Teams to participate in the Bay Area Challenge. The teams include designers, urban planners, architects, engineers, and other resilience experts with local, regional, national, and international expertise. In Phase 2, the 10 teams spent two months touring potential project sites and meeting with community organizations and local government leaders. From this intensive research phase, 10 sites were selected and matched with the 10 teams for five months of collaborative planning and design. Finally, the proposed projects were presented and judged in May 2018. Now, Bay Area stakeholders are turning to the task of financing and implementing these innovative futures.

Interdependence with Other Sectors

In addition to the direct disruption of the transportation network by inundation, the transportation infrastructure is also vulnerable to disruptions in the energy sector, particularly the electrical grid and fuel delivery. Over the longer term, land use and population shifts will be a critical driver of the efficacy of the transportation network and will also simultaneously dictate energy consumption by the transportation system. As discussed below, low-income households are increasingly being displaced inland, increasing demands on the transportation infrastructure to carry this population to employment or medical care in the urban centers of the Bay Area. At the same time, the functioning of the transportation system will affect shifts in population and employment distributions throughout the region. This three-way relationship between land use, transportation infrastructure, and energy systems is perhaps the most critical interdependence in determining the future trajectory of the San Francisco Bay Area.

FIGURE 12

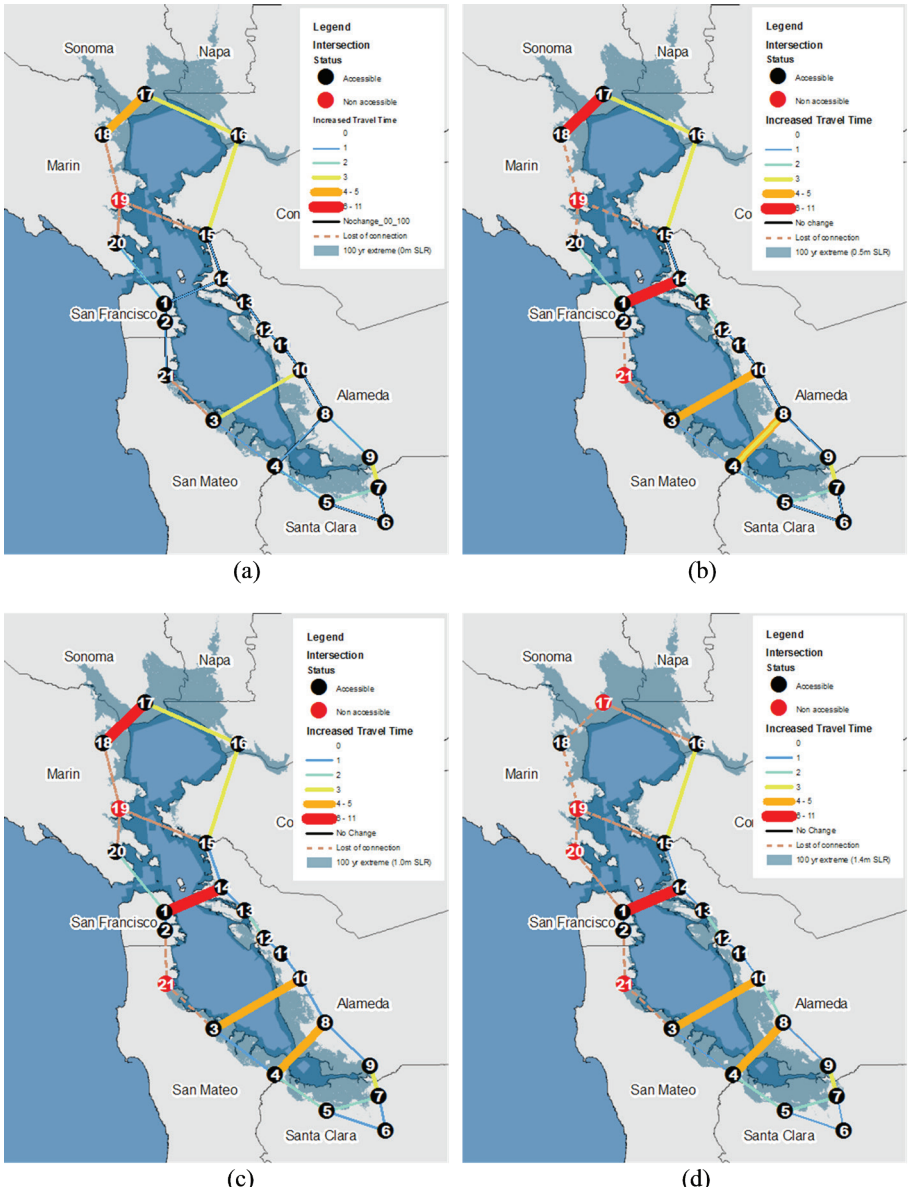

Increased travel time (ratio of impaired to normal travel times) between near neighbor intersections after a 100-year extreme event with different sea-level rise scenarios (none or 0 m, 0.5 m, 1.0 m, and 1.4 m). Source: Biging et al. 2012.

Land Use and Community Development

HIGHLIGHTS

- Future land use decisions will significantly influence the Bay Area's efforts to address climate change, affecting building and transportation energy, urban water demand, and wildfire ignitions.
- Land use choices can also exacerbate climate risks by creating urban heat islands, changing runoff following extreme rain events and other factors.
- The critical lack of affordable housing in the core of the region is forcing households further south, north, and inland, with negative energy and environmental consequences.
- Regional equity issues will be exacerbated in the coming decades as lower income and minority households disproportionately live in the least desirable locations with higher vulnerability to climate and other environmental risks.

Land use in the Bay Area, in which we include housing and non-residential buildings and development, is evolving rapidly due to the interaction of markets and policies. Market forces of particular relevance to the Bay Area include housing supply, real estate prices, increases in population, and employment and growth in high-tech industries and incomes. Policies include both local land use plans and zoning regulations and regional efforts such as Plan Bay Area (see Box 3).

A fundamental crisis for the future of the Bay Area is the lack of affordable housing in the core of the Bay Area, except for a few neighborhoods which are bayfront, at low elevation, and at high risk of current and future flooding. This lack of affordable quality housing, and the climate threat to the housing of that type that does exist, is forcing households further south, north, and inland, in some cases as far as the Central Valley, to find housing they can afford. The movement of "Bay Area" residents further from the urban core increases commuting time and distances, with economic and environmental consequences.

Because of the close connection between the distribution of residents throughout the region and commute distances, transportation and land use are tightly linked. This has always been the case for the Bay Area, raising concerns about disruption due to seismic risk. Now, however, natural risks arising from climate change, including increased flood and fire frequency and magnitude, must be featured in long-term decision-making and planning. Models in support of Plan Bay Area (Box 3) are already incorporating the interaction between transportation, real estate, and climate change risks.

BOX 3: TACKLING CLIMATE CHANGE, SEA LEVEL RISE, AND RESILIENCE THROUGH INTEGRATED PLANNING

Raising the Bar on Regional Resilience

Resilience planning is fast becoming a priority for the Bay Area with its low-lying shorelines susceptible to flooding and rising sea levels, as well as its active earthquake faults and social inequity issues compounded by an affordable housing crisis. Resilience is commonly defined as the ability to recover from setbacks and adapt to change (Ovans 2015). A resilient Bay Area would be well-positioned to manage and respond to the uncertainties and physical hazards associated with the Bay Area's geographic setting and changing climate while protecting vulnerable communities, critical infrastructure, and the natural environment.

With the July 2017 adoption of Plan Bay Area 2040 — including new commitments to resilience-building actions — the region is at an important crossroads where research, planning, design, and management activities focused on resilience are coming together both in policy and on the ground. The plan's adoption is one of several milestones reached in 2017 that demonstrate both how far the region has come and the opportunities ahead to raise the bar on the resiliency of the Bay Area's transportation system and other critical infrastructure, urbanized areas, and environmental systems.

The first milestone in 2017 was the assembly of a critical mass of research and analysis on vulnerability to sea level rise and flooding all around the bay by local and regional partners through the Bay Area Regional Collaborative (BARC) and other efforts. Some of this work — led by the San Francisco Bay Conservation and Development Commission's Adapting to Rising Tides program (BCDC ART) and the Association of Bay Area Government's (ABAG) Resilience Program — identified four areas of vulnerability related to sea level rise and flooding in need of more than just local attention. These regional level vulnerabilities include transportation infrastructure, fragile housing, disadvantaged communities, and natural areas and parklands close to shore.

A second 2017 milestone is the use of this information to identify six actions in Plan Bay Area 2040 (the region's state-mandated Sustainable Communities Strategy) that would help the region address vulnerabilities in an integrated way. These six actions address regional governance, resilient housing, funding, social equity, mitigation, and other issues arising from climate adaptation planning on a regional level. The substance of these actions reflects coordinated work on the part of BARC, BCDC, ABAG, and the Metropolitan Transportation Commission (MTC), as well as the California State Coastal Conservancy and the San Francisco Estuary Partnership. These actions include the completion of a regional assessment that identifies the most vulnerable transportation assets, communities, and natural areas and begins to develop appropriate strategies to address those vulnerabilities in a phased approach. This work is being funded through a grant from Caltrans, with matching funds from the Bay Area Toll Authority (BATA), a strong indication that transportation agencies are seeking solutions to make the region more resilient.

A third 2017 milestone is the launch of the Resilient by Design | Bay Area Challenge, which is now engaging 10 multi-disciplinary design teams in addressing resilience challenges at 10 project locations around the bay. The results, to be completed in summer 2018, will add to the region's toolbox of options for forging more resilient shorelines, cities, and communities.

An important component of integrating resilience planning across the region will be informing the development of the next Sustainable Communities Strategy, a process scheduled to take place between now and 2021. The Sustainable Communities Strategy integrates land use and transportation planning to meet aggressive greenhouse gas reduction targets (required to be updated every five years by Metropolitan Planning Organizations in California through State Bill 375). While Plan Bay Area 2040 is the current version of the state-mandated Regional Transportation Plan/Sustainable Communities Strategy (RTP/SCS), just approved in July 2017, the next version may take a different form. Over the next two years, regional partners will be laying the

groundwork for enhancing this regional planning process so that it more strongly supports multi-hazard, multi-benefit initiatives and strategies that increase the Bay Area's resilience.

Strengthening local and regional resilience through this existing, state-mandated planning process is particularly important since the resulting plans commit the region to focusing growth and development in specific places within the metropolitan Bay Area. The RTP/SCS also prioritizes transportation investments over the next 20 to 30 years. When considered together, and in light of new information about their vulnerability to flooding, sea level rise and other hazards, choices made around these areas identified for future growth and investments will be central to the Bay Area's overall resilience.

In addition, Plan Bay Area 2040's strong focus on the housing affordability crisis highlights the particular vulnerability of people already living within the economic margins of our costly region. Both the affordability and safety of regional housing options are critical components of resilience. This became even more evident in October 2017, when the region lost 3,000 homes within one week in Sonoma, Napa, and Solano counties to devastating wildfires, leaving thousands homeless and many unable to find affordable replacement or temporary housing.

Addressing climate change in the context of regional resilience is a complex challenge for those charged with integrating planning across nine counties, more than a hundred cities, and myriad local jurisdictions and special districts. Clearly, the region must continue to accelerate mitigation of climate impacts by reducing greenhouse gas emissions and improving air quality, activities which the Bay Area Quality Management District, MTC, and ABAG have led for many years. At the same time, the region must work to ensure our longstanding and future residents have safe and affordable places to live. Strengthening our urban and natural infrastructure, ensuring public safety, and growing our regional resilience equitably will require a partnership across regional agencies, local jurisdictions, and non-governmental organizations. They'll also need to work with residents, businesses, designers, builders, academics, health professionals, and others in the community.

Equity issues will be significant as lower income and minority households disproportionately live on the least desirable land, and frequently have higher degrees of vulnerability to environmental risks. At the same time, low-income communities and communities of color are often left out of land use planning and decision-making. This long-term vulnerability is made acute by the fact that these communities may not be sufficiently connected to institutions and agencies that can help them after a climate event.[7] In contrast, we note that high-priced real estate on the urban edge and with views can be among the most vulnerable in the Bay Area to wildfire risk, as occurred in the 1991 Tunnel Fire in the Oakland hills.

7 More details on Climate Justice issues – including the disproportionate impacts and barriers to adaptation faced by several California communities – can be found in a companion Fourth Assessment that covers Climate Justice and Climate Equity issues in-depth (Climate Justice Summary Report 2018).

Interdependence with Other Sectors

Land use in the Bay Area is tightly linked with almost all other considerations of climate change impacts. In fact, it is arguable that population shifts (geographically or in terms of total numbers) may be just as important as (or even more important) climate factors in establishing the future trajectory for the social and built systems of the Bay Area. Shifts in land use will influence energy demand, transportation demand and congestion, public health, and even urban water demand. Further, changes in Bay Area land use will feedback into climate risks, through the creation of urban heat islands, and changes in the runoff response to precipitation potentially exacerbating urban flooding and shifts in the sediment supply to the San Francisco Bay ecosystem.

Urban Water

HIGHLIGHTS

- The Bay Area's water agencies rely on a diverse portfolio of local and imported sources. The reliability of these sources will vary dramatically in both the short and long term as the climate changes.
- Climate impacts — such as earlier melting of snowpack, increasing seawater intrusion into groundwater, increased rates of evapotranspiration, and levee failures or subsidence that contaminate Delta supplies — will affect both the quantity of water available and the quality of supplies.
- Wastewater treatment plants, historically located along bay shorelines where effluent discharge was convenient, are now highly vulnerable to future sea level rise.
- Rising bay water and groundwater levels will also increase salinity intrusion and subsurface flooding. If this groundwater intrudes into sewer systems, treatment processes will become more expensive and wastewater recycling capabilities will be reduced.
- Climate change will require improved stormwater management in the Bay Area as extreme storm events increase in size and frequency.

Urban water systems include the infrastructure and institutions required to: (1) provide, manage and treat water supplies for potable and non-potable uses; (2) collect, treat, and discharge or recycle wastewater; and (3) manage, and, if necessary, treat stormwater after rain events. Historically, these functions often have been planned and operated separately. Increasingly, however, California urban water agencies recognize the need to view all water as a resource and are moving toward more interdependent systems, commonly referred to as "One Water" systems, as interconnections in the following discussion illustrate.

Climate Effects on Water Supply

The Bay Area has 376 community water systems (CWS) (Ekstrom *et al.* 2018). Of those, over 70 are classified as urban water agencies that provide wholesale and retail water supplies. These suppliers rely on a diverse portfolio of sources, including local surface water, groundwater, the State Water and Central Valley Projects, other water imported from outside the region (especially the Sierra Nevada via Hetch Hetchy and Mokelumne Aqueducts), water transferred within the region, groundwater desalination, and water reuse. Figure 13 shows the mix of sources used by urban water suppliers as reported in each agency's 2015 Urban Water Management Plan. Note that this figure aggregates over the entire region, and reliance on local sources is considerably higher in some sub-regions (e.g., Marin and Sonoma Counties) and considerably less in others (e.g., San Francisco).

FIGURE 13

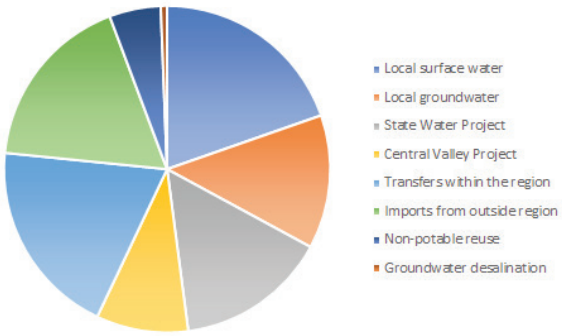

2015 Water Supplies to the Bay Area. Source: Cumulative values from 2015 Urban Water Management Plans for each agency.

The reliability of these sources in both the short and long term will vary dramatically. Hydrologic changes affecting the amount and location of precipitation and snowpack in California's mountainous regions will stress existing storage reservoirs, impacting surface supply, imported water, and water transfer availability, especially in the summer and fall. While many strategies to address scarcity are similar for imported and local supplies (e.g., water recycling), the impacts of climate change on the available quantities of surface water could be different for local supplies (e.g., Marin, Sonoma) than those originating from the Sierras (e.g., San Francisco), as changes in local precipitation patterns are different than changes in snowpack and snowmelt. Recent and potential political decisions may affect the quantity and reliability of Bay Area supplies, including changes to water rights (e.g., to protect environmental flows), the fate of the Delta Tunnels, and implementation of the Sustainable Groundwater Management Act (SGMA) of 2014. Institutional structure can also affect supply reliability. Two-thirds of the region's CWS can be classified as small, self-sufficient (S3) systems that serve less than 10,000 people and are not connected to state or federal water projects (Ekstrom *et al.* 2018). Therefore, S3 systems tend to have fewer resources and alternatives in times of scarcity. In the recent drought (2011-2016), these S3 systems were more likely to experience reliability issues due to water shortage and more likely to address these issues with short-term coping strategies (e.g., outdoor watering restrictions) than with substantial or transformational changes (e.g., developing new water supply). Though there are a large number of S3 systems, they serve a very small portion of the population (<2%) in the highly urbanized Bay Area. Also, some of these systems identified as S3 may be connected to the Hetch Hetchy system and are therefore not be entirely self-reliant.

Climate change will exacerbate reliability concerns as it could potentially affect the quantity of water available and the quality of supplies (e.g., earlier melting of snowpack); increasing seawater intrusion into groundwater; levee failures, either structural or due to subsidence of the levees themselves (Brooks *et al.* 2018) that contaminate Delta supplies). Twenty climate change scenarios were evaluated to determine the economic and hydrologic effects on water supply in

California (Herman, J. *et al.* 2018). Some results, including average water availability and optimal supply portfolios, are reported on a statewide basis. However, costs associated with climate change-related water shortages are reported regionally and, in the Bay Area, may be as high as $200 million per year in extreme conditions.

Reliability concerns can be mitigated with more diverse water supply portfolios, additional water storage infrastructure above and belowground, and innovative groundwater management. Strategies for increasing supply reliability are being pursued by individual agencies and as part of a regional effort called the Bay Area Regional Reliability (BARR) partnership made up of several large water suppliers serving six counties (see Box 4). Alternatives under consideration by BARR and other Bay Area agencies include: expanding storage and conveyance infrastructure; increasing non-potable water recycling; implementing potable reuse and/or seawater desalination; promoting groundwater augmentation, banking, and conjunctive use; constructing interties between systems to enable additional water transfers; and harvesting stormwater.

Reducing water demand can also increase reliability. In 2015, water consumption in the region was 104 gallons per capita per day (gpcd), about 20% lower than the statewide average for urban water agencies that year. For individual agencies, it ranged from 56 to 204 gpcd. (Water consumption in 2015 was lower than a typical year because an executive order required urban water agencies to reduce water use as an emergency drought response.) For comparison, per capita water consumption in Singapore is around 40 gpcd and in Germany is just over 30 gpcd. In Israel and Australia, countries with similar climates to California, water consumption averages about 65 and 90 gpcd, respectively. (Note: Water demands vary by necessity due to, for example, climate and economic drivers. Further, data for consumption rates were obtained through diverse online sources and the underlying accounting methods may not be consistent.) The relatively low per-capita water use in much of the Bay Area reduces the potential for cost-effective conservation at the low end of the reported values. This may explain why water agencies in this region report lower reliance on demand management in times of water shortage than most other regions (Ekstrom *et al.* 2018). Finally, we note that without adequate management, water demand may increase due to climate change-related warmer temperatures, especially for outdoor irrigation or cooling.

Climate Effects on Wastewater

An estimated 200 billion gallons of wastewater are generated in the Bay Area per year (*SF RWQCB staff summary report* 2011). Most wastewater in the region is collected and discharged to San Francisco Bay, directly or indirectly, with a few agencies discharging to the Pacific Ocean (Figure 14). Much of the discharge from inland wastewater treatment plants (WWTPs) shown in the graphic ultimately flows to the San Francisco Bay through surface water channels. Some WWTPs have limits on their discharge volumes. For example, some North Bay plants are not allowed to discharge to the Russian River in the summer to protect public health when recreational uses are common.

The San Francisco Bay ecosystem sits at the center of the region and is a strong driver of policies that limit discharges by volume and quality. Currently, no stringent limitations have been placed on nutrient discharge into the bay due to the fact that the bay ecosystem is limited by other factors, specifically grazing (mostly benthic) and low light levels due to high suspended sediment concentrations. A study of water quality in the bay has indicated a trend toward lower sediment concentrations and clearer waters (Wright & Schoellhamer 2004), as the gold mining sediment pulse works its way through the reservoir and river systems of the Central Valley and San Francisco Bay. If this

trend continues, low light conditions may no longer limit ecosystem growth, raising the potential for eutrophication (excessive plant and algae growth due to high nutrient concentrations) in the bay ecosystem.

This trend would be compounded by a shift in the physics of the bay toward a more persistently stratified condition (Cloern *et al.* 2011), which could be caused by longer, hotter heat waves or increases in precipitation. A more stratified bay would allow phytoplankton to grow at the surface, unchecked by the species that consume them, reinforcing the risk of eutrophication. The future trajectory of the bay ecosystem is uncertain, but if eutrophication occurs, nutrient discharges from WWTPs may need to be limited. Implementation of nutrient reduction technologies at WWTPs would take years to decades and would come at great regional cost. There is currently significant investment in applied research to understand and project future ecosystem conditions, specifically to determine whether WWTPs will need to invest in strategies to reduce nutrient discharges.

Water reuse is being implemented in partnerships between water and wastewater agencies both to reduce the environmental implications of discharging wastewater to the San Francisco Bay and to provide drought-resilient, local water supply. Water agencies in the region project that non-potable reuse will double by 2035, reducing discharges to the bay by an additional 20 billion gallons (10%) per year. In addition, the BARR partnership (Box 4) is evaluating three potable reuse projects that would use advanced methods to treat water to drinking water standards before it is used for groundwater recharge. Demand management strategies that reduce water consumption may potentially reduce wastewater volumes and reuse in the future.

BOX 4: TAKING A REGIONAL APPROACH TO BAY AREA WATER SUPPLY RELIABILITY

Bay Area Regional Reliability Project (BARR)

The Bay Area's largest water agencies are working together to develop a regional solution to improve water supply reliability for over 6 million area residents and thousands of businesses and industries. The BARR partners include Alameda County Water District, Bay Area Water Supply and Conservation Agency, Contra Costa Water District, East Bay Municipal Utility District, Marin Municipal Water District, San Francisco Public Utilities Commission, Santa Clara Valley Water District, and Zone 7 Water Agency. The BARR Partners have joined forces to leverage existing facilities and, if needed, build new ones to bolster regional water supply reliability. The benefits of a ***regional*** approach include:

- Addressing climate resiliency needs
- Facilitating the transfer of water supplies during critical periods of drought or following natural disasters
- Bolstering emergency preparedness
- Leveraging existing infrastructure investments
- Enhancing overall water supply reliability

The 176-page BARR Drought Contingency Plan serves as the first phase of the BARR project. The DCP differs from planning efforts in the past because it focuses on the Bay Area as a region as opposed to individual agencies and integrates all of the required elements into one document.

Many of the region's WWTPs are located along bay shorelines and discharge treated effluents directly to San Francisco Bay waters (Figure 14). While convenient historically, this placement now makes WWTPs vulnerable to inundation if the sea level rises. Using CoSMoS (Barnard *et al.* 2014) model simulations of bay water levels responding to a range of future sea level and tidal forcing, Hummel et al. (2018) found that that WWTPs in the South Bay are most immediately vulnerable to coastal flooding disruption, but other sites, such as Benicia, Paradise Cove, San Pablo, and Southern Marin, are also vulnerable but on longer timelines (Figure 14). The large costs of protecting, retrofitting, or relocating this critical infrastructure must be considered in capital investment plans for these facilities.

Although the results summarized in Figure 14 are based purely on coastal flooding, Hummel et al. (2018) also projected the influence of rising groundwater tables on inundation of WWTPs. Accounting for this flooding mechanism leads to more inundation of WWTPs in the central and northern portions of the Bay Area than appears in Figure 14, over a similar timeframe. As an additional risk, rising bay water and groundwater levels are also associated with increased salinity intrusion into the subsurface, threatening drinking water supplied from these aquifers. If saline groundwater intrudes into sewer systems, the treatment costs associated with wastewater recycling will increase.

WWTPs in the Bay Area are making efforts to mitigate their contributions to climate change. Several agencies that digest sludge anaerobically have implemented programs to augment their digesters with other organic wastes (e.g., slaughterhouse and dairy waste, food waste) to increase their production of methane (natural gas). The East Bay Municipal Utility District, for example, produces electricity with their methane. Though methane burning releases CO_2 as a waste product, this is considered a carbon neutral energy source as it reuses a waste product and offsets purchases of electricity from more carbon-intensive sources.

FIGURE 14

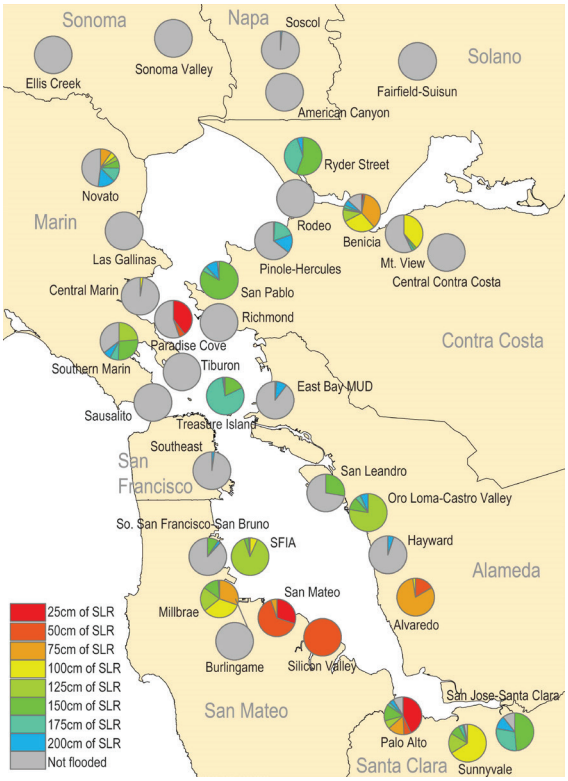

Wastewater treatment plants (WWTPs) in the San Francisco Bay Area. Pie graphs show for each facility the fraction of its footprint that will be inundated for the specified level of sea level rise; colors are cumulative so that the inundation fraction at 100 centimeters is represented by the portion of the pie associated with 25, 50, 75 and 100 centimeters. Many of the region's WWTPs are located along bay shorelines and discharge treated effluents directly to San Francisco Bay waters. Note: Only those facilities on the shorelines of San Francisco Bay are shown here; those on the outer coast are not included. Source: Hummel el at. 2018.

Climate Effects on Stormwater

For much of the region, stormwater is managed through separate sewers from wastewater. San Francisco, however, operates a combined system where wastewater and stormwater are collected and treated through the same infrastructure. Influent volumes to San Francisco's two wastewater treatment plants can be seven times greater during significant rain events (SFPUC 2014). These dramatic shifts in both the quantity and composition of the influent can overwhelm the treatment process and lead to discharges of untreated wastewater to the bay or Pacific Ocean. Other municipalities that operated separate sanitary and storm sewer systems can also experience significant fluctuations in influent volumes and composition to their wastewater treatment plants due to leaks, which allow inflow of stormwater into the collection pipes and manholes with similar results (EBMUD 2013).

Climate change will affect stormwater management in the Bay Area due to changes in the frequency and severity of storm events (see Precipitation section, above). Urban flooding could become more severe, although potentially less frequent, and could vary significantly from year to year. Cities such as San Francisco and Berkeley are investing in green infrastructure (e.g., porous pavements, bioswales, rain gardens) to collect and manage stormwater on a small scale to provide flexible, integrated stormwater management, dampening the flooding and sewer overflow risks associated with storm events. Some water agencies, including the Santa Clara Valley Water District, are planning to expand larger-scale stormwater collection as a potential source of water supply in the future.

Interdependencies with Other Sectors

Population growth is expected in inland communities as individuals and households seek affordable housing. This growth of the inland population, independent of rising temperatures, will lead to increased irrigation and cooling water consumption; warmer climates will contribute further to increased water demand. Public health would be at risk if the water system was significantly disrupted, either due to a lack of potable water or through failures in wastewater treatment systems. Beyond that, the interdependencies that involve the Bay Area water systems are less extensive than in the other sectors discussed in this section, except for some basic dependence of water delivery and wastewater treatment on energy grids, and vice versa.

Energy Distribution

HIGHLIGHTS

- The Bay Area electrical grid is vulnerable to power outages during wind and wildfire events.
- Much of our natural gas transmission system is located along waterways and will be impacted by flooding from sea level rise and extreme storm events.
- California's transportation fuel sector, which distributes oil from refineries to end users, will be increasingly exposed to extreme weather events such as flooding and wildfire.

The generation and distribution of electricity throughout the Bay Area are driven by the need to supply sufficient energy for consumption, which is dominated by buildings and, increasingly, vehicle charging. Distribution of energy resources throughout the region (1/3 of the region's electricity is generated outside of the region) is supported by networked infrastructure systems, including those that distribute electricity, natural gas, and other fuels (BAAQMD 2017). The nature of networked infrastructure systems creates particular vulnerabilities to environmental disruptions, where a local disruption (such as would occur due to flooding or fire) cascades through the infrastructure systems to create a regional impact. Understanding the local-regional interactions created by the infrastructure networks is critical to regional resilience.

Electrical Grid

The electrical grid in the Bay Area consists of both above and belowground links to households and businesses, which leaves neighborhoods and subregions vulnerable to outages during wind and wildfire events. Under scenarios of climate change, extreme storm events with stronger winds may become more frequent, and urban wildfires most certainly will. The combined effect is that aboveground elements of the electrical grid will face more frequent and severe threats in the coming decades.

Natural Gas Distribution

In the Bay Area, extreme storm events coupled with long term sea level rise (SLR) present critical risks for networked infrastructure. In California, the natural gas transmission system is just such an at-risk critical infrastructure structure, with much of it located along the state's waterways and thus vulnerable to greater frequency, duration, and depth of inundation. Such inundation may result in increased buoyancy or pressure forces, erosion, debris flows, disruption of supporting materials, and saline conditions. These conditions have the potential to accelerate structural failures and potentially threaten the functionality of California's natural gas transmission system as a whole.

While household and business electrification are emerging trends in the Bay Area, we remain dependent on an uninterrupted supply of natural gas, both for the economy and the well-being of the region's population. Natural gas supplies meet nearly one-third of California's total energy requirements and natural gas-fired generation is the dominant source of electricity in the state, accounting for 43% of all generation in 2012 (CEC 2014).

Recent work (Radke *et al.* 2016) characterized the vulnerability of the natural gas transmission system to SLR by simulating where assets are likely to be affected by inundation and collaborating with asset operators to analyze the risks that this inundation poses to their system. This analysis integrated geographic information systems (GIS) and a state-of-the art hydrodynamic model, 3Di, to simulate the location and depth of potential inundation in California under realistic extreme storm events coupled with various increments of SLR. Overlaying the resulting inundation projections with the location of natural gas led to the identification of vulnerable locations.

During a near 100-year storm event with no sea level rise, approximately 41 kilometers (26 miles) of PG&E's transmission pipelines are predicted to be inundated. (PG&E voluntarily assessed the risk such inundation poses to their assets and helped inform efforts to design mitigation strategies). This more than doubles to approximately 96 kilometers (60 miles) with a SLR of 0.5 meters and doubles again to 193 kilometers (120 miles) at a SLR of 1.0 m. Finally, when SLR reaches 1.41 meters, the amount of inundated PG&E pipeline increases a further 1.6 times to 308

kilometers (191 miles). However, a simulated SLR of 1.0 meters inundates only 28 km (17 miles) of transmission pipeline to Peak Water Levels (PWLs, which are the highest total water level achieved in the simulation) of more than 2.5 meters and much less, approximately 5 kilometers (3 miles) of more than 3.5 meter PWLs. Although the extent of pipeline inundated is substantial, the amount experiencing deep PWLs is quite small. A simulated SLR of 1.41 meters exposes approximately 53 kilometers (33 miles) of pipeline to PWLs of more than 2.5 meters and approximately 30 kilometers (18 miles) to PWLs of more than 3.5 meters.

As a result, even if a near 100-year storm event may be considered catastrophic for some infrastructure, it may not have a catastrophic effect on natural gas pipeline infrastructure. From a reliability (systemwide) perspective, the worst-case scenario of 1.4 meters in sea level rise with storm surges poses a long-term threat to the PG&E transmission assets. PG&E made a preliminary estimate that the annual cost of natural gas transmission upgrade may be approximately $4 to $7 million and that only about 37 kilometers (23 miles) of transmission pipeline would need to be replaced and secured with a concrete coating. In addition, approximately another 19 kilometers (12 miles) may need to be anchored in place with concrete footings, and less than 1 kilometer (0.6 mile) of pipeline may need to be deactivated. Therefore, the SLR of 1.41 meters plus a near 100-year storm event scenario does not pose a catastrophic threat to the natural gas transmission system as managed by PG&E.

Transportation Fuels Distribution

California's transportation fuel sector (TFS), which distributes oil from its source to end users, will increasingly be exposed to extreme weather events including flooding and wildfire under climate change. Radke and Biging (2018) organized the TFS into a physically and organizationally connected, multi-sector network. Using this network, they projected and analyzed climate change-induced flooding and wildfire exposure at both coarse and fine spatial resolutions, across multiple temporal horizons and climate scenarios, resulting in an assessment of the TFS's exposure and vulnerability. Statewide, the results show that California's TFS assets are minimally exposed to coastal flooding but will suffer increasing exposure due to rising sea levels. Higher proportions of TFS assets are exposed to wildfire (e.g., 28% of refineries in a 5-year period). Direct heat exposure can disrupt fuel distribution, and in extreme instances permanently damage infrastructure. Understanding where wildfires occur, with what frequency, and with what intensity is crucial information to plan for a resilient TFS.

For the Bay Area, fine resolution simulations (Radke *et al.* 2018) indicate that TFS assets in low-lying, flat, and coastal areas, such as the San Francisco Bay Area and the Sacramento-San Joaquin Delta, are vulnerable to coastal flooding. Using 50-meter (164-foot) resolution coastal flood models, Radke et al. (2018) show that a relatively small proportion of each TFS asset type is exposed to any depth of coastal flooding in the state. Docks and terminals are the most exposed assets with on average 12.2% and 11.9% (respectively) flooded between 2000 and 2100, whereas only 0.92% of the state's gas stations are exposed. From the 2000-2020 period to the 2080-2100 period, the exposed proportions of assets increase from 0.44-9.00% (in 2000-2020) to 1.99-21.60% (in 2080-2100). Additionally, increased proportions of the assets are exposed to more severe levels of flooding later in the century. During the 2000-2020 period, 0.01-5.16% of the assets are exposed to extreme flooding with depth greater than 2.0 meters, and these proportions increase to 0.21-6.10% during the 2080-2100 period.

Wildfire threat varies geographically, and Radke et al. (2018) make use of the projections by Westerling (2018) for a regional analysis that estimates the amount of area burned by large (> 1000 acres or 1.56 square miles) future

wildfires. These projections were used to determine which regions and TFS assets in California are potentially threatened by large wildfire events. In a complementary analysis, Radke and Biging (2018) also pursued high spatial resolution analysis (5 meters or 16.4 feet) to assess wildfire hazard with fine precision at the individual asset level. By identifying the wildfire heat exposure hazards, TFS asset managers can assess their own vulnerabilities and damage scenarios, develop targeted risk mitigation strategies, and prepare for wildfire events where firefighters cannot control wildfires around the asset. While the detailed interaction between fire risk and TFS assets analyzed by Radke and Biging (2018) focused on assets in the Sierra foothills, supply lines extend this vulnerability into the San Francisco Bay Area.

Radke et al. (2018) conclude that product pipelines and central distribution terminals are the most critical assets within the TFS network from the perspective of climate vulnerabilities. Their statewide analysis identifies that docks, terminals, and refineries are the most exposed TFS assets to coastal flooding, whereas roads and railroads are the most exposed assets to wildfire. In response, stakeholders are planning to adopt hardening measures, such as improvements on physical infrastructure, as well as resiliency actions, including improvements to behavioral responses at the organizational level. Fine spatial resolution exposure projections are also effective tools to facilitate stakeholder discussions. The fact that many low-income and under-represented communities sit near TFS facilities reinforces the community vulnerabilities through the effects of multiple stressors and limited resources to making preventative investments.

Interdependence with Other Sectors

Radke et al. (2018) concluded that the TFS network depends on supporting inter-connected sectors such as electricity and gas, and that the vulnerability of the TFS network has two external impacts beyond disruption of its own operations: (1) failures in the TFS network disrupt the transportation systems that rely on it for fuel delivery; and (2) disruptions to transportation fuel delivery will place increased pressure on the state's emergency management infrastructure, both through the direct risks associated with TFS failure and through reduced capacity due to a lack of fuel delivery.

Energy Consumption and Distributed Generation

HIGHLIGHTS

- Warmer summers will increase summer energy demand across the region, with the largest increase expected in coastal cities as air conditioning adoption grows there. Warmer winters will lead to decline in winter heating demand.
- Building energy demand is higher in inland regions (warmer summers/cooler winters), so reducing Bay Area energy consumption will strongly depend on where new housing and business growth are located.
- Increasing building energy efficiency and resilience at a regional level will be challenging due to large numbers of older houses, multi-family housing units, and small office buildings.
- Changes in daily and seasonal energy demand, coupled with increased reliance on solar and wind energy, create novel challenges in management of the electrical grid.
- Since transportation accounts for 40% of the Bay Area's GHG emissions, reducing vehicular fossil fuel consumption through both adoption of zero-emission vehicles and by reducing vehicle miles traveled is crucial, a shift that will also produce substantial public health benefits. The shift to electric vehicles will require large investments and innovations in charging infrastructure.

This section examines the demand side of Bay Area energy usage. We consider the energy needs for buildings and vehicles separately, and highlight the expansion of PV installation and its value for building and vehicle energy needs.

Building Design, Smart Buildings

One striking feature of the Bay Area is the age of the building stock[8]. Nearly half of the housing stock was built before 1969, years before the first building codes became law in 1974 (BayREN 2017). Older homes often lack insulation, and most have single-paned windows and can benefit from energy-saving retrofits. Another important element is that the Bay Area has over 700,000 housing units with five or more units in multifamily buildings. This represents 25% of Bay Area housing units and almost a quarter of statewide multifamily units. Multi-family housing is difficult to retrofit because tenants do not own the unit and building owners have little incentive to invest in upgrades. The Bay Area is home to about 62,000 office, retail, hotel, and industrial buildings. The great majority of these buildings (over 90%) are less than 25,000 square feet. These buildings are part of the Small and Medium Business sector and can be difficult to successfully reach for retrofit. Large owner-occupied and government buildings are more accessible for energy efficiency retrofit programs.

Considering anticipated trends in both summer and winter temperatures, we can anticipate how building energy demand for cooling (air-conditioning electricity demand, summer months) and heating (natural gas demand, winter months) will evolve in the coming century. Warmer summers will increase summer energy demand across the region

8 This section draws heavily on data from the Bay Area Regional Energy Network. The BayREN is a collaboration of the nine Bay Area counties led by the Association of Bay Area Governments. Bay Area Regional Energy Network. BayREN Energy Efficiency Business Plan 2018-2025. Jan. 2017.

(Auffhammer 2018), with the most pronounced increase occurring in coastal urban settings as air conditioning adoption grows in these communities (see further discussion below in the context of public health). Milder winter temperatures will decrease winter energy demands (Auffhammer 2018), and the most pronounced effect is likely to occur in inland suburban and exurban regions; the moderating effect of the Pacific Ocean on winter temperatures in coastal regions result in low heating demand under current climates.

A key element of California's energy and environmental policies for buildings is to invest in retrofits and move toward zero net energy (ZNE) buildings. In such units, on a source energy basis, the actual annual consumed energy is less than or equal to the on-site renewable generated energy. The Bay Area's mild climate provides a good location for ZNE buildings - over a dozen ZNE commercial buildings have been built in the region (New Buildings Institute 2016). One notable site, the Zero Net Energy Center in San Leandro, is a training facility for electric workers (Zero-Net-Energy-Center n.d.). The building is designed with advanced energy efficiency to achieve ZNE. The site features natural daylighting with operable skylights, exterior windows, and solar light tubes. The building also uses advanced controls integrated with natural ventilation and passive cooling. The efficient design allows the roof to provide all of the space needed for the photovoltaics (PV) to support ZNE performance.

A related trend in the Bay Area is the growing capability of solar PV systems. In fact, San Francisco alone has more than 6500 buildings with PV systems. Unfortunately, less than 1% of these systems can be used if there is a power outage, which could be caused by emergencies such as earthquakes, distribution circuits overheating, or fires. A recent Department of Energy-funded study led by SF Environment (the city's sustainability office) and supported by the Lawrence Berkeley National Laboratory developed guidelines to improve the use of existing PV systems during an electric outage for resilience and community microgrids.[9]

While the number of ZNE buildings and the greater use of PV systems reduce greenhouse gas (GHG) emissions in the Bay Area, the impacts on the timing of electric loads are problematic. Homes and commercial buildings with PV systems create a sharper ramp-up in the late afternoon, as sunlight decreases, contributing to the so-called "Duck curve." Figure 15 shows California's net load curve (net load is defined as the

FIGURE 15

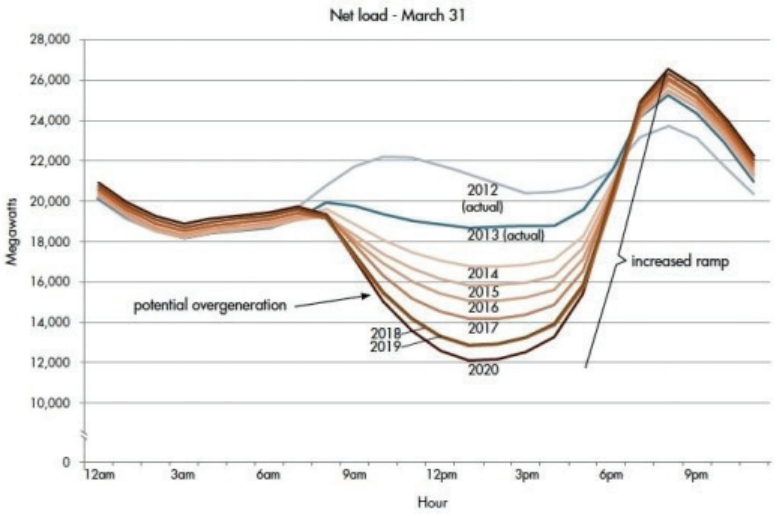

California's Duck Curve showing the daily cycle of net energy load.

Source: https://www.caiso.com/documents/flexibleresourceshelprenewables_fastfacts.pdf

9 https://sfenvironment.org/solar-energy-storage-for-resiliency

energy required from non-renewable sources to supplement on-site renewable generation). The electric system is difficult to manage with such a steep afternoon ramp. This problem is growing and by 2025 will occur not only in spring, but in every month of the year (Alstone *et al.* 2016).

A recent study explored how to mitigate problems related to the Duck curve, in particular by using more electricity in the middle of the day or overnight and less in the late afternoon, thus shifting the daily load curve (Alstone *et al.* 2016). Public service announcements and variable pricing are two mechanisms for shifting individual and household electricity consumption. Buildings can also eventually provide demand response from dynamic and demand-responsive lighting, heating, and cooling. This can be achieved by more time-differentiated pricing as well as fast demand response to adjust building loads dynamically. Another element of this trend is the strong push toward electrification of buildings.

Several cities in the Bay Area (San Jose, San Francisco, Palo Alto) have pledged to reduce their carbon emissions by more than 80% by 2050[10] and the University of California has pledged a zero-emission building footprint by 2025. One key method to reach these GHG goals is to electrify buildings. Natural gas for space and water heating often accounts for greater levels of GHG than electricity use in California. As we move toward using electric heat pumps for cooling as well as space and water heating, we need to ensure these loads are controllable and do not result in the Duck curve having an even steeper afternoon ramp. The evolving Internet of Things supports the control of emerging electric loads. New technology to measure, control, and integrate building end-use loads is developing quickly. In particular, collection and analysis of smart meter data offer new insights into energy use trends.

Electric Vehicle Adoption and Charging Infrastructure

Transportation accounts for about 40% of the Bay Area's GHG emissions[11]. Consequently, reducing California's vehicular fossil fuel consumption through adoption of zero-emission vehicles (ZEVs) (or reducing vehicle miles traveled, see Land Use section, below) is crucial for reducing California's GHG emissions. For the Bay Area, the important role that automobile emissions play in reducing the region's air quality means that a shift to ZEVs will have associated public health benefits. Making ZEVs affordable and convenient for people in the Bay Area will require thoughtful and strategic investments by both public and private sectors.

For the purpose of discussion in this section, we consider the general group of plug-in electric vehicles (PEVs), which replace internal combustion engines with electrochemical batteries and electric motors, to be divided into battery electric vehicles (BEVs) and plug-in hybrid electric vehicles (PHEVs), which still use small amounts of fossil fuel as backup. The economic cost and driving range of PEVs are primarily dictated by battery technology. Over the past 10 years, we have witnessed PEV battery prices fall from 1000 USD/kWh to about 250 USD/kWh (Nykvist & Nilsson 2015). These declining costs, albeit crucial to enabling PEV adoption, are not the only necessary ingredient for transitioning California's fleet to ZEVs. We also require a robust EV charging infrastructure to fuel these vehicles.

There are two distinct categories of non-residential PEV charging infrastructure: *destination charging* and *fast charging*. Destination charging refers to infrastructure placed at destinations, such as homes, work, or shopping centers. These chargers are distributed throughout urban areas and typically achieve a full charge in several hours.

10 https://www.sierraclub.org/ready-for-100/commitments

11 http://www.baaqmd.gov/research-and-data/emission-inventory

Fast charging refers to infrastructure placed along intercity corridors, e.g., between the Bay Area and Southern California. These fast chargers can provide a partial charge in less than one hour, to complete the trip. Both categories of PEV charging infrastructure are required to transition California's transportation fleet.

An integrated approach to PEV charging infrastructure planning requires consideration of both energy and transportation systems, since total ("well to wheel") GHG emissions for PEVs must include emissions created by the electric power generators used to charge the vehicles (Tamayao *et al.* 2015). Consequently, if the objective is to minimize GHG emissions due to transportation, then planning EV charging infrastructure must be considered in tandem with the electric power infrastructure. Recent research has focused on planning EV fast charging stations by jointly analyzing the transportation and electric power networks (Zhang *et al.* 2016, 2017). This work provides one of the first comprehensive approaches to understanding EV charging infrastructure planning across this interdisciplinary boundary.

The implementation of destination charging requires infrastructure to be developed and installed at commercial locations, such as shopping centers, hotels and business parks. Adding EV chargers to these locations can significantly increase electric bill costs, particularly the demand charges associated with peak usage. Demand charges comprise a significant portion of commercial and industrial customers' total electricity costs, typically between 30% and 70%. Adding EV chargers to these sites can significantly increase these costs, further challenging the transition to PEV transportation.

A compelling solution to each of the aforementioned issues is "smart charging." Smart charging refers to automatically controlled charging of PEVs that reshape their power consumption to provide benefits to the PEV infrastructure owner and/or grid operator. At the household level, for example, peak charge structures can create incentives to redistribute demand to periods when regional demand is low. Smart charging can also be applied to minimize the well-to-wheel GHG emissions, by shifting charging to times when the highest percentage of low-carbon electricity sources are online. Recent work has included proof-of-concept computations that scheduled large fleets of PEVs to flatten the Duck curve described in the previous section (Le Floch *et al.* 2016).

A robust PEV charging infrastructure is not yet available. Although significant funds are being allocated to build EV charging infrastructure, such as $100 million per year from California's Alternative and Renewable Fuel and Vehicle Technology Program (ARFVTP, www.energy.ca.gov/altfuels/) and $800 million distributed over 10 years from the Volkswagen settlement for ZEV projects in California, whether the state will efficiently plan and operate this infrastructure remains an open question. To accelerate this transition, we require more investment into research and technology around smart charging and PEV infrastructure planning tools. Moreover, pilot projects should provide open source data to enable rapid scaling and learning. Finally, economically disadvantaged communities often can experience the greatest benefit from ZEV transportation, due to low operational costs and benefits for local air quality. Mechanisms to provide these communities with equitable access must be investigated.

Interdependence with Other Sectors

Future energy demand will be impacted by climate and has important interdependence with land use, transportation and public health. Of particular importance from the perspective of building energy consumption are geographic shifts in population and employment. Building energy demand is higher in inland regions, due to both warmer

summers and cooler winters relative to the coast, so energy consumption in the employment and commercial sector will strongly depend on future regional development. At the same time, shifts in residential distributions may increase or decrease commute times, depending on the trajectory for the region and where densification does or doesn't occur. Longer commutes will create increased energy demand for the transportation sector, but this must be interpreted relative to building energy consumption. Finally, investments in building climate control are critical to reduce public health risks from heat waves, discussed below with reference to the 2017 heat wave in San Francisco.

We conclude this section by noting that each of these steps towards adaptation, whether in buildings or in vehicles, requires the investment of additional resources versus alternative approaches. Low-income individuals and households will have limited capacity to electrify, and renters will have limited control over the structure and function of their homes or apartments. Widespread adoption in the region will therefore be limited by socioeconomic inequalities until and unless these energy-saving strategies become affordable for all.

BOX 5: FIRST COUNTY IN CALIFORNIA WITH ITS OWN CLIMATE AUTHORITY

Sonoma County Regional Climate Protection Authority (RPCA)

Sonoma County's RCPA was formed in 2009 to provide a formal collaborative structure on climate protection for nine cities and multiple countywide agencies. The RCPA helps its stakeholders to set goals, pool resources, and create partnerships across silos. It also coordinates local activities with state and federal entities. The RCPA is governed by a board of 12 elected officials — nine representing cities and three from the County Board of Supervisors — and provides an invaluable forum for in-depth discussions on climate planning, program management, and project delivery. The RCPA has developed Climate Action 2020 (countywide greenhouse gas reduction implementation program), produced a set of Climate Adaptation forums to educate and broaden support for building resilience, created Shift Sonoma County (transportation greenhouse gas reduction), and has assisted with numerous countywide projects such as Sonoma Clean Power and the innovative PAYS financing program for home water improvements. In 2014, the RCPA and the local governments of Sonoma County were designated Climate Action Champions by the White House, in recognition of their outstanding leadership in climate action.

Public Health

HIGHLIGHTS

- Bay Area public health is threatened by a number of climate-related changes, including more extreme heat events, increased air pollution from ozone formation and wildfires, longer and more frequent droughts, and flooding from sea level rise and high-intensity rain events.
- High levels of socioeconomic inequity in the Bay Area create large differences in the ability of individuals to prepare for and recover from heat waves, floods, and wildfires. Financial resources as well as improved social structures are important to enhance community resilience and reduce these disparities.
- Heat waves pose increased health risks due to urban heat islands and the lack of local experience and cooling infrastructure (air conditioning) in bayside cities. These risks are compounded for low-income communities.
- Hazardous waste sites across the region are at risk of flooding with future sea levels. Release of contaminants, particularly in low-income and densely populated communities, creates a serious and direct health risk.
- Climate-related disruption of the transportation network creates three key risks for public health: the capacity of people to evacuate and move away from danger; the difficulty in accessing hospitals and other health-related infrastructure; and the reduced ability of hospitals, clinics, and emergency responders to operate.

Long-term climate change creates a variety of direct and indirect threats to human health, but with geographic variability impacting the severity of each threat. Ekstrom and Moser (2012) outlined the threats for the San Francisco Bay area due to increased frequency and magnitude of extreme heat events, changes in precipitation (including both more intense events and the potential for longer and deeper droughts), and long-term sea level rise. Direct effects include a broad spectrum of heat-related diseases, ranging from heat exhaustion to heat stroke to death, and injuries and fatalities that result from severe weather. Indirect effects of climate change on human health arise from connections of climate and weather conditions with health responses. Examples include air pollution, pollen and allergens, water quality and harmful algal blooms, disease vectors (insects and rodents), and supply of water and food. As climate change transforms conditions for each of these elements, threats to human health emerge. In aggregate, if conditions deteriorate in a region or subregion, human migration will follow, as people seek new homes that can better support their health and well-being.

Health risks due to climate change are strongly influenced by broader issues related to community vulnerability and resilience. While it may be obvious that economic strength and financial resources are important to community preparedness and response, the role that social structures play in preparing communities is now emerging more clearly. An example of the role that social networks and supporting infrastructure can play is seen in the Chicago heat wave of 1995 (Klinenberg 1999). In that instance, the most important factor that reduced death rates in local communities was the presence of strong social networks ensuring that community members were looking out for each other.

Regardless of the particular type of event, it is understood that shifting conditions and increasing disruptions of normal activity by extreme environmental events can have negative effects on mental and emotional health. This risk is elevated among communities in which basic needs themselves are threatened by the changing climate. Social and economic factors impact both the exposure and ability of vulnerable communities to adapt to climate change, and as a result, health outcomes from heat, air quality, wildfires, etc., due to climate change are amplified and multiplied in these communities.

In the Bay Area, the threats of climate change for human health vary within the region, with coastal urban communities having different vulnerabilities than inland suburban and exurban communities due to differences in environmental conditions and the magnitude of climate change impacts. Further, socioeconomic variability is high in the Bay Area, which creates large inequities in the vulnerability to health risks associated with climate change. In the remainder of this section, we develop descriptions of individual and community health vulnerabilities by considering those processes that may be exacerbated by climate change.

Direct Impacts of Heat and Heat Waves in the Bay Area

More frequent, larger magnitude, and longer duration heat waves are already emerging as an important aspect of climate change in the Bay Area (see Regional Climate Science section, above). A key factor in surviving these events is the level of preparedness at both the local and community scale. Because of this, at the moment, coastal regions of the Bay Area are more at risk than inland communities due to differences in both individual acclimatization and investment in protective infrastructure (CNRA 2009). The risk for coastal communities in the Bay Area is exacerbated in urban settings (San Francisco and Oakland) due to the urban heat islands they create, which results in nighttime temperatures that do not cool as they would in natural conditions. Elevated nighttime temperatures, which can be as much as 22°F (12 °C) higher in urban settings (CNRA 2016), eliminate the physiological benefit of periodic cooling leading to cumulative heat effects and elevated risks of illness and death (Chan *et al.* 2001).

As an illustration of the devastating impacts of heat waves in Bay Area urban communities, we need look no further back than the fall of 2017. At the beginning of September, a series of all-time high temperature records were set in San Francisco and Oakland. These events overwhelmed the protective and social infrastructure in San Francisco, resulting in 6 deaths and 38 hospitalizations (Rodriguez 2017). During these heat events, temperatures are just as high or higher in inland suburban communities than they are at the coast, but the preparedness in the inland communities is greater. Not only are individuals in inland communities acclimated to hot temperatures, but more cooling infrastructure is available to protect against severe heat illness (i.e. air conditioning at home, work, stores, and community centers) (CNRA 2014). While some of this difference can be attributed to socioeconomic factors, the commitment of resources to cooling infrastructure and the acclimatization of individuals are due to the high frequency of hot days those communities face.

This vulnerability gap between inland and coastal communities suggests that increased investment in cooling infrastructure in coastal areas of the Bay Area will be an important component of climate adaptation. Nonetheless, the intermittent nature of heat events in the coastal urban communities means less widespread adoption of air conditioning, leaving them more vulnerable than their inland counterparts. This gap is compounded for low-income communities, in which individuals are unable to invest in these protective features, and community-based cooling center availability is likely to be very limited (Ekstrom & Moser 2012).

Impacts of Wildfire on Vulnerable Populations

Wildfires disproportionately impact vulnerable populations, due to health disparities, higher risk of job loss during economic downturns, and lower access to social resources, exacerbated by language barriers, lower internet access, and unwillingness to contact authorities for undocumented individuals (Cornwall *et al.* 2014). Renters and lower-income home owners generally have lower financial capacity to build or upgrade to fire-safe building codes and maintain defensible space, and have higher rates of uninsured or underinsured homes and belongings lost in fires (Cooley *et al.* 2012). The >5,500 structures lost in the Tubbs Fire represented about 5% of the housing stock for the city of Santa Rosa. In a region with elevated housing prices and low availability, these losses have caused considerable displacement, especially for low-income residents.

Air pollution from wildfire smoke, especially particulate matter, creates higher risks for children, elderly, and those suffering from respiratory illness (Lipsett *et al.* 2008). Burning structures and vehicles also release high levels of toxins (from building materials, paints and solvents, etc.) creating greater health risks compared to vegetation fires. Control of particulate matter pollution is a major factor that limits the scope and frequency of prescribed burning, especially near populated areas. However, more research is needed to determine if higher levels of prescribed burning would lead to a net reduction in health risks by reducing the risk of high severity wildfire and associated structure fires. Mechanical fuel treatments can achieve some of the same benefits as prescribed fire, without creating air pollution, and may offer the only viable option near populated areas (Moghaddas *et al.* 2018).

BOX 6: HELPING BAY AREA HEALTH DEPARTMENTS TAKE ON CLIMATE CHANGE

Bay Area Regional Health Inequities Initiative (BARHII)

After a major (and successful) effort with health, social, and environmental justice allies to move health equity issues into the Bay Area's first Sustainable Communities Strategy (Plan Bay Area), BARHII has expanded its focus to include building community resilience to the impacts of climate change.

To support the capacity-building of Bay Area health departments, BARHII has developed five two-page "Quick Guides" on why climate change is a public health and equity issue, the environmental and health co-benefits of climate change action, how to get involved in climate change action planning, and tangible steps to address climate change.

- Guide 1: Climate Change: What's Public Health Got to Do With It?
- Guide 2: Health and Equity Co-Benefits of Addressing Climate Change
- Guide 3: Climate Change and Health Equity
- Guide 4: How Public Health Can Address Climate Change
- Guide 5: Getting Involved in Climate Change Action Planning

Indirect Impacts of Climate Change on Health Due to Air Quality

Three factors dominate the landscape of air quality in the San Francisco Bay Area: (1) ozone pollution during the summer (and, increasingly, the fall); (2) particulate matter during the fall and winter; and (3) allergen production and distribution during the spring and summer. Vulnerable individuals and communities experience the impacts of these contaminants through asthma, lung disease and cardiovascular health risks (Bernard *et al.* 2001). While these risks exist today, we focus here on the direction and mechanisms by which climate change is likely to exacerbate them.

The reactions that create ozone are facilitated by higher ambient temperatures, leading to increases in near-ground and near-source ozone hot spots. While emissions that are the precursors to ozone production may decrease in the coming decades, the net effect for the Bay Area is expected to be an increase in ozone levels (Steiner *et al.* 2006) (Figure 16).

FIGURE 16

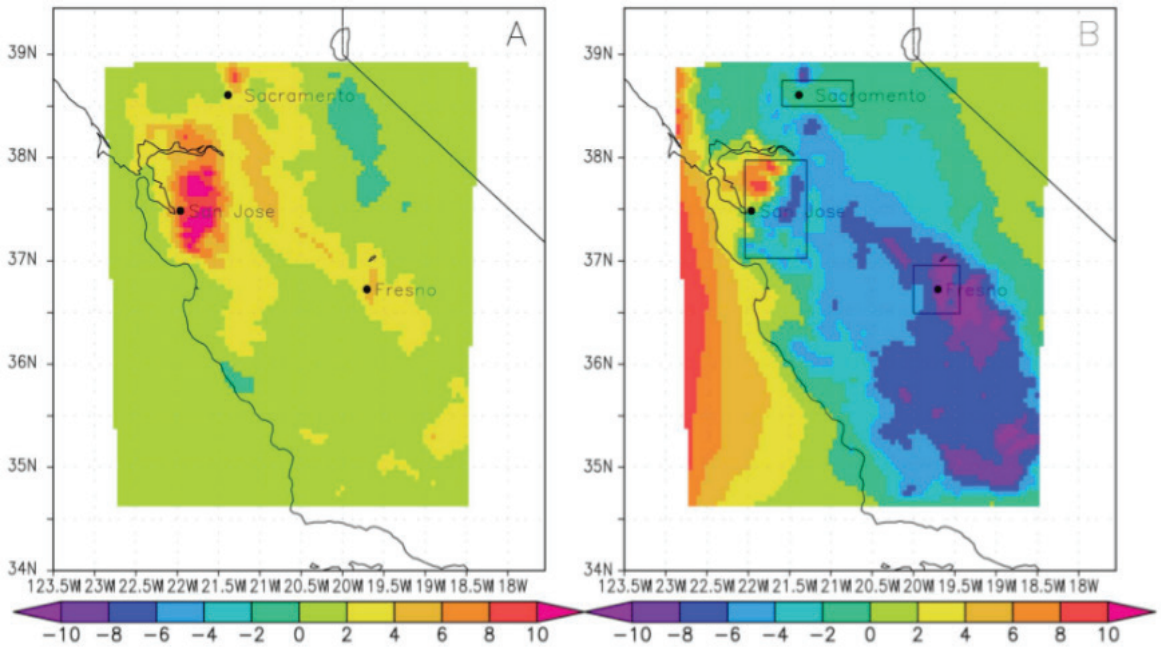

Change in ozone concentration (3 p.m. local time) for (a) combined climate effects; and (b) including emissions reductions. For the Bay Area, increases in ozone concentration mostly increase, except in the far southeast portions of the region, where reduced emissions dominate the increases due to climate factors. Source: Steiner et al. 2006

During the fall and winter months, the dominant consideration in Bay Area air quality conditions is the near-ground trapping of particulate matter by high pressure systems. Recent studies of global circulation have shown that the loss of arctic ice cover has resulted in a change in winter weather patterns. Historically, high pressure systems tended to alternate with low pressure systems over the Western United States on a synoptic timescale of 4-7 days. In recent years, however, high pressure systems have been locked in place over the Western United States for weeks, or even months, during the winter. This response to global climate conditions (termed the "ridiculously resilient ridge" of high pressure) (Swain 2015) not only creates drought conditions for California, but it also leads to deteriorating air quality in inland Bay Area communities due to the persistent trapping of particulate matter in inland valleys.

The combination of heat waves and persistent high-pressure systems during the fall months is leading to wildfires of increased frequency and magnitude. Urban wildfires in the region, and large wildfires to the north and east of the Bay Area, undermine air quality in the Bay Area through the creation and distribution of particular matter in the lower atmosphere, leading to increased hospitalizations and even deaths due to cardiovascular and asthma related emergencies (see further discussion below).

Direct Health Risks due to Extreme Weather Events and Sea Level Rise

The most pronounced risk of life in the Bay Area linked to climate change is likely to be due to wildfires during summer and fall and landslides or sudden flooding due to extreme precipitation and infrastructure failures during the winter. The wildfires in Fall 2017 in the Northern Bay Area (Santa Rosa, Sonoma, Napa County) killed 44 people and hospitalized 185. Prior to this event, the largest urban wildfire in the Bay Area was the 1991 Oakland-Berkeley Hills Fire, which killed 25 (Ekstrom & Moser 2012). As described in the Regional Climate Science section, and as discussed above in the context of land use changes, future heat conditions, combined with development at the urban edge, increases the risk of future wildfire events for human health and lives.

In Bay Area hills, the risk of landslides is a function of the interaction between precipitation and soil conditions (Collins *et al.* 2012), and seismic activity. Climate change creates increased likelihood of extreme precipitation and wildfire events; both create increased risk of slope failures for the coming century.

Sudden flooding events in the greater Bay Area are most likely to result from levee system failures, which are increasingly likely due to higher river flows, higher sea levels, and seismically poor levee structures. Exacerbating this risk is the expansion of impervious surfaces in Bay Area watersheds and the subsidence of bayfront lands to the point that many waterfront communities are already below mean high-water levels. Communities like Alviso in the South Bay or Bethel Island in the Sacramento-San Joaquin Delta are already vulnerable to levee failure-induced flood events. Urbanized lower watersheds, which surround San Francisco Bay, exacerbate the risk of dangerous flood events, as was evident in San Jose during the Coyote Creek flooding of early 2017 (Giwargis 2017).

For low-income residents and communities, risks of isolation and lost resources are elevated in flooding events. Due to the fact that these residents have a lower rate of car ownership than the general population, they are heavily reliant on public transportation and frequently have limited mobility during extreme weather events and emergencies. During climate disasters, such as Hurricane Katrina (New Orleans, 2005) and Hurricane Harvey (Houston, 2017), people who had cars were able to evacuate, and those without (who also had limited public transportation options available) were often unable.

Bayfront nuisance flooding, which is created by sea level rise and high tidal conditions, poses little direct physical threat to human health, although it may undermine regional health through interdependencies described below. A health risk does emerge, however, when considering the mobilization of contaminants, or the deterioration of water quality, in response to long-term change. In the Bay Area, there are dozens of hazardous waste sites at risk of nuisance flooding with future sea levels. The mobilization of these contaminants, particularly in densely populated communities, creates direct health risk due to exposure to metals and petrochemicals (Heberger *et al.* 2009).

From the perspective of drinking water, rising sea levels and more variable precipitation and river flows mean the freshwater supply for much of the Bay Area (and State) is at risk due to salt water intrusion, both into groundwater aquifers (Heberger *et al.* 2009) and into the Sacramento-San Joaquin Delta (Chua & Xu 2014).

Interdependencies with Other Sectors

Interdependencies among different parts of regional infrastructure create risks to human health. Regional infrastructure networks, particularly the transportation, fuel distribution, and power networks, support human function throughout the region, including health-related infrastructure such as hospitals, clinics, and pharmacies.

Disruption of the transportation network, as would occur due to flood or fire, creates two risks for public health: (1) the capacity of the system to evacuate from the event itself may be reduced; and (2) individuals may have difficulty accessing hospitals and other health-related infrastructure. Power and fuel distribution networks provide support for powering health infrastructure, and the capacity of hospitals, clinics, and emergency responders will be reduced by disruptions. Finally, disruptions to the water delivery or wastewater treatment systems would create risks to public health, particularly if the disruptions persisted for more than a few days.

BOX 7: FOCUSING ON VULNERABLE POPULATIONS

San Francisco Climate & Health Profile

San Francisco's Department of Public Health, with funding from the Centers for Disease Control and Prevention, developed a 44-page profile that identifies local climate impacts and associated potential health outcomes, highlighting populations and locations in the city especially vulnerable to these changing conditions.

By systematically using climate projections to prioritize the most critical health impacts and risk factors, the profile reveals essential information needed to take adaptation actions to protect San Francisco residents. By utilizing the best climate science available and engaging community partners to understand vulnerabilities and interventions for communities and populations at highest risk for illness, the profile helps to advance urban health and environmental justice in the climate and health field.

Although all San Franciscans will be affected by climate change, certain San Franciscans will be affected more than others. The profile shows that residents who live, work or recreate along San Francisco's waterfront are more vulnerable to flood risk. Those in areas with poor air quality or limited access to open space are vulnerable to heat-related hazards. In particular, the urban poor are most vulnerable to climate change as its impacts amplify socioeconomic and racial disparities. The degree to which an individual San Franciscan is impacted by climate change often depends on his or her age, race, income, language, educational

BOX 7: FOCUSING ON VULNERABLE POPULATIONS

attainment, housing conditions, and pre-existing physical conditions such as diabetes and mobility disabilities.

After analysis of environmental, demographic, and socioeconomic infrastructure and individual pre-existing indicators, the profile concludes that certain neighborhoods in San Francisco will be disproportionately affected by climate change: Chinatown & Downtown, Bayview Hunters Point, Soma, Excelsior, Crocker Amazon, Visitacion Valley, and Treasure Island.

HAZARD	CLIMATE IMPACT	HEALTH IMPACT
Heat	Average yearly temperature to increase between 4.1 and 6.2 degrees Fahrenheit by 2100	Heat-Related Illness
		• Dehydration
		• Heat Stroke
	Extreme Heat Days (over 85F) to increase by 15-40 by 2050 potentially 90 by 2100	Heat-Related Mortality
		• Heart Disease
		Air Quality Effects
	Increase in heat wave length and frequency	• Respiratory Illness
		• Asthma
		• Allergies
		Mental and Behavioral Health
Sea-level Rise	Sea-levels projected to rise between 7-15 inches by 2050, 25-46 inches by 2100	Fatal and Nonfatal Injury
		Water-borne Disease
		Mental and Behavioral Stressors
		Income Loss
Extreme Storms	As precipitation levels fluctuate year-to-year, in rainy years, the frequency and severity of extreme storms is predicted to increase	Fatal and Nonfatal Injury
		Water-borne Disease
		Mental and Behavioral Stressors
		Strain on public health infrastructure
		Income Loss
Drought	As precipitation levels fluctuate year-to-year, in dry years where the high-pressure system off the coast does not dissipate, the frequency and severity of droughts will increase	Food Insecurity
		• Malnutrition
		Air Quality / Allergens
		• Respiratory Illness
		• Asthma
		• Allergies
		Mental and Behavioral Health
		Income Loss

Natural Infrastructure

HIGHLIGHTS

- Natural infrastructure can play an important role in climate change adaptation, enhancing biodiversity and ecosystem services while reducing societal risks.
- Natural shoreline infrastructure includes options such as oyster beds, marshlands, and dune enhancement that reduce wave energy and shoreline erosion. In some locations, managed retreat may be the only viable option in the face of sea level rise.
- Urban parks and trees enhance cooling and provide shade and can strengthen social ties and local communities.
- The role of natural infrastructure to protect vulnerable communities may face tradeoffs related to displacement and public safety.

In this section, we discuss the role that natural infrastructure can play by providing indirect support for adaptation by either preserving the function of other infrastructure systems or through mitigating the extent of the event that other infrastructure systems must endure. We consider here two distinct types of natural infrastructure that are represented in the Bay Area: first we consider marsh and wetland habitats as an element of shoreline infrastructure and flood protection, and then we consider how urban green or open space may be protective against heat and other community risks.

Shoreline and Flood Protection Infrastructure

When considering the risk of bayfront flooding under scenarios of sea level rise, decision makers must face the multiple threats of sea- and bay-forced flooding (sea level variability plus tidal forcing), groundwater flooding (where the groundwater table emerges above the land surface), and watershed or stormwater flooding (precipitation and runoff). Integrated flood protection infrastructure must be developed with consideration of all of these sources of flooding, which may create the need for supplemental infrastructure systems.

For the Bay Area, the risks associated with sea level rise are of critical importance in the coming decades, including both tidal flooding (created by the daily high tides) and lower watershed flooding (interaction between bay water levels and flows in bay tributaries). The value of natural elements in these protective infrastructure systems lies in their ability to create a more resilient shoreline infrastructure and in the ecosystem benefits that may accrue from the habitats within the natural infrastructure elements (Newkirk *et al.* 2018). These benefits are described in more detail below, but we start with a discussion of the role that natural infrastructure would play in the primary goal of shoreline infrastructure, which is flood protection.

The first, and most important, aspect of shoreline planning and flood mitigation is determining where to place the protective shoreline infrastructure, and what areas are going to be protected from flooding by that infrastructure (Holleman & Stacey 2014; Wang *et al.* 2018). Controlling flood waters with infrastructure (regardless of whether it is engineered or natural) is a containment strategy; allowing flooding to proceed as it would naturally occur is a strategy of flood accommodation. Pursuing flood accommodation as a strategy in an urban environment will necessarily

require retreat – either out of a local region or vertically – or a fundamentally different type of community and its associated infrastructure systems, which can function while intermittently inundated. For any segment of protective shoreline infrastructure, the role that natural approaches can play should be considered within the local context, considering the specifics of the forcing and the needs of the community to be protected by the segment.

In a tidally dominated and urbanized estuary such as San Francisco Bay, the opportunity for truly natural shorelines around San Francisco Bay is relatively limited, due to the requirement that tidal marshes be allowed to progress inland and up the topographic gradient as sea levels rise. We note that this is in contrast to open coastal and beach environments, where natural features have steeper slopes and require less inland space for adjustment. For natural marsh shorelines to be allowed to evolve with forcing from sea level rise in an urbanized or otherwise developed community, retreat would be required. As such, this natural flood protection infrastructure approach, with natural processes allowing the shoreline to evolve in response to environmental variability, may consist primarily of retreat and restoration, and provide limited in-place flood protection for the existing waterfront communities.

For tidal and urbanized systems such as San Francisco Bay, unless a community pursues a flood accommodation strategy, the flood protection infrastructure must have an engineered or artificial element to them to constrain and alter the natural inundation patterns that would occur. The opportunity for natural infrastructure in San Francisco Bay therefore lies in hybrid approaches, in which natural elements are integrated into what would otherwise be engineered structures. The horizontal levee is an example: As seas rise, the fronting marshes in these structures will accrete sediment and their bed elevations will increase. In urban and developed regions that do not retreat, the marshes will not be able to progress landward, however, and the landward edge of the marsh will need to be an engineered structure to transition to lower elevations in the community.

With these limitations in mind, it is important to recognize that the use of natural features in engineered shorelines does bring with it a number of advantages and benefits (Newkirk *et al.* 2018). The presence of marsh or other vegetated habitat on the bay side of engineered structures reduces wave energy (Möller *et al.* 2014), which reduces the wave setup and hence the total water level that the engineered structure must endure. Further, the dissipation of wave energy by the marsh or other habitat leaves less wave energy impinging on the engineered infrastructure that is providing the flood protection. Thus, the use of natural habitats as a fronting feature to engineered structures can be an effective addition to the flood control infrastructure, reducing total water levels and wear-and-tear on engineered protections, creating a more resilient hybrid infrastructure system. Further, the development of natural habitats as a part of the shoreline protective infrastructure creates habitat benefits for Bay ecosystems, including support for endangered species, ecosystem diversity, and recreation.

Urban Green Space and Trees

The role of urban parks and green space in community resilience to climate change and environmental disruption includes both mitigating the effects of climate change itself and providing stronger social connections for the community to respond to events.

First, as noted in the Regional Climate Science section, the density of trees, green space, and irrigation can play an important protective role in urban communities by reducing the heat island effect by several degrees. As discussed above, higher temperatures, particularly during the nighttime, in urban communities increase the risk of heat-related

illness compared to suburban or rural communities. The presence of trees and parks provides a protective element against this risk factor.

Secondly, the presence of parks and open space can create social linkages in the community, even if only at the scale of tree-lined sidewalks or "parklets" (Klinenberg 1999). These social ties are a critical component in establishing the resilience of the community to environmental events, including those worsened by climate change. Using the Chicago heat wave of 1995 as a case study, Klinenberg established that the presence of sidewalks and inviting public space in one neighborhood resulted in strong social networks and a lower fatality rate than in an otherwise similar neighborhood. This type of "natural infrastructure" is frequently overlooked when discussing protective infrastructure because it is through the social system that the protection is achieved, and the social functions are enhanced by the open space.

Disadvantaged Communities

The advantages of natural infrastructure as protection from either flooding or heat-related risks associated with climate change may not be easily achieved in disadvantaged communities. From the perspective of vulnerable communities along the bay shoreline, a retreat-and-restore strategy for flood protection may achieve the same end point as would gentrification: community displacement. Further, urban green space is limited and tree density is small in disadvantaged communities (Jesdale *et al.* 2013), so targeted investment at a relatively large scale would be required to mitigate urban heat island effects. A lower cost opportunity may lie in creating inviting open space to facilitate strong social networks and to improve community resilience.

Economic Resilience

HIGHLIGHTS

- The disruption of Bay Area commerce by climate change will likely be most strongly influenced by inundation and flooding in bayside communities and commercial areas.
- While bayside communities are on the front lines for future flood risk, many of them have limited ability or resources to pursue adaptation strategies.
- Without inclusive engagement among communities, disparities in economic and political power will undermine regional solutions and leave communities acting independently, with highly variable results for resilience and community health.

In a recent interview with the San Jose Mercury News (Baron 2018), former Stanford President John Hennessey identified housing and transportation shortfalls as the biggest risks to the future sustainability of Silicon Valley. Both of these factors are strongly impacted by climate vulnerability and disruptions, as noted above in discussion of the transportation network and changes in land use. The disruption of Bay Area commerce by long-term climate change will likely be most strongly influenced by the interaction of sea level rise with extreme storm events, creating inundation and flooding in lower elevation communities and commercial areas. The "Risky Business" report

concluded that $62 billion worth of property and infrastructure are at risk under moderate (4 feet) end-of-century sea level rise scenarios. Some 160,000 Bay Area residents would face disruptions either at home or at work with sea level rise of just half the end-of-century value. (*Risky Business: The Economic Risks of Climate Change in the United States* 2015)

From a community impact perspective, it is instructive to examine similarities and differences among communities to understand the nature of their vulnerability to long-term sea level rise. Hummel et al. (2017) overlaid inundation projections with census data to define exposures, then used formal clustering analysis to identify similar communities based on variables with particular links to community resilience. The analysis led the authors to two general conclusions. First, communities that are clustered together are frequently not geographically proximate. For example, San Rafael's Canal District and East Palo Alto share many of the same socioeconomic factors that underpin community vulnerability. Secondly, clustering of communities varies significantly through time, with more similarities emerging as sea levels rise. For example, under current conditions, Foster City seems to be unique in the threat that it faces, but by the end of the century, three additional communities will face similar risks to their populations. These results may help to build regional resilience through improved communication about adaptation approaches.

Finally, we must acknowledge the key role that social equity and environmental justice must play in considerations of regional resilience for the Bay Area. There is wide disparity in the ability of Bay Area communities to invest in climate change adaptation, which reinforces a "go-it-alone" approach to shoreline management. Due to historical development patterns and regional investment, low elevation communities (the bayfront communities most susceptible to flooding) are also frequently disadvantaged. While these communities are on the front lines for future flood and inundation risk, they themselves have limited ability or incentive to pursue adaptation strategies. Further, their vulnerability is reinforced by this positioning, and experiences both within the region and beyond have led vulnerable communities to fear that adaptation strategies may increase the attractiveness of their communities to outside investors, resulting in displacement.

Taken together, regional resilience planning will necessarily integrate threats to infrastructure and social systems into discussions that engage all communities around the bayfront. Absent such inclusive discussions, disparities in economic and political power will undermine regional solutions and leave communities acting independently and individually, with highly variable results for resilience and community health.

BOX 8: CREATING A REGIONAL APPROACH FOR SEA LEVEL RISE

RISeR SF Bay — Resilient Infrastructure as Seas Rise (riser.berkeley.edu)

RISeR SF Bay is a silo-busting sea level rise project for the Bay Area looking at hydrodynamics, transportation, governance, and other critical topics. The RISeR team includes engineers from UC Berkeley, transportation experts from New York University Abu Dhabi, political scientists from UC Davis, and ocean and sea level rise experts from the U.S. Geological Survey. A stakeholder advisory group from the Bay Area's public, private, and nonprofit sectors provides important input and feedback for the project.

The first phase of the hydrodynamics work has created state-of-the-art modeling for the San Francisco Bay showing how sea level rise protection projects built in one county would affect water levels and flooding in nearby counties. RISeR is demonstrating that regionalism isn't just a good *idea* — regional collaboration and decision-making on sea level rise will be required to protect and enhance critical infrastructure, human health, and our natural systems. It is also showing how local cities might group themselves for collaborative planning.

Similarly, in RISeR's transportation modeling, the team is showing how flooding of a local segment of a single freeway can produce far-reaching traffic impacts on other sections of the Bay Area transportation network. Again, regional collaboration will be needed to address these regional issues.

In the governance area, RISeR is studying the complex network of actors engaged in Bay Area sea level rise planning and recommending a first set of steps to improve regional decision-making. This work also includes polling and other methods to better understand public knowledge and viewpoints on sea level rise solutions for the region.

BOX 9: COMPREHENSIVE SEA LEVEL RISE VULNERABILITY ASSESSMENTS: 4 BAY AREA COUNTIES

Marin County, San Mateo County, Alameda County & Contra Costa County

Four Bay Area counties have completed detailed, in-depth assessments of their vulnerability to flooding from sea level rise and extreme storm events. These assessments will provide the scientific basis to design, fund, and implement a wide range of strategies to protect infrastructure, natural systems, and human health.

Marin County actually has two assessments, C-SMART for its ocean-facing areas and BayWAVE for Marin's considerable shoreline along San Francisco Bay and San Pablo Bay. Collaboration: Sea level Marin Adaptation Response Team (C-SMART) now includes both the Vulnerability Assessment and the Adaptation Report which identifies options for adaptation strategies for West Marin. The BayWAVE (Marin Bay Waterfront Adaptation Vulnerability Evaluation) Vulnerability Assessment is an informational document that catalogs impacts with six different sea level rise scenarios across the entire bay shoreline.

San Mateo County's extensive countywide effort on sea level rise is called Sea Change San Mateo County and includes assessments, projects, and public engagement activities. Their 215-page Vulnerability Assessment covers both the coast and the bay and looks in-depth at built infrastructure, natural areas, and human communities. The assessment includes regional networked assets as well as local assets and points to specific future actions and research gaps.

Alameda County was the first Bay Area county (2011-2014) to create a comprehensive sea level rise vulnerability assessment as the pilot project for the Bay Conservation and Development Commission's Adapting to Rising Tides program. The project included agencies and organizations from Emeryville to Union City and assessed the vulnerability and risk of shoreline and community resources to sea level rise and storm events. The project led to strategies to help communicate and resolve these complex issues, as well as processes to integrate adaptation into local and regional planning and decision-making. It also jump-started new collaborative adaptation planning efforts including the Hayward Shoreline and Oakland/Alameda Resilience Studies, the Bay Area Transportation Climate Resilience focus area planning efforts, the Capitol Corridor Passenger Rail vulnerability assessment, and the East Bay Regional Park District planning effort.

BCDC collaborated with Contra Costa County and local stakeholders on the Contra Costa County ART Project (2014-2016), covering a diverse shoreline from Richmond all the way to Bay Point. The project area, with its varying local topographies (from bluff to wetland to creek mouth), different types of land uses, diverse communities, and the presence of extensive rail and energy infrastructure, offered an excellent opportunity to better understand the diversity of vulnerabilities and consequences from current and future flooding. The project's Final Report includes assessment of 11 sectors as well as asset-scale evaluation of 15 representative assets.

Emergency Management

Immediate emergency response depends on the interaction between communication networks, transportation networks and public health and safety. Disruption of any of these systems by inundation events, landslides or wildfire would undermine emergency responses and leave populations vulnerable both during and immediately after an environmental event. Further, the reliability and safety of the region's housing stock should be evaluated in the context of emerging climate threats due to the fact that it is easier for a region to respond and recover from an emergency if the housing is habitable post-disaster.

The response time for emergency responders for specific communities under future inundation scenarios was explored by Biging et al (2012). Results for the city of Richmond for an end-of-century storm scenario (1.4 meters of sea level rise, 100-year storm event) are shown in Figure 17.

FIGURE 17

Delay in emergency response due to inundation of transportation network for Richmond, CA. Forcing scenario is 1.4 meters of sea level rise and a 100-year storm event. Areas shaded black are inaccessible due to the depth of inundation. Source: From Biging et al. 2012.

These results from Richmond are illustrative of the type of coupled response one can expect for bayfront communities. Emergencies due to environmental disruptions simultaneously undermine the infrastructure systems needed for the emergency response.

The emergency preparedness and response of vulnerable communities will be shaped by their specific socioeconomic conditions. In advance of any emergency event, low-income households are less likely to invest in preparedness. Thus, during extreme events, houses and structures may be less protected than others in the region and individuals may not be able to move to safety due to a lack of transportation or other resources. In the immediate aftermath of the event, those who rely on food banks, health care facilities, shelters, or churches may not be able to access these resources. Finally, longer-term community recovery may be inhibited by the fact that renters are less likely to have insurance. At the same time, households with limited English proficiency might not be able to understand emergency instructions or might not listen to emergency evacuation instructions because of fears regarding their immigration status.

Natural and Managed Resource Systems

The Bay Area is recognized as a hotspot of biodiversity within California and at a national scale (Myers *et al.* 2000). This diversity is supported by sharp climate gradients, rugged topography and heterogeneous soils, a big beautiful bay, and the majority of tidal wetlands in the state. These ecosystems provide "natural capital" for the region, including improved water quality and supply, carbon sequestration, outdoor recreation, flood control, and enhanced quality of life for a large urban and suburban population.

Plant and animal diversity and distributions in the Bay Area are strongly influenced by climate gradients. The most important of these are the coastal-inland gradient in temperature (including fog frequency and the inland penetration of the marine layer around San Francisco Bay), elevational gradients on local mountain ranges, and distinct rain shadows on the eastern slopes of the Coast Ranges. The Bay Area has about 3000 native plant taxa, with over 50 local endemics (i.e., species or subspecies found nowhere else in the world), and a diverse array of invertebrates and vertebrates occupying terrestrial, freshwater, estuarine, and marine environments.

Habitats and biodiversity of the Bay Area have been profoundly influenced by human activities, from the arrival of Native Americans 13,000 (or more) years ago, to the Spanish, the Gold Rush, and the expansion of urban areas and agriculture through the 20th century and into the 21st. Native Americans altered the California landscape by harvesting, hunting, and extensive burning (Anderson 2006).[12] The arrival of the Spanish brought intensive cattle grazing to California, and the introduction of European alien plants, many of which rapidly invaded and replaced native vegetation, particularly in grasslands and open oak woodlands. Aquatic and coastal ecosystems around the San Francisco Bay and estuary have been transformed by urbanization, dredging and levee construction, especially in the Delta, and the continued impacts of gold mining, dam construction, agriculture, and water diversions on fresh water flows, water quality, and sediment loads.

This section of the regional report draws on a previous report on the impacts of climate change on Bay Area ecosystems from California's Third Climate Change Assessment (Ackerly *et al.* 2012), updated with recent research and expanded discussion of agriculture, grazing lands, and aquatic habitats, including sea level rise impacts on the San Francisco Bay estuary.

12 Further information on how California's Tribal communities face unique threats from climate change – and how these communities are spearheading adaptation and mitigation efforts – can be found in a companion Fourth Assessment report (Tribal and Indigenous Communities Summary Report 2018).

Terrestrial Ecosystems

Impacts of Climate Change on Vegetation and Habitat Distributions

HIGHLIGHTS

- The future climate of the Bay Area will become less suitable for evergreen forests—redwoods and Douglas fir—and more favorable for hot adapted vegetation such as chaparral shrub land.
- Projected trends for grasslands are unclear and management (burning, grazing, etc.) will probably be more influential than climate change.
- The ability of vegetation to respond to the rapidly changing conditions in the 21st century is poorly understood. It is possible that vegetation will be increasingly "out of sync" with climate and vulnerable to heat and drought.

A recent high-resolution map of Bay Area vegetation distinguishes more than 25 major native vegetation types[13], from interior grasslands to coastal redwoods (Figure 18). The distribution of these vegetation types is strongly influenced by the climate gradients identified above, as well as local topographic effects due to solar radiation (south- vs. north-facing slopes), cold air drainages, wind on exposed ridges, and a complex mosaic of different soil types. In general, Bay Area vegetation consists of coniferous forests (redwood and Douglas fir) in the coolest and wettest environments (including areas of high fog influence); oak and other evergreen woodlands on deep soils and areas of moderate rainfall; shrublands on hotter and drier sites, especially steep slopes with thin soils; and grasslands scattered across the region under a wide range of climate conditions.

Future climates will be warmer, and increased temperatures will lead to greater summer aridity, even for future climates with increased winter rainfall (Ackerly *et al.* 2015). Several studies have projected the impacts of climate change on California vegetation at a statewide level (Lenihan *et al.* 2003, 2008; Stralberg *et al.* 2009; Shaw *et al.* 2011; Thorne *et al.* 2017) and in targeted studies of the Bay Area (Ackerly *et al.* 2015) (also see Chornesky et al. 2015). The studies use a variety of methods and different projections for future climates. Despite this range of methods, some consistent results emerge, offering broad guidelines for what to expect in the future.

Projections generally agree that conditions will become less suitable for evergreen conifer forests (redwoods and Douglas fir), and these impacts will be greater if rainfall declines (and, for redwoods, if fog frequency declines). Suitable conditions for these forests will contract toward the coast. Projections are less consistent for mixed evergreen forests and differ depending on the tree species. For example, coast live oak forests may be able to expand in the future, while cool and moist adapted forests such as tanoak, canyon live oak, and Oregon oak will likely decline (Ackerly *et al.* 2015). Projections are also uncertain for blue oak woodlands, with some models predicting the potential for expansion, especially under hotter and lower rainfall scenarios (Ackerly *et al.* 2015). There is general agreement that conditions will become more favorable for chamise chaparral shrubland, with the potential to expand from interior mountains toward the coast. On the other hand, cool adapted montane chaparral and coastal sage

13 Bay Area Open Space Council (2012) The Conservation Lands Network, http://www.bayarealands.org/

scrub are both projected to decline (Figure 18). Projections are least consistent for grasslands, and in many locations management activities (burning, grazing, etc.) are probably more important than climate in determining the distribution of grasslands.

FIGURE 18

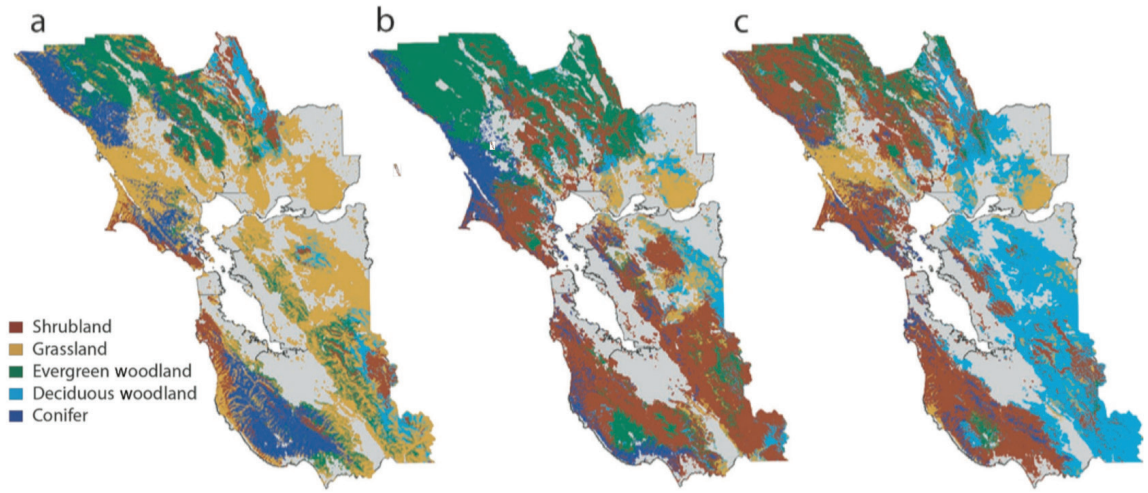

Shifts in potential vegetation of the Bay Area, in response to climate change. Changes were modeled for major vegetation types (e.g. redwood forest, blue oak woodland) and aggregated for illustration. a) historical climates (1951-1980); b) ~7°F (4 °C) warmer with increased rainfall; c) ~7°F (4 °C) warmer with decreased rainfall. See text regarding caveats in interpreting projected changes. Source: Chornesky et al. 2015.

There are three critical considerations to keep in mind about these projections of future change in vegetation. First, all models based on community and vegetation type distributions assume that the currently observed types will persist into the future (Ferrier & Guisan 2006). Models of existing vegetation types do not allow for "non-analog" communities composed of new combinations of existing species, or for novel types invading from outside the region. This problem can be addressed in part through more detailed models of individual species responses. Second, all modeling studies are limited in their ability to make projections under novel climates, i.e., future climate conditions that fall entirely outside the range of conditions observed in the present day. The statewide models are useful in this regard, as conditions found further south and inland provide analogs for future climates in the Bay Area.

Finally, and most importantly, models of vegetation distributions generally rely on an assumption that plant distributions are in equilibrium with historical climate and will rapidly equilibrate to future climate change. The models inform us that the conditions suitable for different species and vegetation types may expand, contract, or shift across the region. But the actual changes will depend on seed dispersal (which can be very limited), interactions with other species including competitors, pathogens, dispersers, pollinators, and herbivores, and the time required for seedlings to grow to adulthood and establish viable populations.

Studies of changes following the ice ages suggest that vegetation can continue to shift for hundreds or thousands of years following a major change in climate. A critical concern in the face of rapid climate change is that vegetation may become "out of sync" with environmental conditions, exposed to levels of heat or drought outside the range of historical variability. This could lead to increased tree mortality, as observed in the 2012-2015 drought, or higher vulnerability to fire (see below); dead trees eventually decompose and release CO_2 to the atmosphere, further contributing to GHG emissions and future climate change.

Wildlife

HIGHLIGHTS

- The most threatening effect of climate change to Bay Area wildlife is the impact of rising sea levels on wetlands because of limited potential for wetlands to move inland and become established.
- Less rainfall, more summer heat, and increased drought will have negative impacts on amphibians and reptiles, while heat and wildfires may negatively affect upland birds, mammals, amphibians, and reptiles.
- Some wildlife species may need to shift locations as the vegetation they inhabit shifts with a changing climate. Barriers to movement are substantial due to habitat fragmentation and urbanization.

The estuaries, wetlands, riparian habitats, forests, ponds, and grasslands of the region are home to a surprisingly diverse array of native wildlife species (mammals, birds, reptiles, and amphibians) supported by the variability of Bay Area microclimates and physiography. For example, birds are the best-known taxa and more than 200 species have been found in the area (BAOSC 2011). Wildlife communities are composed of native species found in California's desert, Central Valley, Coast Ranges, and Pacific Northwest, as well as exotic species that have been introduced from around the world, accidentally or purposefully. The region also includes a large number of threatened or endangered vertebrates[14], listed under the federal and/or California Endangered Species Acts (see Appendix E) (BAOSC 2011) that persist primarily in protected areas within the region (seven mammals, eight birds, two amphibians, and three reptiles).

Climate change is one of many threats faced by wildlife in this urbanized region, including habitat destruction and modification, pollution, pathogens and disease, and predation and competition from nonnative species including domestic cats. A changing climate, however, could exacerbate some of these threats. For example, climate change has been suggested to enhance the spread of exotic disease, such as the chytrid fungus that has decimated amphibian populations (Pounds *et al.* 2006; Clare *et al.* 2016), as well as invasive species in terrestrial and aquatic environments (Hellmann *et al.* 2008; Rahel & Olden 2008).

Arguably the most threatening effect of climate change to wildlife in the Bay Area could come from rising sea levels. Sea level rise is predicted to be severe for the San Francisco Bay estuary from the combined effects of climate warming and land subsidence (see Sea Level Rise section, above). Moreover, there is limited potential in most

14 http://www.Bay Areawildlife.info/species/endangered.htm

locations for these wetlands to move inland and become established within the region. Species specializing in the vegetated portions of marshes may be most vulnerable, since they likely won't find vegetated habitat flooded at a depth that supports them. This might include threatened species, like the California Black Rail, the Light-footed Ridgway's rail, and the salt marsh harvest mouse, as well as many nonthreatened species, such as herons and egrets. On the other hand, subtidal and intertidal mudflats could increase with sea level rise and provide additional habitats for species such as migratory shorebirds (Thorne *et al.* 2018).

Uncertainty in climate predictions characterizes expectations for the future of Bay Area wildlife. However, some general scenarios can be considered. A warmer and drier climate predicted by some analyses would likely have important impacts on riparian wildlife. Streams and riparian areas are key conservation targets for many amphibians and reptiles in the San Francisco Bay region (BAOSC 2011). Decreased winter precipitation and more summer heat, as well as increased intensity of drought, are likely to negatively impact amphibians and reptiles throughout the region. A warmer, drier climate will also lead to increased intensity and frequency of wildfires. These could harm populations of upland birds, mammals, amphibians, and reptiles, especially those persisting in remnants of old-growth forest vegetation.

Some wildlife species may need to shift locations as the vegetation communities they inhabit shift with a changing climate. Enhanced landscape connectivity and habitat corridors are particularly important for more mobile animals. Vegetation shifts from climate change may not be large in the Bay Area (which is buffered by topographic heterogeneity and lower levels of warming compared to inland regions) and may occur slowly (see above). However, barriers to movement may be substantial, especially for amphibians and reptiles, which have limited dispersal.

Invertebrates

HIGHLIGHTS

- The Bay Area is home to a diverse invertebrate fauna. Local extinction of populations of Bay checkerspot butterflies are believed to be due to increasing variability in precipitation, though this cannot be attributed to anthropogenic climate change.
- Phenology, the timing of seasonal events, such as flowering, insect emergence, etc., is highly sensitive to climate and offers important opportunities for monitoring biotic responses and engaging citizen science.

The Bay Area is also home to diverse invertebrates (insects, spiders, etc.), including a number of threatened and endangered species[15] (mostly beetles and butterflies, as they are better studied, and the California freshwater shrimp which is endemic to streams in the North Bay).

Long-term studies of the federally threatened Bay checkerspot butterfly (*Euphydryas editha bayensis*) at Stanford's Jasper Ridge Biological Preserve and other locations in the Bay Area have served as a model for understanding effects of climate and topography on butterfly population dynamics. Checkerspot populations are very sensitive to the timing of larval emergence relative to the flowering time of their native food plants, and larval growth is also closely tied to thermal effects of topographic variation at very small spatial scales (Weiss *et al.* 1988; Weiss & Weiss 1998).

15 http://www.Bay Areawildlife.info/species/endangered.htm

Two of the Jasper Ridge study populations of Bay checkerspots went extinct in 1992 and 1998, and a demographic model strongly suggested that extinction was hastened by an increase in the variability in annual precipitation starting in the 1970s (McLaughlin *et al.* 2002). The later population to go extinct occupied a smaller area, but one with greater topographic heterogeneity, which buffered the impacts of precipitation by providing a greater range of microclimates. The increase in precipitation variability is consistent with projected effects of anthropogenic climate change, though it is not possible to attribute these individual extinction events to anthropogenic impacts.

The timing of seasonal events in plants and animals (known as phenology), such as flowering, hatching, migration timing, etc., is often sensitive to climate. Phenological shifts are important indicators of climate change, and timing mismatches between plants and their pollinators or fruit dispersers may lead to declines in either or both species. In central California, the first flights of butterfly species advanced by almost a month in some cases over the last three decades of the 20th century (Forister & Shapiro 2003). The study of phenology also offers excellent opportunities for community science, and several projects in the Bay Area engage students and community members as part of the California and National Phenology Projects (Charles 2013).

Open Space Protection and Climate-Smart Conservation

HIGHLIGHT

- The Bay Area's mild climate and accessible open spaces are vital to the region's quality of life. Regional conservation efforts, including coordinated open space protection design and implementation of landscape corridors, as well as climate-smart conservation and restoration practices, will enhance success in a changing climate.

With the Gold Rush and the ensuing rapid development of California (which has continued unabated to the present day), the Bay Area was rapidly transformed by logging for timber, bark, and charcoal, the growth of grazing and agriculture, especially related to the wine industry, and most important, by population growth and urbanization. As in other coastal zones, development has been concentrated around the coastline and the bay, leading to large-scale transformation of estuaries and salt marshes.

At the same time, San Francisco served as the heart of California's conservation movement, through its intimate role in conservation battles in the Sierra Nevada and early efforts in local land conservation. Big Basin Redwoods State Park (Santa Cruz County) became the first state park in 1902. Portions of Mt. Tamalpais, Mt. Diablo, the East Bay Hills, and other parcels were acquired for conservation prior to 1950, though formal protection came later in many cases. Large watersheds were set aside surrounding local reservoirs, some storing Sierra Nevada water in transit to the cities, such as Crystal Springs (San Mateo County) and Calaveras Reservoir (Santa Clara County). Development battles in Marin and Sonoma counties in the 1960s and 1970s led to the creation of numerous smaller parks and the preservation of extensive open space and agricultural land (Griffin 1998). These efforts included the creation of Point Reyes National Seashore (1962), one of the largest parks in close proximity to a major metropolitan area in the United States. In addition, the military kept large expanses of land off limits to development (e.g., the Presidio and Marin Headlands). Much of this land has now been converted to open space for public recreation and conservation.

As a result of these efforts, and many others by local, state and federal agencies, as well as non-governmental organizations and private landowners, approximately 25% of the Bay Area's 4 million acres are set aside in protected open space, either in fee title or under conservation easements (BAOSC 2011). Another 25% are urbanized, and approximately 50% are in working landscapes or natural vegetation that lacks formal protection. The mild climate and the accessible open spaces of the Bay Area are vital to the quality of life and the recreational activities of the region, representing a valuable component of the area's natural capital that is supported by native (and in some cases alien) biodiversity. The Bay Area, together with Cape Town, South Africa, probably represent the greatest concentrations in the world of native biodiversity in such close proximity to major metropolitan areas.

The Conservation Lands Network project (CLN) (BAOSC 2011) developed a prioritization for future land acquisition in the Bay Area, with the goal of protecting at least 50% of the area occupied by each major vegetation type in each subregion where they occur, and higher percentages of locations harboring threatened and endangered species and other targeted resources. The CLN has helped to coordinate conservation planning, and several priority locations have been protected in the years since it was released.

The original CLN project did not incorporate climate change into its prioritization scheme. In response to climate change, species movements and expanding or contracting habitats may undermine the conservation goals of the protected area network if species are no longer protected in parks where they once occurred. In response to this concern, conservationists have advocated for an approach of "conserving the stage," i.e., the physical setting and climate gradients that create the template for a diverse landscape, even if we cannot be confident of which species will occupy individual locations in the future (Lawler *et al.* 2015).

The rugged topography and steep climatic gradients of the Bay Area foster considerable habitat diversity within many parks and protected areas. This diversity of both species and physical conditions is expected to buffer impacts of climate change. The greater diversity of species means it is more likely that at least some native plants adapted to future conditions ("future winners") will be found within local landscapes. Heterogeneous conditions also allow species to find sites with suitable future conditions in close proximity, and more likely within natural dispersal distances. Persistent features, such as springs and other hydrologic refugia (McLaughlin *et al.* 2017) may be buffered from climate change impacts, facilitating the persistence of present day biota. However, general predictions are that species occupying cooler and moister locations in a landscape (e.g., north-facing slopes, deeper soils) will be threatened under warmer and drier futures, while those adapted to hot and dry locations (e.g., south facing slopes, thin soils) may spread across the landscape, resulting in homogenization of the biota and reduction of diversity.

Heller et al. (2015) evaluated the robustness of the CLN with respect to local climate gradients, and found that the proposed prioritization scheme, based on vegetation, was largely similar to the results that would be obtained by prioritizing the diversity of climate zones. This positive result largely arises because the plan distributed conservation priorities across the region by targeting vegetation types within 29 "landscape units" (mountain ranges, major valleys, etc.); the goal was to achieve at least 50% protection of each type in each region, with the result that the priorities are broadly distributed across regional gradients of climate and vegetation. CLN2.0 is currently in development, and will incorporate climate goals more explicitly, including maximizing topo-climate diversity and habitat connectivity for climate change adaptation.

A second major conservation priority in the face of conservation change is enhanced landscape connectivity and corridors, both for the traditional goals of enhancing wildlife movement and increasingly out of concern for facilitating species range shifts. To adapt to climate change, many of California's species will need to shift their distributions. Landscape planning for climate resilience should focus on maintaining and restoring habitat corridors that can facilitate species range shifts. Such corridors function by protecting climate refugia and places with slower rates of climate change and then linking protected areas to sites that will offer suitable conditions under future climates. To counter ongoing habitat loss and fragmentation and increase ecosystem resilience to climate change, it is urgent that the region speed up corridor implementation through land conservation and restoration. Targeted efforts to address regulatory barriers and incentives for resource agencies and private landowners could play an important role in this regard. Regional collaborations can create a common vision of connected landscapes, articulate the multiple benefits of corridors, build partnerships between stakeholders, and involve the public in corridor conservation. Scientific data, such as identifying animal movement paths and connectivity models are important for siting and justifying connectivity projects. California's Fourth Climate Change Assessment (Fourth Assessment) report "Climate-wise Landscape Connectivity: Why, How, and What Next" (Keeley *et al.* 2018) provides recommendations for selecting climate-wise modeling approaches and offers a framework to guide on-the-ground connectivity implementation.

These principles have been applied in the Bay Area-based "Building Habitat Connectivity for Climate Adaptation" project[16], integrating habitat mapping, threat assessment, and climate change projections to enhance connectivity and climate resilience in the Mayacamas to Berryessa Coast Ranges (Napa, Sonoma, Lake, and Mendocino counties). The project is evaluating terrestrial and riparian connectivity across the study region to generate linkages between existing protected areas, then determining climate connectivity across the protected area network by calculating the climate benefit offered by each linkage (e.g. connecting warmer to cooler locations).

The development of landscape-scale planning efforts for conservation and connectivity poses new challenges for leadership and cooperative action among public, NGO and private land owners, and government agencies from the local to federal level. While individual agencies may manage networks of protected areas, sometimes across large regions, the open space, parks, and preserves within local landscapes have an array of owners often with contrasting goals, obligations, and jurisdiction for resource stewardship. Land managers are recognizing they need more tools to sustain the health of the lands that have been acquired; public ownership or protected status alone does not necessarily equal resiliency and sustainability. New initiatives in cooperative landscape governance and stewardship are emerging in California[17] and elsewhere to tackle shared challenges posed by climate change, land use change, population growth and other factors. Looking ahead, the United States is expected to see an emergence of more nascent landscape-scale partnerships, as well as deepening levels of collaboration and integration among existing partners[18].

16 https://californialcc.org/projects/building-habitat-connectivity-climate-adaptation-s

17 http://landscapeconservation.org/california-landscape-stewardship-network/who-we-are/

18 The Center for Natural Resources and Environmental Policy at The University of Montana, http://naturalresourcespolicy.org/the-center/

While landscape-scale stewardship partnerships are not a new idea, those committed to long-term action at a regional or landscape level are still not widespread. Recent shifts within the field towards embracing these kinds of innovative partnerships mean that the time is right time to make a collaborative, landscape-scale approach the new norm for California. In the Bay Area, the Tamalpais Lands Collaborative — and its community-facing initiative OneTam — is an exemplary effort bringing municipal, county, state, and federal agencies together with a conservation-based NGO to focus on management of Mt. Tamalpais and surrounding lands in Marin County. Using a collective impact model, the NGO provides the backbone support to leverage this public-private partnership and scale the partners' resources to achieve restoration, stewardship, research, education, and sustainability goals. Within four years, OneTam has developed, prioritized, and is implementing collective conservation and stewardship goals through aggregating and analyzing hundreds of partner data sets, which establishes a baseline understanding of the mountain's overall ecological heath across jurisdictional boundaries.

A third priority for climate-smart conservation is adapting restoration practice to ensure success in a changing climate. One example is expanding planting palettes (e.g. the range of genotypes or species used in a project), utilizing a broad range of climate tolerances as well as species with diverse flowering and fruiting times to provide more resilience in food resources for animals. The latter principles are embodied in the climate-smart Students and Teachers Restoring a Watershed (STRAW[19]) program run by Point Blue Conservation Science underway in the San Francisco Bay Area. STRAW, a community-based restoration program, has restored 36 miles of stream with over 46,000 plants and 45,000 students. STRAW has integrated the climate-smart approach into restoration projects, with the goal of providing enhanced water quality and wildlife benefits, as well as added carbon sequestration of restored woody vegetation.

BOX 10: CO-CREATING CLIMATE SCIENCE PRODUCTS TO MEET LOCAL RESOURCE MANAGERS' LONG-TERM PLANNING NEEDS

Climate Ready North Bay

To create a framework for adapting to climate change, decision makers working in the Bay Area's watersheds need to define climate vulnerabilities in the context of local opportunities and constraints in water supply, land use suitability, wildfire risks, ecosystem services, and biodiversity. Climate Ready North Bay, a public-private initiative spearheaded by Sonoma County's Regional Climate Protection Authority and funded by the California Coastal Conservancy's Climate Ready program, provides a valuable case study of a facilitated engagement process that effectively bridges the science-management divide.

Climate Ready North Bay succeeded in generating an innovative set of customized, "actionable" data products grounded in site-specific management objectives. The success of the project hinged on all participants (staff from eight municipal entities across three counties and a team of six climate scientists) committing to an in-depth facilitated exchange over a two-year period.

19 http://www.pointblue.org/our-science-and-services/conservation-science/conservation-training/straw-program

The project tapped into high-resolution downscaled watershed data products developed by the Terrestrial Biodiversity Climate Change Collaborative co-chaired by UC Berkeley and the Pepperwood Preserve. By working directly with staff (local water districts, parks and open space districts, and planning agencies) from the very start of the process to define their resource-specific information needs, Climate Ready North Bay developed spatially-explicit data products to help local agencies advance key climate adaptation strategies. Generated products include maps, graphs, data sets, and summary technical reports customized to client jurisdictions and management concerns. For full project documentation and sample products, click here.

Lessons learned:

- Use an iterative process, an extended dialogue (12+ months) and multiple in-person exchanges.
- Frame resource-specific management questions at the project kickoff.
- Make sure managers participate in scenario selection to ensure relevancy and to learn why an ensemble approach is needed to capture model uncertainties.
- A critical member of the team is an "information broker" who speaks the languages of both "science" and "management" to facilitate discussions.
- Once results are available, managers need additional support from the technical team to scope how to translate results to specific planning applications.

Climate Ready North Bay provides a model of how to introduce municipal agencies to available climate science products and chart pathways for integrating those products into resource plans. Data packages are now being applied to multiple long-term resource plans (and on-line planning tools) including:

- Sonoma County Water Agency's climate adaptation plan
- Napa County's Groundwater Sustainability planning initiative
- Marin Municipal Water District's Urban Water Management Plan
- OneTAM's Mountain Health Scorecard
- Sonoma County Agricultural Preservation and Open Space District's Vital Lands initiative
- Sonoma Regional Conservation Partnership Program: Venture Conservation
- BAOSC Conservation Lands Network 2.0 and Explorer Tool
- Bay Area Greenprint
- TBC3's Bay Area Climate Smart Watershed Analysis

Forest Management, Fire Risk and Carbon sequestration

HIGHLIGHT

- Forests can play an important role in carbon sequestration. Fuel and fire management will be critical, as fire is the primary source of carbon loss from forests. Recently, carbon loss from fires exceeded carbon uptake by vegetation in California.

As noted above, fire is a recurrent event in the Bay Area, as in most of California. Native plants in California have evolved in the presence of fire and exhibit a range of life history strategies to promote post-fire regeneration. Some species, such as Bishop pine and some chaparral shrubs, are dependent on fire for regeneration from seed, and many species resprout from the base of the trunk or the larger branches following fire. As in the Sierra Nevada, fire suppression in the 20th century has led to the buildup of a dense understory of conifers, hardwoods, and shrubs in woodlands and forests throughout the region. At a landscape level, there is evidence that woodlands have expanded over the past 100+ years, while shrublands have declined, consistent with the effects of reduced fire frequencies (Evett *et al.* 2013). Douglas fir, the dominant native conifer in the region, is quite fire sensitive when young. In the absence of fire, the seedlings establish and grow rapidly under the canopy of other trees, eventually overtopping shrubs and hardwoods leading to vegetation conversion and reduction of habitat diversity.

The buildup of dense understories and higher density of small trees, especially conifers, enhance the risk of high severity fires under hot, dry, and windy conditions. While these negative effects of fire suppression are well documented in Sierra Nevada conifer forests, their impacts on fire in oak woodlands and mixed hardwood forests of the Coast Ranges are less well understood. In addition, tree mortality due to drought and sudden oak death (Metz *et al.* 2013) have increased densities of dead fuels and likely contributed to higher fire risk in the Bay Area. It is well established that vegetation removal, either by prescribed burning, herbivory (i.e., goats), or mechanical thinning, reduces the risk or severity of fire in the immediate vicinity of the treatments and can help to limit fire spread (Agee & Skinner 2005). Under moderate conditions, oak woodlands generally present low fire risk, and treatments that remove understory fuels further reduce risk of high severity fire. It is harder to determine how aggressive fuels management would alter fire behavior under extreme fire conditions, as experienced at the outset of the 2017 North Bay fires. High severity fire increases risk, even when it occurs far from populated areas, as the fire is more likely to grow and spread quickly; production of burning embers carried on the wind can lead to rapid spread beyond the immediate perimeter, and these are often the primary cause of ignition for structures. Fire behavior in mixed hardwoods is not well characterized in the current generation of fire models, and more research is needed to be able to evaluate future fire risks, especially under a changing climate, and the scale and type of fuels management that could effectively reduce risk to structure loss.

Forests also play a critical role in carbon sequestration, and the management of natural and working lands is one of the pillars of California's emissions reduction policies (FCAT 2018) (see discussion of rangelands below)[20]. Fire management is critical as fire is the primary source of carbon loss from forests and in the last decade losses exceeded carbon uptake at a statewide level (Gonzalez *et al.* 2015). Redwood forests are especially important as they have the highest aboveground carbon density of any ecosystem on earth (Van Pelt *et al.* 2016). With their disease resistant wood, large size, high densities, and the lower risk of fire along the coast, redwoods have an exceptional potential

20 https://www.arb.ca.gov/cc/pillars/pillars.htm

to sequester carbon for long periods of time. While the largest stands are found further north, redwoods make important contributions to Bay Area vegetation in the Santa Cruz mountains, Mt. Tamalpais in Marin County, and along the Sonoma County coast.

California has played an important role in the development of carbon offset protocols for sustainable forest management, creating an income stream for management actions that enhance carbon sequestration by participating in California's cap-and-trade market. One Bay Area forest—Preservation Ranch in Sonoma County—is currently a registered carbon offset project, receiving credits for enhanced annual sequestration of about 2% of the standing stock (i.e., sequestration credited to sustainable management practices, over and above the baseline scenario of forest growth in the absence of these practices). It is unknown, however, whether future climatic conditions will allow these forests to persist and sustain these sequestration levels. Climate change adaptation planning to facilitate range shifts and species conversions is generally lacking from forest management guidance (e.g., FCAT 2017). Given their conservation value and iconic status, we can probably assume protection of redwood forests in this region to be a priority. Even so, it is not clear yet how to buffer these ecosystems, and the carbon they store, from the compound effects of novel pathogens, climates and fire regimes simultaneously.

Aquatic Systems

HIGHLIGHTS

- Nearly every aspect of Bay-Delta ecosystems will be affected by climate change as a result of rising sea levels, increases in air temperatures, changes in precipitation, changes in sediment supply, and more. Natural areas of the shore will need to adapt or transform.
- The interruption of natural processes over the past 200 years as the region has developed has decreased natural Bay-Delta resiliency. A dynamic, resilient ecosystem has become a rigid landscape with brittle features that will have trouble adapting.
- New approaches that use natural shoreline infrastructure, like beaches, marshes, and mudflats, together with managed retreat where necessary, can create more resilient shorelines that respond well to changing conditions.

Delta Baylands and Coast

The San Francisco Bay-Delta estuary consists of highly valuable ecosystems. Californians depend on the Bay and Delta for fresh water supply, shoreline protection, water quality, food web productivity, biodiversity support, carbon sequestration, and recreation. The cities and other infrastructure of the Bay Area and Delta are built around the geography of the estuary, which both shows the importance of these ecosystems and makes the impacts of climate change to Bay-Delta tidal wetlands very relevant to people.

Although naturally resilient, these ecosystems are threatened by climate change. The interruption of natural processes over the past 200 years as the region has developed has decreased that resilience. San Francisco Bay is now highly urbanized, with billions of dollars of infrastructure built up to and on top of tidal wetlands (Heberger *et al.* 2012). Much of the shoreline is protected by a series of earthen berms and marshes, rather than by engineered levees (SFEI 2016). The Golden Gate watershed (approximately 40% of California's land) is highly modified, so that the sediment

and water flows that reach the estuary are very different from their natural patterns of timing and magnitude. Tidal wetland habitats have been fragmented and isolated (Goals Project 2015), and several endangered and otherwise protected species are found only in these marshes (see Wildlife section). In sum, a dynamic, resilient ecosystem has become a rigid landscape with many brittle features that cannot adapt and must instead be protected. Impacts to the various elements of the Bay-Delta ecosystem are detailed below, and at the end of this section we discuss approaches for restoring natural process and resilience while protecting people and property and upgrading infrastructure.

Nearly every aspect of Bay-Delta ecosystems is likely to be affected by climate change, including physical, chemical, and biological elements. Effects that will stem from increasing sea levels include: changes in precipitation patterns (including storm intensity and timing of runoff); changes in freshwater supply and management of that supply; changes in sediment supply; increases in air temperature; more severe drought; and infrastructure adjustments in response to climate change. Across the elevation gradient from shallow subtidal to the tidal-terrestrial transition zone, natural areas of the shore will necessarily adapt or transform.

At the highest elevations of the Bay-Delta ecosystem, which are closest to people and built infrastructure, is the estuarine-terrestrial transition zone. This zone is a critical area for ecological functions, supporting many endemic species, and for ecosystem services, acting as a buffer for the wetland and aquatic habitats of the bay (Goals Project 2015). The transition zone of today becomes the tidal wetlands of tomorrow as marshes migrate inland in keeping with sea level rise. Much of the transition zone is already developed; little of what is undeveloped is protected (SFEP 2015). Barriers like berms, levees, and seawalls minimize and eliminate the transition zone, foreclosing the opportunity for tidal wetlands to migrate inland. This means that tidal wetlands are squeezed between a rising sea and levees and will lose their ability to protect the shoreline and its infrastructure from flooding and erosion. The fluvial-tidal transition zone (where rivers and creeks enter the estuary) is a critical area with increased value for its functions and benefits and also with increased flooding problems in developed areas.

Slightly lower in elevation than the estuarine-terrestrial transition zone is the intertidal area. Tidal marsh is the dominant natural intertidal habitat of this estuary, and a large effort is being made to restore tidal marshes across the estuary (Goals Project 2015), especially with the recent funding of the San Francisco Bay Restoration Authority (http:// Bay Areayrestore.org/).

Mudflats are found in the lower intertidal zone. Mudflats and tidal marsh are both extremely productive, providing food for fish, marsh wildlife (including several threatened and endangered species - see Wildlife section), and millions of migratory and resident shorebirds. Marshes are also important for water quality in terms of nutrient cycling and contaminant sequestration and breakdown.

Both mudflats and tidal marsh play critical roles in protecting the shoreline behind them. These habitats attenuate waves, reducing erosion of the shoreline. Thus, developed areas with substantial intertidal habitats adjacent require less substantial engineered protection from sea level rise. Recent studies from around the nation have shown that these types of natural shoreline protection perform better than engineered solutions and cost less (Gittman *et al.* 2014; Smith *et al.* 2017).

These intertidal habitats are very resilient to sea level rise, given enough sediment supply that they can keep accreting vertically or enough space that they can migrate inland. However, sediment supplies have recently decreased (Schoellhamer 2011), and modeling results indicate that San Francisco Bay marshes may not be able to keep up with

sea level rise in the long term, unless management practices change (Stralberg *et al.* 2011; Schile *et al.* 2014). Thus, sediment management choices in the bay and its watersheds are critical to outcomes for intertidal habitats and the shorelines behind them.

Sediment delivery to the shore could be increased by infrastructure updates to dams, changes in reservoir management, changes in creek alignments near the bay, and flood risk management approaches. Management of freshwater is equally critical because brackish and freshwater tidal marshes are able to increase in elevation rapidly by creating peat. Evidence of historical freshwater tidal marsh accretion rates in the Delta (Drexler *et al.* 2009) and modeling results (Swanson *et al.* 2015) indicate that these marshes may be sustainable at the lower end of projected sea level rise rates later this century (OPC 2018), but their long-term persistence may be jeopardized at higher rates. Placement and delivery of freshwater around the shoreline should be viewed as a resource to create resilient, protective marshes. Most of the edge of the estuary is leveed, so intertidal areas have very little space to move inland (SFEI 2016).

Intertidal habitats that have been largely removed from the bay, particularly beaches, and (transitioning into the subtidal area) eelgrass and oyster beds, are also resilient elements of the shore that can help protect built infrastructure while adding habitat value. Efforts to restore these habitats are in the nascent stages and could happen faster and at a larger scale.

Novel and managed habitats are common throughout the historic intertidal zone of the estuary, and these managed ponds, leveed areas, duck clubs, deepened and widened channels, and flooded islands are largely a liability in terms of climate change. These areas are prevalent in North and South San Francisco Bay, Suisun Bay, and the Delta. Where land has been kept dry for agriculture and other uses, the land surface continues to subside as the ancient marshes underneath lose CO_2 to the atmosphere. This increases future flooding risk and well as increasing greenhouse gases in the atmosphere.

Failure of levees around subsided lands, as well as sea level rise alone, will cause the estuary to grow in size, drawing in more saline water. As the estuary becomes saltier, habitat will shift from brackish to salt and from fresh to brackish. This is already a problem for fresh water supply in the Delta. The gradient of fresh to salt water and fresh to salt marsh will migrate inland, prompting the need to plan ahead for where natural communities can be supported in the Delta and Central Valley, where wetlands have been largely removed in the past two centuries (SFEI-ASC 2014). Many so-called levees around the estuary are berms made of peat, rather than engineered structures (SFEI 2016). They fail regularly due to flooding and could fail at a large scale in an earthquake. Such a levee failure in the Delta would cause the limited volume of tidal water passing through the Carquinez Strait to be spread over a larger area, thus reducing tidal range and intertidal area.

The way that people respond to the changing climate will determine the fate of estuarine habitats. The relationship between constructed systems, management choices, and natural systems is critical. Removal and interruption of the natural flooding processes of rivers and tides have created the current rigid landscape that cannot adapt over time, is difficult to protect from climate change impacts, and provides few benefits beyond flood risk management. Further removal and interruption of natural processes by tidal barriers, sea walls, and other engineered structures will exacerbate the situation (see Natural Infrastructure section, above). However, new approaches that use natural infrastructure, like beaches, marshes, and mudflats, and different management practices, such as planned flooding

during certain times of the year, can create more resilient shorelines that can respond to changing conditions and provide multiple benefits (Newkirk et al. 2018). Hybrid natural and engineered solutions are likely to be necessary in many areas. Beyond choices at the shoreline, the management of rivers, creeks, reservoirs and stormwater in watersheds will also be critical. Sediment and water coming off the land are the building materials of estuarine habitats, and how they are delivered is of paramount importance.

Incorporating natural elements into shoreline adaptation and watershed management requires advance planning, as well as changes in policies, funding, and coordination. Because the natural systems of the estuary are large in scale and some natural processes take time to play out, planning to incorporate natural elements needs to be at a large enough scale and far enough ahead to consider the full system and its multiple benefits. Pilot projects are underway that show the feasibility and efficacy of these approaches, including realignment of San Tomas Aquino Creek for better sediment delivery, the redesign of SR 37 for flood risk management and reduced impact to intertidal habitats, restoration of oyster reefs for shoreline protection, and pulsed flows in the Yolo bypass to create food web productivity for fish.

Local residents support this focus on restoring the estuary as the climate continues to change. In a recent historic vote, Bay Area residents levied upon themselves the first regional parcel tax measure in California's history (Measure AA). It passed with 70% approval across the nine-county region and went into effect in 2017. This parcel tax will raise approximately $25 million annually, or $500 million over 20 years, to fund habitat restoration projects in the Bay Area, including flood control and shoreline access elements of those projects.

BOX 11: BIG MONEY FOR RESTORING THE BAY (WHAT A CONCEPT!)

Measure AA: The San Francisco Bay Restoration Authority

This $12/year parcel tax passed in 2016 by 70% of Bay Area voters is the first regional parcel tax in California history! The Authority is now handing out its first checks for bay wetlands restoration projects. The Authority will dispense $25 million each year for 20 years with a number of the projects expected to address sea level rise as part of their focus.

Projects that benefit disadvantaged communities are among Measure AA's priorities and, working with representatives of environmental justice groups on the Advisory Committee, the Restoration Authority adopted a new definition of an economically disadvantaged community that considers income-based metrics as well as environmental and other burdens.

The first funded projects include:

- Deer Island Wetlands (Marin) - $1 million
- Encinal Dune (Alameda) - $450,000
- India Basin remediation (San Francisco) - $5 million
- Lower Sonoma Creek (Sonoma) - $150,000
- Montezuma Wetlands (Solano) - $2 million
- North Bay wetland restoration (Sonoma, Marin) - $3 million
- San Leandro Treatment Wetland (Alameda) - $1 million
- South Bay Salt Pond Restoration Project (San Mateo, Alameda, Santa Clara) - $8 million
- South San Francisco Bay Shoreline Project (Santa Clara) - $4 million

Freshwater Systems

The ecology of freshwater systems and the dynamics of fish populations are tightly linked to water flows and water temperature, both of which are sensitive to climate change. Water flows in the Bay-Delta are directly coupled to winter precipitation, and the amount and timing of snowmelt in the Sierra Nevada. Rainfall is highly variable from year to year in California, and models project this variability may increase, with more extreme wet years and increased risk of drought; there is still considerable uncertainty, especially in central California, about whether average rainfall will increase or decrease (see Precipitation section, above). In the 3rd California Climate Change Assessment, Moyle et al. (2012) compiled a thorough estimate of the factors affecting the California fish fauna and ranked all members of that fauna, both native and alien, by their baseline vulnerability to extinction and by their sensitivity to climate change.

SALMONIDS

Salmonids have received considerable attention in relation to climate and conservation, reflecting their iconic life history and their long-standing economic importance. As the Delta is the entry point for populations throughout

the Central Valley and Sierra, potential impacts of climate change have widespread importance. In a recent review, Moyle et al. (2017) concluded that climate change is a major threat to salmon populations throughout California, and that the historic 2012-2016 drought contributed to continuing declines in recent years. The lack of cold water and low flows from Shasta Dam and other dams in the Central Valley contributed to the high mortality of eggs and fry (juvenile fish). The Russian River watershed, in Sonoma and Mendocino counties, is home to three threatened and endangered salmonid species: Chinook salmon (*Oncorhynchus tshawytscha*), coho salmon (*Oncorhynchus kisutch*), and steelhead (*Oncorhynchus mykiss*). Current efforts by the Sonoma County Water Agency to enhance habitat conditions for salmonids include improvements to reservoir reliability to maintain a cold water pool in Lake Mendocino through the summer for downstream juvenile steelhead rearing and into the fall for adult salmonid migration. This could help reduce the impact of drought on rearing and migrating salmonids.

Emergency efforts to protect salmon during the drought led to a focus on restoring the original portfolio of salmon's adaptive strategies to California's variable climate. This support would include better providing for all life stages; different life stages fare better in different years, so diverse strategies increase the likelihood that some will be appropriate for whatever conditions occur in a given year and place. Broadening the salmon's genotypic and phenotypic portfolio requires different hatchery management practices and improved quantities and access to habitats of diverse types used by different salmon life stages.

NON-SALMONID FISHES

A diverse array of non-salmonid fish occur in the Delta and have been carefully monitored for many years[21]. Changes in these populations, coupled with analysis of life histories, have been used to rank species from critically sensitive to least sensitive to climate change. The most vulnerable species are Sacramento Perch and Sacramento Splittail, whose populations spike in the wet years and decline precipitously in dry years. Delta Smelt and Tule Perch are also highly vulnerable species, although their dynamics are less dependent on annual rainfall. Both species are tolerant of high salinities, but exhibit low thermal tolerance (Swanson et al. 2000, Moyle 2002) and have been declining in recent years. No Delta smelt were captured in 2017. Precipitation patterns are not firmly agreed upon for California's future climate, but the increase in temperature is common to all local models, suggesting that these two species will be highly vulnerable to continued change.

Several exotic species have established themselves in the Delta. One of these, American Shad, has populations that fluctuate with rainfall, like some of the natives, suggesting greater vulnerability in a future climate. Others, including Mississippi Silverside, Striped Bass, and Largemouth Bass, have more steady population sizes and high thermal tolerances and appear to be quite resilient in the face of variable rainfall and warming temperatures.

MANAGEMENT IMPLICATIONS FOR RESIDENT NATIVE FISHES

California's native fish fauna is adapted to a highly variable climate. However, much of California's water development has aimed to reduce the impacts of this variable climate on water supply to farms and cities. As climate change progresses, or as historical variability in flows is restored, the resident species have the adaptations to take advantage of good conditions and spawn prodigiously. However, habitat change and invasive species reduce their ability to survive through the intervening dry years. Restoration of diverse habitats used by native fishes will likely improve

21 https://view.officeapps.live.com/op/view.aspx?src=https://www.fws.gov/lodi/juvenile_fish_monitoring_program/data_management/Metadata_Updated_September_09_2014.doc

their survival. Hydrologic isolation of some of the restored habitats could offer refuge from environmental hazards that are more intense in drier years and thereby enhance survival and protect populations.

BAY AREA RIVERS AND CREEKS

Climate change could impact Bay Area creeks and rivers in several ways. On the one hand, longer dry seasons and more frequent and severe droughts could greatly reduce the quantity and quality of water in waterways. Droughts and higher mean temperatures could reduce the quantity of water available for flow in creeks and rivers in the Bay Area. Instream flows may be affected by longer dry seasons; increased evaporation; greater water demands from riparian vegetation due to higher rates of evapotranspiration; increased direct diversion and groundwater pumping by adjacent property owners; and reduced contributions to flow from adjacent groundwater aquifers (Micheli *et al.* 2016). On the other hand, increased frequency and magnitude of extreme precipitation events could lead to more flooding and erosion (NBCAI 2013).

Catastrophic wildfires associated with climate change, such as those that occurred in the North Bay in 2017, increase the risk of delivering ash, debris, and sediment to waterways during subsequent rain events. Toxins, particularly from urban fires, can directly affect invertebrates, fish, amphibians, and other species[22]. Fine sediments can impact spawning habitat for threatened and endangered salmonids, such as Chinook salmon, coho salmon, and steelhead present in the Russian River watershed. Introduction of dissolved organic carbon and other contaminants could impact downstream water supply operations. For example, a catastrophic wildfire in the watershed upstream of Lake Sonoma, a reservoir located in the Russian River watershed, would impact the primary drinking water source for approximately 600,000 North Bay residents and could affect the Sonoma County Water Agency's ability to supply clean, safe drinking water (SCWA 2018). The Water Agency is developing a fire risk and water quality assessment as part of its climate adaptation planning process to better understand how wildfire could affect hydrology and water quality in the Russian River watershed.

Flooding is already a significant problem in some Bay Area communities. The Russian River, located in Sonoma and Mendocino counties, is a major source of flooding in Sonoma County, which contains the highest number of properties suffering repetitive flood losses of any community in California (SCHMP 2017). Atmospheric rivers play a large part in these flooding events and recent studies (see Regional Climate Science section, above) suggest that intense atmospheric rivers will occur more frequently as mean temperatures rise. The SCWA is working with the National Oceanic and Atmospheric Administration, Scripps Institution of Oceanography, and others to improve atmospheric river forecasting in region[23]. Additionally, SCWA is developing a new flood model for the Russian River as part of its climate adaptation planning process[24].

IMPACTS OF DROUGHT

The 2012-2016 drought produced, in intense form, several of the expected long-term effects of climate change. Reduced precipitation caused lower stream flows, including the complete drying of some stream reaches, and reduced lake and reservoir levels. Reduced snowfall caused higher water temperatures, flashier hydrographs, and lower summertime flows. Higher air temperatures caused higher water temperatures and more rapid evaporation. Higher water temperatures produce physiological stress on fish, greater disease susceptibility, and higher rates of

22 https://ca.water.usgs.gov/wildfires/wildfires-water-quality.html

23 http://www.scwa.ca.gov/aqpi/

24 http://cw3e.ucsd.edu/firo/

primary productivity, including harmful algal blooms. Additional impacts were caused by tree mortality in forests, sedimentation following wildfire and changes in outflow, and salinity in estuaries. Many of these impacts were immediate, while some are still affecting fish populations. Impacts to fish populations are likely to continue for years even if higher precipitation years return.

Bay Ecosystem

The open water and benthic components of the San Francisco Bay ecosystem have undergone a series of fundamental changes in the past century, starting with a sediment flux resulting from hydraulic mining and the Gold Rush, followed by an invasive species of clams. A series of changes are anticipated in the coming century. In this section, we start with a discussion of current conditions in the bay, and how those conditions were shaped by historical conditions and change. We then consider the coming century and how the ecosystem is likely to be transformed.

The San Francisco Bay ecosystem is quite high in nutrient concentrations, due to the high levels of wastewater and urban water returns to the bay. In the South Bay, nutrient concentrations are comparable to those observed in Chesapeake Bay, but San Francisco Bay does not experience the same eutrophication evident in the Chesapeake, due to a number of physical factors that limit growth in the system.

In San Francisco Bay today, phytoplankton growth is not limited by nutrient concentrations, but instead biomass is limited by the combination of low light levels and high grazing rates. Low light levels in San Francisco Bay are a result of high sediment concentrations, which are suspended from the bed by energetic tidal flows and surface waves. The extensive shallows of San Francisco Bay play an important role in maintaining these high concentrations. They are, in part, a result of the pulse of sediment that entered the bay following hydraulic mining and the Gold Rush, which continues to work its way through California's rivers and reservoir system to the bay.

The grazing of phytoplankton in San Francisco Bay is dominated by benthic clams, which have sufficient density in portions of the bay to filter the entire water column in less than 2-3 days. The particular species of clam that dominates the benthos was introduced from Asia in the ballast waters of ships in the 1980s, and now helps to control phytoplankton growth throughout the bay. Physically, the ability of a benthic species to effectively filter the entire water column depends on the bay mixing regularly, which occurs in San Francisco Bay as a result of strong tidal forcing in relatively shallow channels. This is another contrasting characteristic to Chesapeake Bay, which remains stratified (unmixed) for months, eliminating the possibility of benthic grazers acting to reduce the high biomass that develops as it eutrophies during the summer.

Looking to the future, the key concern is whether the current limitations on biomass (low light levels due to high sediment concentrations; extensive benthic grazing due to high clam populations and mixed conditions) may be relaxed, thus allowing much more extensive growth in the bay in response to high nutrient levels.

THE KNOWN UNKNOWNS

There are two key trends that may alter physical conditions in the bay, although the resulting changes in the ecosystem are uncertain. First, sediment concentrations are declining due to end of the post-Gold Rush hydraulic mining pulse. Recent analysis (Schoellhamer 2011) has indicated that there may be a significant decline in bay sediment concentrations in the coming century, which would result in higher light levels and more phytoplankton growth. The second key trend is toward more intense and longer heat waves, which will lead to thermally stratified conditions and

phytoplankton growth in the surface layer, including possibly harmful species (Cloern *et al.* 2011). There is uncertainty as to whether a threshold (and, if so, what the level of threshold) will be met in either case that would result in a transformation of the bay ecosystem. Ongoing research is attempting to determine the level of risk.

THE UNKNOWN UNKNOWNS

The introduction of the Asian clam species in the 1980s fundamentally altered the San Francisco Bay ecosystem. The coming century will almost certainly involve additional ecological disruptions with uncertain consequences. Increases in clam predators, for example, would reduce or eliminate the ability of the clams to filter the bay and limit phytoplankton biomass. The probability of some kind of ecological disruption in the coming century is quite high, but the details and the consequences of that disruption are, of course, unknown at present.

Agriculture

HIGHLIGHTS

- Nearly 70% of California's existing area of wine production will be vulnerable under future climate change projections by mid-century. Wine grape production in the Bay Area could be vulnerable to extreme temperatures and temperature-related water scarcity.
- The sensitivity of Bay Area rangeland vegetation to precipitation dynamics makes these ecosystems particularly vulnerable to climate change. Changes in rainfall regimes are likely to affect plant production and associated patterns in soil carbon and greenhouse gas production.
- Grazing and rangeland management practices can play a significant role in enhancing soil moisture and below-ground carbon sequestration. Current research highlights the potential role of compost together with grazing on California pasturelands as a targeted strategy to increase carbon sequestration.

Climate Change and Wine Grape Production in the San Francisco Bay Area

The Bay Area supports a diverse portfolio of crops (NASS 2012). While wine grapes are its most notable crop, 32,600 acres of field-grown vegetables[25] produce annual sales of $193.8 million[26]. An additional $4.2 million come from vegetables grown in protected conditions (i.e., tunnels, greenhouses) and $5.1 million in sales are produced from just 373 acres of berries. Production of horticulture and floriculture crops contributes $125.5 million in sales. Production of fruit and tree nuts contributes the greatest regional value, with $1.259 billion in annual sales, largely due to wine grape production. The North Bay first began producing wines in the early 20th century and has since become one of the world's premier growing regions. More recently, parts of the East and South Bay have also emerged as producers of high quality wines (Figure 19). The region's diverse climate allows a wide range of cultivars, but the usual suspects rise to the top (*Grape Crush Final Report 2016* 2017). Listed in decreasing acreage, the top five red varieties are Cabernet

25 Includes seeds and transplants

26 Sales – Definition from USDA-NASS glossary: "Refers to both dollars ($) received and quantities of commodities (e.g., head or bushels) sold or removed from the operation. Includes landlord share and value of product removed under production contract. Depending upon the data series, may refer to marketings or cash receipts. Excludes government payments. Used alone, *sales* refers only to the data item."

Sauvignon, Pinot noir, Merlot, Zinfandel and Petite Sirah, with nearly similar acreage from Syrah, Petit Verdot, Malbec and Cabernet Franc. The top white varieties are Chardonnay, Sauvignon blanc and Pinot gris, and Gewurztraminer, with Viognier, Semillon, Chenin blanc and White Riesling coming in at a near tie.

Nearly 70% of California's existing area of wine production may be vulnerable under future climate change projections by mid-century (Hannah *et al.* 2013). Recent spatial analysis of grape production across California used mean summer mid-century temperature projections to identify potential regions of vulnerability for grapes (Elias *et al.* 2015). The historic mean summer temperatures where grapes were grown in California were used as an estimate of suitable temperature conditions for grape production. When temperatures increased beyond historic means where 95% of California wine grapes were grown, the area was considered a new temperature regime. Mean summer temperature increase caused more than 60,000 acres of varied land use in northern Solano and Napa counties to exceed the normal historic temperatures. In contrast, portions of Marin, Sonoma and San Mateo counties along the coast transitioned to typical mean summer temperatures where grapes are grown (Figure 19). Only northern Solano County had a small area presently growing grapes that is predicted to shift outside the 95% percentile of optimal temperatures.

FIGURE 19

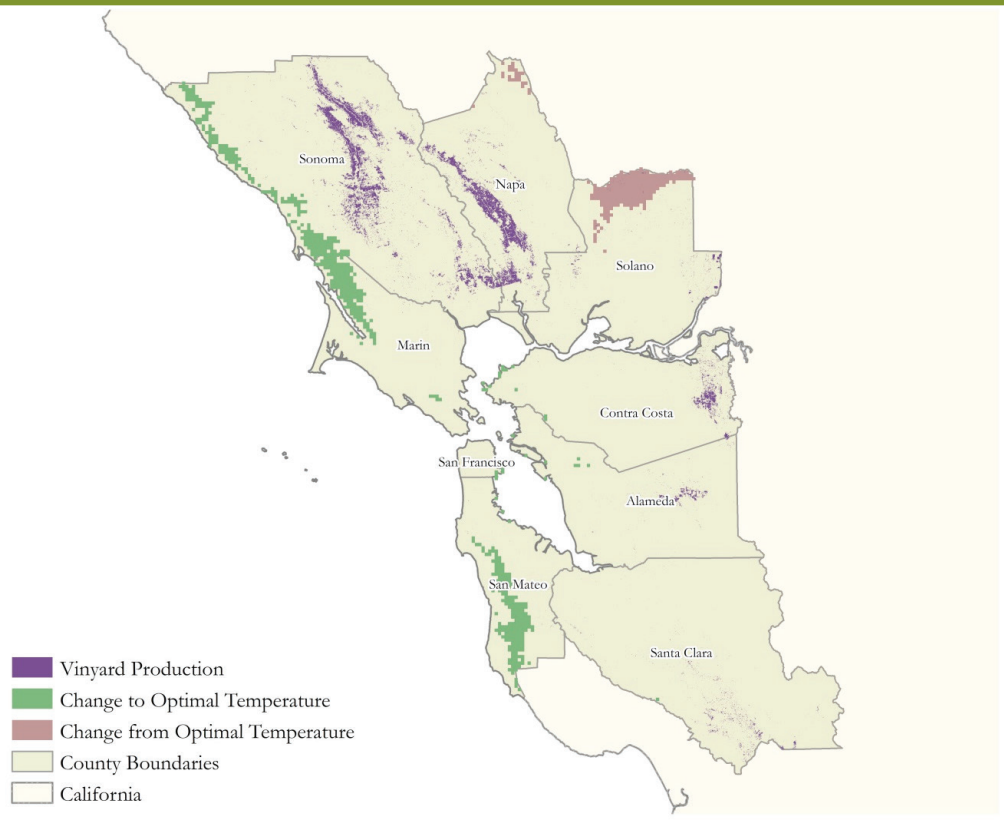

Changes in climatic suitability for wine grapes Source: Elias et al. 2015.

The pattern of decreased inland suitability but increased coastal suitability has been reported independently (Hannah *et al.* 2013; Elias *et al.* 2015). While mean temperatures may have minimal impact on Bay Area grape production by mid-century, wine grape acreage in the Bay Area could be vulnerable to extreme temperatures and temperature-related water scarcity by mid-century. When the composition and acreage of the specialty crops in all of California's counties were evaluated for sensitivity at mid-century, the nine counties in the Bay Area ranked in the mid-level of sensitivity for summer and winter changes in temperature because wine grapes have the relative potential to tolerate such increases better than other specialty crops more susceptible to increasing temperatures at key phenological stages (Kerr *et al.* 2017). Despite anticipated vulnerabilities, loss of wine grape production from the region is unlikely due to the heavy investment in institutional knowledge, capital and land, infrastructure, and supply chains to support the industry (A. Walker, pers. comm.). The varieties of wine grapes grown in the Bay Area likely will have to shift to accommodate changes in resource availability and climate.

Vines planted today will have a 20- to 30-year lifespan; thus, mid-century climate projections provide the relevant context for current adaptation and investment decisions. In the absence of adaptation efforts, climate change will likely have strong consequences for long-term growth and production. Wine grapes are a woody perennial crop that establishes the buds for one growth season in the preceding season; thus, management and weather events in the preceding and current growth season can cumulatively impact production and vine balance (Celette *et al.* 2009; Ripoche *et al.* 2010). Alterations in flavor development and accumulation of sugars in grapes may result from increases in absolute temperature and in the differential between day and night temperatures (Spayd *et al.* 2002; Keller *et al.* 2010; Nicholas & Durham 2012). Risk of Pierce's disease may increase as the infection rate of *Xylella fastidiosa* and the survival of its vector, the mealy bug, will benefit from increasing winter temperatures (A. Walker, pers. comm.). Continued prophylactic management of trunk diseases will be imperative. Warmer winter temperatures already lead to earlier growth of vines in spring, increases in yield in some cases, and risk of later frost damage, although this risk may be mitigated by reduced frost incidence in the future. High temperatures (>95 °F or 35 °C) during bloom can also hinder subsequent fruit set.

Similar to other agricultural systems, practices like cover crops, compost, and no-till soil management can improve soil health. They promote soil organic matter, stability of soil aggregates, stable pools of soil organic matter (SOM), water infiltration, microbiological activity, weed suppression, and trends for reductions in nitrate leaching and net greenhouse gas emissions (Steenwerth & Belina 2008b, a; Garland *et al.* 2011; Verhoeven & Six 2014; Belmonte *et al.* 2016; Yu *et al.* 2017). This body of work on wine grapes and other specialty crops has been incorporated into the USDA-NRCS tools, COMET-Farm, and COMET-Planner to support growers in implementing conservation practices that will reduce greenhouse gas emissions and improve soil organic matter and other aspects of soil health (Zhu *et al.* 2015). A yet unexamined concern is the potential limit of soils in the region to provide long-term stabilization of soil organic matter using these conservation practices under increasing climatic temperatures and any changes in quantity and timing of irrigation and rainfall.

Cover crops, compost, and no-till practices that improve soil health can provide adaptation, but vegetation on the vineyard floor can compete with the vines (Ripoche *et al.* 2010). Fortunately, irrigated vines in California are to some extent decoupled from effects of vineyard floor management compared to dry farm grapes. For instance, impacts of annual cover crops on vine nutrition and yields were not evident in a drip irrigated 12-year-old vineyard over three years (Steenwerth *et al.* 2016). Should future rainfall patterns limit available water for irrigation and subsurface sources,

vine balance and nutrition will be more sensitive to vineyard floor management, and effects will likely be evident two to four years after implementation (Celette *et al.* 2009). Managing irrigation with surface renewal and supporting continued investment in integrated technologies such as sensors at the vine and remote sensing scales will aid growers in precise, site-specific irrigation management (e.g., GRAPEX[27])

Novel approaches to adaptation were highlighted at a recent joint meeting involving university researchers, USDA-ARS scientists, and wine industry members (National Grape and Wine Initiative, Portland, November 2017). Surface renewal was developed decades ago, but recent advancements are enabling its diffusion into the wine grape industry to finely manage deficit irrigation. Development of rootstock germplasm and evaluation of tolerances to disease, deficit irrigation, and salt- and chloride-affected water sources are underway (See work by A. Walker – UC Davis, A. McElrone – USDA/ARS). Preliminary examination of wastewater streams from wineries using potassium-based cleaners and municipalities indicates that they can be tolerated by vineyard soil types with little observed impact on vines and wines in California (Mosse *et al.* 2013; Weber *et al.* 2014; Buelow *et al.* 2015b, a; Hirzel *et al.* 2017) and other Mediterranean regions (Quayle *et al.* 2009; Laurenson *et al.* 2012). Sun exposure and heat loading can be adjusted through changes in vine training, trellis type, and row orientation at planting to reduce sun exposure and heat loading, although these are less ideal adaptive measures due to inflexibility and potentially significant costs (Spayd *et al.* 2002). Effects of trellis type on wine grape quality for current and emerging varieties are not well understood, and efficient techniques to reduce temperatures across whole vineyards must still be developed.

The wine grape industry, and agriculture in general, also must mitigate risks of climate change on human capital, such as retention and access to seasonal labor and maintaining safe working conditions in extreme conditions. Job losses in the agricultural sector will disproportionately impact low-income communities, and these workers have limited access to labor and occupational health protections, especially for the undocumented community (Shonkoff *et al.* 2009). At a national level, crop workers experience elevated risk of mortality from heat stroke (CDC 2008). These risks are much lower in the Bay Area due to the coastal climate, but the lack of preparation and experience with extremes can increase vulnerability to heat waves (see Public Health section, above).

Rangelands and Belowground Carbon Sequestration

Rangelands are the dominant cover type in California, covering approximately 23 million hectares or over 40% of the state (*Forest and Rangelands Assessment Program* 2010). Rangelands are defined as ecosystems with plant cover suitable for grazing that are dominated by grasses, grass-like plants, forbs, or shrubs. Bay Area rangelands are dominated by oak savanna and annual grassland ecosystems (grasslands are here defined as rangelands dominated by grasses and forbs). Rangelands can include native and introduced plant species (*Summary Report: 2007 National Resources Inventory* 2009). Throughout California, including the Bay Area, annual plant species, especially exotic grasses, are the most common vegetation type in rangelands (D'Antonio *et al.* 2007). In the Bay Area, rangelands cover approximately 1.7 million hectares, or 40% of the land area (CDC 2009).

California's rangelands play an important role in the beef cattle and dairy industries. Livestock and livestock products in California accounted for 25% of the state's gross agricultural cash receipts in 2015 *(California Agricultural Statistics Report 2015-2016* 2016*)* which amounted to $15.3 billion in 2014 and $12 billion in 2015. Dairy products are the

27 https://www.ars.usda.gov/northeast-area/beltsville-md/beltsville-agricultural-research-center/hydrology-and-remote-sensing-laboratory/docs/grapex/).

state's leading commodity. The California dairy industry was responsible for 18% of the annual dairy receipts of the US in 2015. In 2016, revenue from milk and cream amounted to $6.07 billion, while beef cattle revenue was $2.53 billion (*2016 Crop Year Report CDFA* n.d.). The Bay Area supports over 230,000 head of cattle ("USDA NASS" 2016). Marin and Sonoma counties are the largest dairying regions in the Bay Area with 2% of the state's dairy cows on 7% of the dairies ("CDFA California Dairy Statistics Annual 2016" 2016).

Bay Area rangelands experience a Mediterranean climate with cool wet winters and hot dry summers. Plant productivity in California's rangelands is tightly coupled with patterns in precipitation. The high inter-annual variability in rainfall leads to large inter-annual differences in aboveground biomass (e.g. forage) production (Huntsinger & Bartolome 2014). The sensitivity of rangeland vegetation to precipitation dynamics makes these ecosystems particularly vulnerable to climate change. Changes in rainfall regimes are likely to affect plant production and associated patterns in soil carbon and greenhouse gas production (Jackson *et al.* 2007; Ma *et al.* 2007; Chou *et al.* 2008; Grant *et al.* 2012; Schwalm *et al.* 2012).

Climate models yield varying results for precipitation in the Bay Area. Under a wetter future scenario, some Bay Area counties could see an increase in forage production (Shaw *et al.* 2011), depending upon how that rainfall is distributed (George *et al.* 2010). Timing of rainfall is important to the physiology and growth of California's annual grassland species, as well as soil carbon dynamics (Chou *et al.* 2008). An increase in summer rainfall events with climate change is likely to stimulate soil respiration (Xu & Baldocchi 2004; Baldocchi *et al.* 2006; Chou *et al.* 2008). Simulated increases in early and late season rainfall events (i.e., September and May–July) increased microbial activity and associated decomposition of carbon stored in soils (Chou *et al.* 2008). Increased rainfall during the rainy season had little effect on carbon pools and fluxes. Drought leads to low net primary production and can result in a significant net source of carbon to the atmosphere in California rangelands as microbial respiration exceeds plant carbon uptake (Xu & Baldocchi 2003; Ma *et al.* 2007). Drought can also increase plant mortality, particularly in oak woodlands, leading to lower carbon uptakes and higher soil respiration losses (Fellows & Goulden 2013). An increase in fire associated with droughts and higher temperatures is also likely to lead to large carbon losses from Bay Area rangelands.

The effects of increased temperature on rangeland ecosystems is unclear. In a modeling experiment, Chaplin-Kramer (2013) found increased forage production in most Bay Area rangelands, particularly toward the end of the century. However, periodic drought, which was assumed to occur two to four times over a 30-year period, led to dramatic declines in aboveground production in all areas except the North Bay (Chaplin-Kramer 2013). The model projections also predicted a shorter growing season, particularly in the South Bay, which could partially offset the benefits of increased growth.

Rangelands have the potential to have large soil carbon pools. Periods of low rainfall and the occurrence of dry seasons favor plant species with high carbon allocation to root biomass. High root biomass stocks tend to facilitate the development of carbon-rich soils. A meta-analysis of research on California's rangelands showed that soils stored about 140 megagrams of carbons per hectare in the top meter of the profile (Silver *et al.* 2010) (for comparison, above-ground carbon in grasslands is generally <2 megagram of carbon per hectare). Carbon stocks in surface soils (0-20 cm depth) were similar to those of Midwestern perennial grasslands, but when the top meter was considered, California's annual grasslands generally had lower soil carbon stocks than perennial systems. Owen and Silver (2015) reported soil carbon stocks that ranged from 60 ± 2 to 223 ± 6 Mg C ha^{-1} in the top 50 centimeters of soil on rangelands in Marin and Sonoma counties.

Soil carbon sequestration in rangelands has been proposed as a means to help mitigate climate change (Conant 2011; *CA Healthy Soils Initiative* 2016; Flint *et al.* 2018). Livestock manure is a common amendment on rangelands. A recent study of Bay Area rangelands showed that manure amendments significantly increased soil carbon stocks, but also stimulated the emissions of nitrous oxide (N_2O), a potent greenhouse gas (Owen & Silver 2015). Results suggested that rangelands are a net source of CO_2e[28] to the atmosphere under this management regime. Composting livestock manure with green waste, combined with grazing, can lower greenhouse gas emissions of organic matter amendments (DeLonge *et al.* 2013; Ryals & Silver 2013). Marin County rangelands experienced a net sink of approximately 1 Mg C ha^{-1} y^{-1} over the first three years following a single application of compost to surface soils (Ryals & Silver 2013; Ryals *et al.* 2014). There was no significant increase in N_2O emissions relative to untreated control plots. A lifecycle assessment model suggested that applying compost to only 5% of California's rangelands (an area equivalent to 68% of Bay Area's rangelands) could offset all of the annual livestock emissions for the state. Compost amendments significantly increased above and belowground net primary productivity over multiple years (Ryals & Silver 2013). Model output suggested that the net sink would persist for several decades (Ryals *et al.* 2015).

The effects of compost amendments on soil carbon storage was robust under different future climate change scenarios when modeled for seven locations across the state (Silver *et al.* 2018). Bay Area rangelands in Marin County showed a maximum increase of 6 Mg CO_2e ha^{-1} relative to untreated soils 15 years after compost application. The same magnitude of benefit occurred under both an RCP 4.5 and RCP 8.5 scenario. The model predicted a similar benefit in Solano County, with a slightly greater 15-year impact under the RCP 8.5 scenario (6.49 Mg CO_2e ha^{-1} relative to untreated soils) (Silver *et al.* 2018).

Soils high in organic matter stocks, and thus carbon content, can also play an important role in adaptation to climate change. Soil organic matter content plays an important role in the ecohydrology of rangelands. Organic matter generally holds more moisture than minerals in soils, and thus organic rich soils may be better buffered against drought. Bay Area rangelands that received organic matter amendments had higher water holding capacity than untreated soils (Ryals & Silver 2013). Flint et al. (2018), in a report for California's Fourth Climate Change Assessment, conducted a modeling study that suggested benefits of organic matter amendments would be widespread in California, with significant gains in water holding capacity and resilience to drought (Flint *et al.* 2018). They found that a 1% increase in soil organic matter content led to a 3.2% increase in soil moisture storage. When modeling with both a wetter and drier future climate scenario (both RCP 8.5), Flint et al. found that 97% of California's rangeland and cropland benefited hydrologically from compost application. Rangelands with a wetter climate, typical of Bay Area locations, were more likely to benefit from higher soil water storage than more arid regions.

28 CO2e refers to CO2 equivalents, a metric of the cumulative heat-trapping potential of gases emitted to the atmosphere, including methane, NOx, etc., in equivalent units of CO2 emissions.

Conclusion

The Bay Area faces a panoply of challenges triggered by a changing climate. The region also has a unique economic, political, and social fabric, buttressed by California's national and global leadership on climate change mitigation and adaptation. While the challenges loom large, novel ideas and innovations are rapidly emerging that could show the way to a resilient future. The pace of change in the physical environment that is projected in the coming decades will outpace any episode in recent human history, and a similarly unprecedented pace of societal change may be necessary in response. This report, along with the summary reports for other regions of California and the contributions of California's most recent Climate Change Assessment, provide the knowledge base to design and test adaptation strategies and identify uncertainties and knowledge gaps that will need to be addressed moving forward.

The joint effort by Bay Area scientists and stakeholders to produce this report can also serve as a foundation for an on-going science-to-action collaboration among academics, government officials and staff, community organizations, and the private sector. To start, the data and information contained here, along with guidance on how to interpret and apply it, can be distributed widely to inform decision-making at the regional and local levels. This can include slide decks, printed and web-based materials, social media, and other channels. It can spotlight the growing number of exciting solutions and innovative pilot projects that are being developed in our region to respond to the challenge of climate change.

Moreover, the new Bay Area Climate Adaptation Network (BayCAN) and its partners can use this report and related materials to engage the public and elected leaders for in-depth discussions on how the Bay Area will accelerate its work to build a strong and resilient Bay Area for all. This campaign can include school activities, community meetings, facilitated discussions in workplaces and faith-based communities, and other approaches. Finally, this process of engagement can identify the key information and knowledge gaps that will be the focus of the next rounds of climate adaptation research. In this way, the Bay Area Regional Report can be seen as the *beginning* of a deep partnership between academic experts and a broad range of regional stakeholders that will help build the equitable and resilient 21st century Bay Area.

Works Cited

2016 Crop Year Report CDFA. (n.d.). Available at: www.cdfa.ca.gov/statistics/. Accessed 29 August 2018.

Abatzoglou, J.T. & Williams, A.P. (2016). Impact of anthropogenic climate change on wildfire across western US forests. Proc. Natl. Acad. Sci., 113, 11770–11775.

Ackerly, D.D., Cornwell, W.K., Weiss, S.B., Flint, L.E. & Flint, A.L. (2015). A geographic mosaic of climate change impacts on terrestrial vegetation: Which areas are most at risk? PLoS One, 10(6): e0130629.

Ackerly, David D., Rebecca A. Ryals, Will K. Cornwell, Scott R. Loarie, Sam Veloz, Kelley D. Higgason, Whendee L. Silver, and Todd E. Dawson. 2012. Potential Impacts of Climate Change on Biodiversity and Ecosystem Services in the San Francisco Bay Area. California Energy Commission. Publication number: CEC-500-2012-037.

Agee, J.K. & Skinner, C.N. (2005). Basic principles of forest fuel reduction treatments. In: Forest Ecology and Management, 211, 83–96.

Ahlm, L., Jones, A., Stjern, W.C., Muri, H., Kravitz, B. & Kristjánsson, J.E. (2017). Marine cloud brightening - As effective without clouds. Atmos. Chem. Phys., 17, 13,071–13,087.

Allan, J.C. & Komar, P.D. (2006). Climate Controls on US West Coast Erosion Processes. J. Coast. Res., 223, 511–529.

Allen, M.R. & Ingram, W.J. (2002). Constraints on future changes in climate and the hydrologic cycle. Nature. 419. 224-32.

Alstone, P., Potter, J., Piette, M.A., Schwartz, P., Berger, M.A., Dunn, L.N., et al. (2016). 2015 California Demand Response Potential Study - Charting California's Demand response Future: Interim Report on Phase 1 Results. Available at: http://eta-publications.lbl.gov/sites/default/files/2015_dr_potential_study_phase1_final_report.pdf. Accessed 28 August 2018.

Anderson, K. (2006). Tending the Wild: Native American Knowledge and the Management of California's Natural Resources. University of California Press, Berkeley, California.

Angélil, O., Stone, D., Wehner, M., Paciorek, C.J., Krishnan, H. & Collins, W. (2017). An independent assessment of anthropogenic attribution statements for recent extreme temperature and rainfall events. J. Clim., 30, 5–16.

Auffhammer, M. (2018). Climate Adaptive Response Estimation: Short and Long Run Impacts of Climate Change on Residential Electiricty and Natural Gas Consumption Using Big Data. California's Fourth Climate Change Assessment. Publication number: CCCA4-EXT-2018-005

BAAQMD. (2017). Bay Area Clean Air Plan. Available at: www.baaqmd.gov/plans-and-climate/air-quality-plans/current-plans. Accessed 28 August 2018.

Baldocchi, D., Tang, J. & Xu, L. (2006). How switches and lags in biophysical regulators affect spatial-temporal variation of soil respiration in an oak-grass savanna. J. Geophys. Res. Biogeosciences, 111, G2.

Ballard, G., Barnard, P.L., Erikson, L., Fitzgibbon, M., Higgason, K., Psaros, M., et al. (n.d.). Our Coast Our Future (OCOF) web tool. Available at: www.ourcoastourfuture.org. Accessed 26 August 2018.

BAOSC. (2011). The Conservation Lands Network: San Francisco Bay Area Upland Habitat Goals Project Report. Available at: www.Bayarealands.Org. Accessed 26 August 2018.

Barnard, P.L., Hoover, D., Hubbard, D.M., Snyder, A., Ludka, B.C., Allan, J., et al. (2017). Extreme oceanographic forcing and coastal response due to the 2015-2016 El Niño. Nat. Commun., 8, 14365.

Barnard, P.L., van Ormondt, M., Erikson, L.H., Eshleman, J., Hapke, C., Ruggiero, P., et al. (2014). Development of the Coastal Storm Modeling System (CoSMoS) for predicting the impact of storms on high-energy, active-margin coasts. Nat. Hazards, 74, 1095–1125.

Barnard, P.L., Short, A.D., Harley, M.D., Splinter, K.D., Vitousek, S., Turner, I.L., et al. (2015). Coastal vulnerability across the Pacific dominated by El Niño/Southern Oscillation. Nat. Geosci., 8, 801–807.

Baron, E. (2018). Silicon Valley's housing and traffic woes put it at risk for replacement: former Stanford president John Hennessy. Mercury News. Available at: www.mercurynews.com/2018/03/21/silicon-valleys-housing-and-traffic-woes-put-it-at-risk-for-replacement-former-stanford-president-john-hennessy/. Accessed 27 August 2018.

Bay-Area-IRWMP. (n.d.). Bay Area Integrated Regional Water Management Plan. Available at: http://bayareairwmp.org/. Accessed 26 August 2018.

BayREN. (2017). BayREN Energy Efficiency Business Plan 2018-2025. Available at: abag.ca.gov/bayren/documents/BayREN_BusinessPlan_20170123_PDFA.pdf. Accessed 29 August 2018.

BCDC. (2009). Living with a Rising Bay: Vulnerability and Adaptation in the San Francisco Bay and its Shoreline. Available at: http://www.bcdc.ca.gov/proposed_bay_plan/bp_1-08_cc_draft.pdf. Accessed 26 August 2018.

Belmecheri, S., Babst, F., Wahl, E.R., Stahle, D.W. & Trouet, V. (2016). Multi-century evaluation of Sierra Nevada snowpack. Nat. Clim. Change 6, 2.

Belmonte, S.A., Celi, L., Stanchi, S., Said-Pullicino, D., Zanini, E. & Bonifacio, E. (2016). Effects of permanent grass versus tillage on aggregation and organic matter dynamics in a poorly developed vineyard soil. Soil Res., 54, 797–808.

Berg, N. & Hall, A. (2017). Anthropogenic warming impacts on California snowpack during drought. Geophys. Res. Lett., 44, 2511–2518.

Bernard, S.M., Samet, J.M., Grambsch, A., Ebi, K.L. & Romieu, I. (2001). The potential impacts of climate variability and change on air pollution-related health effects in the United States. Environ. Heal. Perspect., 109, 199–209.

Biging, Greg S., John D. Radke, and Jun Hak Lee. (2012). Impacts of Predicted Sea-Level Rise and Extreme Storm Events on the Transportation Infrastructure in the San Francisco Bay Region. California Energy Commission. Publication number: CEC-500-2012-040.

Bindoff, N.L., Stott, P.A., AchutaRao, K.M., Allen, M.R., Gillett, N., Gutzler, D., et al. (2013). Detection and Attribution of Climate Change: from Global to Regional. In: Climate Change 2013: The Physical Science Basis. Contribution of Working Group I to the Fifth Assessment Report of the Intergovernmental Panel on Climate Change, Eds: Stocker, T.F., D. Qin, G.-K. Plattner, M. Tignor, S.K. Allen, J. Boschung, A. Nauels, Y. Xia, pp. 1217–1308.

Bromirski, P.D., Miller, A.J., Flick, R.E. & Auad, G. (2011). Dynamical suppression of sea level rise along the Pacific coast of North America: Indications for imminent acceleration. J. Geophys. Res. Ocean., 116, C7.

Brooks, B., Telling, J.T., Ericksen, T., Glennie, C.L., Knowles, N., Cayan, D., et al. (2018). High Resolution Measurement of Levee Subsidence Related to Energy Infrastructure in the Sacramento-San Joaquin Delta. Available at: http://climateassessment.ca.gov/techreports/docs/20180827-Energy_CCCA4-CEC-2018-003.pdf. Accessed 29 August 2018.

Buelow, M.C., Steenwerth, K. & Parikh, S.J. (2015a). The effect of mineral-ion interactions on soil hydraulic conductivity. Agric. Water Manag., 152, 277–285.

Buelow, M.C., Steenwerth, K., Silva, L.C.R. & Parikh, S.J. (2015b). Characterization of winery wastewater for reuse in California. Am. J. Enol. Vitic., 66, 302–310.

Burgess, S.S.O. & Dawson, T.E. (2004). The contribution of fog to the water relations of Sequoia sempervirens (D. Don): Foliar uptake and prevention of dehydration. Plant, Cell Environ., 27, 1023–1034.

Bürgmann, R., Hilley, G., Ferretti, A. & Novali, F. (2006). Resolving vertical tectonics in the San Francisco Bay Area from permanent scatterer InSAR and GPS analysis. Geology, 34, 221–224.

Burns, E. E. (2017). Understanding Sequoia sempervirens. Gen. Tech. Rep. PSW-GTR-258. Albany, CA: US Department of Agriculture, Forest Service, Pacific Southwest Research Station: 9-13, 258.

Butsic, V., Kelly, M. & Moritz, M. (2015). Land Use and Wildfire: A Review of Local Interactions and Teleconnections. Land, 4, 140–156.

CA Healthy Soils Initiative. (2016). Available at: https://www.cdfa.ca.gov/healthysoils/. Accessed 26 August 2018.

Cai, W., Borlace, S., Lengaigne, M., Van Rensch, P., Collins, M., Vecchi, G., et al. (2014). Increasing frequency of extreme El Niño events due to greenhouse warming. Nat. Clim. Chang., 4, 111–116.

California Agricultural Statistics Report 2015-2016. (2016). Available at: www.cdfa.ca.gov/statistics/PDFs/2016Report.pdf. Accessed 26 August 2018.

California Department of Water Resources. (2015). California Climate Science and Data for Water Resources Management. Calif. Clim. Sci. Data, Climate Change Program. Available at: www.water.ca.gov/LegacyFiles/climatechange/docs/CA_Climate_Science_and_Data_Final_Release_June_2015.pdf. Accessed 26 August 2018.

Cayan, D.R., Bromirski, P.D., Hayhoe, K., Tyree, M., Dettinger, M.D. & Flick, R.E. (2008). Climate change projections of sea level extremes along the California coast. Clim. Change, 87, 57–73.

Cayan, D.R. & Peterson, D.H. (1993). Spring climate and salinity in the San Francisco Bay Estuary. Water Resour. Res., 29, 293–303.

Cayan, D.R., Pierce, D.W. & Kalansky, J.F. (2018a). Climate, drought, and sea level rise scenarios for the Fourth California Climate Assessment.

Cayan, D.R., Pierce, D.W. & Kalansky, J.F. (2018b). Climate, Drought, and Sea Level Rise Scenarios for the Fourth California Climate Assessment.

CDC. (2008). Heat-related deaths among crop workers--United States, 1992--2006. MMWR. Morb. Mortal. Wkly. Rep., 57, 649–53.

CDC. (2009). Farmland Mapping and Monitoring Program. Available at: http://www.conservation.ca.gov/dlrp/fmmp. Accessed 26 August 2018.

CDFA California Dairy Statistics Annual 2016. (2016). Available at: https://www.cdfa.ca.gov/dairy/pdf/Annual/2016/2016_Statistics_Annual.pdf. Accessed 26 August 2018.

CEC. (2014). California Natural Gas Data and Statistics. Available at: https://www.energy.ca.gov/almanac/naturalgas_data/. Accessed 26 August 2018.

Celette, F., Findeling, A. & Gary, C. (2009). Competition for nitrogen in an unfertilized intercropping system: The case of an association of grapevine and grass cover in a Mediterranean climate. Eur. J. Agron., 30, 41–51.

Chan, N.Y., Stacey, M.T., Smith, A.E., Ebi, K.L. & Wilson, T.F. (2001). An empirical mechanistic framework for heat-related illness. Clim. Res., 16, 133–143.

Chaplin-Kramer, R. 2013. Climate Change and the Agricultural Sector in the San Francisco Bay Area: Changes in Viticulture and Rangeland Forage Production Due to Altered Temperature and Precipitation Patterns. California Energy Commission. Publication number: CEC-500-2012-033.

Charles, J. (2013). The phenology project: Getting kids involved in science. Bay Nature, April-June 2013.

Cheng, L., Hoerling, M., Aghakouchak, A., Livneh, B., Quan, X.W. & Eischeid, J. (2016). How has human-induced climate change affected California drought risk? J. Clim., 29, 111–120.

Chornesky, E.A., Ackerly, D.D., Beier, P., Davis, F.W., Flint, L.E., Lawler, J.J., et al. (2015). Adapting California's ecosystems to a changing climate. Bioscience, 65, 247-262.

Chou, W.W., Silver, W.L., Jackson, R.D., Thompson, A.W. & Allen-Diaz, B. (2008). The sensitivity of annual grassland carbon cycling to the quantity and timing of rainfall. Glob. Chang. Biol., 14, 1382–1394.

Chua, V.P. & Xu, M. (2014). Impacts of sea-level rise on estuarine circulation: An idealized estuary and San Francisco Bay. J. Mar. Syst., 139, 58–67.

Chung, M., Dufour, A., Pluche, R. & Thompson, S. (2017). How much does dry-season fog matter? Quantifying fog contributions to water balance in a coastal California watershed. Hydrol. Process., 31, 3948–3961.

Clare, F.C., Halder, J.B., Daniel, O., Bielby, J., Semenov, M.A., Jombart, T., et al. (2016). Climate forcing of an emerging pathogenic fungus across a montane multi-host community. Philos. Trans. R. Soc. B Biol. Sci., 371, 20150454.

Clark, P.U., Shakun, J.D., Marcott, S.A., Mix, A.C., Eby, M., Kulp, S., et al. (2016). Consequences of twenty-first-century policy for multi-millennial climate and sea-level change. Nat. Clim. Chang. 2923, 10.

Clemesha, R.E.S., Gershunov, A., Iacobellis, S.F. & Cayan, D.R. (2017a). Daily variability of California coastal low cloudiness: A balancing act between stability and subsidence. Geophys. Res. Lett., 44, 3330–3338.

Clemesha, R.E.S., Guirguis, K., Gershunov, A., Small, I.J. & Tardy, A. (2017b). California heat waves: their spatial evolution, variation, and coastal modulation by low clouds. Clim. Dyn., 1–17.

Cloern, J.E., Knowles, N., Brown, L.R., Cayan, D., Dettinger, M.D., Morgan, T.L., et al. (2011). Projected evolution of California's San Francisco bay-delta-river system in a century of climate change. PLoS One(9): e24465.

CNRA. (2009). California Climate Adaptation Strategy. Available at: http://www.climatechange.ca.gov/adaptation/strategy/index.html. Accessed 26 August 2018.

CNRA. (2014). Safeguarding California: Reducing Climate Risk. Available at: http://resources.ca.gov/docs/climate/Final_Safeguarding_CA_Plan_July_31_2014.pdf. Accessed 26 August 2018.

CNRA. (2016). Safeguarding California: Implementation Action Plans. Available at: http://resources.ca.gov/docs/climate/safeguarding/Safeguarding%20California-Implementation%20Action%20Plans.pdf. Accessed 26 August 2018.

Collins, M., An, S.-I., Cai, W., Ganachaud, A., Guilyardi, E., Jin, F.-F., et al. (2010). The impact of global warming on the tropical Pacific Ocean and El Niño. Nat. Geosci., 3, 391–397.

Collins, M., Chandler, R.E., Cox, P.M., Huthnance, J.M., Rougier, J. & Stephenson, D.B. (2012). Quantifying future climate change. Nat. Clim. Chang, 2, 403.

Collins, M., Knutti, R., Arblaster, J., Dufresne, J.-L., Fichefet, T., Friedlingstein, P., et al. (2013). Long-term Climate Change: Projections, Commitments and Irreversibility. In: Climate Change 2013: The Physical Science Basis. Contribution of Working Group I to the Fifth Assessment Report of the Intergovernmental Panel on Climate Change, pp. 1029–1136.

Conant, R.T. (2011). Sequestration through forestry and agriculture. Wiley Interdiscip. Rev. Clim. Change 2, 238-254.

Cook, E.R., Seager, R., Heim, R.R., Vose, R.S., Herweijer, C. & Woodhouse, C. (2010). Megadroughts in North America: Placing IPCC projections of hydroclimatic change in a long-term palaeoclimate context. J. Quat. Sci., 25, 48–61.

Cooley, H., Moore, E., Heberger, M. & Allen, L. (2012). Social Vulnerability to Climate Change in California.

Cornwall, C., Moore, S., DiPietro, D., Veloz, S., Micheli, L., Casey, L., et al. (2014). Climate Ready Sonoma County: Climate Hazards and Vulnerabilities. Available at: http://rcpa.ca.gov/wp-content/uploads/2016/03/Climate-Ready_Hazards_Vulnerabilities-FINAL.pdf. Accessed 26 August 2018.

D'Antonio, C.M., Malmstrom, C., Reynolds, S.A., Gerlach, J., Stromberg, M. & Corbin, J. (2007). Ecology of Invasive Non-Native Species in California Grassland. In: California Grasslands: Ecology and Management (eds. Stromberg, M.R., Corbin, J.D.C. & D'Antonio, C.M.). University of California Press, pp. 67–83.

Dangendorf, S., Marcos, M., Wöppelmann, G., Conrad, C.P., Frederikse, T. & Riva, R. (2017). Reassessment of 20th century global mean sea level rise. Proc. Natl. Acad. Sci., 114, 5946–5951.

Dawson, T.E. (1998). Fog in the California redwood forest: Ecosystem inputs and use by plants. Oecologia, 117, 476–485.

DeConto, R.M. & Pollard, D. (2016). Contribution of Antarctica to past and future sea-level rise. Nature, 531, 591–597.

DeLonge, M.S., Ryals, R. & Silver, W.L. (2013). A Lifecycle Model to Evaluate Carbon Sequestration Potential and Greenhouse Gas Dynamics of Managed Grasslands. Ecosystems, 16, 962–979.

Dettinger, M.. & Anderson, M.L. (2015). Storage in California's Reservoirs and Snowpack in this Time of Drought. San Fr. Estuary Watershed Sci., 13(2).

Dettinger, M. (2011). Climate change, atmospheric rivers, and floods in California - a multimodel analysis of storm frequency and magnitude changes. J. Am. Water Resour. Assoc., 47, 514–523.

Dettinger, M.D. (2013). Atmospheric Rivers as Drought Busters on the U.S. West Coast. J. Hydrometeorol., 14, 1721–1732.

Dettinger, M.D., Ralph, F.M., Das, T., Neiman, P.J. & Cayan, D.R. (2011). Atmospheric Rivers, Floods and the Water Resources of California. Water, 3, 445–478.

Diffenbaugh, N.S., Swain, D.L. & Touma, D. (2015). Anthropogenic warming has increased drought risk in California. Proc. Natl. Acad. Sci., 112, 3931–3936.

Dorman, C.E., Mejia, J., Koračin, D. & McEvoy, D. (2017). Worldwide Marine Fog Occurrence and Climatology. In: Marine Fog: Challenges and Advancements in Observations, Modeling, and Forecasting. Editors: Koračin, D., Dorman, C.E., pp. 7–152.

Drexler, J.Z., de Fontaine, C.S. & Brown, T.A. (2009). Peat accretion histories during the past 6,000 years in marshes of the sacramento-san joaquin delta, CA, USA. Estuaries and Coasts, 32, 871–892.

EBMUD. (2013). All About EBMUD. Available at: www.ebmud.com/index.php/download.../1365/?All-About-EBMUD-2013.pdf. Accessed 26 August 2018.

Egli, S., Thies, B., Drönner, J., Cermak, J. & Bendix, J. (2017). A 10 year fog and low stratus climatology for Europe based on Meteosat Second Generation data. Q. J. R. Meteorol. Soc., 143, 530–541.

Ekstrom, Julia A., and Susanne C. Moser. (2012). Climate Change Impacts, Vulnerabilities, and Adaptation in the San Francisco Bay Area: A Synthesis of PIER Program Reports and Other Relevant Research. California Energy Commission. Publication number: CEC-500-2012-071.

Ekstrom, Julia A., Meghan R. Klasic, Amanda Fencl, Mark Lubell, Ezekiel Baker, Frances Einterz. (2018). Drought Management and Climate Adaptation among Small, Self-Sufficient Water Systems in California. California's Fourth Climate Change Assessment, California Natural Resources Agency.

Elias, E., Brody-Lopez, N., Dialesandro, J., Steele, C., Rango, A. 2015. Impacts of projected mid-century temperatures on thermal regimes for select specialty and fieldcrops common to the southwestern U.S. [abstract]. American Geophysical Union 2015 Fall Meeting, December 14-18, 2015, San Francisco, CA. GC13D-1186.

Erikson, L.H., Hegermiller, C.A., Barnard, P.L., Ruggiero, P. & van Ormondt, M. (2015). Projected wave conditions in the Eastern North Pacific under the influence of two CMIP5 climate scenarios. Ocean Model., 96, 171–185.

Evett, R.R., Dawson, A. & Bartolome, J.W. (2013). Estimating vegetation reference conditions by combining historical source analysis and soil phytolith analysis at pepperwood preserve, northern california coast ranges, U.S.A. Restor. Ecol., 21, 464–473.

FCAT. (2018). California Forest Carbon Plan: Managing our forest landscapes in a changing climate. Sacramento, CA. Available at: http://resources.ca.gov/wp-content/uploads/2018/05/California-Forest-Carbon-Plan-Final-Draft-for-Public-Release-May-2018.pdf. Accessed 26 August 2018.

Fellows, A.W. & Goulden, M.L. (2013). Controls on gross production by a semiarid forest growing near its warm and dry ecotonal limit. Agric. For. Meteorol., 169, 51–60.

Ferretti, A., Novali, E., Bürgmann, R., Hilley, G. & Prati, C. (2004). InSAR permanent scatterer analysis reveals ups and downs in San Francisco Bay Area. EOS Trans. Am. Geophys. Union, 85, 317, 324.

Ferrier, S. & Guisan, A. (2006). Spatial modelling of biodiversity at the community level. J. Appl. Ecol., 43, 393-404.

Flint, L., Flint, A., Stern, M., Mayer, A., Vergara, S., Silver, W., et al. (2018). Increasing Soil Organic Carbon to Mitigate Greenhouse Gases and Increase Climate Resiliency for California.

Flint, L.E., Flint, A.L., Thorne, J.H. & Boynton, R. (2013). Fine-scale hydrologic modeling for regional landscape applications: The California Basin Characterization Model development and performance. Ecol. Process., 2, 1–21.

Le Floch, C., Belletti, F. & Moura, S. (2016). Optimal Charging of Electric Vehicles for Load Shaping: A Dual-Splitting Framework With Explicit Convergence Bounds. IEEE Trans. Transp. Electrif., 2, 190–199.

Forest and Range Assessment: Data. 2010. Available at: http://frap.fire.ca.gov/data/frapgisdata-sw-rangeland-assessment_data. Accessed 29 August 2018.

California Department of Forestry and Fire Protection. 2010. California's forest and rangelands: 2010 assessment. Sacramento, CA, USA: Forest and Rangelands Assessment Program. p. 39–40. Available at: http://frap. re.ca.gov/assessment/2010/ assessment2010.php. Accessed 26 August 2018.

Forister, M.L. & Shapiro, A.M. (2003). Climatic trends and advancing spring flight of butterflies in lowland California. Glob. Chang. Biol., 9, 1130–1135.

Fu, C. & Dan, L. (2018). The variation of cloud amount and light rainy days under heavy pollution over South China during 1960–2009. Environ. Sci. Pollut. Res., 25, 2369–2376.

Garland, G.M., Suddick, E., Burger, M., Horwath, W.R. & Six, J. (2011). Direct N2O emissions following transition from conventional till to no-till in a cover cropped Mediterranean vineyard (Vitis vinifera). Agric. Ecosyst. Environ., 144, 423–428.

Gemmrich, J., Thomas, B. & Bouchard, R. (2011). Observational changes and trends in northeast Pacific wave records. Geophys. Res. Lett., 38 (22), 5.

George, M.R., Larsen, R.E., McDougald, N.M., Vaughn, C.E., Flavell, D.K., Dudley, D.M., et al. (2010). Determining drought on california's mediterranean-type rangelands: The noninsured crop disaster assistance program. Rangelands, 32, 16–20.

Gershunov, A. & Guirguis, K. (2012). California heat waves in the present and future. Geophys. Res. Lett., 39, L18710.

Gimeno, L., Nieto, R., VÃ¡zquez, M. & Lavers, D.A. (2014). Atmospheric rivers: a mini-review. Front. Earth Sci., 2, 2.

Gittman, R.K., Popowich, A.M., Bruno, J.F. & Peterson, C.H. (2014). Marshes with and without sills protect estuarine shorelines from erosion better than bulkheads during a Category 1 hurricane. Ocean Coast. Manag., 102, 94–102.

Giwargis, R. (2017). San Jose flood: Hundreds return home as questions swirl about surprise flood. San Jose Mercury News. 24 February 2017.

Goals_Project. (2015). The Baylands and Climate Change: What We Can Do. Baylands Ecosystem Habitat Goals Science Update. Oakland. Available at: https://baylandsgoals.org/science-update-2016/. Accessed 26 August 2018.

Gonzalez, P., Battles, J.J., Collins, B.M., Robards, T. & Saah, D.S. (2015). Aboveground live carbon stock changes of California wildland ecosystems, 2001-2010. For. Ecol. Manage., 348, 68–77.

Graham, N.E., Cayan, D.R., Bromirski, P.D. & Flick, R.E. (2013). Multi-model projections of twenty-first century North Pacific winter wave climate under the IPCC A2 scenario. Clim. Dyn., 40, 1335–1360.

Grant, R.F., Baldocchi, D.D. & Ma, S. (2012). Ecological controls on net ecosystem productivity of a seasonally dry annual grassland under current and future climates: Modelling with ecosys. Agric. For. Meteorol., 152, 189–200.

Grape Crush Final Report 2016. (2017). California Department of Food and Agriculture. Issued March 10, 2017, 1-160.

Gray, E., Baldocchi, D.D. & Goldstein, A.H. (2016). Influence of NOx Emissions on Central Valley Fog Frequency and Persistence. Abstract A21L-04 presented at 2016 Fall Meeting, American Geophysical Union, San Francisco, CA, 12-16 December 2016.

Griffin, D. & Anchukaitis, K.J. (2014). How unusual is the 2012 – 2014 California drought ? Geophys. Res. Lett., 41, 9017–9023.

Griffin, L.M. (1998). Saving the Marin-Sonoma Coast. Sweetwater Springs Press, Healdsburg, California.

Guan, B., Molotch, N.P., Waliser, D.E., Fetzer, E.J. & Neiman, P.J. (2013). The 2010/2011 snow season in California's Sierra Nevada: Role of atmospheric rivers and modes of large-scale variability. Water Resour. Res., 49, 6731–6743.

Guan, B., Waliser, D.E., Ralph, F.M., Fetzer, E.J. & Neiman, P.J. (2016). Hydrometeorological characteristics of rain-on-snow events associated with atmospheric rivers. Geophys. Res. Lett., 43, 2964–2973.

Hamlington, B.D., Cheon, S.H., Thompson, P.R., Merrifield, M.A., Nerem, R.S., Leben, R.R., et al. (2016). An ongoing shift in Pacific Ocean sea level. J. Geophys. Res. Ocean., 121, 5084–5097.

Hanes, D.M. & Erikson, L.H. (2013). The significance of ultra-refracted surface gravity waves on sheltered coasts, with application to San Francisco Bay. Estuar. Coast. Shelf Sci., 133, 129–136.

Hannah, L., Roehrdanz, P.R., Ikegami, M., Shepard, A. V., Shaw, M.R., Tabor, G., et al. (2013). Climate change, wine, and conservation. Proc. Natl. Acad. Sci., 110, 6907–6912.

Harpold, A., Dettinger, M. & Rajagopal, S. (2017). Defining Snow Drought and Why It Matters. Eos, 98, 1–10.

Heberger, M., Cooley, H., Herrera, P., Gleick, P.H. & Moore, E. (2009). The impacts of sea-level rise on the California coast. California Climate Change Center.

Heberger, M., Cooley, H., Moore, E. & Herrera, P. (2012). The Impacts of Sea Level Rise on the San Francisco Bay. Available at: https://uc-ciee.org/downloads/Impacts%20of%20Sea%20Level%20Rise%20on%20the%20San%20Francisco%20Bay.pdf. Accessed 26 August 2018.

Heller, N.E., Kreitler, J., Ackerly, D.D., Weiss, S.B., Recinos, A., Branciforte, R., et al. (2015). Targeting climate diversity in conservation planning to build resilience to climate change. Ecosphere, 6, 65.

Hellmann, J.J., Byers, J.E., Bierwagen, B.G. & Dukes, J.S. (2008). Five potential consequences of climate change for invasive species. Conserv. Biol., 22, 534-543.

Herckes, P., Marcotte, A.R., Wang, Y. & Collett, J.L. (2015). Fog composition in the Central Valley of California over three decades. Atmos. Res., 151, 20-30.

Herman, J., M., Fefer, M., Dogan, M., Jenkins, M., Medellín-Azuara, J. & Lund, J. (2018). Advancing Hydro-Economic Optimization to Identify Vulnerabilities and Adaptation Opportunities in California's Water System.

Hirzel, D.R., Steenwerth, K., Parikh, S.J. & Oberholster, A. (2017). Impact of winery wastewater irrigation on soil, grape and wine composition. Agric. Water Manag., 180, 178–189.

Holleman, R.C. & Stacey, M.T. (2014). Coupling of Sea Level Rise, Tidal Amplification, and Inundation. J. Phys. Oceanogr., 44, 1439-1455.

Hu, Y. & Fu, Q. (2007). Observed poleward expansion of the Hadley circulation since 1979. Atmos. Chem. Phys., 7, 5229-5236.

Hummel, M.A., Berry, M.S. & Stacey, M.T. (2018). Sea level rise impacts on wastewater treatment systems along the US coasts. Earth's Futur., 6, e312.

Hummel, M.A., Wood, N.J., Schweikert, A., Stacey, M.T., Jones, J., Barnard, P.L., et al. (2017). Clusters of community exposure to coastal flooding hazards based on storm and sea level rise scenarios—implications for adaptation networks in the San Francisco Bay region. Reg. Environ. Chang., 1–13.

Huntsinger, L. & Bartolome, J.W. (2014). Cows in California Rangelands and Livestock in the Golden State. Rangelands, 36, 4–10.

Jackson, L., Potthoff, M., KL, S., AT, O., MR, S. & KM, S. (2007). Soil biology and carbon sequestration. In: Ecology and management of California grasslands (eds. Corbin, J., D'Antonio, C. & Stromberg, M.). University of California Press, Berkeley, CA, pp. 107–118.

Jesdale, B.M., Morello-Frosch, R. & Cushing, L. (2013). The racial/ethnic distribution of heat risk–related land cover in relation to residential segregation. Environ. Heal. Perspect, 121.7, 811.

Jevrejeva, S., Moore, J.C., Grinsted, A., Matthews, A.P. & Spada, G. (2014). Trends and acceleration in global and regional sea levels since 1807. Glob. Planet. Change, 113, 11–22.

Johnstone, J.A. & Dawson, T.E. (2010). Climatic context and ecological implications of summer fog decline in the coast redwood region. Proc. Natl. Acad. Sci., 107, 4533–4538.

Kaplan, M.L., Tilley, J.S., Hatchett, B.J., Smith, C.M., Walston, J.M., Shourd, K.N., et al. (2017). The Record Los Angeles Heat Event of September 2010: 1. Synoptic-Scale-Meso-β-Scale Analyses of Interactive Planetary Wave Breaking, Terrain- and Coastal-Induced Circulations. J. Geophys. Res. Atmos., 122, 10,729-10,750.

Keeley, A., Ackerly, D., Basson, G., Cameron, D., Hannah, L., Heller, N., et al. (2018). Migration corridors as adaptation to climate change: why, how, and what next.

Keller, M., Tarara, J.M. & Mills, L.J. (2010). Spring temperatures alter reproductive development in grapevines. Aust. J. Grape Wine Res., 16, 445–454.

Kerr, A., Dialesandro, J., Steenwerth, K., Lopez-Brody, N. & Elias, E. (2017). Vulnerability of California specialty crops to projected mid-century temperature changes. Clim. Change, 1–18.

Kharin, V. V., Zwiers, F.W., Zhang, X. & Wehner, M. (2013). Changes in temperature and precipitation extremes in the CMIP5 ensemble. Clim. Change, 119, 345–357.

Klinenberg, E. (1999). Denaturalizing Disaster: A Social Autopsy of the 1995 Chicago Heat Wave. Theory and Society, 28, 239-295.

Kopp, R.E., Horton, R.M., Little, C.M., Mitrovica, J.X., Oppenheimer, M., Rasmussen, D.J., et al. (2014). Probabilistic 21st and 22nd century sea-level projections at a global network of tide-gauge sites. Earth's Futur., 2, 383–406.

Koračin, D. (2017). Modeling and Forecasting Marine Fog. In:Marine Fog: Challenges and Advancements in Observations, Modeling, and Forecasting. Eds: Koračin, D., Dorman, C., pp. 425–475.

Koračin, D., Dorman, C.E., Lewis, J.M., Hudson, J.G., Wilcox, E.M. & Torregrosa, A. (2014). Marine fog: A review. Atmos. Res., 143, 142-175.

Kottek, M., Grieser, J., Beck, C., Rudolf, B. & Rubel, F. (2006). World map of the Köppen-Geiger climate classification updated. Meteorol. Zeitschrift, 15, 259–263.

Krawchuk, M. A., and M. A. Moritz. (2012). Fire and Climate Change in California. California Energy Commission. Publication number: CEC-500-2012-026.

Krawchuk, M.A. & Moritz, M.A. (2014). Burning issues: statistical analyses of global fire data to inform assessments of environmental change. Environmetrics, 25, 472–481.

LaDochy, S. & Witiw, M. (2012). The continued reduction in dense fog in the southern California region: Possible causes. Pure Appl. Geophys., 169, 1157–1163.

Laurenson, S., Bolan, N.S., Smith, E. & Mccarthy, M. (2012). Review: Use of recycled wastewater for irrigating grapevines. Aust. J. Grape Wine Res., 18, 1-10.

Lawler, J.J., Ackerly, D.D., Albano, C.M., Anderson, M.G., Dobrowski, S.Z., Gill, J.L., et al. (2015). The theory behind, and the challenges of, conserving nature's stage in a time of rapid change. Conserv. Biol., 29, 618–629.

Lenihan, J.M., Bachelet, D., Neilson, R.P. & Drapek, R. (2008). Response of vegetation distribution, ecosystem productivity, and fire to climate change scenarios for California. Clim. Change, 87, 215–230.

Lenihan, J.M., Drapek, R., Bachelet, D. & Neilson, R.P. (2003). Climate change effects on vegetation distribution, carbon, and fire in California. Ecol. Appl., 13, 1667–1681.

Lipsett, M.B., Materna, B., Stone, S.L., Therriault, S., Blaisdell, R. & Cook, J. (2008). Wildfire Smoke: A Guide for Public Health Officials. Available at: http://www.arb.ca.gov/smp/progdev/pubeduc/wfgv8.pdf. Accessed 27 August 2018.

Van Loon, A.F. (2015). Hydrological drought explained. Wiley Interdiscip. Rev. Water, 2, 359–392.

Ma, S., Baldocchi, D.D., Xu, L. & Hehn, T. (2007). Inter-annual variability in carbon dioxide exchange of an oak/grass savanna and open grassland in California. Agric. For. Meteorol., 147, 157–171.

Malamud-Roam, F., Dettinger, M., Ingram, L.B., Hughes, M.K. & Florsheim, J.L. (2007). Holocene Climates and Connections between the San Francisco Bay Estuary and its Watershed: A Review. J. San Fr. Estuary Watershed Sci., 5, 1–28.

Mann, M.E. & Gleick, P.H. (2015). Climate change and California drought in the 21st century: Fig. 1. Proc. Natl. Acad. Sci., 112, 3858–3859.

Mann, M.L., Batllori, E., Moritz, M.A., Waller, E.K., Berck, P., Flint, A.L., et al. (2016). Incorporating anthropogenic influences into fire probability models: Effects of human activity and climate change on fire activity in California. PLoS One, 11(4), p.e0153589.

McLaughlin, B.C., Ackerly, D.D., Klos, P.Z., Natali, J., Dawson, T.E. & Thompson, S.E. (2017). Hydrologic refugia, plants, and climate change. Glob. Chang. Biol., 8, 2941-2961.

McLaughlin, J.F., Hellmann, J.J., Boggs, C.L. & Ehrlich, P.R. (2002). Climate change hastens population extinctions. Proc. Natl. Acad. Sci., 99, 6070–6074.

Menéndez, M., Méndez, F.J., Losada, I.J. & Graham, N.E. (2008). Variability of extreme wave heights in the northeast Pacific Ocean based on buoy measurements. Geophys. Res. Lett., 35(L22607), 6.

Metz, M.R., Varner, J.M., Frangioso, K.M., Meentemeyer, R.K. & Rizzo, D.M. (2013). Unexpected redwood mortality from synergies between wildfire and an emerging infectious disease. Ecology, 94, 2152–2159.

Micheli, E., Flint, L., Veloz, S., Johnson, K. & Heller, N. (2016). Climate Ready North Bay Vulnerability Assessment Data Products: North Bay Region Summary. http://climate.calcommons.org/crnb/key-findings-northbay-region, Accessed 27 August 2018

Moghaddas, J., Roller, G., Long, J., Saah, D., Moritz, M., Stark, D., et al. (2018). Fuel Treatment for Forest Resilience and Climate Mitigations: A Critical Review for Coniferous Forests of the Sierra Nevada, Southern Cascade, Coast, Klamath, and Transverse Ranges.

Möller, I., Kudella, M., Rupprecht, F., Spencer, T., Paul, M., Van Wesenbeeck, B.K., et al. (2014). Wave attenuation over coastal salt marshes under storm surge conditions. Nat. Geosci., 7, 727–731.

Mosse, K.P.M., Lee, J., Leachman, B.T., Parikh, S.J., Cavagnaro, T.R., Patti, A.F., et al. (2013). Irrigation of an established vineyard with winery cleaning agent solution (simulated winery wastewater): Vine growth, berry quality, and soil chemistry. Agric. Water Manag., 123, 93–102.

Mote, P.W., Li, S., Lettenmaier, D.P., Xiao, M. & Engel, R. (2018). Dramatic declines in snowpack in the western US. npj Clim. Atmos. Sci., 1, 2.

Mote, P.W., Rupp, D.E., Li, S., Sharp, D.J., Otto, F., Uhe, P.F., et al. (2016). Perspectives on the causes of exceptionally low 2015 snowpack in the western United States. Geophys. Res. Lett., 43, 10,980-10,988. Available at: https://doi.org/10.1002/2016GL069965. Accessed 29 August 2018.

Moyle, Peter B., Rebecca M. Quiñones, and Joseph D. Kiernan (2012). Effects of Climate Change on the Inland Fishes of California: With Emphasis on the San Francisco Estuary Region. California Energy Commission. Publication number: CEC-500-2012-029.

MTC (2007). San Francisco Bay Area Regional Rail Plan, Final Report. https://mtc.ca.gov/our-work/plans-projects/other-plans/regional-rail-plan, accessed 28 August 2018

MTC, and Caltrans - D4 (2008). Bay Area Transportation: State of the System 2008 (Oakland, California) Available at: http://www.mtc.ca.gov/library/state_of_the_system/index_2003-07.htm. Accessed 26 August 2018.

Myers, N., Mittermeier, R.A., Mittermeier, C.G., da Fonseca, G.A.B. & Kent, J. (2000). Biodiversity hotspots for conservation priorities. Nature, 403, 853–858.

NASS. (2012). National Agricultural Statistics Service. Available at: www.nass.usda.gov. Accessed 26 August 2018.

North Bay Climate Adaptation Initiative, Climate Smart North Bay. Rivers, Creeks and Climate Change. (2013). Available at: http://www.lagunadesantarosa.org/pdfs/Climate%20Smart%20North%20Bay%20-%20Riparian.pdf. Accessed 28 August 2018.

New Buildings Institute. (2016). 2016 List of Zero Net Energy Buildings. Available at: https://newbuildings.org/2016-list-zero-net-energy-buildings/. Accessed 27 August 2018.

Newkirk, S., Veloz, S., Hayden, M., Heady, W., Leo, K., Judge, J., et al. (2018). Toward Natural Infrastructure to Manage Shoreline Change in California.

Nicholas, K.A. & Durham, W.H. (2012). Farm-scale adaptation and vulnerability to environmental stresses: Insights from winegrowing in Northern California. Glob. Environ. Chang., 22, 483–494.

NOAA. (2018). Tides & Currents. Available at: http://tidesandcurrents.noaa.gov/. Accessed 27 August 2018.

National Research Council (NRC). (2008). Potential Impacts of Climate Change on U.S. Transportation. Transportation Research Board Special Report 290. Transportation Research Board, Washington, DC.

National Research Council (NRC). 2012. Sea-Level Rise for the Coasts of California, Oregon, and Washington: Past, Present, and Future. National Academies Press, 260.

Nykvist, B. & Nilsson, M. (2015). Rapidly falling costs of battery packs for electric vehicles. Nat. Clim. Chang., 5, 329–332.

O'Brien, T.A., Sloan, L.C., Chuang, P.Y., Faloona, I.C. & Johnstone, J.A. (2013). Multidecadal simulation of coastal fog with a regional climate model. Clim. Dyn., 40, 2801–2812.

OPC (2018). State of California Sea-Level Rise Guidance: 2018 Update. Ocean Protection Council and California Natural Resources Agency.

Ovans, A. (2015). What Resilience Means, and Why It Matters. Harv. Bus. Rev. Available at: https://hbr.org/2015/01/what-resilience-means-and-why-it-matters. Accessed 27 August 2018.

Owen, J.J. & Silver, W.L. (2015). Greenhouse gas emissions from dairy manure management: A review of field-based studies. Glob. Chang. Biol. 21: 550-565.

Pall, P., Patricola, C.M., Wehner, M.F., Stone, D.A., Paciorek, C.J. & Collins, W.D. (2017). Diagnosing conditional anthropogenic contributions to heavy Colorado rainfall in September 2013. Weather Clim. Extrem., 17, 1–6.

Van Pelt, R., Sillett, S.C., Kruse, W.A., Freund, J.A. & Kramer, R.D. (2016). Emergent crowns and light-use complementarity lead to global maximum biomass and leaf area in Sequoia sempervirens forests. For. Ecol. Manage., 375, 279–308.

Pierce, D.W. & Cayan, D.R. (2013). The uneven response of different snow measures to human-induced climate warming. J. Clim., 26, 4148–4167.

Pierce, D.W., Cayan, D.R. & Thrasher, B.L. (2014). Statistical Downscaling Using Localized Constructed Analogs (LOCA)*. J. Hydrometeorol., 15, 2558–2585.

Poland, J.F. & Ireland, R.L. (1988). Land subsidence in the Santa Clara Valley, California, as of 1982. U.S. Geological Survey Professional Paper 497-F, 66.

Pounds, J.A., Bustamante, M.R., Coloma, L.A., Consuegra, J.A., Fogden, M.P.L., Foster, P.N., et al. (2006), Widespread amphibian extinctions from epidemic disease driven by global warming. Nature. 439:161-167.

Prein, A.F., Liu, C., Ikeda, K., Trier, S.B., Rasmussen, R.M., Holland, G.J., et al. (2017). Increased rainfall volume from future convective storms in the US. Nat. Clim. Chang., 7, 880–884.

Quayle, W.C., Fattore, A., Zandona, R., Christen, E.W. & Arienzo, M. (2009). Evaluation of organic matter concentration in winery wastewater: a case study from Australia. Water Sci. Technol., 60, 2521–2528.

Radke, J.D, G.S. Biging, K. Roberts, M. Schmidt-Poolman, H. Foster, E. Roe, Y. Ju, S. Lindbergh, T. Beach, L. Maier, Y. He, M. Ashenfarb, P. Norton, M. Wray, A. Alruheil, S. Yi, R. Rau, J. Collins, D. Radke, M. Coufal, S. Marx, D. Moanga, V. Ulyashin, A. Dalal. (2018). Assessing Extreme Weather-Related Vulnerability and Identifying Resilience Options for California's Independent Transportation Fuel Sector. California's Fourth Climate Change Assessment, California Energy Commission.

Radke, J.D., Biging, G.S., Schmidt-Poolman, M., Foster, H., Roe, E., Ju, Y., et al. (2016). Assessment of Bay Area Natural Gas Pipeline Vulnerability to Climate Change. California Energy Commission. Publication number: CEC-500-2017-008.

Rahel, F.J. & Olden, J.D. (2008). Assessing the effects of climate change on aquatic invasive species. Conserv. Biol. 22:521-533.

Ralph, F.M. & Dettinger, M.D. (2011). Storms, floods, and the science of atmospheric rivers. Eos (Washington. DC)., 92, 265–266.

Ralph, F.M., Neiman, P.J., Wick, G.A., Gutman, S.I., Dettinger, M.D., Cayan, D.R., et al. (2006). Flooding on California's Russian River: Role of atmospheric rivers. Geophys. Res. Lett., 33(13).

Rhoades, A.M., Ullrich, P.A. & Zarzycki, C.M. (2018). Projecting 21st century snowpack trends in western USA mountains using variable-resolution CESM. Clim. Dyn., 50, 261–288.

Ripoche, A., Celette, F., Cinna, J.P. & Gary, C. (2010). Design of intercrop management plans to fulfil production and environmental objectives in vineyards. Eur. J. Agron., 32, 30–39.

Risky Business: Risky Business Project, "Risky Business: The Economic Risks of Climate Change in the United States," 06/2014. Available at: http://riskybusiness.org/site/assets/uploads/2015/09/RiskyBusiness_Report_WEB_09_08_14.pdf. Accessed 26 August 2018.

Risser, M.D. & Wehner, M.F. (2017). Attributable Human-Induced Changes in the Likelihood and Magnitude of the Observed Extreme Precipitation during Hurricane Harvey. Geophys. Res. Lett., 44, 12,457-12,464. Available at: https://doi.org/10.1002/2017GL075888. Accessed 26 August 2018.

Rodriguez, J.F. 38 hospitalized for heat-related illnesses in SF. San Fr. Exam., 4 September 2017.

Rossow, W.B. & Dueñas, E.N. (2004). The International Satellite Cloud Climatology Project (ISCCP) Web Site: An Online Resource for Research. Bull. Am. Meteorol. Soc., 85, 167-172.

Ryals, R., Hartman, M.D., Parton, W.J., Delonge, M.S. & Silver, W.L. (2015). Long-term climate change mitigation potential with organic matter management on grasslands. Ecol. Appl., 25, 531–545.

Ryals, R., Kaiser, M., Torn, M.S., Berhe, A.A. & Silver, W.L. (2014). Impacts of organic matter amendments on carbon and nitrogen dynamics in grassland soils. Soil Biol. Biochem., 68, 52–61.

Ryals, R. & Silver, W.L. (2013). Effects of organic matter amendments on net primary productivity and greenhouse gas emissions in annual grasslands. Ecol. Appl., 23, 46–59.

Ryan, H., Gibbons, H., Hendley, J.W. & Stauffer, P. (1999). El Niño sea-level rise wreaks havoc in California's San Francisco Bay Region. USGS Fact Sheet 175–99. Available at: http://pubs.usgs.gov/fs/1999/fs175-99/. Accessed 26 August 2018.

Sawaske, S.R. & Freyberg, D.L. (2015). Fog, fog drip, and streamflow in the Santa Cruz Mountains of the California Coast Range. Ecohydrology, 8, 695–713.

Schile, L.M., Callaway, J.C., Morris, J.T., Stralberg, D., Thomas Parker, V. & Kelly, M. (2014). Modeling tidal marsh distribution with sea-level rise: Evaluating the role of vegetation, sediment, and upland habitat in marsh resiliency. PLoS One, 9: e88760.

Schmidt, D.A. & Bürgmann, R. (2003). Time-dependent land uplift and subsidence in the Santa Clara valley, California, from a large interferometric synthetic aperture radar data set. J. Geophys. Res. Solid Earth, 108(B9), 2416.

Sonoma County Hazard Mitigation Plan Update. (2017), FH-27 and -28. Available at: https://sonomacounty.ca.gov/PRMD/Long-Range-Plans/Hazard-Mitigation/Approved-Update/. Accessed 26 August 2018.

Schoellhamer, D.H. (2011). Sudden Clearing of Estuarine Waters upon Crossing the Threshold from Transport to Supply Regulation of Sediment Transport as an Erodible Sediment Pool is Depleted: San Francisco Bay, 1999. Estuaries and Coasts, 34, 885–899.

Schwalm, C.R., Williams, C.A., Schaefer, K., Baldocchi, D., Black, T.A., Goldstein, A.H., et al. (2012). Reduction in carbon uptake during turn of the century drought in western North America. Nat. Geosci., 5, 551-556

SCWA. (2018). Sonoma County Water Agency public draft LHMP 2018.

Seager, R., Hoerling, M., Schubert, S., Wang, H., Lyon, B., Kumar, A., et al. (2015). Causes of the 2011-14 California drought. J. Clim., 28, 6997–7024.

SF RWQCB staff summary report. (2011).

SFEI-ASC (2014). A Delta Transformed: Ecological Functions, Spatial Metrics, and Landscape Change in the Sacramento-San Joaquin Delta. Prepared for the California Department of Fish and Wildlife and Ecosystem Restoration Program. A Report of SFEI-ASC's Resilient Landscapes Prog., Publication #729, San Francisco Estuary Institute-Aquatic Science Center, Richmond, CA.

SFEI (2016). San Francisco Bay Shore Inventory: Mapping for Sea Level Rise Planning. SFEI Publication #779. San Francisco Estuary Institute-Aquatic Science Center, Richmond, CA.

SFEP (2015). The State of the Estuary. San Francisco Estuary Partnership, San Francisco, CA.

SFPUC. (2014). San Francisco's Wastewater Treatment Facilities Fact Sheet. Available at: https://sfwater.org/modules/showdocument.aspx?documentid=5801 Accessed 27 August 2018.

Shaw, M.R., Pendleton, L., Cameron, D.R., Morris, B., Bachelet, D., Klausmeyer, K., et al. (2011). The impact of climate change on California's ecosystem services. Clim. Change, 109, 465–484.

Shirzaei, M. & Bürgmann, R. (2018). Global climate change and local land subsidence exacerbate inundation risk to the San Francisco Bay Area. Sci. Adv., 4 (3).

Shirzaei, M., Bürgmann, R. & Fielding, E.J. (2017). Applicability of Sentinel-1 Terrain Observation by Progressive Scans multitemporal interferometry for monitoring slow ground motions in the San Francisco Bay Area. Geophys. Res. Lett., 44, 2733–2742.

Shonkoff, S.B., Morello-Frosch, R., Pastor, M. & Sadd, J. (2009). Minding the Climate Gap: Environmental Health and Equity Implications of Climate Change Mitigation Policies in California. Environ. Justice, 2, 173–177.

Silver, W.L., Ryals, R. & Eviner, V. (2010). Soil Carbon Pools in California's Annual Grassland Ecosystems. Rangel. Ecol. Manag., 63, 128–136.

Silver, W.L., Vergara, S. & Mayer, A. (2018). Carbon sequestration and greenhouse gas mitigation potential of composting and soil amendments on California's rangelands.

Smith, C.S., Gittman, R.K., Neylan, I.P., Scyphers, S.B., Morton, J.P., Joel Fodrie, F., et al. (2017). Hurricane damage along natural and hardened estuarine shorelines: Using homeowner experiences to promote nature-based coastal protection. Mar. Policy, 81, 350–358.

Spayd, S.E., Tarara, J.M., Mee, D.L. & Ferguson, J.C. (2002). Separation of sunlight and temperature effects on the composition of Vitis vinifera cv. Merlot berries. Am. J. Enol. Vitic., 53, 171–182.

Steenwerth, K. & Belina, K.M. (2008a). Cover crops and cultivation: Impacts on soil N dynamics and microbiological function in a Mediterranean vineyard agroecosystem. Appl. Soil Ecol., 40, 370–380.

Steenwerth, K. & Belina, K.M. (2008b). Cover crops enhance soil organic matter, carbon dynamics and microbiological function in a vineyard agroecosystem. Appl. Soil Ecol., 40, 359–369.

Steenwerth, K.L., Calderón-Orellana, A., Hanifin, R.C., Storm, C. & McElrone, A.J. (2016). Effects of various vineyard floor management techniques on weed community shifts and grapevine water relations. Am. J. Enol. Vitic., 67, 153–162.

Steiner, A.L., Tonse, S., Cohen, R.C., Goldstein, A.H. & Harley, R.A. (2006). Influence of future climate and emissions on regional air quality in California. J. Geophys. Res. Atmos., 111(D18).

Stralberg, D., Brennan, M., Callaway, J.C., Wood, J.K., Schile, L.M., Jongsomjit, D., et al. (2011). Evaluating Tidal Marsh Sustainability in the Face of Sea-Level Rise: A Hybrid Modeling Approach Applied to San Francisco Bay. PLoS One, 6, e27388.

Stralberg, D., Jongsomjit, D., Howell, C.A., Snyder, M.A., Alexander, J.D., Wiens, J.A., et al. (2009). Re-shuffling of species with climate disruption: A no-analog future for California birds? PLoS One, 4, e6825.

Sugimoto, S., Sato, T. & Nakamura, K. (2013). Effects of synoptic-scale control on long-term declining trends of summer fog frequency over the pacific side of Hokkaido Island. J. Appl. Meteorol. Climatol., 52, 2226–2242.

Summary Report: 2007 National Resources Inventory, Natural Resources Conservation Service, Washington, DC, and Center for Survey Statistics and Methodology, Iowa State University, Ames, Iowa. 123 pages. Available at: https://www.nrcs.usda.gov/Internet/FSE_DOCUMENTS/stelprdb1041379.pdf. Accessed 26 August 2018.

Swain, D.L. (2015). A tale of two California droughts: Lessons amidst record warmth and dryness in a region of complex physical and human geography. Geophys. Res. Lett., 42, 9999.

Swain, D.L., Horton, D.E., Singh, D. & Diffenbaugh, N.S. (2016). Trends in atmospheric patterns conducive to seasonal precipitation and temperature extremes in California. Sci. Adv., 2, e1501344.

Swain, D.L., Langenbrunner, B., Neelin, J.D. & Hall, A. (2018). Increasing precipitation volatility in twenty-first-century California. Nat. Clim. Chang., 8, 427–433.

Swanson, K.M., Drexler, J.Z., Fuller, C.C. & Schoellhamer, D.H. (2015). Modeling Tidal Freshwater Marsh Sustainability in the Sacramento–San Joaquin Delta Under a Broad Suite of Potential Future Scenarios. San Fr. Estuary Watershed Sci., 13(1).

Sweet, W.V., Kopp, R.E., Weaver, C.P., Obeysekera, J., Horton, R.M., Thieler, E.R., et al. (2017). Global and regional sea level rise scenarios for the United States. NOAA Technical Report NOS CO-OPS 083, NOAA/NOS Center for Operational Oceanographic Products and Services.

Syphard, A.D., Radeloff, V.C., Keeley, J.E., Hawbaker, T.J., Clayton, M.K., Stewart, S.I., et al. (2007). Human influence on California fire regimes. Ecol. Appl., 17, 1388–1402.

Tamayao, M.-A.M., Michalek, J.J., Hendrickson, C. & Azevedo, I.M.L. (2015). Regional Variability and Uncertainty of Electric Vehicle Life Cycle CO2 Emissions across the United States. Environ. Sci. Technol., 49, 8844–8855.

Thorne, J.H., Choe, H., Boynton, R.M., Bjorkman, J., Whitneyalbright, W., Nydick, K., et al. (2017). The impact of climate change uncertainty on California's vegetation and adaptation management. Ecosphere, 8, e02021.

Thorne, K., MacDonald, G., Guntenspergen, G., Ambrose, K., Buffington, B., Dugger, B., et al. (2018). Pacific coastal wetland resilience and vulnerability to sea-level rise. Sci. Adv., 4, eaao3270.

Torregrosa, A., Combs, C. & Peters, J. (2016). GOES-derived fog and low cloud indices for coastal north and central California ecological analyses. Earth Sp. Sci., 3, 46–67.

Torregrosa, A., O'Brien, T.A. & Faloona, I.C. (2014). Coastal Fog, Climate Change, and the Environment. Eos, Trans. Am. Geophys. Union, 95, 473–474.

USDA NASS. (2016). Available at: https://www.nass.usda.gov. Accessed 27 August 2018.

USGCRP. (2017). Climate Science Special Report: Fourth National Climate Assessment, Volume 1. Washington, DC.

Vahmani, P. & Jones, A.D. (2017). Water conservation benefits of urban heat mitigation. Nat. Commun., 8, 1072.

Verhoeven, E. & Six, J. (2014). Biochar does not mitigate field-scale N2O emissions in a Northern California vineyard: An assessment across two years. Agric. Ecosyst. Environ., 191, 27–38.

van Vuuren, D.P., Edmonds, J.A., Kainuma, M., Riahi, K. & Weyant, J. (2011). A special issue on the RCPs. Clim. Change, 109, 1–4.

Walker, C.L. & Anderson, M.R. (2016). Cloud impacts on pavement temperature and shortwave radiation. J. Appl. Meteorol. Climatol., 55, 2329–2347.

Wang, M. & Ullrich, P. (2018). Marine air penetration in California's Central Valley: Meteorological drivers and the impact of climate change. J. Appl. Meteorol. Climatol., 57, 137–154.

Wang, R.Q., Stacey, M.T., Herdman, L.M.M., Barnard, P.L. & Erikson, L. (2018). The Influence of Sea Level Rise on the Regional Interdependence of Coastal Infrastructure. Earth's Futur., 6, 677-688.

Weber, E., Grattan, S.R., Hanson, B.R., Vivaldi, G.A., Meyer, R.D., Prichard, T.L., et al. (2014). Recycled water causes no salinity or toxicity issues in Napa vineyards. Calif. Agric., 68, 59-67.

Wehner, M.F., Arnold, J.R., Knutson, T., Kunkel, K.E. & LeGrande, A.N. (2017). Droughts, floods, and wildfires, Climate Science Special Report: Fourth National Climate Assessment, Volume I. Washington, DC.

Wehner, M.F., Reed, K.A., Li, F., Prabhat, Bacmeister, J., Chen, C.T., et al. (2014). The effect of horizontal resolution on simulation quality in the Community Atmospheric Model, CAM5.1. J. Adv. Model. Earth Syst., 6, 980–997.

Wehner, M.F., Smith, R.L., Bala, G. & Duffy, P. (2010). The effect of horizontal resolution on simulation of very extreme US precipitation events in a global atmosphere model. Clim. Dyn., 34, 241–247.

Weiss, S.B., Murphy, D.D. & White, R.R. (1988). Sun, slope, and butterflies: topographic determinants of habitat quality for Euphydryas editha. Ecology, 69, 1486–1496.

Weiss, S.B. & Weiss, A.D. (1998). Landscape-Level Phenology of a Threatened Butterfly: A GIS-Based Modeling Approach. Ecosystems, 1, 299–309.

Westerling, A.L. (2018). Wildfire Simulations for the Fourth California Climate Assessment: Projecting Changes in Extreme Wildfire Events with a Warming Climate.

Westerling, A.L., Hidalgo, H.G., Cayan, D.R. & Swetnam, T.W. (2006). Warming and earlier spring increase Western U.S. forest wildfire activity. Science, 313, 940–943.

Williams, A.P., Schwartz, R.E., Iacobellis, S., Seager, R., Cook, B.I., Still, C.J., et al. (2015). Urbanization causes increased cloud base height and decreased fog in coastal Southern California. Geophys. Res. Lett., 42, 1527–1536.

Wingfield, D.K. & Storlazzi, C.D. (2007). Spatial and temporal variability in oceanographic and meteorologic forcing along Central California and its implications on nearshore processes. J. Mar. Syst., 68, 457–472.

Witiw, M.R. & Ladochy, S. (2015). Cool PDO phase leads to recent rebound in coastal southern California fog. Erde, 146, 232–244.

Wright, S. a. & Schoellhamer, D.H. (2004). Trends in the sediment yield of the Sacramento River, California, 1957-2001. San Fr. Estuary Watershed Sci., 2, 1–14.

Xu, L. & Baldocchi, D.D. (2003). Seasonal trends in photosynthetic parameters and stomatal conductance of blue oak (Quercus douglasii) under prolonged summer drought and high temperature. Tree Physiol., 23, 865–877.

Xu, L. & Baldocchi, D.D. (2004). Seasonal variation in carbon dioxide exchange over a Mediterranean annual grassland in California. Agric. For. Meteorol., 123, 79–96.

Yu, O.T., Greenhut, R.F., O'Geen, A.T., Mackey, B., Horwath, W.R. & Steenwerth, K.L. (2017). Precipitation Events and Management Practices Affect Greenhouse Gas Emissions from Vineyards in a Mediterranean Climate. Soil Sci. Soc. Am. J., 81, 138-152.

Zero-Net-Energy-Center. Available at: https://www.znecenter.org/. Accessed 26 August 2018.

Zhang, H., Moura, S., Hu, Z. & Song, Y. (2016). PEV Fast-Charging Station Siting and Sizing on Coupled Transportation and Power Networks. IEEE Trans. Smart Grid, 1–1

Zhang, H., Moura, S.J., Hu, Z., Qi, W. & Song, Y. (2017). A Second Order Cone Programming Model for Planning PEV Fast-Charging Stations. IEEE Trans. Power Syst., 33, 2763-2777.

Zhang, S., Chen, Y., Long, J. & Han, G. (2015). Interannual variability of sea fog frequency in the Northwestern Pacific in July. Atmos. Res., 151, 189–199.

Zhu, X., Zhang, L., Ran, R. & Mol, A. (2015). Regional restrictions on Environmental Impact Assessment approval in China: The legitimacy of environmental authoritarianism. J. Clean. Prod., 92, 100-108.